



TECHNISCHE UNIVERSITÄT MÜNCHEN

Wissenschaftszentrum Weihenstephan für Ernährung, Landnutzung und Umwelt

Lehrstuhl für Mikrobiologie

Identification of naphthalene carboxylase subunits
of the sulfate-reducing enrichment culture N47

Janina Stephanie Kölschbach

Vollständiger Abdruck der von der Fakultät Wissenschaftszentrum Weihenstephan für Ernährung, Landnutzung und Umwelt der Technischen Universität München zur Erlangung des akademischen Grades eines

Doktors der Naturwissenschaften

genehmigten Dissertation.

Vorsitzende(r):

Univ.-Prof. Dr. Wolfgang Liebl

Prüfer der Dissertation:

1. Priv.-Doz. Dr. Tillmann Lüders
2. Univ.-Prof. Dr. Rainer U. Meckenstock
(Universität Duisburg-Essen)
3. Univ.-Prof. Dr. Johann Heider
(Philipps-Universität Marburg)

Die Dissertation wurde am 06.07.2015 bei der Technischen Universität München eingereicht und durch die Fakultät Wissenschaftszentrum Weihenstephan für Ernährung, Landnutzung und Umwelt am 06.10.2015 angenommen.

Für Mama, Papa, Jessica, Janka und Maximilian

Abstract

Non-substituted polycyclic aromatic hydrocarbons are very difficult to degrade in the absence of molecular oxygen and the underlying anaerobic biochemical reactions are only poorly understood. Metabolite analyses have indicated that for the model compound naphthalene, carboxylation was the first reaction activating such a chemically stable molecule. Moreover, Mouttaki et al. (2012) brought biochemical evidence confirming the carboxylation reaction in the sulfate-reducing culture N47. Naphthalene carboxylase converts naphthalene and ^{13}C -labeled bicarbonate to 2-[carboxyl- ^{13}C]naphthoic acid at a rate of $0.12 \text{ nmol min}^{-1} \text{ mg}^{-1}$ of protein in crude cell extracts of N47. Additionally, it exhibits an isotopic exchange capability indicating the formation of free reversible intermediates. Previous proteogenomic studies on N47 and the marine naphthalene-degrading strain NaphS2 allowed the identification of a gene cluster which products were suggested to be carboxylase-like subunits potentially involved in the initial reaction of naphthalene degradation. The focus of the present PhD project was on the identification of the naphthalene carboxylase and its subunits. Initially, it was planned to purify the protein complex under native conditions from N47 cells. Due to the slow growth and the little biomass obtained from N47, the native purification of such an oxygen sensitive enzyme (complex) is difficult. In order to purify the naphthalene carboxylase from small sample volumes under strict anoxic conditions, a commercially available chromatography system was modified in a way that it could be operated inside of an anaerobic chamber. Different cell lysis methods such as sonication, bead beating and treatment with lysozyme or detergents were tested. However, none of the used methods generated cell-free extracts that preserved naphthalene carboxylase activity. Therefore, we developed alternative strategies to identify the native naphthalene carboxylase subunits. A differential protein induction analysis on Blue native PAGE led to the identification of potential subunits of the naphthalene carboxylase of N47 in native conformation. Due to the obtained results, the naphthalene carboxylase protein complex is proposed to consist of at least eight different subunits including three carboxylase-like subunits with a total apparent molecular mass of around 750 kDa. Moreover, the identified subunits are encoded in an operon structure with a size of 8.9 kbp within the previously mentioned naphthalene carboxylase gene cluster. These findings were supported by a pull-down approach revealing *in vitro* interaction partners of a heterologously produced GST-tagged naphthalene carboxylase subunit. In the present PhD thesis, the interaction of the gene products of the naphthalene carboxylase gene cluster was shown for the first time. Furthermore, a final experiment demonstrated naphthalene carboxylase activity in cell-free extracts of N47 cells, which were opened by a French Press. The results identified naphthalene carboxylase as a potential ATP-dependent enzyme.

The enrichment culture N47 consists of two major organisms, the naphthalene-degrading Deltaproteobacterium and a spirochete. In the environment, uncultivated members of the family *Spirochaetaceae* were detected in contaminated sites and co-occurred with key degrader organisms. The ecological function of *Spirochaetaceae* within this niche is unknown. It was speculated that they might support the degradation of (poly-)aromatic and chloro-organic compounds. In a complementary project, the novel anaerobic spirochete *Cand. Treponema contaminophilus* sp. strain HM^T was isolated from the naphthalene-degrading enrichment culture N47 and characterized. Even though *Cand. Treponema contaminophilus* sp. strain HM^T is a stable member of the naphthalene-degrading culture, it was not able to degrade naphthalene under sulfate-reducing conditions in pure culture. In contrast to the majority of described spirochete species, *Cand. Treponema contaminophilus* sp. strain HM^T showed a rod-shaped morphology and was non-motile. The strain grew between 12 to 50 °C with an optimum at 37 °C. The new isolate was able to ferment various sugars including D-glucose, D-fructose, lactose, sucrose but only in the presence of yeast extract. Based on its characteristics, e.g. its unusual morphology compared to its relatives from the *Treponema* species and the phylogenetic distance, the new strain could be clearly distinguished from cultivated members.

In a cooperation project, a protocol was established to analyze N47 cells using stable isotope Raman microspectroscopy. Raman microspectroscopy is a non-invasive method, which allows the chemical analysis of cells on the single cell level. Different methods were tested to prepare N47 cells for stable isotope Raman microspectroscopy and the obtained spectra were compared. The sharpest bands with the highest reproducibility were obtained after fixing N47 cell with PFA followed by a treatment with stepwise increased concentrations of ethanol. In a final experiment using ¹³C₁₀-labeled naphthalene, the region of the phenylalanine marker band at 1001 cm⁻¹ was analyzed by stable isotope Raman microspectroscopy. The isotopic shift of the phenylalanine Raman band (990, 978 and 968 cm⁻¹) indicated successful incorporation of the label into the biomass of N47. The four Raman bands represented the different isotopologues of phenylalanine.

In summary, this thesis provides new insights into the biochemistry of naphthalene carboxylase and its subunits. The gained knowledge will contribute to the understanding of the complex pathways in the anaerobic degradation of polycyclic aromatic hydrocarbons, which are ubiquitous and persistent environmental pollutants. Moreover, *Cand. Treponema contaminophilus* sp. strain HM^T, which is the first isolate of a new phylogenetic branch of spirochetes co-occurring in contaminated sites, will help to understand the role of spirochetes in these habitats and might be of use to reveal a potential interaction with the key degrading microorganisms. Furthermore, our newly established protocol will allow the analysis of slow

growing microorganisms that anaerobically degrade complex substrates such as naphthalene by stable isotope Raman microspectroscopy.

Zusammenfassung

Der aerobe Abbau von polyzyklischen aromatischen Kohlenwasserstoffen wurde intensiv untersucht und die zugehörigen biochemischen Reaktionen aufgeklärt. In Abwesenheit des Co-Substrates Sauerstoff ist der Abbau dieser inerten Substanzen jedoch schwierig und bisher konnten nur einige biochemische Reaktionen näher untersucht werden. Metabolit-Analysen von Kulturüberständen zeigten, dass Naphthalin, eine Modelsubstanz im anaeroben Abbau von polyzyklischen Kohlenwasserstoffen, in einer initialen Reaktion carboxyliert und dadurch aktiviert wird. Die ersten Hinweise drauf konnten in Zellextrakten des Sulfat-reduzierenden Modelorganismus N47 biochemisch bestätigt werden. Mouttaki et al. (2012) zeigten, dass die Naphthalin Carboxylase in N47-Zellextrakten Naphthalin und ^{13}C -markiertes Bicarbonat zu 2-[Carboxyl- ^{13}C]Naphthoesäure umsetzt. Die spezifische Aktivität betrug dabei $0.12 \text{ nmol min}^{-1} \text{ mg}^{-1}$ Protein. Darüberhinaus katalysiert das Enzym eine Austauschreaktion, welche auf die Bildung eines freien Intermediates während der Katalyse deutet. Eine solche charakteristische Austauschreaktion wurde für nicht-Biotin abhängige Carboxylasen häufig beschrieben. In zwei unabhängigen proteogenomischen Analysen wurden in N47 und dem marinen Naphthalin-Abbauer NaphS2 vergleichbare Gencluster identifiziert, in welchen Carboxylase-ähnliche Proteine codiert werden. Es wurde vermutet, dass diese Carboxylase-ähnlichen Proteine an der initialen Aktivierung von Naphthalin beteiligt sind. Das Ziel dieser Doktorarbeit war die Identifizierung der Naphthalin Carboxylase und deren Untereinheiten in dem Modelorganismus N47. Der Enzymkomplex sollte unter nativen Bedingungen aus zellfreiem Extrakt von N47 gereinigt werden. Schon vor Beginn des Projektes war bekannt, dass die Naphthalin Carboxylase sehr instabil und sensitiv gegenüber Sauerstoff ist. Zudem ist die verfügbare Biomasse von N47 stark limitierend, da die Zellen bei Sulfat-reduzierendem Wachstum mit Naphthalin als Kohlenstoffquelle nur sehr langsam (bis zu 3 Monate) und in geringen Zelldichten wachsen. Um das Protein dennoch aus geringen Probenvolumen und unter anoxischen Bedingungen reinigen zu können, wurde ein Chromatographiesystem modifiziert und partiell in ein Anaerobenzelt integriert. Desweiteren wurden verschiedenen Methoden zur Zellyse getestet, um einen zellfreien Extrakt zu erzeugen in welchem die Naphthalin Carboxylase Aktivität erhalten blieb. N47-Zellen wurden unter anderem mit Hilfe von Ultraschall, einer Kugelmühle, Lysozym und Detergenzien aufgeschlossen, die Aktivität des Enzymes konnte jedoch in keinem der erzeugten zellfreien Extrakte nachgewiesen werden. Daher wurde eine alternative Methode entwickelt, um die Untereinheiten der Naphthalin Carboxylase zu identifizieren. Hierbei führte eine differenzielle Proteomanalyse mittels „Blue native PAGE“ zur Identifizierung von potentiellen Naphthalin Carboxylase Untereinheiten in nativer Konformation. Ausgehend von den hier erhaltenen Daten weist die Naphthalin Carboxylase eine apparente molekulare Masse von ungefähr 750 kDa auf und besteht aus mindestens acht verschiedenen

Untereinheiten, darunter drei Carboxylase-ähnliche Untereinheiten. Die identifizierten Untereinheiten werden in einem Operon von 8.9 kbp codiert, welches innerhalb des putativen Naphthalin Carboxylase Geneclusters liegt. Unter Verwendung einer heterolog produzierten und GST-getaggen Naphthalin Carboxylase Untereinheit wurden in einem „Pull-down“-Experiment Interaktionspartner *in vitro* identifiziert. Die gefundenen Interaktionspartner unterstützten die erhaltenen Daten der „Blue native PAGEs“. In der vorliegenden Arbeit wurde die Interaktion der Genprodukte des Naphthalin Carboxylase Geneclusters zum ersten Mal gezeigt. In einem abschließenden Experiment, welches mit French Press-geöffneten N47-Zellen aus einem Fermenter durchgeführt wurde, konnte die Naphthalin Carboxylase Aktivität letztlich auch im zellfreien Extrakt gemessen werden. Die hierbei generierten Ergebnisse lassen darauf schließen, dass die Naphthalin Carboxylase möglicherweise ein ATP-abhängiges Enzyme ist.

Die Anreicherungskultur N47 besteht überwiegend aus zwei Mikroorganismen, einem Naphthalin-abbauenden Deltaproteobacterium und einem Spirochäten. An kontaminierten Standorten treten nicht-kultivierte Mitglieder der Familie *Spirochaetaceae* häufig zusammen mit sogenannten mikrobiellen „Key Playern“ auf. Während die mikrobiellen „Key Player“ den entsprechenden Schadstoff anaerob abbauen, ist die ökologische Funktion der Spirochäten innerhalb dieser Nische vollkommen unbekannt. Es wird jedoch vermutet, dass Spirochäten den Abbau von (poly-)aromatischen und chloro-organischen Substanzen unterstützen. Hier wurde der neuartige anaerobe Spirochät *Cand. Treponema contaminophilus* sp. Stamm HM^T charakterisiert, welcher zuvor aus der Anreicherungskultur N47 isoliert wurde. Obwohl *Cand. Treponema contaminophilus* sp. Stamm HM^T aus der Naphthalin-abbauenden Kultur N47 isoliert wurde, war die Reinkultur nicht fähig unter Sulfat-reduzierenden Bedingungen Naphthalin abzubauen. Das unbewegliche und stäbchenförmige Bakterium zeigte Wachstum zwischen 12 bis 50 °C, wobei das Optimum bei 37 °C lag. *Cand. Treponema contaminophilus* sp. Stamm HM^T fermentierte in Anwesenheit von Hefeextrakt eine Vielzahl von Zuckern unter anderem D-Glucose, D-Fructose, Laktose und Saccharose. Bedingt durch die abweichende Morphologie sowie die phylogenetische Distanz unterscheidet sich das neue Isolat eindeutig von seinen bereits kultivierten Verwandten.

Im Rahmen dieser Doktorarbeit wurde in einem Kooperationsprojekt mit der Technischen Universität München ein Protokoll etabliert, welches es ermöglichte den Einbau von stabilen Isotopen in N47-Zellen mittels Raman-Mikrospektroskopie zu untersuchen. Die Raman-Mikrospektroskopie ist eine nicht-invasive Methode, die eine chemische Analyse einzelner Zellen ermöglicht. Es wurden verschiedene Methoden zur Probenvorbereitung von N47-Zellen getestet und die erhaltenen Spektren verglichen. Die exaktesten Spektren mit der höchsten Reproduzierbarkeit wurden dabei erhalten, wenn die Zellen zuvor in Paraformaldehyd fixiert und anschließend mit einer stufenweise erhöhten Konzentration von

Ethanol behandelt wurde. In einem abschließenden Experiment unter Verwendung von $^{13}\text{C}_{10}$ -markiertem Naphthalin konnte der Einbau des stabilen Isotopes in die Zellmasse von N47 mittels Raman-Mikrospektroskopie erfolgreich nachgewiesen werden. Der Einbau von markiertem Naphthalin wurde dabei durch eine charakteristische Rotverschiebung der Phenylalanin Raman-Bande von 1001 cm^{-1} auf 990 cm^{-1} , 978 cm^{-1} und 968 cm^{-1} sichtbar. Diese zusätzlichen Raman-Banden repräsentierten dabei die verschiedenen Isotopologe des Phenylalanins.

Die neu erhaltenen Einblicke in die Biochemie der Naphthalin Carboxylase und die Identifikation ihrer Untereinheiten werden zu einem besseren Verständnis der komplexen Abbauege von aromatischen Kohlenwasserstoffen beitragen, welche weitverbreitete und persistierende Umweltschadstoffe darstellen. Darüber hinaus ist *Cand. Treponema contaminophilus* sp. Stamm HM^T der erste kultivierbare Vertreter eines neuen phylogenetischen Zweigs von Spirochäten, welche an kontaminierten Standorten detektiert wurden. Daher kann *Cand. Treponema contaminophilus* sp. Stamm HM^T als Modelorganismus verwendet werden, um die Rolle von Spirochäten in diesen Habitaten zu verstehen und eine mögliche Interaktion mit den Schadstoff-abbauenden Mikroorganismen zu analysieren. Zudem erlaubt unser neu etabliertes Protokoll der Stabilisotopen-Raman-Mikrospektroskopie die Analyse langsam wachsender Bakterien, die komplexe Substrate wie beispielsweise Naphthalin anaerob abbauen.

Abbreviations

°C	Celsius	Nms	naphthyl-2-methyl-succinate synthase
¹² C	Carbon isotope with standard atomic weight of 12 u	OD	Optical density
¹³ C	Stable carbon isotope with atomic weight of 13 u	PAH	Polycyclic aromatic hydrocarbon
16S rRNA	Ribosomal RNA, small subunit (bacteria)	PBS	Phosphate buffered saline
ADMA	4-amino-N,N-dimethylaniline sulfate	PEG	Polyethylene glycol
APS	Ammonium persulfate	PFA	Paraformaldehyde
BMC	Bacterial microcompartment	P _i	Orthophosphate PO ₄ ³⁻
BNP	Blue native PAGE	Ppc	Phenylphosphate carboxylase
Bss	Benzylsuccinate synthase	PP _i	Pyrophosphate
cDNA	Complementary DNA	RNase	Ribonuclease
CIAP	Calve intestine alkaline phosphatase	rpm	Rounds per minute
ddH ₂ O	Double-distilled water	RT	Room temperature
DDM	<i>n</i> -Dodecyl-β-D-maltopyranoside	RT-PCR	reverse transcriptase-PCR
DHNC ₂ CoA	5,6-Dihydro-2-naphthyl-CoA	s	Seconds
DMSO	Dimethyl sulfoxide	SEM	Scanning Electron Microscopy
dNTP	Desoxynucleoside triphosphate	SERS	Surface enhanced Raman spectroscopy
EBP	Bacterial enhancer-binding proteins	SIP	Stable isotope probing
FAM	6-carboxyfluorescein	T-RFLP	Terminal restriction fragment length polymorphism
Fig.	Figure	Tab.	Table
G+C content	Guanine + Cytosine content	TAE	Tris-acetate-EDTA
gDNA	genomic DNA	TEMED	Tetramethylethylenediamine
h	Hours	THNCoA	5,6,7,8-Tetrahydro-2-naphthoyl-CoA
HHNCoA	Hexahydro-2-naphthoyl-CoA	U	Unit of enzyme activity, conversion of 1 μmol substrate min ⁻¹
HMN	2,2,4,4,6,8,8-Heptamethylnonane	v/v	Volume per volume
IPTG	Isopropyl β-D-1-thiogalactopyranoside	w/v	Wight per volume
kDa	Kilodalton		
MCS	Multiple Cloning Site		
min	Minutes		
NCR	2-Naphthoyl-CoA reductase		

Table of contents

Abstract	I
Zusammenfassung	IV
Abbreviations	VII
1. INTRODUCTION.....	1
1.1 Aromatic hydrocarbons.....	1
1.2 Aromatic hydrocarbon contaminated sites.....	3
1.2.1 Spirochaetes in hydrocarbon-contaminated sites	4
1.3 Anaerobic degradation of non-substituted polycyclic aromatic hydrocarbons.....	5
1.3.1 Anaerobic degradation of benzene	5
1.3.2 Anaerobic degradation of naphthalene	10
1.3.3 Anaerobic degradation of other polycyclic aromatic hydrocarbons- Anthracene, Phenanthrene, Biphenyl	17
1.4 The enrichment culture N47.....	18
Anaerobic degradation of 2-methynaphthalene	19
1.5 Carboxylases.....	20
(i) Autotrophic carboxylases	21
(ii) Assimilatory carboxylases in anaerobic degradation	22
(iii) Anaplerotic carboxylases	26
(iv) Biosynthetic carboxylases	27
1.6 Objectives.....	29
2. MATERIALS AND METHODS.....	30
2.1 Organisms, vectors and synthetic oligonucleotides.....	30
2.2 Chemicals, biochemicals and gases.....	33
2.3 Media and buffers.....	33
2.3.1 Medium for the cultivation of <i>E. coli</i>	33
2.3.2 Medium for the cultivation of N47	34
2.3.3 Medium for the cultivation of NaphS2	36
2.3.4 Medium for the cultivation of <i>Cand. Treponema contaminophilus</i> sp.	38
2.4 Cultivation and maintenance of bacterial strains and preparation of cell-free extracts.....	39
2.4.1 <i>In vitro</i> overexpression of plasmid-encoded genes in <i>E.coli</i>	39
2.4.2 Cultivation and maintenance of the strict anaerobic cultures N47, NaphS2 and <i>Cand. T. contaminophilus</i> sp.	39
i. N47 and NaphS2	40
ii. <i>Cand. Treponema contaminophilus</i> sp.	40

2.4.3	Cell harvesting and preparation of cell-free extracts	41
	i. <i>E. coli</i>	41
	ii. N47 and NaphS2	41
2.5	Molecular Methods	43
2.5.1	Polymerase chain reaction (PCR)	43
2.5.2	Terminal restriction fragment length polymorphism (T-RFLP)	45
2.5.3	Restriction	45
2.5.4	Purification of DNA	46
2.5.5	Isolation of plasmids	46
2.5.6	Isolation of RNA	46
2.5.7	Reverse transcription polymerase chain reaction (RT-PCR)	47
2.5.8	Isolation of chromosomal DNA	47
2.5.9	Gel extraction of DNA	48
2.5.10	Dephosphorylation of plasmids	48
2.5.11	Ligation	48
2.5.12	Transformation of plasmids	49
2.5.13	Preparation of chemical competent <i>E. coli</i>	49
2.5.14	Separation of DNA by agarose gels electrophoresis	49
2.6	Analytical methods	50
2.6.1	Bradford assay	50
2.6.2	Sulfide measurement	50
2.6.3	High-pressure liquid chromatography (HPLC)	50
2.6.4	Determination of fatty acid composition	51
2.6.5	DNA base composition	52
2.6.6	Determination of bacterial morphological characteristics	52
2.6.7	Microscopy	52
	i. Electron Microscopy	52
	ii. Raman microspectroscopy	53
2.6.8	Flow cytometry for absolute microbial cells counting	54
2.6.9	Proteomic analysis	55
	i. In-Gel tryptic digest	55
	ii. Mass spectrometric measurements	55
	iii. Label-free quantitative analysis	56
2.7	Biochemical methods	57
2.7.1	Enzyme purification	57
	i. GST purification	57
	ii. HIS purification	57
	iii. Desalting and concentration of proteins	58
2.7.2	Polyacrylamide gel electrophoresis	58
	i. SDS polyacrylamide gel electrophoresis	58
	ii. Blue native polyacrylamide gel electrophoresis	59
2.7.3	Extraction of proteins from BNPs	59
2.7.4	<i>In vitro</i> protein interaction analysis (Pull-down experiment)	59
2.8	Enzyme assays	60
2.8.1	Naphthalene carboxylase enzyme assays	60
2.8.2	Naphthoate-CoA ligase enzyme assay	60

3. RESULTS.....	62
Project 1	
Identification of naphthalene carboxylase subunits of N47.....	62
3.1 Native purification of naphthalene carboxylase of N47.....	62
3.1.1 Small scale purification using the 'ÄKTAmicro' system under strict anoxic conditions	62
3.1.2 Storage of N47 and NaphS2 cells	64
3.1.3 Cell lysis methods and naphthalene carboxylase activity	66
Cell membrane and naphthalene carboxylase activity	68
Naphthalene carboxylase in cell-free extract generated by a French Press	69
2-naphthoate CoA-ligase activity during the isotopic exchange reaction assay	72
3.2 Transcriptional analysis – Operon mapping by RT-PCR.....	73
3.2.1 RNA extraction and RT-PCR	73
3.2.2 Operon mapping	74
3.3 Blue native polyacrylamide gel electrophoresis.....	78
Blue native PAGE- Method development	78
3.3.1 Blue native polyacrylamide gel electrophoresis using N47 cells	79
i. Blue native PAGE band with a size of around 750 kDa	83
ii. Blue native PAGE band with a size of around 560 kDa	83
iii. Blue native PAGE band with a size of around 400 kDa	84
Extraction of native proteins from a BNP and subsequent separation on a SDS-PAGE	84
3.3.2 In-gel naphthalene carboxylase activity	86
3.3.3 Analysis of the 2-methylnaphthalene specific 220 kDa protein band	87
3.3.4 Blue native polyacrylamide gel electrophoresis using NaphS2 cell-free extracts	89
i. Blue native PAGE band with a size of around 750 kDa	90
ii. Blue native PAGE band with a size of around 400-450 kDa	91
3.4 In vitro protein interaction assays.....	92
3.4.1 Heterologous production and purification of N47_K27540	93
i. Production and purification of His-tagged N47_K27540	93
ii. Production and purification of GST-tagged N47_K27540	94
3.4.2 Pull-down assay	95
Project 2	
Characterization of <i>Cand. Treponema contaminophilus</i> sp. strain HM^T.....	100
3.5 Characterization of <i>Cand. Treponema contaminophilus</i> sp. strain HM^T.....	100
3.5.1 Morphology of <i>Cand. Treponema contaminophilus</i> sp. strain HM ^T cells	100
3.5.2 Physiology of strain HM ^T	101
i. Substrate utilization	101
ii. Temperature, pH and oxygen range of growth	103
3.5.3 Membrane	105
3.5.4 Motility of strain HM ^T	105
3.5.5 DNA G+C base content	106
3.5.6 16S rRNA gene sequence of <i>Cand. T. contaminophilus</i> sp. strain HM ^T	106
Project 3	
Raman microspectroscopy of N47.....	108
3.6 Raman microspectroscopy of N47.....	108
3.6.1 Preparation and analysis of N47 cells by stable isotope Raman	109

Stable isotope Raman microspectroscopy of N47	111
Flow cytometry using N47 cells	112
3.6.2 Scanning Electron Microscopy of N47	112
4. DISCUSSION.....	113
Project 1	
Identification of naphthalene carboxylase subunits of N47.....	113
4.1 Biochemistry of naphthalene carboxylase - Activity in cell-free extracts.....	113
4.1.1 Naphthalene carboxylase activity located in the pellet fraction	113
i. Is the naphthalene carboxylase encapsulated in microcompartments?	114
ii. Is the activity in the pellet fraction detectable due to intact cells?	114
4.1.2 Naphthalene carboxylase activity in cell-free extracts in presence of ATP	115
i. Is naphthalene carboxylase activity in cell-free extracts coupled to the direct esterification of 2-naphthoic acid?	115
ii. Naphthalene carboxylase- an additional ATP-dependent enzyme in anaerobic degradation of naphthalene by the sulfate reducer N47?	118
4.2 Molecular biological investigation on naphthalene carboxylase - Organization of the naphthalene carboxylase operon.....	121
4.3 Naphthalene carboxylase complex and its subunits.....	122
4.3.1 Potential regulation of the naphthalene carboxylase	124
i. Transcriptional regulation of the naphthalene carboxylase	124
ii. Post-translational regulation of naphthalene carboxylase	125
4.4 Interaction of naphthalene carboxylase with other proteins.....	125
i. 2-naphthoate-CoA ligase N47_I06840	125
ii. Interaction of naphthalene carboxylase with membrane proteins	126
iii. The FAD-binding protein N47_A07150	127
4.5 Complexes involved in anaerobic 2-methylnaphthalene degradation.....	127
4.6 Naphthalene carboxylase in NaphS2.....	129
4.7 UbiD-like (de)carboxylases involved in anaerobic degradation of aromatic compounds- A new class of enzymes with common properties?.....	130
4.7.1 UbiD in ubiquinone biosynthesis	131
i. UbiX- An isoenzyme of UbiD in ubiquinone biosynthesis?	132
ii. UbiX-like proteins in the anaerobic degradation of aromatic compounds	132
4.7.2 Comparison of naphthalene carboxylase with phenylphosphate carboxylase, the prototype of UbiD-like enzymes in anaerobic degradation of aromatic compounds	133
4.7.3 UbiD-like (de)carboxylases involved in anaerobic degradation of aromatic compounds	134
i. Benzene carboxylase	134
ii. Non-oxidative hydroxyarylic acid decarboxylases/ phenol carboxylases	135
iii. Terephthalate decarboxylase	136
iv. Aniline carboxylase	137
v. Carboxylases acting on higher molecular weight PAHs	138
4.7.4 Phylogenetic analysis of UbiD-like enzymes involved in the anaerobic degradation	138
4.8 Potential reaction mechanisms for naphthalene carboxylase.....	140

Project 2	
Characterization of <i>Cand. Treponema contaminophilus</i> sp. strain HM^T	141
4.9 Characterization of <i>Cand. Treponema contaminophilus</i> sp. strain HM^T	141
Project 3	
Cooperation project Raman microspectroscopy of N47.....	145
4.10 Raman microspectroscopy of N47.....	145
5. CONCLUSION AND OUTLOOK.....	147
6. LITERATURE.....	151
PUBLICATION AND AUTHORSHIP CLARIFICATION.....	172
ACKNOWLEDGEMENTS - DANKSAGUNG.....	174
LEBENS LAUF.....	175
APPENDIX.....	176

1. Introduction

Aromatic hydrocarbons are ubiquitous and persistent environmental pollutants. The biodegradation of these compounds is difficult due to their high chemical stability and low aqueous solubility. Therefore, aromatic hydrocarbons accumulate in the environment. They are found widespread in oxic and anoxic habitats such as aquifers, marine and terrestrial sediments, freshwater, and soil.

Aromatic hydrocarbon pollution in the environment is caused by human activities such as crude oil spillage, fossil fuel combustion, and gasoline leakage (Foght, 2008). Additionally, natural processes like combustion of wood or natural petroleum seepage lead to their discharge. Due to their carcinogenic potential and health risk, the anthropogenic release of aromatic hydrocarbons represents a serious danger for humans and the environment. Therefore, it is a matter of public interest to study microbial aromatic hydrocarbon degradation in detail to understand the biodegradation processes in order to develop bioremediation technologies. The knowledge about metabolic pathways and in particular the involved enzymes will be of use to improve the performance of naturally occurring organisms or even to engineer new artificial pathways in the future.

1.1 Aromatic hydrocarbons

Aromatic hydrocarbons are cyclic compounds exhibiting a characteristic aromatic ring with delocalized π -electrons. Following Hückel's rule these π -electrons lead to a low-energy molecule when its number equals $4n+2$ and the molecule is fully conjugated. The C-atoms of the aromatic rings are sp^2 -hybridized resulting in a planar structure of the rings. In addition, all aromatic compounds have in common a great stability due to resonance energy and inertness of C–H and C–C bonds (Boll et al., 2002).

Aromatic compounds are the second most abundant class of compounds found in nature (Boll et al., 2002). They are found in every organism, for instance in form of the three aromatic amino acids (phenylalanine, tryptophan, and tyrosine). The largest compound class is lignin, a structural aromatic polymer formed from phenylpropane units, in higher plants. Even though plants are the main producers of aromatic compounds, they lack pathways to degrade and recycle the carbon from these substances (Fuchs et al., 2011). Animals have only limited capacities concerning degradation of aromatic compounds, except for aromatic amino acids and a few others (e.g. pyrimidine) (Löffler et al., 2006). Thus, the degradation and mineralization of aromatic compounds is predominantly performed by aerobic and anaerobic bacteria and aerobic fungi (Fuchs et al., 2011).

Aromatic hydrocarbons consist exclusively of carbon and hydrogen. Monoaromatic hydrocarbons like benzene, toluene, ethylbenzene, and the three xylene isomers, summarized in the abbreviation BTEX compounds, contain just one aromatic ring. Polycyclic aromatic hydrocarbons (PAH), e.g. naphthalene, anthracene, phenanthrene, and benzo[a]pyrene have at least two fused aromatic rings sharing two neighboring carbon atoms (Fig. 1).

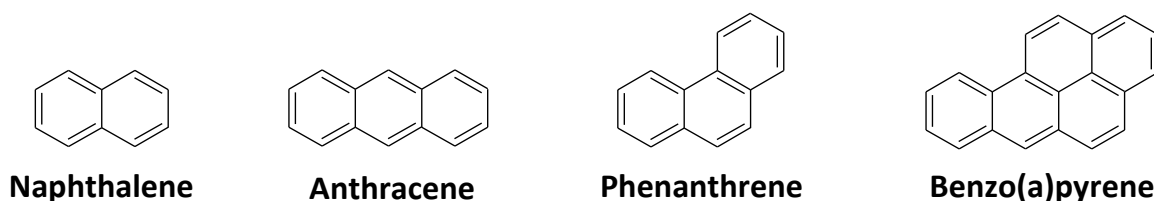


Figure 1: Chemical structure of selected polycyclic aromatic hydrocarbons. Further details are given in the text.

Naphthalene consists of two fused benzene rings and is the simplest polycyclic aromatic hydrocarbon. Moreover, it is an abundant component of coal tar and crude oil and is generated by combustion of wood and fossil fuels. Naphthalene is also produced in commercial quantities from either coal tar or petroleum (United States Environmental Protection Agency, 2003). Furthermore, there are some biological sources such as endophytic fungi (Daisy et al., 2002), *Magnolia* flowers (Azuma et al., 1996), special deer hair (Gassett et al., 1997), and termite nests (Chen et al., 1998).

Even though naphthalene is less toxic than higher molecular weight PAHs such as anthracene or benzo(a)pyrene, animal experiments revealed carcinogenic effects associated to naphthalene exposure (National Toxicology Program, 2000). Therefore, it was reclassified as a potential human carcinogen (Preuss et al., 2003). Exposure to large amounts of naphthalene was reported to cause damage of red blood cells (U.S. Department of Health & Human Services, 2005). Particularly, children consuming naphthalene-containing mothballs suffered from hemolytic anemia. Exposure of pregnant women to naphthalene resulted in neonatal hemolytic anemia in the newborn (Anziulewicz et al., 1959). It is likely that long-term exposure to naphthalene might lead to the development of cataracts even though a possible correlation with the presence of impurities in naphthalene samples could not be excluded (Koch et al., 1976; U.S. Department of Health & Human Services, 2005). However, animal testing supported the development of naphthalene-induced cataracts. Acute intoxication with naphthalene may result in headache, drowsiness, nausea, loss of appetite, and diarrhea (GESTIS-Stoffdatenbank).

Due to its solubility in water (3.1×10^{-2} g/L), naphthalene is often used as a model compound for studying the degradation of polycyclic aromatic hydrocarbons (PAHs).

1.2 Aromatic hydrocarbon contaminated sites

In the 20th century, mono- and polycyclic aromatic hydrocarbons originating from industrial coal gasification were released to the environment and led to the contamination of soil and aquifers (Johnsen et al., 2005). To date, field sites such as Düsseldorf-Flingern, Germany or the Stuttgart-Testfeld Süd, Germany demonstrate the persistence of anthropogenic hydrocarbon contamination (Zamfirescu and Grathwohl, 2001; Anneser et al., 2008).

Due to the high carbon load, oxygen was suggested to be depleted rapidly in hydrocarbon-contaminated aquifers while redox compartments along the contaminated anoxic plume were formed (Lovley, 1991; Christensen et al., 2000; Christensen et al., 2001). However, for the hydrocarbon-contaminated site Düsseldorf-Flingern, it was demonstrated that the degradation of the contaminants was enhanced at the plume fringes, where electron donors and electron-acceptors (in this particular case SO_4^{2-}) mix together (Anneser et al., 2008; Bauer et al., 2008; Bauer et al., 2009). These hot-spots of degradation were characterized as the 'plume fringe concept' (Bauer et al., 2008; Bauer et al., 2009).

Anaerobic degradation of monocyclic aromatic hydrocarbons such as BTEX compounds (benzene, toluene, ethylbenzene, and xylenes) by microbial communities was monitored in the mentioned field site (Griebler et al., 2004; Anneser et al., 2008; Winderl et al., 2008). Moreover, the polycyclic aromatic hydrocarbon naphthalene was also shown to be degraded within the anoxic zone (Griebler et al., 2004; Anneser et al., 2008).

During the Deepwater Horizon accident in 2010, around 4.6 million barrels of oil were released to the Gulf of Mexico (Griffiths, 2012). While human intervention combined with natural processes were capable of removing most of the oil, the fate of around 20% of the released oil remained unclear (Ramseur, 2010; Kimes et al., 2013). Later, it was shown that the remaining contamination persisted in the water column affecting deep-sea sediments (Passow et al., 2012; Schrope, 2013). Kimes et al. (2013) revealed that in deeper layers of the deep-sea sediment where the oxygen content is low, Deltaproteobacteria able to anaerobically degrade aromatic hydrocarbons were enriched. More recently, Mason et al. (2014) demonstrated by using growth experiments with ^{14}C -labeled substrates and metagenomic analyses that bacteria in the oxic sediment surface of the Gulf of Mexico were not able to degrade PAHs which as a consequence accumulated in the sediment. Subsequently, exposure to these hydrocarbons in the deeper sediment led to the change in

the microbial population and anaerobic bacteria possibly able to degrade recalcitrant PAHs are enriched (Kimes et al., 2013).

1.2.1 Spirochaetes in hydrocarbon-contaminated sites

Spirochetes are ubiquitous in the environment and were isolated from fresh water (Zuelzer, 1912; Veldkamp, 1960) as well as from marine habitats (Hespell and Canale-Parola, 1970; Harwood and Canale-Parola, 1983). Moreover, some species were adapted to extreme habitats such as deep-sea sediments (Harwood et al., 1982; Imachi et al., 2008), high salinity (around 1.4 M sodium chloride) (Greenberg and Canale-Parola, 1976; Magot et al., 1997; Reddy et al., 2013), high alkalinity (up to pH 10) (Zhilina et al., 1996; Pikuta et al., 2009; Reddy et al., 2013) or high temperature (up to 73 °C) (Aksenova et al., 1992; Pohlschroeder et al., 1994). Species of the family *Spirochaetaceae* are free-living or host-associated and some are known to be pathogenic to human and animal. Human pathogens can be found in the genus *Borrelia* and *Treponema* causing Lyme disease (*B. burgdorferi* and related species) or syphilis (*T. pallidum*).

Spirochetes were described as Gram-negative, helical-shaped or wave-curved bacteria, with a typical ultrastructural cell organization (Canale-Parola, 1984). In contrast to other bacteria, the periplasmic flagella, which are required for motility, are localized within the periplasmic space (Paster and Canale-Parola, 1980; Li et al., 2000; Charon and Goldstein, 2002). For the pathogenic spirochetes, the periplasmic flagella were shown to be essential for invasion and infection of the host tissue. Indeed, when the motility genes were deleted, their pathogenicity was attenuated (Rosey et al., 1996; Lux et al., 2001; Lambert et al., 2012; Guyard et al., 2013).

For a long time, helical morphology and motility represented one of the fundamental characteristics of the phylum *Spirochaetes* (Paster and Canale-Parola, 1980; Paster and Dewhirst, 2000). However, recently three coccoidal and non-motile isolates belonging to the new genus *Sphaerochaeta* were described (Dröge et al., 2006; Ritalahti et al., 2012). Their genomes lacked genes for motility whereas genes involved in carbohydrate transport and metabolism were increased compared to other available spirochetal genomes (Abt et al., 2012; Caro-Quintero et al., 2012). The high proportion of carbohydrate metabolism genes was not directly linked to the unusual morphology but rather indicated a fermentative lifestyle (Caro-Quintero et al., 2012). Solely *Sphaerochaeta smaragdinae*, which was isolated from an oil field, showed a similar high number of genes involved in carbohydrate metabolism (Magot et al., 1997; Abt et al., 2012).

Sphaerochaeta globosa Buddy^T and *Sphaerochaeta pleomorpha* Grapes^T were isolated from a reductively dechlorinating consortium (Ritalahti et al., 2012). It was hypothesized that

members of the genus *Sphaerochaeta* interact with species of the genus *Dehalococcoides* (Caro-Quintero et al., 2012). Bacteria of the genus *Dehalococcoides* are reported to transform a variety of chloro-organic compounds such as tetrachloroethene (PCE) and trichloroethene (TCE) via reductive dechlorination (Ritalahti and Löffler, 2004; He et al., 2005; Duhamel and Edwards, 2006; Taş et al., 2010). However, the type of interaction remains to be elucidated.

A so far uncharacterized spirochete strain is a stable member of the naphthalene-degrading culture N47 (see Introduction 1.4) (Selesi et al., 2010). Interestingly, the strain shared high similarity to 16S rRNA gene sequences of uncultured members of the family *Spirochaetaceae* that co-occur with bacteria which anaerobically degrade (poly)-aromatic hydrocarbons and (poly-)chlorinated aromatics and ethenes in contaminated environments.

1.3 Anaerobic degradation of non-substituted polycyclic aromatic hydrocarbons

The aerobic degradation of aromatic compounds is well understood and studied in detail (for PAHs: (Cerniglia, 1993; Habe and Omori, 2003; Karlsson et al., 2003)), whereas first insights into the anaerobic degradation were gained in the last three decades. The anaerobic degradation of mono-aromatic hydrocarbons revealed so far unknown and surprising biochemical reaction mechanisms (Sawers and Watson, 1998; Beller and Spormann, 1999; Selmer and Andrei, 2001). However, to date most of the pathways for anaerobic degradation of PAHs are proposed based on metabolite analyses and only some key enzyme reactions such as the naphthalene carboxylase and three reductases, the 2-naphthoyl-CoA reductase, the DHNCoA reductase, and the THNCoA reductase, could be elucidated due to the slow growth and the little biomass obtained from the model organisms (Zhang and Young, 1997; Meckenstock et al., 2000; Annweiler et al., 2002; Mouttaki et al., 2012; Eberlein et al., 2013b; Eberlein et al., 2013a; Estelmann et al., 2015).

1.3.1 Anaerobic degradation of benzene

Bacteria which are able to aerobically degrade benzene have been known for around 100 years (Söhngen, 1913; Vogt et al., 2011), whereas anaerobic degradation was first reported about 30 years ago. However, the underlying biochemical pathways and especially the initial reaction of benzene degradation still remain elusive.

In the literature, sulfate- (Lovley et al., 1995; Phelps et al., 1996; Ulrich and Edwards, 2003; Vogt et al., 2007; Mancini et al., 2008; Musat and Widdel, 2008; Abu Laban et al., 2009;

Berlendis et al., 2010), nitrate- (Major et al., 1988; Nales et al., 1998; Burland and Edwards, 1999; Luo et al., 2014), iron- (Kazumi et al., 1997; Villatoro-Monzón et al., 2003; Jahn et al., 2005; Botton and Parson, 2006; Kunapuli et al., 2007b), and manganese(IV)-dependent (Villatoro-Monzón et al., 2003; Villatoro-Monzón et al., 2008) benzene mineralization has been described. Initially, benzene degradation was observed under methanogenic conditions in microcosm experiments (Wilson et al., 1986; Grbić-Galić and Vogel, 1987).

In 1987, Grbić-Galić and Vogel demonstrated the mineralization of ^{14}C -labeled benzene in the absence of molecular oxygen. However, only around 6% of the labeled benzene was converted to $^{14}\text{CO}_2$. Later, complete mineralization of benzene to equal proportions of methane and carbon dioxide was shown (Weiner and Lovley, 1998). In this study, addition of potential extracellular intermediates of anaerobic benzene degradation such as phenol, acetate, and propionate inhibited growth of the culture. Therefore, the authors hypothesized these compounds as likely intermediates of anaerobic benzene degradation. Moreover, they suggested that for anaerobic degradation of benzene under methanogenic conditions a microbial consortium was required. At the current state of knowledge, it is assumed that syntrophic interactions between fermenting microorganisms, aceticlastic methanogens and hydrogenotrophic methanogens exist in all benzene-degrading cultures under methanogenic conditions (Vogt et al., 2011). In such a syntrophic consortium the methanogens most likely consume the hydrogen, acetate and/or other potential substrates released by the fermenting organism. This sequential degradation of benzene under methanogenic conditions was supported by the fact that methanogens have not been described to degrade aromatic hydrocarbons (Evans and Fuchs, 1988; Sakai et al., 2009).

In addition, syntrophic interactions within benzene-degrading cultures grown under sulfate-reducing, iron-reducing, and nitrate-reducing conditions were often discussed (Botton et al., 2007; Kunapuli et al., 2007a; Musat and Widdel, 2008; Luo et al., 2014). The hypothesis of a syntrophic degradation of benzene was supported by long lag-phases of most of the cultures and the presence of multiple species, which could so far not be separated. Furthermore, protein-SIP (protein-based stable isotope probing) experiments analyzing carbon fluxes using labeled benzene or ^{13}C -labeled carbonate revealed multiple microbial functional groups within a sulfate-reducing benzene-degrading culture (Taubert et al., 2012). Microorganisms, which showed incorporation of ^{13}C , were affiliated to Clostridiales, Deltaproteobacteria and Bacteroidetes/Chlorobi. The Clostridiales-related key organisms (group I) were involved in benzene degradation and used high amounts of carbonate as a carbon source. The identified Deltaproteobacteria (group II) were suggested to degrade the fermentation products of group I and the Bacteroidetes/Chlorobi (group III) most likely lived on dead cells. Organisms of group I/II putatively were sulfate reducers as proteins produced in both groups

were related to dissimilatory sulfate reduction. This study nicely demonstrated the close interaction of different organisms within a benzene-degrading consortium.

However, only few benzene-degrading pure cultures have been described. Two *Dechloromonas* strains (strain RCB and JJ) were successfully isolated from lake sediments degrading benzene under nitrate-reducing conditions (Coates et al., 2001). Additionally, two denitrifying *Azoarcus* strains (strain DN11 and AN9) identified by SIP experiments were isolated from gasoline-contaminated groundwater (Kasai et al., 2006) and a chlorate-reducing strain (strain BC) was isolated from a benzene-degrading enrichment culture (Weelink et al., 2008). It should be noted that in the last step of chlorate-reduction the chlorite dismutase converts chlorite to oxygen and chloride. Therefore, the authors suggested that in strain BC benzene was attacked by oxygenases using the oxygen formed by the chlorite dismutase (Weelink et al., 2008). In conclusion, benzene was proposed to be metabolized via the catechol pathway.

Even though *Dechloromonas aromatica* strain RCB is able to degrade benzene, its genome lacks key enzymes such as the benzylsuccinate synthase genes (*bssABC*) and the benzoyl-CoA pathway which are known to be involved in anaerobic degradation of aromatic compounds (Salinero et al., 2009). Therefore, the enzymes responsible for the so far unknown degradation pathways remain to be identified. Recently, Ettwig et al. (2010) showed formation of oxygen linked to denitrification within a methane-degrading culture. The responsible enzyme is still unknown but a similar reaction involved in benzene degradation could be possible for *Dechloromonas aromatica* strain RCB (Weelink et al., 2010; Meckenstock and Mouttaki, 2011; Vogt et al., 2011). Therefore, an oxygen-dependent benzene metabolism cannot be ruled out for nitrate-reducing bacteria.

Under strict anoxic conditions, the pure benzene-degrading Euryarchaeon *Ferroglobus placidus* was described (Holmes et al., 2011). Recently, *Geobacter metallireducens* and *Geobacter* strain Ben were reported to degrade benzene under iron-reducing conditions (Zhang et al., 2012b).

Mechanisms to activate benzene

Due to the π -electron system of the aromatic ring and the lack of substituents, benzene is a very stable molecule. The anaerobic activation mechanism of benzene is still under debate. Based on metabolite analyses and proteogenomic studies, three potential activation mechanisms of benzene such as methylation to toluene (Coates et al., 2002; Ulrich et al., 2005), direct carboxylation to benzoate (Caldwell and Sufliata, 2000; Kunapuli et al., 2008; Abu Laban et al., 2009; Abu Laban et al., 2010; Holmes et al., 2011; Luo et al., 2014) and hydroxylation to phenol (Vogel and Grbić-Galić, 1986; Grbić-Galić and Vogel, 1987; Caldwell and Sufliata, 2000; Chakraborty and Coates, 2005; Zhang et al., 2013, 2014) have been

proposed (Fig. 2).

In metabolite analyses, Ulrich et al. (2005) detected ^{13}C -labeled toluene in culture supernatants of a methanogenic and a denitrifying culture growing with ^{13}C -labeled benzene. The detection of the potential metabolite led to the hypothesis that the initial step in anaerobic degradation of benzene proceeded via methylation to toluene. Subsequently, the methyl group of toluene should be added to the double bond of fumarate, which is catalyzed by the benzylsuccinate synthase (Bss) (Biegert et al., 1996; Leuthner et al., 1998; Leutwein and Heider, 1999). The formed benzylsuccinate would then be converted via β -oxidation reactions to the central intermediate benzoyl-CoA (Leuthner and Heider, 1999; Leutwein and Heider, 1999). Additionally, Ulrich et al. (2005) detected benzoate, whereas other metabolites such as benzylsuccinate or known β -oxidation products of benzylsuccinate degradation could not be detected in the culture supernatants.

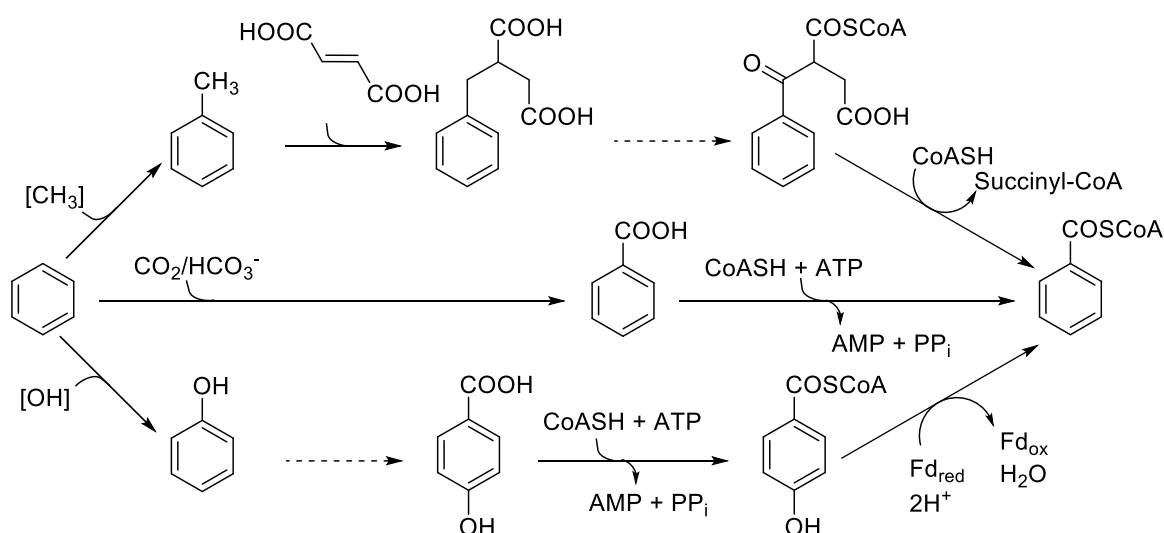


Figure 2: Proposed activation reactions in anaerobic benzene degradation. Methylation of benzene to toluene and further degradation through the toluene pathway. Direct carboxylation of benzene to benzoate. Hydroxylation of benzene to phenol and further degradation through the phenol pathway. Further explanations are given in the text. The degradation of phenol is intensively discussed in the introduction section 1.5.

Due to the very high dissociation energy of the C-H bond (473 kJ/mol) (Thauer and Shima, 2008), a direct carboxylation of benzene is chemically difficult. Biochemical data demonstrating the carboxylation of benzene are still pending. However, new hints came from genomic studies. The anaerobic degradation of benzene was studied in the iron-reducing enrichment culture BF, the Euryarchaeon *Ferroglobus placidus* (Holmes et al., 2011) and recently in the metagenome of a benzene degrading, nitrate-reducing enrichment culture

(Luo et al., 2014). Abu Laban et al. (2010) identified a benzene-induced protein (putative anaerobic benzene carboxylase, AbcA) on SDS-PAGE which shared 43% sequence identity with the phenylphosphate carboxylase subunit PpcA of *A. aromaticum* strain EbN1. Therefore, the enzyme AbcA was proposed to be involved in the carboxylation of benzene. The putative benzene carboxylase gene *abcA* was part of a gene cluster encoding a phenylphosphate carboxylase γ -subunit-like gene *abcD*, the already mentioned carboxylase-like gene *abcA*, a putative benzoyl-CoA ligase gene (*bzIA*), and an UbiX-like gene. Luo et al. (2014) verified a similar gene organization within the genome of a benzene-degrading nitrate-reducing enrichment culture. However, in the genome of *F. placidus* reported as well to degrade benzene, only a *abcA* homolog was identified (Holmes et al., 2011).

In the first studies on anaerobic benzene degradation, addition of ^{18}O -labelled water to the medium led to the formation of ^{18}O -labelled phenol (Vogel and Grbic-Galic, 1986). Therefore, hydroxylation of benzene to phenol was suggested in which the hydroxyl group originated from water. Phenol was often observed as a potential metabolite of anaerobic benzene degradation (Weiner and Lovley, 1998; Caldwell and Suflita, 2000; Chakraborty and Coates, 2005; Kunapuli et al., 2008; Abu Laban et al., 2009). However, different studies indicated rather an abiotic formation of phenol from benzene by contact with air during sampling of culture media from an iron- or from a sulfate-reducing culture (Kunapuli et al., 2008; Abu Laban et al., 2009).

Recently, hydroxylation of benzene to phenol was reported for *Geobacter metallireducens* (Fig. 2) (Zhang et al., 2013). The authors showed that phenol was a potential intermediate in benzene degradation and the deletion of key enzymes (PpsA, PpcB, PpcC) of the phenol degradation pathway resulted in the inability of *G. metallireducens* to grow with benzene. Later, microarray analysis identified 11 up-regulated genes in benzene-grown *G. metallireducens* cells, among them six genes were excluded as their function was connected to other processes (Zhang et al., 2014). For the other five genes, deletion strains were constructed to investigate their impact on benzene degradation. A protein of unknown function and a zinc-containing oxidoreductase were identified and proposed as potential enzymes catalyzing the hydroxylation of benzene. As co-localization for genes encoding these two proteins could only be seen in the genome of *G. metallireducens*, it can be suggested that the mechanism for hydroxylation of benzene is unique to *G. metallireducens*.

1.3.2 Anaerobic degradation of naphthalene

In 1988, Mihelcic et al. first reported microbial degradation of naphthalene as well as for naphthol and acenaphthene under denitrifying conditions in soil-water systems (Mihelcic and Luthy, 1988). Some years later, mineralization of naphthalene under sulfate-reducing conditions (Thierrin et al., 1993; Coates et al., 1996), iron-reducing conditions (Lovley et al., 1994) and methanogenesis (Chang et al., 2006) was confirmed. A few PAH-degrading strains are available in pure cultures e.g. the sulfate-reducing strain NaphS3 enriched from a Mediterranean lagoon (Musat et al., 2009), NaphS2 isolated from a fluidized bed reactor, seeded with PAH-contaminated marine sediment (Galushko et al., 1999), and the two nitrate-reducing strains NAP-3-1, NAP-3-2, and NAP-4 (Rockne et al., 2000). Upon request, the nitrate-reducing and naphthalene-degrading strains NAP-3-1, NAP-3-2, and NAP-4 have been lost during the cultivation and are no longer available.

Mechanisms to activate naphthalene

To date, different hypotheses about the initial activation of the non-substituted polycyclic aromatic compound naphthalene were stated (Fig. 3). In particular, carboxylation (Zhang and Young, 1997; Meckenstock et al., 2000; Musat et al., 2009) and methylation (Safinowski and Meckenstock, 2006) have been discussed as likely reaction mechanisms to activate the ring system in position 2.

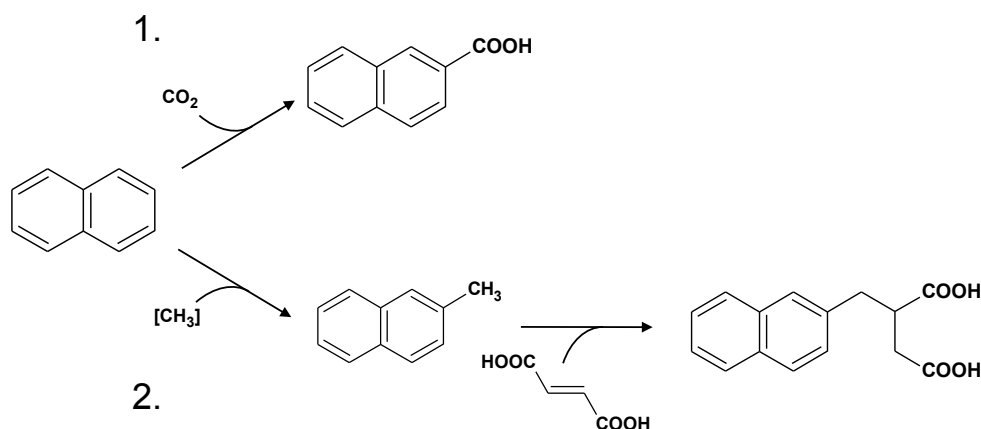


Figure 3: Two proposed initial activation reactions in anaerobic naphthalene degradation. (1) Direct carboxylation to 2-naphthoic acid. (2) Methylation to 2-methylnaphthalene and a further degradation through the 2-methylnaphthalene pathway. Further explanations are given in the text.

Bedessem et al. (1997) analyzed the mineralization of [1-¹⁴C]naphthalene to CO₂ in sulfate-rich, coal tar-contaminated aquifers. Using GC/MS analysis, formation of naphthol was observed and the authors suggested naphthol as potential metabolic intermediate. However,

hydroxylation of naphthalene to naphthol (aka naphthalenol) as activation reaction is unlikely because N47 (Meckenstock et al., 2000) as well as NaphS2 and NaphS3 (Musat et al., 2009) seemed not to be able to grow with 1- or 2-naphthol and those two metabolites could not be detected in supernatant of naphthalene-grown cells (Meckenstock et al., 2000).

Studies on anaerobic degradation of naphthalene by a sulfate-reducing culture revealed 2-naphthoic acid as potential intermediate (Zhang and Young, 1997). Furthermore, incorporation of [^{13}C]bicarbonate into the carboxyl group of 2-naphthoic acid indicated a direct carboxylation of naphthalene (Zhang and Young, 1997; Meckenstock et al., 2000). The carbon atom in position 2 is the most electronegative of all the carbons. Therefore, an electrophilic aromatic substitution reaction mechanism to yield 2-naphthoic acid could be more likely than in the 1 position (Fig. 4). Alternatively, a reaction mechanism involving a radical intermediate might be possible.

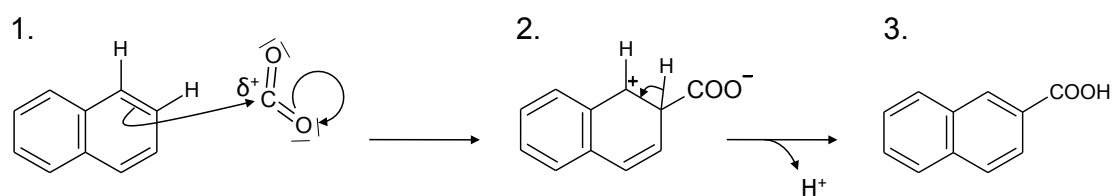


Figure 4: Putative initial activation reaction by direct carboxylation in anaerobic degradation of naphthalene. The reaction mechanism is based on an electrophilic aromatic substitution reaction. The electrophile, carbon dioxide, is attacked by the electrons of the aromatic ring system (1) resulting in a carbocation (2). This carbocation is unstable, owing both to the positive charge on the molecule and to the temporary loss of aromaticity. Finally, a proton leaves the intermediate and the end product, 2-naphthoic acid, is formed (3).

During growth of N47 with naphthalene, metabolites specific for anaerobic 2-methylnaphthalene degradation e.g. naphthyl-2-methyl-succinate and naphthyl-2-methylene-succinate were identified in culture supernatant (Safinowski and Meckenstock, 2006). In anaerobic degradation of 2-methylnaphthalene, the initial reaction is an addition reaction of 2-methylnaphthalene to the double bond of fumarate to yield the first intermediate naphthyl-2-methylene-succinate (Annweiler et al., 2000; Safinowski and Meckenstock, 2004). The reaction is catalyzed by naphthyl-2-methyl-succinate synthase (Nms), a glyceryl radical enzyme analogous to benzylsuccinate synthase (Bss) involved in anaerobic degradation of toluene (Biegert et al., 1996; Leuthner and Heider, 1999).

In 2009, Musat et al. quantified metabolites in NaphS2, NaphS3 as well as in NaphS6. As expected, 2-naphthylmethyl-succinate was the most abundant metabolite in 2-methylnaphthalene-grown cells. It was 20-fold higher than 2-naphthoic acid. The other way around, in naphthalene-grown cells the amount of 2-naphthoic acid was 100-fold higher than that of 2-naphthylmethyl-succinate. As impurity of naphthalene by 2-methylnaphthalene could be excluded, some authors suggested the production of 2-naphthylmethyl-succinate from 2-naphthoyl-CoA and the ubiquitous metabolite succinyl-CoA as a potential side reaction in anaerobic degradation of naphthalene (Musat et al., 2009; Meckenstock and Mouttaki, 2011).

Safinowski and Meckenstock (2006) detected the activities of several enzyme reactions involved in the anaerobic 2-methylnaphthalene degradation in naphthalene-grown N47 cells. The activities of naphthyl-2-methyl-succinate synthase, naphthyl-2-methyl-succinyl-CoA transferase, and naphthyl-2-methenyl-succinyl-CoA dehydrogenase measured in naphthalene-grown cells were comparable to those ones determined in 2-methylnaphthalene-grown cells. As a consequence, a methylation reaction was suggested as the initial step in the anaerobic degradation of naphthalene. Based on a proteomic approach, this result could be verified because under both growth conditions, with naphthalene and 2-methylnaphthalene as substrates, all enzymes involved in 2-methylnaphthalene degradation were produced (Bergmann et al., 2011b). In contrast, SDS-PAGE performed with NaphS2 (NaphS3 and NaphS6) showed strong induction of naphthyl-2-methyl-succinate synthase (Nms) in 2-methylnaphthalene-grown cells, which is absent when naphthalene or benzoate served as substrate (Musat et al., 2009). Thus, carboxylation was suggested as initial reaction in NaphS2, NaphS3 and NaphS6.

Proteogenomic studies on N47

In 2011, the genome of N47 was sequenced and annotated (Bergmann et al., 2011a). It was estimated that approximately 98% of the total genome sequence was covered with the 17 contigs. In a proteogenomic approach, Bergmann et al. (2011b) analyzed the differential production profiles of N47 growing with different substrates to identify proteins which might be involved in the anaerobic degradation of naphthalene. In this study, they identified a UbiD-like subunit which was differentially produced in naphthalene-grown N47 cells, sharing 45% sequence identity with the alpha subunit of phenylphosphate carboxylase of *Aromatoleum aromaticum* EbN1 and 48% with the alpha subunit of the putative anaerobic benzene carboxylase of the benzene-degrading iron-reducing culture BF (AbcA) (Abu Laban et al., 2010). Among others, this carboxylase-like subunit (N47_K27540) was differentially abundant when cells were grown on naphthalene compared to 2-methylnaphthalene. This

fact allowed the identification of a gene cluster containing a few genes which products were suggested to be carboxylase-like subunits, potentially involved in the activation of naphthalene (Fig. 5).

Furthermore, a comparable gene cluster was identified in the recently sequenced Deltaproteobacterium NaphS2 (Fig. 5) with genes sharing up to 84% sequence identity with N47 (DiDonato et al., 2010). Interestingly, these two strains are related only distantly on the 16S rRNA gene level (Selesi et al., 2010).

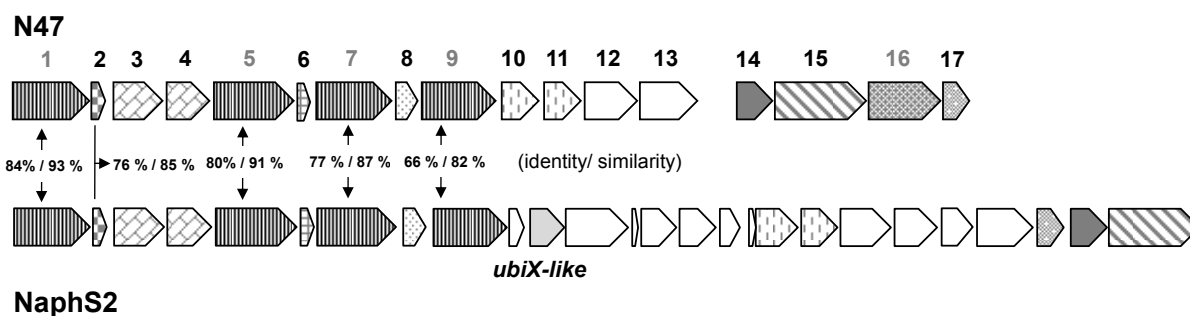


Figure 5: Organization of the gene cluster encoding enzymes potentially involved in the initial carboxylation reaction of naphthalene degradation in the sulfate-reducing Deltaproteobacteria N47 (GI:308273914 to GI:308273898) and NaphS2 (GI:300443517 to GI:300443519). Open reading frames are represented by arrows. Black-striped arrows represent *ubiD*-like genes. *UbiX*-like genes are indicated by light grey. ORFs which products share high homology between the strains have the same filling. Annotated function of the gene products: 1, putative phenylphosphate carboxylase, alpha subunit; 2, putative phenylphosphate carboxylase, gamma subunit; 3, MRP, Fer4_NifH superfamily; 4, ParA/MinD ATPase like, MRP, Fer4_NifH superfamily; 5, UbiD family decarboxylase; 6, conserved hypothetical protein; 7, UbiD family decarboxylase; 8, conserved hypothetical protein; 9, UbiD family decarboxylase; 10 & 11, HAD hydrolase; 12, membrane protein involved in aromatic hydrocarbon degradation; 13, IS4 transposase; 14, succinate dehydrogenase and fumarate reductase iron-sulfur protein; 15, putative succinate dehydrogenase flavoprotein subunit; 16, UbiD family decarboxylase; 17, pyridoxamine 5'-phosphate oxidase family protein.

Recently, Mouttaki et al. (2012) provided biochemical evidence for the carboxylation reaction of naphthalene to 2-naphthoic acid in crude extracts of N47.

Further degradation of the metabolite 2-naphthoic acid

The produced 2-naphthoic acid is subsequently activated to 2-naphthoyl-CoA by an ATP-dependent ligase. The central intermediate 2-naphthoyl-CoA is the substrate for the first ATP-independent reductase (Fig. 6). Initial investigations on the native 2-naphthoyl-CoA reductase of N47 indicated a four-electron reduction of 2-naphthoyl-CoA to 5,6,7,8-tetrahydro-2-naphthoyl-CoA (THNCoA) (Eberlein et al., 2013b). The enzyme was purified and the identified subunit N47_G38220 formed a homodimer (α_2) of around 150 kDa in its native conformation. This enzyme showed sequence similarity to members of the flavin-containing old-yellow enzyme family (Eberlein et al., 2013b). This new prototype of reductases has been classified as a class III arylcarboxyl-CoA reductases and was oxygen-resistant. The cofactors are FAD, FMN and an iron sulfur-cluster.

However, very recently Estelmann et al. (2015) demonstrated that actually two consecutive enzymes are involved in the conversion of 2-naphthoyl-CoA to 5,6,7,8-tetrahydro-2-naphthoyl-CoA and catalyze two-electron reduction steps. The first enzyme, 2-naphthoyl-CoA reductase N47_G38220 (NCR), catalyzes the reduction of 2-naphthoyl-CoA to 5,6-dihydro-2-naphthoyl-CoA whereas the second enzyme, 5,6-dihydro-2-naphthoyl-CoA reductase N47_G38210 (5,6-DHNCR), reduces 5,6-dihydro-2-naphthoyl-CoA to 5,6,7,8-tetrahydro-2-naphthoyl-CoA. Interestingly, the 5,6-DHNCR activity was 20-times higher than the one for the 2-naphthoyl-CoA reduction. Moreover, 2-naphthoyl-CoA reductase showed high 2-naphthoyl-CoA-forming dihydro-2-naphthoyl-CoA oxidase activity which was suggested to represent the ability of N47 to detoxify small amounts of oxygen (Estelmann et al., 2015).

In the genome of NaphS2, two genes encoding putative 2-naphthoyl-CoA reductase were identified. The NADH oxidase-like proteins NPH_1753 and NPH_5475 shared a sequence identity of 67% and 65% respectively with the 2-naphthoyl-CoA reductase N47_G38220. Furthermore, NPH_5475 was shown to be differentially abundant in cells grown with naphthalene compared to benzoate and therefore suggested to be involved in reduction of 2-naphthoyl-CoA (DiDonato et al., 2010). Estelmann et al. (2015) biochemically proved that NPH_1753 and NPH_5475 both are NCRs whereas NPH_5476 showed 5,6-DHNCR activity. All five characterized enzymes represent members of the flavin-containing old-yellow enzyme family.

In a second reductive dearomatization step, 5,6,7,8-tetrahydro-2-naphthoyl-CoA (THNCoA) is converted to hexahydro-2-naphthoyl-CoA (HHNCoA) (Eberlein et al., 2013a). The reaction is extremely sensitive to oxygen. Surprisingly, THNCoA reductase is ATP-dependent and showed characteristics of class I dearomatizing benzoyl-CoA reductases which catalyze the reduction of benzoyl-CoA by a two-electron step to form cyclohexa-1,5-diene-1-carboxyl-CoA

(1,5-dienoyl-CoA) (Boll and Fuchs, 1995; Eberlein et al., 2013a). With the exception of the hyperthermophilic archaeon *Ferroglobus placidus* (Holmes et al., 2012), class I dearomatizing benzoyl-CoA reductases are usually encoded within the genome of facultative anaerobes (Boll and Fuchs, 1995). In contrast, strict anaerobic bacteria show ATP-independent class II dearomatizing benzoyl-CoA reductases (Kung et al., 2009; Löffler et al., 2011). Genes sharing high sequence similarities to class I dearomatizing benzoyl-CoA reductase genes from *Azoarcus* species (*bzdNOPQ*) were identified within the genome of N47 (N47_E41460-E41490) (Selesi et al., 2010; Bergmann et al., 2011b) and NaphS2 (NPH_5888-NPH_5891) (DiDonato et al., 2010).

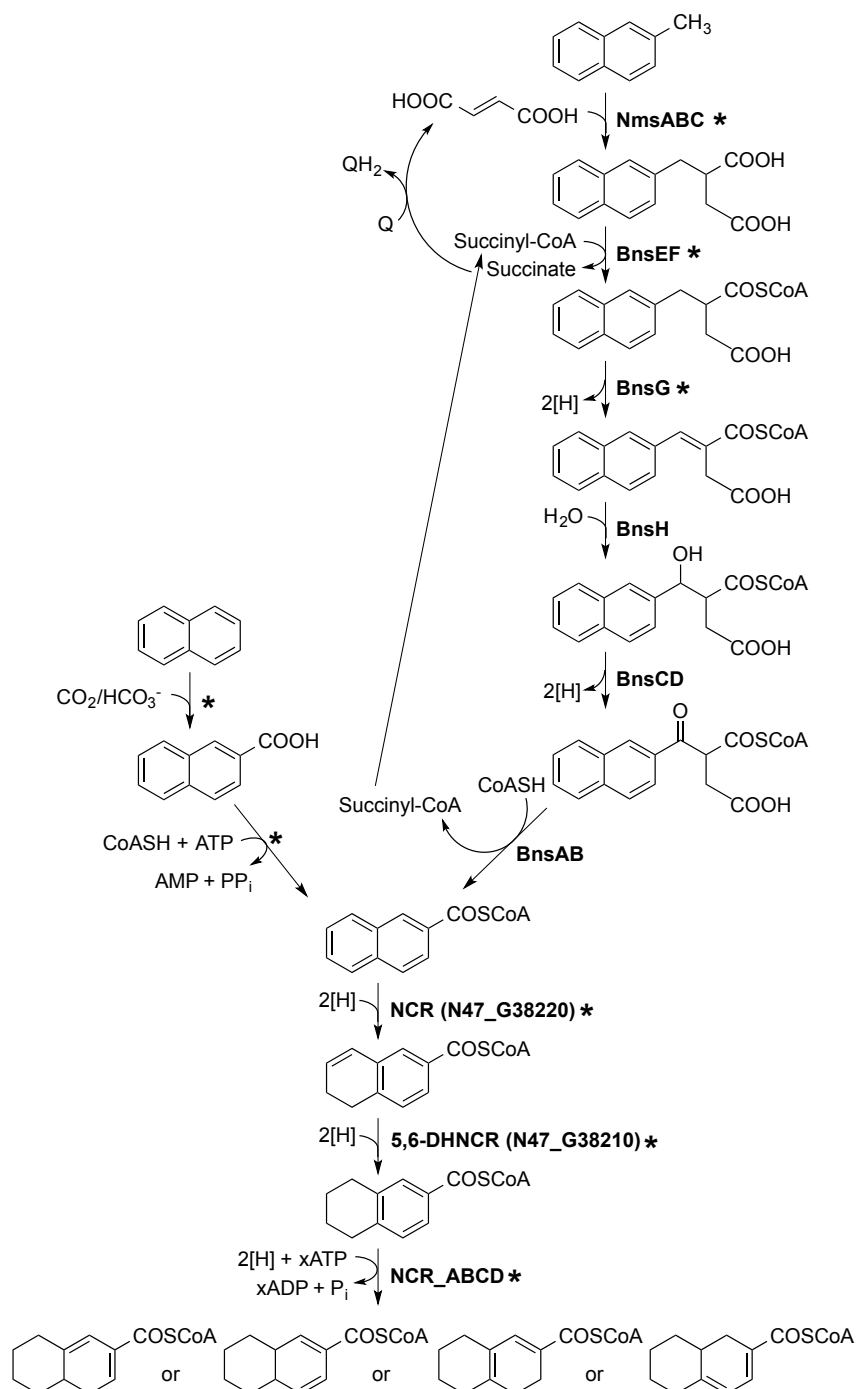


Figure 6: Proposed pathways for anaerobic naphthalene and 2-methylnaphthalene degradation in the enrichment culture N47. Naphthoyl-CoA represents the central metabolite. NmsABC, naphthyl-2-methyl-succinate synthase; BnsEF, naphthyl-2-methyl-succinate CoA transferase; BnsG, naphthyl-2-methyl-succinyl-CoA dehydrogenase; BnsH, naphthyl-2-methylene-succinyl-CoA hydratase; BnsCD, naphthyl-2-hydroxymethyl-succinyl-CoA dehydrogenase; BnsAB, naphthyl-2-oxomethyl-succinyl-CoA thiolase; NCR N47_G38220, 2-naphthoyl-CoA reductase; 5,6-DHNCR N47_G38210, 5,6-dihydro-2-naphthoyl-CoA reductase; NcrABCD, 5,6,7,8-tetrahydro-2-naphthoyl-CoA (THNCoA) reductase. Reactions which have been identified and the activity measured in N47 cells grown with naphthalene or methylnaphthalene, respectively are marked with asterisks (modified from Eberlein et al. (2013a)).

1.3.3 Anaerobic degradation of other polycyclic aromatic hydrocarbons- Anthracene, Phenanthrene, Biphenyl

Higher molecular weight PAHs such as anthracene and phenanthrene were shown to be degraded by anaerobic microbial consortia. However, reports about microbial anthracene-degradation are rare. Zhang et al. (2012a) identified anthracene degraders in microcosms under methanogenic conditions via DNA-based stable isotope probing (SIP). In this study, they found three different proteobacteria which were putatively involved in the degradation process. The anthracene degraders were classified within the genera *Methylibium*, *Legionella*, and some unclassified *Rhizobiales*. Moreover, degradation of anthracene in mixture with phenanthrene was observed by a sulfate-reducing enrichment culture (Selesi and Meckenstock, 2009).

Phenanthrene-degrading bacteria were isolated under sulfate-reducing (Coates et al., 1996; Coates et al., 1997; Zhang and Young, 1997; Davidova et al., 2007; Selesi and Meckenstock, 2009), nitrate-reducing (Rockne and Strand, 2001; Ambrosoli et al., 2005), and methanogenic conditions (Chang et al., 2006; Maillacheruvu and Pathan, 2009). In addition to naphthalene and benzene, the non-substituted three-ringed PAH phenanthrene was proposed to be activated via carboxylation (Zhang and Young, 1997; Davidova et al., 2007). To date, the anaerobic degradation pathway of phenanthrene is unknown and no enzymes have been identified. The extremely slow growth (around 33 weeks (Davidova et al., 2007)) and the absence of a highly enriched or pure culture represent problems in studying the enzymes which are involved in the anaerobic phenanthrene metabolism. Nevertheless, Davidova et al. (2007) demonstrated that two Deltaproteobacteria, Phe4A (Gene bank accession no. EF467179) and Phe4C (Gene bank accession no. EF467180), were the key players within a sulfate-reducing phenanthrene-degrading enrichment culture.

A biphenyl-degrading enrichment culture grown under strict anoxic conditions was characterized by Selesi and Meckenstock (2009). The key players within the enrichment culture BiphS1 were affiliated to the Gram-positive genus *Desulfotomaculum*. Furthermore, metabolite analyses revealed biphenyl-4-carboxylic acid as an intermediate in biphenyl degradation supporting the hypothesis that also anaerobic biphenyl degradation is potentially initiated by a direct carboxylation. So far, no biochemical evidence supporting the direct carboxylation of biphenyl is available. As already seen with the phenanthrene-degrading cultures, BiphS1 showed very slow growth and oxidized biphenyl completely to CO₂ in about 29 weeks (Selesi and Meckenstock, 2009).

Additionally, biphenyl degradation was reported under methanogenic (Bauer et al., 2008; Bauer et al., 2009), nitrate-reducing (Rockne and Strand, 1998, 2001; Ambrosoli et al., 2005), and sulfate-reducing conditions (Rockne and Strand, 1998; Yang et al., 2008).

1.4 The enrichment culture N47

The highly enriched sulfate-reducing culture N47 was isolated from soil material of a contaminated aquifer from a former coal gasification site near Stuttgart, Germany, with naphthalene as sole carbon and energy source (Meckenstock et al., 2000). The culture is able to use naphthalene and 2-methylnaphthalene as growth substrate under strict anoxic, sulfate-reducing conditions at 30 °C. In T-RFLP analyses and sequencing of the 16S rRNA genes (Fig. 7), it was shown that N47 basically consists of two major organisms: a Deltaproteobacterium (513-bp T-RF) and a spirochete (208/212-bp T-RF) (Selesi et al., 2010; Bergmann et al., 2011b). In the past, efforts were made to obtain a pure culture (only the Deltaproteobacterium), but so far without any success.

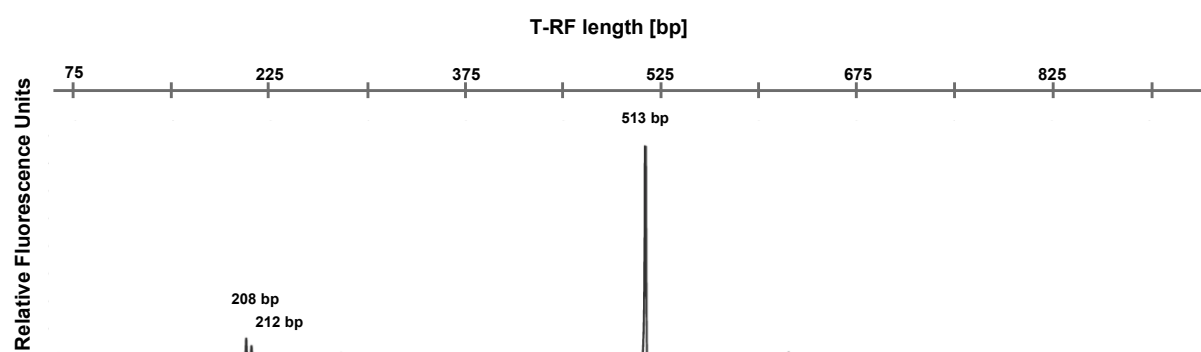


Figure 7: T-RFLP analysis of bacterial 16S rRNA gene sequence of the sulfate-reducing enrichment culture N47 grown with naphthalene. The length of major T-RFs is indicated.

The culture grows very slowly (two to three months; Fig. 8). Nevertheless, growth can be enhanced to eight weeks of incubation time by decreasing the amount of reducing agent (Na_2S) in the medium and regular transfers, which reduce and even eliminate the lag phase (Dr. Housna Mouttaki, personal communication).

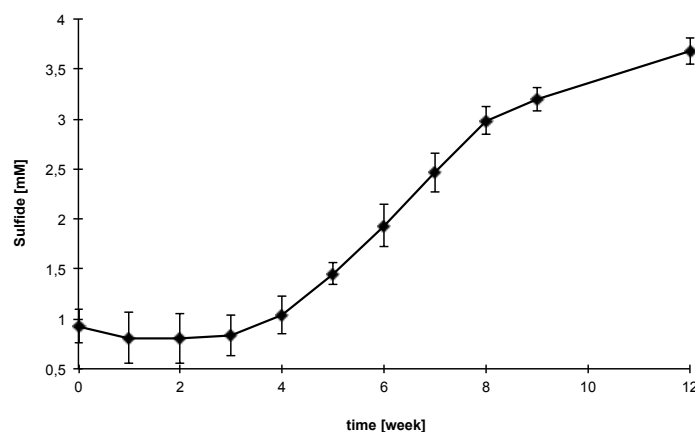


Figure 8: Sulfide formation by the enrichment culture N47 grown with naphthalene.

The sulfate-reducing culture N47 and the marine strain NaphS2, which is available as pure culture (Galushko et al., 1999), became the model organisms for studying the anaerobic degradation of naphthalene.

Anaerobic degradation of 2-methylnaphthalene

N47 is able to degrade 2-methylnaphthalene under anoxic conditions (Selesi et al., 2010). Here, the initial reaction is an addition reaction of the methyl group of 2-methylnaphthalene to the double bond of fumarate to yield the intermediate naphthyl-2-methyl-succinate (Fig. 6). Analogous to the initial reaction in toluene degradation in *T. aromatica*, catalyzed by the glycol radical enzyme benzylsuccinate synthase (Bss), the initial step in 2-methylnaphthalene degradation is catalyzed by the naphthyl-2-methyl-succinate synthase (Nms) (Leuthner et al., 1998; Safinowski and Meckenstock, 2004). The benzylsuccinate synthase is composed of α , β and γ -subunits and is encoded by the *nmsABC* genes (Selesi and Meckenstock, 2009). The enzyme has a putative apparent molecular weight of around 220 kDa ($\alpha_2\beta_2\gamma_2$). Within the genome of N47, in close vicinity to *nmsABC* a gene encoding the activating enzyme NmsD could be identified.

In the following enzymatic steps, naphthyl-2-methyl-succinate is converted via β -oxidation reactions to the central intermediate 2-naphthoyl-CoA (Safinowski and Meckenstock, 2004). The enzymes are encoded within the *bns*-operon (β -oxidation of naphthyl-2-methyl-succinate) consisting of eight genes (*bnsABCDEFGH*) (Selesi et al., 2010).

In vitro, the activities of benzylsuccinate synthase (NmsABC), naphthyl-2-methyl-succinate CoA transferase catalyzing the CoA-transfer (BnsE and BnsF) from naphthyl-2-methyl-succinyl-CoA to succinate (back reaction was assayed) and naphthyl-2-methyl-succinyl-CoA dehydrogenase (BnsG) catalyzing the oxidation of naphthyl-2-methyl-succinyl-CoA to naphthyl-2-methylene-succinyl-CoA, were measured (Annweiler et al., 2000; Safinowski and

Meckenstock, 2004). Analogous to the reactions in the anaerobic degradation of toluene, the double bond of naphthyl-2-methylene-succinyl-CoA is suggested to be hydrated and the formed naphthyl-2-hydroxymethyl-succinyl-CoA is most likely oxidized to naphthyl-2-oxomethyl-succinyl-CoA (Fig. 6). Subsequently, this compound is proposed to be thiolitically cleaved to 2-naphthoyl-CoA and succinyl-CoA.

1.5 Carboxylases

The main topic of this PhD project is about the naphthalene carboxylase. In the following paragraphs some well-studied carboxylases are described to give a general overview about the enzyme family.

Carboxylases belong to the enzyme class of ligases (forming carbon-carbon bonds; EC 6.4.1) whereas decarboxylases are assigned to the class of lyases (carboxy-lyases; EC 4.1.1). To ensure that the reaction proceeds only in one of the two possible directions, (de)carboxylation reactions can be irreversible under physiological conditions, however, some enzymes are able to catalyze both reactions. In the latter case, the function of the enzyme depends on the downstream reactions. The direct depletion of the produced product for example can pull the equilibrium of a thermodynamically unfavorable (de)carboxylation reactions.

Carboxylases are enzymes catalyzing the incorporation of carbon dioxide (CO_2) into organic matter. Even though CO_2 -fixation is a common feature, the underlying mechanisms were shown to be very diverse in nature. In most carboxylases, metal ions (which are prosthetic groups) and/or cofactors are required for the activity (Aresta and Dibenedetto, 2007). As prosthetic group, metal ions like Mg^{2+} , Mn^{2+} , Co^{2+} , Fe^{2+} can frequently be found, while Co^{3+} , Al^{3+} , Fe^{3+} are less present. Carboxylases use either carbon dioxide or the hydrated form bicarbonate (HCO_3^-). At physiological pH, bicarbonate is available in higher concentrations than gaseous CO_2 . However, carbon dioxide and bicarbonate differ regarding their chemical reactivity. Due to the partial positive charge of the carbon atom of CO_2 , it is very reactive towards nucleophilic attacks whereas bicarbonate is less reactive (Inoue and Yamazaki, 1982; O'Leary, 1992; Glueck et al., 2010). During (de)carboxylation reactions, C-H and C-C bonds are exchanged and negatively charged intermediates are usually formed (Fig. 9). The stability of these anionic intermediates is rate determining for the reactions (O'Leary, 1992). In many cases, the enolate intermediates are stabilized by metal ion complexation.

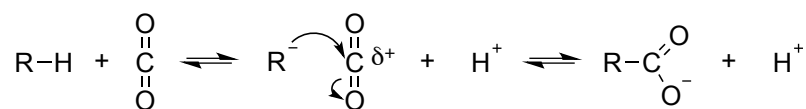


Figure 9: Formation of an anionic intermediate in (de)carboxylation reactions.

It is estimated that 98% of CO₂ entering the biological carbon circle is fixed by carboxylases (Erb, 2011). All together 100 Gt of CO₂ are estimated to be embedded into organic material per year (net primary production) (Field et al., 1998).

Moreover, the very important, autotrophic carboxylase RuBisCO (ribulose-1,5-bisphosphate carboxylase/oxygenase) not only enables plants and other photosynthetic organisms to maintain their requirement for organic carbon, it also provides carbon sources, oxygen, and energy for heterotrophic and other organisms (Glueck et al., 2010). It is the most abundant protein on earth (Ellis, 1979), what correlates with its bad catalytic activity, possibly.

According to their function within the organism, carboxylases were classified into five different groups: (i) autotrophic, (ii) assimilatory, (iii) anapleurotic, (iv) biosynthetic and (v) redox-balancing carboxylases (Erb, 2011) (Fig. 10).

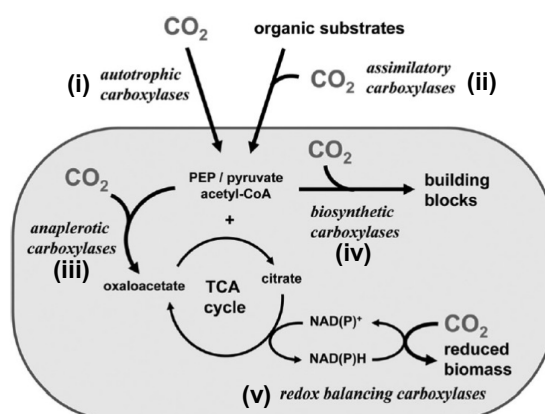


Figure 10: Classification of carboxylases by function. Carboxylases were divided in five different groups: (i) autotrophic, (ii) assimilatory, (iii) anapleurotic, (iv) biosynthetic and (v) redox-balancing carboxylases. Based on the huge variety in amino acid sequences and the underlying reaction mechanisms, it is reasonable to separate them by function (modified from Erb (2011)).

(i) Autotrophic carboxylases

As already mentioned, most of CO₂ is fixed by RuBisCO (EC 4.1.1.39), the key enzyme of Calvin-Benson-Bassham cycle (Bassham et al., 1950). It catalyzes the carboxylation and subsequent cleavage of ribulose-1,5-bisphosphate into two molecules of 3-phosphoglycerate (3-PGA) (Frey and Hegeman, 2006). Due to an intrinsic reactivity of the enediolate

intermediate with oxygen, also oxygenative cleavage into one molecule of 3-PGA and one molecule of phosphoglycolate occurs.

RuBisCO needs special activation in the ϵ -amino group of lysine within the active site. Mg^{2+} and CO_2 do not only serve as cofactor and substrate, they are also involved in the activation reaction (Lorimer et al., 1976). The lysine residue binds CO_2 as *N*-carbamate and forms the active state of the enzyme. Mg^{2+} binds after carbamylation of lysine for stabilization (Frey and Hegeman, 2006). Moreover, Mg^{2+} orients all reactants in the active site of the enzyme e.g. ribulose-1,5-bisphosphate. Ribulose-1,5-bisphosphate forms an enediolate which attacks CO_2 generating a C6-sugar (Nelson and Cox, 2008). The molecule is then hydroxylated at the C3 carbonyl and by cleavage the first molecule 3-phosphoglycerate is produced. Protonation of the remaining carbanion will generate a second molecule 3-phosphoglycerate. This CO_2 -fixation pathway can be found in many plants, algae, and some bacteria (Fuchs et al., 2011).

In general, autotrophic carboxylases allow the transformation of inorganic carbon dioxide into the biomass. Depending on the energy requirements of the organism, its tolerance towards molecular oxygen and the availability of the respective reducing equivalents and cofactors, alternative pathways to the already mentioned Calvin-Benson-Bassham cycle are used (Fuchs and Schlegel, 2006). Five other CO_2 fixation pathways have been discovered so far: the reductive citric acid cycle (Evans et al., 1966), the reductive acetyl-CoA pathway (Ragsdale and Pierce, 2008), the 3-hydroxypropionate bicycle (Zarzycki et al., 2009), the 3-hydroxypropionate/4-hydroxybutyrate cycle (Berg et al., 2007), and the dicarboxylate/4-hydroxybutyrate cycle (Huber et al., 2008). For all this pathways, carboxylases are the key enzymes (except of the reductive acetyl-CoA pathway, but there is also a carboxylation reaction involved, catalyzed by pyruvate ferredoxin oxidoreductase).

(ii) Assimilatory carboxylases in anaerobic degradation

Assimilatory carboxylases transform organic compounds into central precursor molecules (Erb, 2011). In anaerobic bacteria, carboxylation was reported as an alternative to an oxygen-dependent functionalization reaction to activate inert compounds such as acetone, acetophenone and phenol (Schühle and Fuchs, 2004; Jobst et al., 2010; Schühle and Heider, 2011). Following, all of these carboxylation products are activated to their corresponding CoA-esters and further metabolized into central intermediates (reviewed in (Boll et al., 2014)).

Acetone and acetophenone carboxylase are members of the same enzyme family. Both enzymes are ATP-dependent and biotin-independent. It is suggested that one ATP is consumed for the activation of bicarbonate to carboxyphosphate and a second one for the formation of a phospho-*enol*-intermediate (Jobst et al., 2010; Schühle and Heider, 2011).

Acetophenone carboxylase is involved in the anaerobic degradation of ethylbenzene and acetophenone. However, the activity was shown not to be oxygen-sensitive (Jobst et al., 2010). Within the genome of *A. aromatoleum*, it is encoded in an operon, *apcABCDE*, and forms a $(\alpha\beta\gamma\delta)_2$ -heterooctamer. During the purification, acetophenone carboxylase dissociated into two parts, the subcomplex ApcABCD and the subunit ApcE and the enzyme was inactive. The activity could be restored by the addition of the heterologously produced ApcE (Jobst et al., 2010). The enzyme contained Zn^{2+} and was dependent on the presence of Mg^{2+} or Mn^{2+} .

Acetone carboxylase from the denitrifying bacterium *A. aromaticum* converts acetone and HCO_3^- to acetoacetate under both oxic and anoxic conditions. Subsequently, acetoacetate is activated to acetoacetyl-CoA and thiolitically cleaved to yield acetyl-CoA (Schühle and Heider, 2011). Additionally, the enzyme is involved in the butanone metabolism in *A. aromatoleum*. Schühle and Heider (2011) demonstrated the carboxylation of butanone to 3-oxopentanoic acid by acetone carboxylase *in vitro*. Acetone carboxylase contains zinc and iron and is composed of three subunits, AcxABC. The active enzyme forms a heterohexamer $(\alpha\beta\gamma)_2$.

The activation of acetone via carboxylation and further conversion to acetyl-CoA consumes three ATP equivalents. Gutiérrez Acosta et al. (2013) postulated an alternative activation mechanism for the strict anaerobic sulfate reducer *Desulfococcus biacutus*. They demonstrated a carbonylation reaction of acetone with CO to acetoacetaldehyde. The reaction was ATP-dependent and could be enhanced by addition of NH_4^+ . The presence of acetoacetaldehyde dehydrogenase activity in cell-free extracts of acetone-grown cells strongly supported a further degradation to acetoacetyl-CoA. Due to the high reactivity of acetoacetaldehyde, the authors hypothesized the carbonylating enzyme to be a multi-enzyme complex, harboring both enzymatic activities. Further analyses revealed thiamine pyrophosphate (TPP) as a potential cofactor of the so far unknown enzyme (Gutiérrez Acosta et al., 2014). The mechanism of TPP involvement in this reaction remained unclear. Moreover, the products of ATP-cleavage were shown to be AMP and pyrophosphate, excluding a possible phosphorylation of acetone to phospho-*enol*-acetone.

The first step in anaerobic phenol degradation is the ATP-dependent activation of phenol to phenylphosphate via phenylphosphate synthase (PpsABC) (Fig. 11) (Schmeling et al., 2004). For the phenylphosphate synthase activity, only the PpsA and PpsB subunits are required, however, the activity can be simulated several fold in presence of the PpsC subunit (Schmeling et al., 2004).

Subsequently, the activated intermediate is carboxylated in the *para* position by the metal-dependent (Mg^{2+} or Mn^{2+} and K^+) phenylphosphate carboxylase (Fig. 11) (Schühle and Fuchs, 2004). The divalent metal ions potentially act as Lewis acid by increasing the electrophilic character of CO_2 or they interact with the phenolic hydroxyl group (Lack and Fuchs, 1992; Schühle and Fuchs, 2004). K^+ was reported to support the chemical *para* carboxylation in this biological Kolbe-Schmitt carboxylation. During the phenylphosphate carboxylation, the free energy of the phosphate ester hydrolysis ensures substrate binding even at low substrate concentration and shifts the equilibrium towards the carboxylation reaction (Schmeling and Fuchs, 2009; Boll et al., 2014).

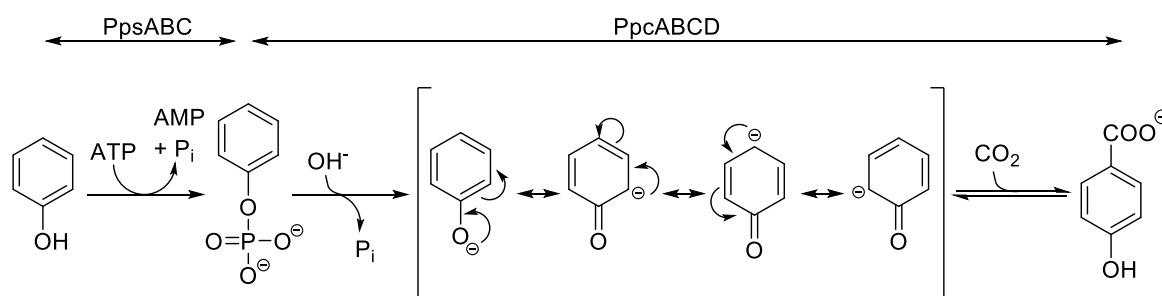


Figure 11: First enzymatic reactions involved in the anaerobic degradation of phenol in *T. aromatica*. Phenol is first activated by the phenylphosphate synthase PpsABC and the phosphorylated intermediate is subsequently carboxylated to 4-hydroxybenzoate. The formation of the enzyme-bound phenolate is most likely unidirectional (exergonic) (Schühle and Fuchs, 2004). Moreover, this step was suggested to be the rate-limiting step in the reaction. Based on the isotopic exchange reaction of $^{14}CO_2$ with the carboxyl group of [^{12}C]4-hydroxybenzoate, the phenylphosphate carboxylation seems to be freely reversible.

The purified enzyme from *T. aromatica* was composed of four subunits- two UbiD-like proteins ($\alpha\beta$, 54 and 53 kDa), a hypothetical protein (γ , 10 kDa), and a phosphatase-like protein (δ , 18 kDa) (Schühle and Fuchs, 2004). The authors suggested the enzyme to be a trimer ($\alpha\beta\gamma\delta$)₃. During purification, the phenylphosphate carboxylase decomposed into a core complex ($\alpha\beta\gamma$) and the phosphatase-like δ -subunit. However, the core complex ($\alpha\beta\gamma$) without the δ -subunit was only capable of catalyzing the exchange reaction between $^{14}CO_2$ and the

carboxyl group of 4-hydroxybenzoate but not the phenylphosphate carboxylation per se. The activity could be restored by the addition of the heterologously produced δ -subunit.

Phenol degradation initiated by phenylphosphate synthase and phenylphosphate carboxylase was reported in the denitrifying bacteria *T. aromatica*, *A. aromaticum* strain EbN1, *Magnetospirillum* sp., the sulfate-reducing bacterium *Desulfatiglans anilini* strain AK1, and the iron-reducer *G. metallireducens* GS-15 (Fig. 12) (Schmeling et al., 2004; Schühle and Fuchs, 2004; Ahn et al., 2009; Schleinitz et al., 2009; Schmeling and Fuchs, 2009; Suzuki et al., 2014). However, homologs of the genes encoding the phenylphosphate carboxylase subunits PpcA and PpcD were not identified within the genome of *G. metallireducens* GS-15 (Schleinitz et al., 2009). Therefore, the authors suggested variations in the enzymatic properties. Indeed, phenylphosphate carboxylase activity of *G. metallireducens* GS-15 was comparable to the one detected in *T. aromatica* but did not catalyze the characteristic $^{14}\text{CO}_2$ isotope exchange reaction.

Beside phenol, phenylphosphate synthase and phenylphosphate carboxylase initiated the anaerobic degradation of catechol (1,2-dihydroxybenzene) (Ding et al., 2008). Catechol is first activated to catechylphosphate and subsequently carboxylated to protocatechuate. Therefore, Ding et al. (2008) suggested that the ability to degrade catechol was due to unspecific reactions of some promiscuous enzymes such as phenylphosphate carboxylase.

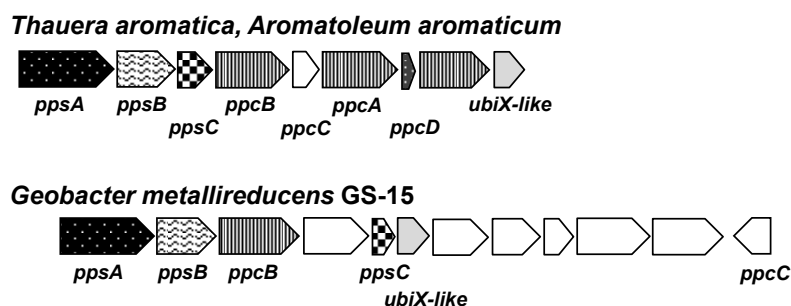


Figure 12: Organization of the phenol gene cluster in *T. aromatica*, *A. aromaticum*, and *G. metallireducens*. The phenylphosphate synthase PpsABC and the phenylphosphate carboxylase PpcABCD are encoded within the phenol gene clusters in the nitrate-reducers *Thauera aromatica* (GI:10697118 to GI:10697125), *Aromatoleum aromaticum* strain EbN1 (GI:56477200 to GI:56475432) and the iron-reducer *Geobacter metallireducens* GS-15 (GI:300245886 to GI:300245892). Open reading frames are represented by arrows. Black-striped arrows represent *ubiD*-like genes. Phenylphosphate synthase genes are indicated by black pattern fill and *ubiX*-like genes by light grey. ORFs which products shares high homology between the strains have the same filling. Further details are mentioned in the text.

The recently described naphthalene carboxylase, which will be the central part of this PhD project, fits well into this last subgroup of carboxylases. As already mentioned, it catalyzes the conversion of naphthalene and [^{13}C]bicarbonate to [^{13}C]2-naphthoic acid (Mouttaki et al., 2012). Furthermore, it catalyzes a much faster exchange of ^{13}C -labeled bicarbonate with the carboxyl group of [^{12}C]2-naphthoic acid. The oxygen-sensitive carboxylation reaction is biotin-independent and neither metal ions nor ATP are needed under the tested conditions. It was also described that strong reducing reagents such as sodium dithionite strongly inhibited naphthalene carboxylation, leading to the suggestion that a redox active group could be necessary for the enzyme activity (Mouttaki et al., 2012). Otherwise, dithionite (or rather its decomposition product SO_2^-) as well as oxygen can act as a radical trapping reagent (Schühle and Fuchs, 2004). So far, a radical mechanism for naphthalene carboxylase cannot be excluded.

To date, a carboxylation reaction as initial step in the anaerobic degradation of naphthalene could be biochemically demonstrated in the sulfate-reducing cultures N47 and NaphS2 and in the iron-reducer N49 (Mouttaki et al., 2012; Cunha Tarouco et al., 2013).

(iii) Anaplerotic carboxylases

For the synthesis of important intermediates, compounds of central metabolic cycles are constantly used (Fuchs and Schlegel, 2006). To maintain all central metabolic pathways running, there are specific enzymes catalyzing the so-called anaplerotic reactions which allow to refill the consumed intermediates. Oxaloacetate is one of the central intermediates often used as a precursor molecule for biosynthesis of amino acids. Because oxaloacetate is needed for condensation with acetyl-CoA as the first step in citric acid cycle, two different carboxylases, phosphoenolpyruvate carboxylase and biotin-dependent pyruvate carboxylase, replenish the oxaloacetate pool.

Phosphoenolpyruvate carboxylase is ATP-independent, but it requires Mg^{2+} . The enzyme uses HCO_3^- rather than CO_2 (Maruyama et al., 1966; Cooper and Wood, 1971). A transfer of ^{18}O from ^{18}O -labelled bicarbonate to inorganic phosphate P_i supports the proposed reaction mechanism in which the formation of a bicarbonate-phosphate intermediate in form of a carbonic-phosphoric anhydride (carboxyphosphate) is suggested (Maruyama et al., 1966). In the next step, the CO_2 formed by the decarboxylation of carboxyphosphate carboxylates enolpyruvate to the end product oxaloacetate (Fig. 13). Moreover, isotope effect studies suggested that the formation of the enzyme-bound carboxyphosphate intermediate was the rate-determining step (O'Leary et al., 1981).

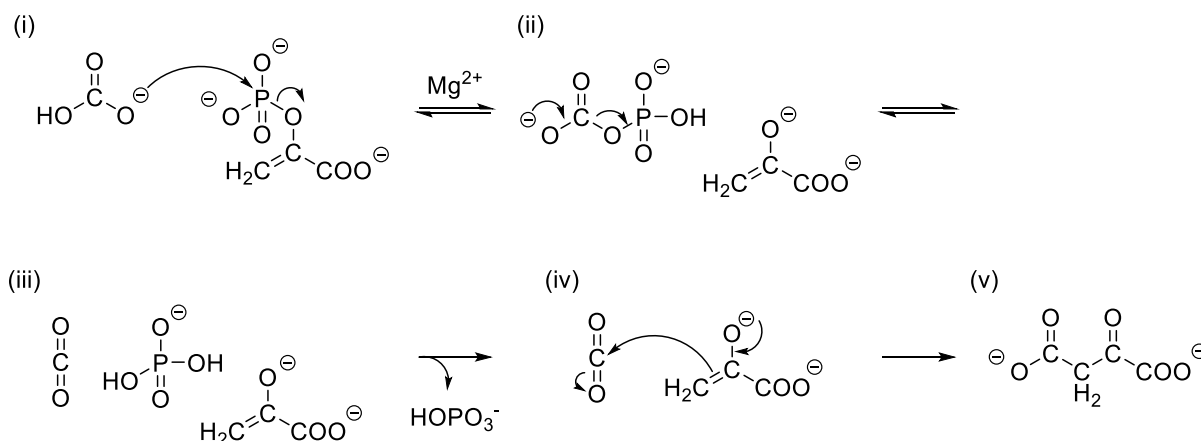


Figure 13: Proposed reaction mechanism for phosphoenolpyruvate carboxylase. (i) The reaction starts with bicarbonate and phosphoenolpyruvate. (ii) Formation of enolpyruvate and a bicarbonate-phosphate-intermediate in form of a carbonic-phosphoric anhydride (carboxyphosphate). (iii) Dephosphorylation of carboxyphosphate and release of P_i . (iv) Carboxylation of enolpyruvate to oxaloacetate (v) (Frey and Hegeman, 2006).

In biotin-dependent carboxylases, CO_2 is delivered to the active site in form of carboxybiotin. To produce carboxybiotin, CO_2 is required in its activated form, carboxyphosphate, which is generated via HCO_3^- coupled to ATP-hydrolysis (Berg et al., 2003). Biotin-dependent enzymes such as pyruvate carboxylase exclusively accept HCO_3^- and require a metal ion for catalysis (O'Leary, 1992). The biotin cofactor is covalently bound to the enzyme by an amide linkage to a lysine residue (Nelson and Cox, 2008). In a second sequence, which takes place in a different catalytic site of the enzyme, the released CO_2 reacts with pyruvate to form oxaloacetate and the biotinyl-enzyme is regenerated. The biotin attached to the lysine side chain enables the movement between the two catalytic active sites of the enzyme.

As mentioned earlier, CO_2 is very reactive towards nucleophilic attacks but the CO_2 concentration at the physiological pH is low and its ability to bind to enzymes limited. Biotin-dependent enzymes solve this issue by binding the higher available hydrated form HCO_3^- and combining it to ATP hydrolysis into the more reactive CO_2 leading to a high local concentration prior to the carboxylation reaction itself (Jencks, 1975; O'Leary, 1992).

(iv) Biosynthetic carboxylases

As the name implies, biosynthetic carboxylases provide specific building blocks for synthesis of molecules. For example, in fatty acid biosynthesis in eukarya and bacteria, malonyl-CoA functions as a building block. Malonyl-CoA is provided by an ATP-dependent carboxylation of acetyl-CoA using acetyl-CoA carboxylase (Formica and Brady, 1959). Furthermore, the

assimilation of some amino acids as well as the degradation of branched and odd-chain fatty acids proceeds via biotin-dependent propionyl-CoA carboxylase (Fuchs and Schlegel, 2006). In addition, biosynthetic pathways to polyketide secondary metabolites involve essential carboxylation reactions (Erb, 2011).

In table 1, all mentioned carboxylases are described with their preferred substrate, subunit composition and requirement of prosthetic groups and energy.

Table 1: Characteristics of some carboxylases. All carboxylases are also mentioned in the text. Comparison of different types of carboxylases underlines the high variation within this group.

Enzyme	Substrate	Subunit composition	Cofactor	ATP	CO ₂ /HCO ₃ ⁻	Organism	Ref.
RuBisCO (Spinach)	Ribulose	Heterohexadecamer	Mg ²⁺	-	CO ₂	C3-Plants, also higher	(Andersson and Backlund, 2008)
Phenylphosphate carboxylase	Phenylphosphate	(αβγ) ₃ + (δ) ₃	Mg ²⁺ / Mn ²⁺ , K ⁺	-	CO ₂	<i>T. aromatica</i> and others	(Schühle and Fuchs, 2004)
Acetophenone carboxylase	Acetophenone	(αβγδ) ₂ -heterooctamer	Mg ²⁺ / Mn ²⁺ 1 Zn ²⁺	+	HCO ₃ ⁻	<i>A. aromaticum</i> EbN1 and others	(Jobst et al., 2010)
Acetone carboxylase	Acetone, Butanone	(αβγ) ₂	complex Mg ²⁺ , 1 Zn ²⁺ + 2 Fe/	+	HCO ₃ ⁻	<i>A. aromaticum</i> EbN1 and others	(Schühle and Heider, 2011)
Acetone carbonylase	Acetone	Unknown	heterohexamers Most likely TPP	+	CO	<i>D. biacutus</i>	(Gutiérrez Acosta et al., 2013; Gutiérrez Acosta et al., 2014)
Phosphoenolpyruvate carboxylase	Phosphoenolpyruvate	Homotetramer	Mg ²⁺	-	HCO ₃ ⁻	Bacteria, C3-Plants	(Mazelis and Vennesland, 1957)
Pyruvate carboxylase	Pyruvate	Homotetramer	Mn ²⁺ / Biotin	+	HCO ₃ ⁻	All life-forms, except plants	(Berg et al., 2003)
Acetyl-CoA carboxylase	Acetyl-CoA	depends on organism	Mg ²⁺ / Biotin	+	HCO ₃ ⁻	All life-forms	UniProt
Propionyl-CoA carboxylase	Propionyl-CoA	α-, β-SU in different comp.	Mg ²⁺ / Biotin	+	HCO ₃ ⁻	All life-forms	UniProt

1.6 Objectives

Non-substituted polycyclic aromatic hydrocarbons are very difficult to degrade in the absence of molecular oxygen and the underlying anaerobic biochemical reactions are only poorly understood. Nevertheless, the model compound naphthalene is degraded by the enrichment culture N47 under sulfate-reducing conditions. The initial reaction activating such an inert polycyclic aromatic compound under anoxic conditions is of special scientific interest. In the anaerobic degradation of naphthalene by N47, the initial step was suggested to be a carboxylation of naphthalene to 2-naphthoic acid. Recently, the naphthalene carboxylase activity could be measured by Mouttaki et al. (2012). The subunit(s) of the naphthalene carboxylase remained unknown. Therefore, the aim of the present study was to identify the subunit(s) of the naphthalene carboxylase complex in the sulfate-reducing culture N47. Due to the slow growth and the little biomass obtained from N47, the native purification of such an oxygen sensitive enzyme (complex) is extremely difficult. To this end, alternative approaches such as transcriptional analysis, differential protein production analysis, and *in vitro* protein interaction assays were developed to identify the naphthalene carboxylase subunits.

The enrichment culture N47 consists of two major organisms, the naphthalene-degrading Deltaproteobacterium and a spirochete. Interestingly, in the environment uncultivated members of the family *Spirochaetaceae* usually co-occurred in sites contaminated with hydrocarbons and chlorinated compounds. Based on 16S rRNA gene sequences, these uncultivated species are closely related to the N47 spirochete. This supports the hypothesis that spirochetes might play an important ecological role in the degradation of (poly-)aromatic and chloro-organic compounds. To get insights into this group of uncharacterized spirochetes, the spirochete strain was isolated from the enrichment culture N47 and characterized by standard microbiological and molecular methods in pure culture.

2. Materials and Methods

2.1 Organisms, vectors and synthetic oligonucleotides

Organisms, vectors and oligonucleotide sequences, which were used in the present study, are listed in the tables below.

Table 2: Organisms.

Strain	Genotype	Reference
<i>Escherichia coli</i> DH5 α	F ⁻ endA1 glnV44 thi-1 recA1 relA1 gyrA96 deoR nupG Φ 80dlacZ Δ M15 Δ (lacZYA-argF)U169 hsdR17(r _K ⁻ m _K ⁺) λ -	Woodcock et al. (1989)
<i>Escherichia coli</i> BL21 (DE3)	F ⁻ <i>ompT</i> hsdS _B (r _B ⁻ m _B ⁻) <i>gal dcm</i> (DE3)	Studier and Moffatt (1986)
<i>Escherichia coli</i> Rosetta™ 2 (DE3)pLysS	F ⁻ <i>ompT</i> hsdS _B (r _B ⁻ m _B ⁻) <i>gal dcm</i> (DE3) pLysSRARE2 (Cam ^R)	Novagen®
Enrichment culture N47	Wild type	Meckenstock et al. (2000)
Deltaproteobacterium NaphS2	Wild type	Galushko et al. (1999)
<i>Cand. Treponema</i> <i>contaminophilus</i> sp. strain HM ^T	Wild type	Present study

Table 3: Vectors.

Plasmid	Genotype	Reference
pHAT	amp ^r , T7 promoter, Lac-inducible, N-terminal His-tag	Peränen et al. (1996)
pGEX-6P1	amp ^r , <i>tac</i> promoter, Lac-inducible, N-terminal GST-tag, PreScission™ cleavage site	GE Healthcare Europe (Freiburg, Germany)
pETM-13	kan ^r , T7 promoter, Lac-inducible, C-terminal His-tag	EMBL-made vector by Gunter Stier
pET-21a-d(+)	amp ^r , T7 promoter, Lac-inducible, C-terminal His-tag	Novagen®/ Merck KGaA (Darmstadt, Germany)
pGEX-6P1_N47K27540	pGEX-6P1 plus N47_K27540	Present study
pETM13_N47K27540	pGEX-6P1 plus N47_K27540	Present study
pHAT_N47K27540	pHAT plus N47_K27540	Present study

Plasmid	Genotype	Reference
pET21a_N47K27540	pET-21a-d(+) plus N47_K27540	Present study
pGEX-6P1_N47K27400	pGEX-6P1 plus N47_K27400	Present study
pGEX-6P1_N47K27460	pGEX-6P1 plus N47_K27460	Present study
pGEX-6P1_N47K27480	pGEX-6P1 plus N47_K27480	Present study
pGEX-6P1_N47K27520	pGEX-6P1 plus N47_K27520	Present study

Table 4: Primer sets designed and utilized for molecular cloning.

Primers' name	Sequence (5'-3')
pGEX_Sall_540_for	GTA <u>GTCGAC</u> TGATGGCGTTTAAAGATTTGAG
pET21a_pGEX_NotI_540_rev	GTA <u>GCGGCCGC</u> GAATCCATATTTATTCCAATTG
pHAT_NotI_540_for	GTA <u>GCGGCCGC</u> AATGGCGTTTAAAGATTTGAG
pHAT_HindIII_540_rev	GTA <u>AAGCTT</u> TCAGAATCCATATTTATTCCAATTG
pET21a_NheI_540_for	GTA <u>GCTAGC</u> ATGGCGTTTAAAGATTTGAG
pETM13_PscI_for	GTA <u>ACATGT</u> TAGCGTTTAAAGATTTGAGGGAG
pGEX_BamHI_400_for	GTA <u>GGATCC</u> ATGGTGAAATGAGTTGCGA
pGEX_NotI_400_rev	GTA <u>GCGGCCGC</u> GTTTCCCGGACGGAGATAAGAC
pGEX_BamHI_460_for	GTA <u>GGATCC</u> ATGTTTAGTGATTTTCGCGG
pGEX_NotI_460_rev	GTA <u>GCGGCCGC</u> TCTCCGATGACTTAAATAAGAC
pGEX_Sall_480_for	GTA <u>GTCGAC</u> TGATGAGTTCATTAAGAGAA
pGEX_NotI_480_rev	GTA <u>GCGGCCGC</u> GTCCATAACCACTGGTTCCTGC
pGEX_BamHI520_for	GTA <u>GGATCC</u> ATG GAAGAACGTGAAATACT
pGEX_NotI520_rev	GTA <u>GCGGCCGC</u> TGCTTTCTCCTCCTGTACTTCT

Restriction sites were underlined.

Table 5: Primers used for sequencing.

Primers' name	Sequence (5'-3')	Reference
N47_Seq_540_for	CCACCGTGATCGGCGGCGATC	Present study
N47_Seq_540_rev	CTCAATGTCCACGGTCTCGCAT	
pGex_for	ATAGCATGGCCTTTGCAGG	Eurofins Genomics (Ebersberg, Germany)
pGex_rev	GAGCTGCATGTGTCAGAGG	
Ba27f (-FAM) ^{a,b}	FAM-AGAGTTTGATCMTGGCTCAG	(Pilloni et al., 2011)
Ba907r ^b	CCGTCAAATTCCTTTGAGTTT	
Ba1492r ^a	CGGYTACCTTGTTACGACTT	(Weisburg et al., 1991)
Spiro_640f ^a	TTGAGTTATGGAGAGGGAGCTAG	Present study
Spiro_731r ^a	CGCACCTCAGCGTCAGTCATCGG	

^a Primer used for direct sequencing of 16S rRNA genes. ^b Primer used for T-RFLP.

Table 6: Primer set utilized for the detection of flagella genes in spirochetes.

Primers' name	Sequence (5'-3')	Reference
flaBU	GCAGGAGATGATGCTTCTGGT	Heuner et al. 2000,
flaBR	ATTTGCTTGGGCAAGCATTGC	Ritalahti et al., 2012

Table 7: Primer sets designed and utilized for transcriptional analysis (operon mapping).

Primer set	Primers' name	Sequence (5'-3')	Amplicon size (bp)
-1.1	53306f	TATTAACGTAAAGGCAGGC	1239
	52068r	TTTCCAAGAGCTCAATAAACT	
-1	52641f	ATTATCAGAAGGGCTGTTTAA	574
	52068r	TTTCCAAGAGCTCAATAAACT	
1	50736f	AAAGATGTTTCAGGAAAAGGT	538
	50199r	GCACTTCATCATGATGTTG	
2	49346f	GAAGTACAGGAGGAGAAAGC	1107
	48240r	CTTCATTGACTTCCACAAGT	
3	46832f	AGATCGACTGGCACAAGAAGT	473
	46360r	TGCGACATGGCACAGATAG	
4	45060f	TAGAGATCGTGTGGTGGCTTT	580
	44481r	TTCGCCTGAATGATTGAGG	
5	43268f	AAGATAGGCTTGGATGCCAC	913
	42356r	TCCAGGATAACACCCCTGATAT	
5.1	43268f	AAGATAGGCTTGGATGCCAC	496
	42773r	GGTCGAGGTAACAATGCCTATT	
1A	pGEX6P1_Sall_52110f	GTAGTCGACTGATGGCGTTTAAAGATTTGAG	1923
	50199r	GCACTTCATCATGATGTTG	
2B	pGEX6P1_BamHI_50243f	GTAGGATCCATGGAAGAACGTGAAATACT	1837
	48416r	AAATCAATGACGCTCTTGCCTATCTT	
3C	48303f	ATGGACACTAGAGAATTGGT	1944
	46360r	TGCGACATGGCACAGATAG	
4D	pGEX6P1_Sall_46472f	GTAGTCGACTGATGAGTTCATTAAGAGAA	2003
	44481r	TTCGCCTGAATGATTGAGG	

The oligonucleotides were synthesized by Eurofins Genomics (Ebersberg, Germany) or biomers.net (Ulm, Germany).

2.2 Chemicals, biochemicals and gases

Chemicals used in the present study were purchased from AppliChem (Darmstadt, Germany), Fluka (Neu-Ulm, Germany), Merck KGaA (Darmstadt, Germany), Carl Roth (Karlsruhe, Germany), Sigma Aldrich (St. Louis, MO) and GE Healthcare Europe (Freiburg, Germany) in *p.a.* quality. Biochemicals were ordered from Bio-Rad Laboratories (Hercules, CA), Life Technologies (Carlsbad, CA), Promega (Fitchburg, WI), Thermo Fisher Scientific (Waltham, MA), Roche (Basel, Switzerland) and 5Prime (Hamburg, Germany).

Nitrogen gas (99,999%) and Biogon® (C20 E941/E29; carbon dioxide 20% ± 2%, rest nitrogen) were purchased from Linde AG (Pullach, Germany).

2.3 Media and buffers

Chemical solutions and growth media were prepared in MilliQ water (Merck KGaA, Darmstadt, Germany). Growth medium as well as heat-resistant solutions and equipment were autoclaved (120 °C, 45 min), whereas heat-sensitive solutions were filtrated (22 µm). Glassware was sterilized in dry heat (180 °C, 2 h). Buffers used for chromatography were filtrated (45 µm) to avoid impurities on the chromatography matrix.

Anoxic buffers and solutions were flushed with nitrogen or N₂/CO₂ (80:20, v/v) for at least 20 min.

2.3.1 Medium for the cultivation of *E. coli*

E. coli cells were grown in LB medium (see Tab. 8). For selective media, respective antibiotics (see Tab. 9) were added after autoclaving (120 °C, 30 min). Solid medium was prepared by the addition of 15 g/L agar-agar.

Table 8: LB medium.

<u>LB medium</u>	Weighed-in quantity
Tryptone	10 g/L
Yeast extract	5 g/L
NaCl	10 g/L

Table 9: Antibiotics.

Antibiotic	Concentration of stock solutions and their final concentration
Ampicillin	100 mg/mL in MilliQ water (stock) final concentration in the medium 100 µg/mL
Chloramphenicol	34 mg/mL in ethanol (stock); final concentration in the medium 34 µg/mL
Kanamycin	50 mg/mL in MilliQ water (stock); final concentration in the medium 50 µg/mL
Rifampicin	0.5 mg/mL in MilliQ water (stock); final concentration in the medium 10 µg/mL

2.3.2 Medium for the cultivation of N47

The sulfate-reducing enrichment culture N47 was grown under strict anoxic conditions. The medium (see Tab. 14) was incubated at 100 °C for at least 1 h and subsequently flushed with N₂/CO₂ (80:20, v/v) until it was cooled down to RT. Before sterilization, trace elements, selenite-tungsten solution and resazurin (see Tab. 16) were added. If required, the medium was filled into serum bottles under a stream of N₂/CO₂ (80:20, v/v). The bottles were sealed with blue butyl stoppers (Glasgerätebau Ochs, Bovenden, Germany) and aluminum caps prior to autoclaving. All other additives and the carbon source were added to the sterile medium from sterile and anoxic stock solutions (see Tab. 16).

Table 10: Stock solution (50X) for the anaerobic cultivation of N47.

	Weighed-in quantity
NaCl	50 g/L
MgCl ₂ • 6 H ₂ O	20 g/L
KH ₂ PO ₄	10 g/L
NH ₄ Cl	12.5 g/L
KCl	25 g/L
CaCl ₂ • 2 H ₂ O	7.5 g/L

Table 11: Trace elements SL10 (1000X; Widdel et al. (1983)).

	Weighed-in quantity
FeCl ₂ • 4 H ₂ O	1500 mg/L
ZnCl ₂	70 mg/L
MnCl ₂ x • 4 H ₂ O	100 mg/L
CoCl ₂ • 6 H ₂ O	190 mg/L
CuCl ₂ • 2 H ₂ O	2 mg/L
NiCl ₂ • 6 H ₂ O	24 mg/L
Na ₂ MoO ₄ • 2 H ₂ O	36 mg/L
H ₃ BO ₃	6 mg/L
HCl (25%)	10 mL/L

Table 12: Vitamin solution VL-7 (1000X; Pfennig (1978)).

	Weighed-in quantity
Cyanocobalamin (B12)	10 mg/ 200 mL
p-Aminobenzoate	10 mg/ 200 mL
D(+)-Biotin	2 mg/ 200 mL
Nicotinate	20 mg/ 200 mL
Ca-D(+)-Pantothenate	5 mg/ 200 mL
Pyridoxamine dihydrochloride (B6)	50 mg/ 200 mL
Thiamine dihydrochloride (B1)	10 mg/ 200 mL

Table 13: Selenite-tungsten solution (1000X).

	Weighed-in quantity
NaOH	500 mg/L
Na ₂ SeO ₃ • 5 H ₂ O	3 mg/L
Na ₂ WO ₄ • 2 H ₂ O	4 mg/L

Table 14: Medium without supplements.

	Amount
Stock solution (50X)	18 mL
Na ₂ SO ₄	1,14 g (final concentration 10 mM)
MilliQ water	ad 780 mL

Table 15: Supplements added to the anoxic medium from stock solutions.

Stock solution	Weighed-in quantity	Final concentration in the medium
1 M NaHCO ₃	12.6 g/150 mL	30 mM
0.5 M Na ₂ S • 9 H ₂ O	6 g/ 50 mL	0.5 mM
0.4% Resazurin	0.4 g/ 100 mL	0.0004%
1.5% Naphthalene in HMN	1.5 g/ 100 mL	
1.5% 2-Methylnaphthalene in HMN	1.5 g/ 100 mL	

Table 16: Supplemented medium for the anaerobic cultivation of N47.

	Added amount of stock solution
Carbonate buffer ^a (Tab. 15)	30 mL/L
Reducing agent (Na ₂ S) ^a (Tab. 15)	1 mL/L
Vitamin solution ^a (Tab. 12)	1 mL/L
Trace elements (Tab. 11)	0.5 mL/L
Selenite-tungsten solution (Tab. 13)	0.5 mL/L
Resazurin (Tab. 15)	1 mL/L
Naphthalene ^a /	20 mL/L
2-Methylnaphthalene ^a (Tab. 15)	

^a Added from sterile and anoxic stock solution to the sterile medium.

2.3.3 Medium for the cultivation of NaphS2

The marine naphthalene-degrading strain NaphS2 was cultivated under strict anoxic conditions. The medium (see Tab. 17) was boiled and subsequently flushed with N₂/CO₂ (80:20, v/v) until it was cooled down to RT. Before sterilization, trace elements, selenite-tungsten solution and resazurin (see Tab. 16) were added. If required, the medium was filled into serum bottles under a stream of N₂/CO₂ (80:20, v/v). The bottles were sealed with blue butyl stoppers (Glasgerätebau Ochs, Bovenden, Germany) and aluminum caps prior to autoclaving. All other additives and the carbon source were added to the sterile medium from sterile and anoxic stock solutions (see Tab. 19). When 2-naphthoate served as the substrate, it was directly added to the medium prior to autoclaving with a final concentration of 2 mM.

Table 17: Medium for the anaerobic cultivation of NaphS2.

	Weighed-in quantity
Na ₂ SO ₄	2.4 g/ 770 mL
KH ₂ PO ₄	0.16 g/ 770 mL
NH ₄ Cl	0.24 g/ 770 mL
NaCl	16.8 g/ 770 mL
MgCl ₂ • 6 H ₂ O	2.4 g/ 770 mL
KCl	0.4 g/ 770 mL
CaCl ₂ • 2 H ₂ O	0.12 g/ 770 mL

Table 18: Vitamin solution (100X; DSMZ medium 141).

	Weighed-in quantity
D(+)-Biotin	2 mg/L
Folic acid	2 mg/L
Pyridoxine-HCl	10 mg/L
Thiamine-HCl • 2 H ₂ O	5 mg/L
Riboflavin	5 mg/L
Nicotinic acid	5 mg/L
Ca-D(+)-Pantothenate	5 mg/L
Cyanocobalamin (B12)	0.1 mg/L
p-Aminobenzoate	5 mg/L
Lipoic acid	5 mg/L

Table 19: Supplemented medium for the anaerobic cultivation of NaphS2.

	Added amount from stock solution
Carbonate buffer ^a (Tab. 15)	30 mL/L
Reducing agent (Na ₂ S) ^a (Tab. 15)	1 mL/L
Vitamin solution ^a (Tab. 18)	1 mL/L
Trace elements (Tab. 11)	0.5 mL/L
Selenite-tungsten solution (Tab. 13)	0.5 mL/L
Resazurin (Tab. 15)	1 mL/L
Naphthalene ^{a/}	20 mL/L
2-Methylnaphthalene ^a (Tab. 15)	

^a Added from sterile and anoxic stock solution to the sterile medium.

2.3.4 Medium for the cultivation of *Cand. Treponema contaminophilus* sp.

Cand. T. contaminophilus sp. strain HM^T is a pure strain isolated from the anaerobic enrichment culture N47. The anoxic medium for the regular cultivation of *Cand. T. contaminophilus* sp. was prepared according to the protocol of N47 (see 2.3.2) with minor changes (see Tab. 21).

Table 20: Supplements added to the medium from stock solutions.

Stock solution	Weighed-in quantity	Final concentration in the medium
20% Yeast extract	20 g/ 100 mL	0.1%
1 M Glucose	18 g/ 100 mL	10 mM
1 M NH ₄ Cl	1.07 g/ 20 mL	1 mM
0.2 M CaCl ₂	1.45 g/ 50 mL	0.4 mM
0.08 M MgSO ₄	19.7 g/50 mL	0.16 mM

Table 21: Supplemented medium for the anaerobic cultivation of *Cand. T. contaminophilus* sp..

	Added amount from stock solution
Carbonate buffer ^a (Tab. 15)	30 mL/L
Reducing agent (Na ₂ S) ^a (Tab. 15)	1 mL/L
Trace elements (Tab. 11)	0.5 mL/L
Selenite-tungsten solution (Tab. 13)	0.5 mL/L
Resazurin (Tab. 15)	1 mL/L
Yeast extract (Tab. 20)	5 mL/L
Glucose (Tab. 20)	10 mL/L

To determine the optimum pH for growth of the strain, an alternative minimal medium was used. The pH of the mineral medium was adjusted using KOH or HCl. Before sterilization, trace elements and the selenite-tungsten solution (see Tab. 11, Tab. 13) were added. The bottles were sealed with blue butyl stoppers (Glasgerätebau Ochs, Bovenden, Germany) and aluminum caps and flushed with nitrogen gas for at least 20 min prior to autoclaving. The nitrogen source as well as MgSO₄ and CaCl₂ were added to the sterile medium from sterile and anoxic stock solutions (see Tab. 22).

Table 22: Supplemented medium for pH experiments with *Cand. T. contaminophilus* sp..

	Added amount of stock solution
10 mM Potassium phosphate buffer + 0.1% NaCl	
Trace elements (Tab. 11)	32 µL/ 50 mL
Selenite-tungsten solution (Tab. 13)	32 µL/ 50 mL
NH ₄ Cl ^a	50 µL/ 50 mL
CaCl ₂ ^a	50 µL/ 50 mL
MgSO ₄ ^a	50 µL/ 50 mL
Yeast extract ^a (Tab. 21)	250 µL/ 50 mL
Glucose ^a (Tab. 21)	500 µL/ 50 mL

^a Added from sterile and anoxic stock solution to the sterile medium.

2.4 Cultivation and maintenance of bacterial strains and preparation of cell-free extracts

2.4.1 *In vitro* overexpression of plasmid-encoded genes in *E. coli*

Liquid cultures were cultivated in 30-40% (v/v) filled Erlenmeyer flasks. If required, antibiotics were added. The cultures were incubated on a shaker at 37 °C. At an optical density of 0.5-0.7 at 578 nm (OD_{578nm}), gene expression was induced by addition of 0.2-0.5 mM IPTG. In some cases, to improve solubility of the produced proteins, the cells were incubated at RT and incubated on a stirring plate for additional 3 h. The cells were harvested at 4.000 rpm for 15 min at 4 °C and the pellet was stored at -20 °C until further use.

For cultivation on solid medium, the culture plates were incubated at 37 °C over night.

For the preparation of glycerol stocks of *E. coli*, 800 µL of an exponentially grown culture were mixed with 200 µL sterile glycerol and transferred into a 2 mL-cryovial (Nalgene, Wiesbaden, Germany). The glycerol stocks were stored at -80 °C.

2.4.2 Cultivation and maintenance of the strict anaerobic cultures N47, NaphS2 and *Cand. T. contaminophilus* sp.

Anoxic conditions were retained during the whole cultivation process. Therefore, the Hungate technique was used to cultivate the enrichment culture N47, NaphS2 and *Cand. T. contaminophilus* sp.. During cultivation, bottles were sealed with blue butyl stoppers (Glasgerätebau Ochs, Bovenden, Germany) and aluminum caps to avoid penetration of molecular oxygen. Moreover, the used glassware (Glasgerätebau Ochs, Bovenden,

Germany) was able to resist higher gas pressure. On one hand, the cells actively produced gas and on the other hand overpressure was kept within the bottle to avoid influx of oxygen during sampling.

All used solutions were flushed with N₂ or N₂/CO₂ (80:20, v/v) for at least 20 min, depending on the headspace of the flask and the volume of the water body. In case it was impossible to work in closed bottles, experiments were performed using the anaerobic chamber under a N₂- or N₂/H₂-atmosphere.

i. N47 and NaphS2

For routine cultivation of the sulfate-reducers N47 and NaphS2, the PAHs naphthalene or 2-methylnaphthalene served as growth substrates (see Materials and Methods 2.3.2/ 2.3.3). Only in case of NaphS2, 2-naphthoate was used as alternative substrate. The bottles were inoculated using 10% of a pre-culture and incubated for 6-8 weeks at 30 ° C in the dark.

It was not possible to measure naphthalene carboxylase activity in N47 cells which were stored at -80 °C. Therefore, the cultures were transferred on regular basis.

ii. *Cand. Treponema contaminophilus* sp.

For routine cultivation of *Cand. Treponema contaminophilus* sp. strain HM^T, 10 mM glucose and 0.1% yeast extract were added to the medium (see Materials and Methods 2.3.4). The bottles were inoculated using 10% of a pre-culture and incubated for 1-2 weeks at 30-37 °C in the dark. *Cand. T. contaminophilus* sp. strain HM^T could be stored at 4 °C.

Substrate utilization tests

Substrate utilization tests were done in triplicates. To avoid substrate carryover, the cells were grown with the new substrate and transferred at least twice with the new substrate. For batch cultures experiments, the tested substrates were prepared in anoxic stock solutions and added at a final concentration of 5 mM to the freshwater medium. In experiments testing for alternative electron acceptors, they were added at a final concentration of 10 mM.

BIOLOG AN MicroPlates

For substrate utilization tests using BIOLOG AN MicroPlates (Hayward, CA), freshwater medium without sodium sulfide or substrate but supplemented with 0.1% yeast extract was used. Prior to inoculation, the cells were washed three times with the modified medium described above to avoid substrate carryover. The plates were inoculated with a cell density of 1x10⁸ cells/mL and incubated in an anaerobic jar at 30 ° C in the dark with an atmosphere

of N₂/CO₂. Growth was measured in a plate reader (Wallac Victor³ 1420; PerkinElmer, Waltham, MA) at 595 nm. When growth could be observed on the BIOLOG MicroPlates with a specific substrate, that same substrate was tested in batch experiments.

Experiments to test various growth parameters

To determine the salinity growth profile, sodium chloride concentrations were tested between 0.1 up to 5% in the freshwater medium. The oxygen sensitivity of the strain was analyzed in thioglycollate broth (Sigma Aldrich, St. Louis, MO) as recommended by the manufacturer. The temperature growth profile was determined in triplicates over a range between 12 to 60 °C and the pH growth profile was tested between pH 5 and 9.

2.4.3 Cell harvesting and preparation of cell-free extracts

i. *E. coli*

Preparation of cell-free extracts by sonication

The pellets of *E. coli* cells containing heterologously produced proteins (see Materials and Methods 2.4.1) were resuspended on ice in one mL buffer (composition depending on the further application) per one g wet cells with lysozyme (Sigma Aldrich, St. Louis, MO), DNase I (AppliChem, Darmstadt, Germany) and 0.2-1% IGEPAL[®] CA-630 (Sigma Aldrich, St. Louis, MO). The cells were disrupted by 4-6 cycles of sonication (1 cycle 3-5 min) at a frequency of 30 kHz with a 50% pulse and an amplitude of 60% (UP50H, Hielscher Ultrasonics GmbH, Teltow, Germany) with a resting time of 2-5 min on ice. The cell lysis status was controlled microscopically. The crude extract was centrifuged (14,000 rpm, 4 °C, 20 min; Heraeus Multifuge X3/X3R; Thermo Fisher Scientific, Waltham, MA) and the generated cell-free extract collected for further experiments.

ii. N47 and NaphS2

Preparation of cell-free extracts by sonication

For the preparation of cell-free extracts, cells were harvested in the mid-exponential phase of growth in an anaerobic chamber (Labstar, MBRAUN, Garching, Germany). To avoid contact with traces of oxygen, the plastic consumables were transferred into the anaerobic chamber at least 12 h before the experiment started.

The cells were separated from the HMN phase by using a separation funnel. After 5 min, the HMN phase was clearly separated from the aqueous medium phase. The medium was filled into Falcon tubes and centrifuged (4000 rpm, 4 °C, 45 min; Heraeus Multifuge X3/X3R;

Thermo Fisher Scientific, Waltham, MA). Afterwards, the cells were washed and depending on the used culture volume resuspended in up to 1.5 mL buffer. Depending on the further application, different buffers were used to wash and resuspend N47 or NaphS2 cells.

The cells were disrupted by 3-4 cycles of sonication (1 cycle 15-20 s) at a frequency of 30 kHz with a 50% pulse and an amplitude of 40% (UP50H, Hielscher Ultrasonics GmbH, Teltow, Germany) in a pre-chilled metallic block followed by a 20 min centrifugation step (14,000 rpm, 4 °C). The supernatant was collected for further experiments. To prevent protein degradation, a 1X complete protease inhibitor cocktail (Roche, Basel, Switzerland) was added to cell-free extracts of all conducted approaches.

Preparation of cell-free extracts by French Press

The French Press was used to disrupt N47 cells harvested from a fermenter. The lysis method is known to be very mild and effective. The French Press was used in the group of Prof. Dr. Matthias Boll at the Albert-Ludwigs University Freiburg. The harvested cells (see Preparation of cell-free extracts by sonication) were resuspended in up to 3.5 mL MOPS/KOH buffer (100 mM, pH 7.3), filled into a pre-chilled mini-cell (max. 3.7 mL total volume; Thermo Fisher Scientific, Waltham, MA) and opened by 1 passage through the French Press cell. The crude extract was collected in an anoxic Hungate tube sealed with a rubber stopper. In the anaerobic chamber, the extract was transferred to ultracentrifuge tubes and tightly closed. After centrifugation (40 K, 4 °C, 1 h; Optima L90-K Ultrazentrifuge, Beckman Coulter, Krefeld, Germany), the cell-free extract was removed from the pellet fraction with a Pasteur pipette and stored at 4 °C under anoxic conditions not longer than some hours.

Preparation of cell-free extracts by bead beating

The cell pellets (see Preparation of cell-free extracts by sonication) were resuspended in up to 1 mL respective buffer and transferred to Lysis Matrix B (for protein extraction) or E (for DNA extraction) tubes (MP Biomedicals, Santa Ana, CA). The tubes were fixed in a homogenizer (FastPrep®-24 Instrument, MP Biomedicals, Santa Ana, CA) and cells were disrupted for 10-40 s with a speed of 4-6 m/s. Afterwards, the tubes were centrifuged (14,000 rpm, 4 °C, 20 min) and the supernatant carefully removed without touching the matrix.

Preparation of cell-free extracts by chemical treatment

A chemical treatment e.g. with detergent represents a mild alternative to disrupt cells without mechanical force and thereby without the generation of heat. To open the cells the following concentrations of different detergents were tested: 20% (v/v) BugBuster® Protein Extraction

Reagent (Merck KGaA, Darmstadt, Germany), 0.02-1% IGEPAL[®] CA-630 (Sigma-Aldrich, St. Louis, MO), 0,15 mM Dodecyl- β -D-maltosid (Carl Roth, Karlsruhe, Germany), 0.03% LDOA (*N,N*-Dimethyldodecylamine *N*-oxide, Sigma-Aldrich, St. Louis, MO), 30 mM Octyl β -D-glucopyranoside (Sigma-Aldrich, St. Louis, MO) and 0.01-1% Triton X 100 (Carl Roth, Karlsruhe, Germany). The cells were incubated with the respective detergent for 20 min at 4 °C. Moreover, incubation with 1 mg/mL lysozyme for 30 min at 30 °C was tested.

2.5 Molecular Methods

2.5.1 Polymerase chain reaction (PCR)

The polymerase chain reaction was used to amplify DNA fragments or genes, respectively. A standard PCR reaction was mixed in a 0.5 mL PCR cup and contained nuclease-free water (Promega, Fitchburg, WI), 1X Taq PCR buffer, 1.5 mM MgCl₂, 0.2 mM dNTPs, 0.5 μ M primer (forward and reverse, each) and 1.25 U *Taq* polymerase (Fermentas, Thermo Fisher Scientific, Waltham, MA) in a final volume of 20-100 μ L.

For the amplification of genes, which were inserted into expression vectors, Phusion Hot Start II High-Fidelity DNA Polymerase (Thermo Fisher Scientific, Waltham, MA) with a proofreading function was used. These reactions contained nuclease-free water (Promega, Fitchburg, WI), 1X GC buffer, 0.2 mM dNTPs, 0.5 μ M primer (forward and reverse, each) and 0.5 U Phusion polymerase in a final volume of 50 μ L.

Table 23: PCR program for the amplification of the 16S rRNA gene fragment (primer set Ba27f-FAM/ 907r).

Temperature	Time	
94 °C	5 min	
94 °C (Denaturation)	30 s	← 25 cycles
52 °C (Annealing)	30 s	
72 °C (Elongation)	1 min	
72 °C	5 min	
8 °C	Hold	

For direct sequencing of the 16S rRNA gene fragment from *Cand. T. contaminophilus* sp. strain HM^T (primer set Ba27f-FAM/ Ba1492r) the elongation time was increased to 90 s.

Table 24: PCR program for amplification of flagella genes (primer set flaBU/ flaBR).

Temperature	Time	
94 °C	5 min	
94 °C (Denaturation)	30 s	← 30 cycles
55 °C (Annealing)	35 s	
72 °C (Elongation)	2:12 min	
72 °C	5 min	
8 °C	Hold	

Table 25: Intergenic regions were amplified via PCR using the primer sets listed in Tab. 7.

Temperature	Time	
94 °C	5 min	
94 °C (Denaturation)	30 s	← 35 cycles
52-57 °C (Annealing)	15 s	
72 °C (Elongation)	1 kb/60 s	
72 °C	5 min	
8 °C	Hold	

Table 26: PCR program for amplification of *N47_K27540* (~ 1.5 kbp).

Temperature	Time	
98 °C	30 s	
98 °C (Denaturation)	10 s	← 30 cycles
55 °C (Annealing)	20 s	
72 °C (Elongation)	45 s	
72 °C	5 min	
8 °C	Hold	

All genes or inserts, which were subsequently cloned into expression vectors, were amplified using the program defined in Tab. 26.

The annealing temperatures varied between the different PCR reactions and were experimentally optimized. Moreover, the elongation time was dependent on the length of the DNA fragment and the used polymerase- *Taq* polymerases need 1 min for the synthesis of 1 kb, whereas the Phusion polymerase synthesizes the same DNA fragment within 15-30 s.

2.5.2 Terminal restriction fragment length polymorphism (T-RFLP)

T-RFLP analyses were performed to visualize the composition of bacterial communities or to check for purity of a culture. For T-RFLP analyses, the 16S rRNA gene was partially amplified via PCR (see Materials and Methods 2.5.1, Tab. 23) using the 5'-end 6-carboxyfluorescein-labeled (FAM) forward primer Ba27f-FAM. The purified amplicons (see Materials and Methods 2.5.4) were digested with *MspI* (Fermentas, Thermo Fisher Scientific, Waltham, MA) for 2 h at 37 °C (see Materials and Methods 2.5.3; Tab. 27) and desalted with DyeEx columns following the manufacturer's instructions (Qiagen, Hilden, Germany). The T-RFLP run was conducted on an ABI 3730 DNA analyzer (Applied Biosystems, Grand Island, NY) at the Genome Analysis Center, Helmholtz Zentrum München and the electropherograms were processed with the PeakScanner (version 1.0) and GeneMapper® (version 4.0, Applied Biosystems, Grand Island, NY).

2.5.3 Restriction

The method was used for standard molecular cloning, T-RFLP analyses (see Materials and Methods 2.5.2) and to check if a DNA fragment was successfully inserted into an expression vector (see Materials and Methods 2.5.11). The restriction of DNA by restriction enzymes was performed according to the manufacturer's protocols. To ensure sufficient restriction, it was important to consider the individual enzyme activity in the used buffer system when more than one enzyme was included in the reaction. The reactions were incubated at 37 °C for 2 h for circular DNA (vectors) or over night for DNA fragments (inserts). Subsequently, the linear DNA fragments were purified to remove the restriction enzymes (see Materials and Methods 2.5.4). In the present study, restriction enzymes were purchased from Thermo Fisher Scientific (Waltham, MA) or New England Biolabs (Ipswich, MA).

Table 27: Restriction of 16S rRNA amplicons for T-RFLP.

	Amount
PCR fragment (16 S rRNA, ~ 80 ng)	1 µL
Buffer Tango	1 µL
<i>MspI</i> (10 U/µL)	0,3 µL
H ₂ O	7,7 µL
	10 µL

2.5.4 Purification of DNA

Amplicons were purified using the PCRextract kit (5Prime, Hamburg, Germany) according to the manufacturer's protocol.

Genomic DNA, which was sent for sequencing, was purified via QIAamp MinElute columns following the protocol 'Cleanup of Genomic DNA' (QIAamp DNA Mini Kit, Qiagen, Hilden, Germany).

2.5.5 Isolation of plasmids

Plasmids were isolated according to the GeneJET™ Plasmid Miniprep Kit (Thermo Fisher Scientific, Waltham, MA) and sent for sequencing (Eurofins Genomics, Ebersberg, Germany) to ensure precise expression of heterologous genes.

2.5.6 Isolation of RNA

RNA was extracted using the SV Total RNA Isolation System by Promega (Fitchburg, WI) as described by the manufacturer.

To get a higher yield of RNA, the modified method by Schmitt et al. (1990) was applied. Cell pellets from 150 mL culture of N47 naphthalene-grown cells were resuspended in 300 µL of buffer AE (50 mM Na-Acetate, pH 5.3; 10 mM Na-EDTA) and 200 µL sodium phosphate buffer (200 mM sodium phosphate, pH 5.6). Then, 50 µL of a 20% (w/v) SDS solution and 450 µL phenol/AE were added and the mixture was incubated for 10 min at 65 °C. After centrifugation (14,000 rpm, 4 °C, 5 min), the supernatant was transferred to a gel lock heavy tube (5Prime, Hamburg, Germany) and extracted consecutively with 1 volume phenol-chloroform-isoamylalcohol [PCI, 24:24:1 (v/v/v)] and 1 volume chloroform-isoamylalcohol [CI, 24:1 (v/v)] prior to precipitation (14,000 rpm, 4 °C, 30 min) with 2 µL glycogen (Roche, Basel, Switzerland) and 2 volumes of polyethylene glycol. Subsequently, the nucleic acid pellet was washed with 150 µL 70% ethanol and resuspended in 40 µL RNase-free water (Promega, Fitchburg, WI).

Prior to RT-PC (see Materials and Methods 2.5.7), the co-extracted DNA was digested with RQ1 RNase-free DNase (Promega, Fitchburg, WI) according to the manufacturer's instructions. The RNA was visualized on standard agarose gel electrophoresis (see Materials and Methods 2.5.14) and analyzed by using NanoDrop (NanoDrop Technologies, Inc., Wilmington, DE) to estimate the quality. RNA was stored at -80 °C until further use.

2.5.7 Reverse transcription polymerase chain reaction (RT-PCR)

The RNA was reversibly transcribed into cDNA by GoScript™ reverse transcriptase (Promega, Fitchburg, WI). In a pre-step to anneal the primers, the extracted RNA (up to 5 µg) was incubated at 70 °C for 5 min with random hexamer primers (0.5 µg per reaction; Thermo Fisher Scientific, Waltham, MA) or with gene specific reverse primers (Tab. 7; 50199r, 48240r, 46360r, 44481r; 5 pmol each per reaction). To stop the reaction, the pre-mix was incubated on ice for 5 min. The final RT-PCR contained 1X GoScript™ reaction buffer, 2.5 mM MgCl₂ (Promega, Fitchburg, WI), 0.5 mM of each dNTP (Thermo Fisher Scientific, Waltham, MA), 0.5 µL recombinant RNasin® ribonuclease inhibitor (Promega, Fitchburg, WI), 7.5 µL RNA-primer pre-mix and 1 µL GoScript™ reverse transcriptase in a total volume of 20 µL. As a negative control, a reaction was set up without the reverse transcriptase to monitor eventual residual genomic DNA contamination. For cDNA synthesis, the following program was used: annealing for 5 min at 25 °C, extension for 55 min at 42 °C and inactivation of the reverse transcriptase for 15 min at 70 °C. The cDNA was stored at -20 °C.

2.5.8 Isolation of chromosomal DNA

Genomic DNA was extracted with the DNasy Minikit (Qiagen, Hilden, Germany) from exponentially grown cultures (150 mL N47 culture, 5 mL *Cand. T. contaminophilus* sp.) as described by the manufacturer.

For sequencing of the genomic DNA from *Cand. T. contaminophilus* sp. strain HM^T, a higher amount of DNA was required. Therefore, the gDNA was isolated following a modified method by Lueders et al. (2004) and Gabor et al. (2003). The cell pellet of *Cand. T. contaminophilus* sp. from a 150 mL culture was resuspended in 650 µL PTN buffer (pH 8.0, 120 mM sodium phosphate buffer, 125 mM Tris/HCl, 0.25 mM NaCl). Afterwards, 200 µL 20% (w/v) SDS solution and 100 µL phenol-chloroform-isoamylalcohol [PCI, 24:24:1 (v/v/v), pH 8] were added and the mixture was transferred to a 2 mL screw-capped bead beating vial filled with 0.2 mL zirconia (0.1 mm)/ silica beads (0.7 mm) (ratio 1:1; BioSpec, Bartlesville, OK). The cells were disrupted by bead beating for 20 s at 6 m/s (see Materials and Methods 2.4.3). After centrifugation (7500 rpm, 20 °C, 5 min), the supernatant (~ 750µL) was transferred to a gel lock heavy tube (5Prime, Hamburg, Germany) and extracted consecutively with 1 volume PCI and 1 volume chloroform-isoamylalcohol [CI, 24:1 (v/v)] (14,000 rpm, 4 °C, 5 min). To precipitate the DNA, the supernatant (~ 650µL) was mixed with 2 volumes of polyethylene glycol (30% PEG, 1.6 M NaCl), incubated 2 h at 4 °C and centrifuged (14,000 rpm, 4 °C, 30 min). Subsequently, the nucleic acid pellet was washed with 500 µL 70% ethanol, dried to remove residual ethanol and resuspended in 30 µL EB buffer (10 mM Tris/HCl, pH 8.5).

To yield a higher purity, the extracted gDNA was additionally purified (see Materials and Methods 2.5.4). Moreover, the samples were treated with RNase. 1 μ L RNase A (10 mg/mL; Thermo Fisher Scientific, Waltham, MA) was mixed with 50 μ L of the sample and incubated for 30 min at 37 °C.

The concentration of gDNA was estimated by comparison to known concentrations of phage lambda-DNA (100-3.125 ng/ μ L; Thermo Fisher Scientific, Waltham, MA) on an agarose gel (see Materials and Methods 2.5.14). The isolated and treated gDNA was stored at -20 °C.

2.5.9 Gel extraction of DNA

DNA was extracted from agarose gels e.g. when small parts within the multiple cloning site of the vector were removed before a DNA fragment could be inserted or to separate different amplicons in one PCR reaction for sequencing. For gel extraction, the NucleoSpin® Gel and PCR Clean-up kit by MACHEREY-NAGEL (Düren, Germany) was used. The DNA was separated on an agarose gel (see Materials and Methods 2.5.14) and one part, which served as a ruler, stained with SYBR® Safe DNA Gel Stain (Life Technologies, Carlsbad, CA), visualized by blue light (470 nm) and cut.

2.5.10 Dephosphorylation of plasmids

The vectors were incubated with CIAP (Thermo Fisher Scientific, Waltham, MA) to prevent recircularization and religation of linearized vector DNA by removing phosphate groups. 1 μ L CIAP was added and the mixture was incubated for 30 min at 37 °C. The procedure was repeated once.

2.5.11 Ligation

For the ligation, vector and insert DNA were combined in a molar ratio of 3:1 or 5:1. Vector and insert were treated with restriction enzymes beforehand (see Materials and Methods 2.5.3) and the vector was dephosphorylated (see Materials and Methods 2.5.10). The total reaction volume was 20 μ L in the presence of 1 U T4 DNA Ligase (Thermo Fisher Scientific, Waltham, MA). The ligation reaction was incubated for 2 h at RT. Subsequently, 5-8 μ L of the reaction were transformed (see Materials and Methods 2.5.12) with competent *E. coli* cells (see Materials and Methods 2.5.13).

2.5.12 Transformation of plasmids

50 µL chemically competent *E. coli* cells (see Materials and Methods 2.5.13) were thawed for 10 min on ice. After addition of 1 µL plasmid DNA, the cells were incubated for 10 more minutes and shocked for 30 s at 42 °C to improve the efficiency of DNA absorption. Then, the cells were incubated for 2 min on ice and 150 µL LB medium (Tab. 8) were added. The mixture was incubated at 37 °C while shaking (850 rpm) for 1 h. Afterwards, the cells were streaked onto selective LB plates (see Tab. 9). The plates were incubated at 37 °C over night.

2.5.13 Preparation of chemical competent *E. coli*

The preparation of chemical competent *E. coli* cells followed the method by Inoue et al. (1990). In a first step, 5 mL of LB medium (Tab. 8) were inoculated with a single colony of the *E. coli* strain and incubated at 37 °C over night. On the next day, this culture was used to inoculate 300 mL SOB medium (2% (w/v) tryptone, 0.5% (w/v) yeast extract, 10 mM NaCl, 2.5 mM KCl, 10 mM MgCl₂, 10 mM MgSO₄). The culture was incubated at 18 °C until an optical density (OD_{578nm}) of 0.6 at 578 nm was reached. The cells were incubated for 10 min in ice and centrifuged for 5 min (5000 rpm, 4 °C). The supernatant was discarded and the cells resuspended in 80 mL pre-chilled TB (transformation) buffer (10 mM PIPES, 15 mM CaCl₂, 250 mM KCl (pH 6,7); 55 mM MnCl₂). The mixture was incubated on ice for 10 min and centrifuged again (5000 rpm, 4 °C, 5 min). Afterwards, the cells were resuspended in 20 mL pre-chilled TB buffer and carefully mixed with 1.4 mL DMSO. After additional 10 min on ice, samples were aliquoted, frozen in liquid nitrogen and stored at -80 °C.

2.5.14 Separation of DNA by agarose gels electrophoresis

DNA, which was amplified via PCR (see Materials and Methods 2.5.1) or extracted from cells (see Materials and Methods 2.5.5-8), was checked for correct length, quality and integrity by gel electrophoresis. Moreover, for gel extraction (see Materials and Methods 2.5.9) or restriction analyses during molecular cloning (see Materials and Methods 2.5.3), the DNA was separated on agarose gels. 4 µL DNA was mix with Loading Dye (Thermo Fisher Scientific, Waltham, MA; 10 mM Tris/HCL, pH 7.6; 0,03% bromophenol blue; 0,03% xylene cyanol FF; 60% glycerol; 60 mM EDTA) and applied to a 1.2% (w/v) agarose gel. To estimate the size and the concentration of a DNA sample, the GeneRuler™ 1 kb DNA Ladder (Thermo Fisher Scientific, Waltham, MA) was used. Gel electrophoresis was performed in 1X TAE-Puffer (50X TAE-Puffer: 242 g Tris; 57.1 mL acetic acid; 50 mM EDTA;

ad 1 L ddH₂O) at 90-120 V. Subsequently, the gels were stained with PAGE GelRed™ (Biotium, Hayward, CA) and visualized by UV light (312 nm).

2.6 Analytical methods

2.6.1 Bradford assay

The protein concentration was determined by the method of Bradford (1976) using Quick Start™ Bradford Dye Reagent (Bio-Rad Laboratories, Hercules, CA) and bovine serum albumin as standard. The samples were diluted according to the calibration curve (0-10 µg/mL or 0-0.4 mg/mL) and 10 µL were mixed with 200 µL 1X Bradford reagent in a 96-well microtiter plate (Greiner, Frickenhausen, Germany). The sample were incubated for 5 min in the dark and then photometrically measured in a plate reader (Wallac Victor³ 1420; PerkinElmer, Waltham, MA) at 595 nm.

2.6.2 Sulfide measurement

Dissolved hydrogen sulfide (H₂S, HS⁻, S²⁻), which is produced by growing sulfate-reducing bacteria, was determined as described by Fischer (1924) and Cline (1969). All solutions except for the Fe(III) solution (RT) were stored at 4 °C. To prevent the oxidation of dissolved sulfide, 1 mL of zinc acetate (2 g zinc acetate in 100 mL MilliQ water; if required 2 mL acetic acid were added to dissolve it) was mixed with 3 mL MilliQ water and 200 µL of a bacterial culture. 1 mL of ADMA (2 g ADMA were dissolved in 200 mL MilliQ water and 200 mL concentrated H₂SO₄ added slowly, ad 1 L), 1 mL Fe(III) solution (5 g ferric ammonium were dissolved in 40 mL MilliQ water and 1 mL concentrated H₂SO₄ added, ad 1 L) and 4 mL MilliQ water were successively added. After mixing all components for 10 s, the mixes were incubated for 30-120 min. Within this time frame, methylene blue was formed which could be measured photometrically at 670 nm (Cary 50 Bio UV-Vis Spectrophotometer; Varian, CA). The concentrations were calculated according to the calibration curve (0-10 mM Na₂S).

2.6.3 High-pressure liquid chromatography (HPLC)

Acetate and lactate were measured on the HPLC (Shimadzu, Japan) with an Aminex HPX-87H column (Bio-Rad Laboratories, Hercules, CA) set to 35 °C. As mobile phase, 5 mM H₂SO₄ with a flow rate of 0.4 ml min⁻¹ was used. The acetate and lactate were detected via the UV detector at 220 nm with a retention time of 23 and 21 min, respectively. Samples were prepared according to Marozava (2013). 0.5 mL samples were mixed with 55 µL

35% perchloric acid and incubated for 10 min on ice. Afterwards, 27 μL 7 M KOH was added, the sample centrifuged (14,000 rpm, 2 min, RT) and 300 μL of the supernatant transferred to a HPLC (VWR International, Radnor, PA).

To monitor the conversion of substrates to the respective products in the enzyme assays (see Materials and Methods 2.8), a C18-reversed-phase UPLC (ACQUITY UPLC H-Class System; Waters, Eschborn, Germany) analysis was performed according to Estelmann et al. (2015) in the group of Prof. Dr. Boll at the Albert-Ludwigs University Freiburg. After centrifugation (14,000 rpm, 4 °C, 30 min), the supernatant of the naphthalene carboxylase and naphthoate-CoA ligase enzyme assays (see Materials and Methods 2.8) were analyzed by using a acetonitrile gradient (15–35%) in 10 mM potassium phosphate buffer (pH 6.8) at a flow rate of 0.2 ml min⁻¹. Free acids and CoA esters were identified by comparing their retention times and UV/Vis absorption spectra with standards which were established by members of Prof. Dr. Boll's group.

2.6.4 Determination of fatty acid composition

The membrane lipids of *Cand. T. contaminophilus* sp. strain HM^T were extracted at the Institute of Groundwater Ecology, Helmholtz Zentrum München. The tried samples were sent to the Helmholtz Zentrum für Umweltforschung (UFZ) in Leipzig, Germany and the analysis was done by Dr. Hermann J. Heipiper, Department Umweltbiotechnologie.

The extraction of membrane lipids was performed according to Bligh and Dyer (1959) and Morrison and Smith (1964). Membrane lipids were extracted from 65 mg of *Cand. T. contaminophilus* sp. cells grown with glucose. The pellet was resuspended into 0.5 mL of water, 1 mL of methanol, and 2 mL of chloroform. After vortexing the mixture for 3 min, an additional 0.5 mL of water was added and mixed again for 30 s. The sample was then centrifuged 10 min, at 3000 rpm and RT and the chloroform phase was transferred to a new vial. The chloroform was removed completely using a nitrogen stream. To methylate the extracted fatty acids to FAME, 0.6 mL BF₃ in methanol was added and the sample was incubated at 95 °C for 15 min. Finally, 0.3 mL of water and 0.3 ml of hexane were added and mixed for 60 s and the final hexane phase was transferred into a GC-vial and used for analysis using an Agilent 6890N gas chromatograph with an FID detector (Agilent Technologies, Santa Clara, CA). The CP-Sil 88 capillary column (Agilent Technologies, Santa Clara, CA) was 50 m in length with an internal diameter of 0.25 mm. The oven temperature was set to 40 °C for 2 min followed by a temperature gradient to a final temperature of 220 °C with an increase of 8 °C/min. The injector was at 240 °C, the flow was in splitless mode with helium as carrier gas. The detector was set at 270 °C. A qualitative

standard of bacterial FAMES (Supelco; Sigma Aldrich, St. Louis, MO) was used to identify the detected peaks.

2.6.5 DNA base composition

The DNA G+C content of the strain HM^T was measured at the DSMZ in Braunschweig, Germany. The genomic DNA was extracted from the cell pellets according to a modified protocol described by Marmur (1961). The DNA was hydrolyzed using P1 nuclease and the nucleotides were dephosphorylated with bovine alkaline phosphatase (Mesbah et al., 1989). The resulting deoxyribonucleosides were analyzed by HPLC (Tamaoka and Komagata, 1984). The data were analyzed using the CLARITY (version 2.4.1.93) software package (DataApex Ltd., Czech Republic). The analytical column was a C₁₈-column (VYDAC 201SP54, 250x4.6 mm; Vydac, Hesperia, CA). The temperature of the column was set to 45 °C, the sample injection volume was 10 µL and the solvent used was 0.3 M (NH₄)H₂PO₄/acetonitrile [40:1 (v/v), pH 4.4] at a flow rate of 1.3 mL/min (adapted from (Tamaoka and Komagata, 1984)). Lambda-DNA and three DNAs with published genome sequences representing a G+C range of 43-72 mol% were used as standards. The G+C values were calculated from the ratio of deoxyguanosine and thymidine according to the method of Mesbah et al. (1989).

2.6.6 Determination of bacterial morphological characteristics

Gram staining was performed by using the Gram staining kit (Sigma Aldrich, St. Louis, MO) as defined by the manufacturer. Catalase activity was determined by placing 30% hydrogen peroxide (Carl Roth, Karlsruhe, Germany) on a cell pellet of a freshly grown culture on a fluted filter. Oxidase activity was determined by a solution of 1% (w/v) N, N, N', N'-teramethyl-1,4-phenyldiammonium dichloride (Wurster's blue). An oxidase-positive assay was indicated by formation of a blue color. *B. subtilis* and *E. coli* were used as reference strains.

2.6.7 Microscopy

i. Electron Microscopy

Electron microscopy was done in collaboration with Dr. Carolin Meyer (former member of the Institute of Groundwater Ecology, Group of Anaerobic Degradation, Helmholtz Zentrum

München) and Prof. Dr. Reinhard Rachel (Zentrum für Elektronenmikroskopie der Fakultät für Biologie und Vorklinische Medizin) at the University of Regensburg.

For TEM analysis, *Cand. Treponema contaminophilus* sp. strain HM^T cells were fixed with 2.5% (final concentration) glutaraldehyde for 30 min at RT. Cells were concentrated by centrifugation and applied to carbon-coated 200 mesh copper grids (Plano, Wetzlar, Germany). The samples were either platinum-carbon shadowed at 15 °C (CFE 50; Cressington Ltd., Watford, UK) or negatively stained with 2% uranyl acetate for approximately 1 min. TEM micrographs were taken on a Phillips CM 12 transmission electron microscope (voltage 120 kV, FEI, Eindhoven, The Netherlands) and recorded using a slow-scan charged-coupled device camera (TEM-1000, TVIPS-Tietz, Gauting).

ii. Raman microspectroscopy

The sample preparation for Raman microspectroscopy was developed and performed at the Institute of Groundwater Ecology, Helmholtz Zentrum München. Raman microspectroscopy was done by Patrick Kubryk and Dr. Natalia P. Ivleva at the Institute of Hydrochemistry, Chair for Analytical Chemistry, Technische Universität München.

The samples were prepared according to Amann et al. (1990) and Giovannoni et al. (1988) with minor changes. Twenty-five mL of N47 culture were harvested (4000 rpm, 35 min) and washed in PBS buffer (pH 7.4; 137 mM NaCl, 2.7 mM KCl, 8 mM Na₂HPO₄ • 2 H₂O, 1.5 mM KH₂PO₄; 4000 rpm, 10 min). The cells were fixed with freshly prepared 4% PFA (in PBS). One volume of PFA was added to 3 volumes of cell suspension and the mixture was incubated at 4 °C for 12 h. Afterwards, the cells were pelleted by centrifugation (4000 rpm, 4 °C, 10 min), washed with PBS to remove any residual PFA, centrifuged again and treated with a stepwise increased concentration of ethanol (50%, 80%, absolute ethanol). The fixed cells in ethanol were stored at –20 °C. For Raman microspectroscopic studies, 10 µL of the bacterial suspension was dropped onto a CaF₂ plate and was analyzed shortly after evaporation of the ethanol.

A Lab-RAM HR Raman microscope (Horiba Scientific, Japan) integrated with an Olympus BXFM microscope was used for the Raman analysis. The measurements were carried out with a frequency-doubled Nd:YAG laser (532 nm, 32 mW at the sample) or a He-Ne-Laser (633 nm, 14 mW at the sample). The laser beam was focused onto the sample with a 100X objective (Olympus MPlan N, NA = 0.9). The full laser power and an acquisition time of 100 s was chosen for the measurements of the reference compounds and *Deltaproteobacterium* N47. The Raman scattering was collected in a 180° backscatter geometry. The Rayleigh

scattering and the Anti-Stokes Raman scattering were removed by an edge filter. The Stokes Raman scattered light was passed through a diffraction grating (600 lines/mm) and a spatial pinhole (100 μm). Lateral and axial resolution was ca. 1 μm and ca. 2 μm , respectively. The signal was detected with a -72 °C-Peltier-cooled CCD detector. Usually the Raman spectra were recorded over a spectral range from 50 cm^{-1} to 4000 cm^{-1} . The wavelength calibration was performed by focusing the laser beam on a silicon wafer with a 50X objective (Olympus MPlan N, NA = 0.75) and evaluating the first-order phonon band of silicon at 520.7 cm^{-1} . SERS samples were directly analyzed on glass slides. All other samples were measured on CaF_2 plates. With its sharp band at 320 cm^{-1} CaF_2 was also used as an internal standard to ensure a proper calibration and correct the measured spectra if necessary.

2.6.8 Flow cytometry for absolute microbial cells counting

Growth curves of N47 and *Cand. T. contaminophilus* sp. were based on the total number of microbial cells within a sample. The cells were counted by flow cytometry. Technical assistance and method development was provided by Nina Weber (Institute of Groundwater Ecology, Group of Microbial Ecology, Helmholtz Zentrum München).

The reference beads (Trucount™ Absolute Counting Tubes, BD Bioscience, Franklin Lakes, NJ) were resuspended in 4 mL sterile filtered PBS (pH 7.4; 137 mM NaCl, 2.7 mM KCl, 8 mM $\text{Na}_2\text{HPO}_4 \cdot 2 \text{H}_2\text{O}$, 1.5 mM KH_2PO_4), 3 times inverted and vortexed for 10 s. Afterwards, the reference solution was incubated for 10 min to ensure soaking of the beads. The final sample, which was used for the FACS measurements, contained 980 μL reference solution, 100 μL bacterial culture (if necessary already diluted) and 3 μL SYBR® Green I (1.000X; Sigma-Aldrich, St. Louis, MO) to stain the DNA within the bacterial cells. For dead-live staining, 1 μL propidium iodide (1 mg/mL; Sigma-Aldrich, St. Louis, MO) and 1 μL propidium iodide plus 1 μL SYBR® Green I (1.000X; Sigma-Aldrich, St. Louis, MO) for a double stain were used. The samples were incubated for 10 min in the dark and subsequently analyzed using the Cytomics FC 500 (Serial No. AM27235; Beckman coulter, Krefeld, Germany). The flow cytometer was equipped with a 488 nm (40 mW) and a 638 nm (25 mW) laser. The maximum measuring time was set to 300 s in which a maximum of 1 million events was counted. The flow rate was set to medium corresponding to 30 $\mu\text{L}/\text{min}$. The discriminator was set to FL1 (green fluorescence) with a threshold of 1. For detection following parameters were applied: forward scatter 586 V, gain 2.0; sideward scatter 791 V, gain 2.0; FL1 416 V, gain 1.0; FL3 485 V, gain 1.0. Readings were collected in logarithmic mode (at least 500 reference events per sample) and analyzed with the CXP software (version 2.2; Beckman coulter, Krefeld, Germany). Each sample was measured in duplicates. After detection of 500

reference events, the measurement was stopped and the bacterial counts were calculated to the final number using the following formula:

$$\frac{\text{bacteria counted} \times \text{total number of beads in the tube}}{\text{beads counted} \times \text{amount added sample}} \times \text{dilution factor}$$

2.6.9 Proteomic analysis

The proteomic analyses were done by Dr. Juliane Merl-Pham (Research Unit Protein Science, Helmholtz Zentrum München).

i. In-Gel tryptic digest

Coomassie-stained excised gel-pieces were digested as described previously (Merl et al., 2012). The gel-pieces were destained using acetonitrile (ACN) and after rehydration the cysteines residues were reduced using dithiothreitol (DTT) and alkylated using 2-iodoacetamide (IAA). After washing, the proteins in the gel-pieces were digested for approx. 18 h using trypsin (Sigma-Aldrich, St. Louis, MO) in 50 mM ammonium bicarbonate (ABC) solution. Digestion was stopped with trifluoroacetic acid (TFA) and peptides were eluted by successive ACN steps. The eluted peptides were dried and stored at -20 °C until further use.

ii. Mass spectrometric measurements

Dried digested samples were thawed and dissolved in 45 µL of 2% ACN/0.5% TFA. After brief centrifugation, LC-MS/MS analysis was performed on an Ultimate3000 nano HPLC system (Dionex, Sunnyvale, CA) online coupled to a LTQ OrbitrapXL mass spectrometer (Thermo Fisher Scientific, Waltham, MA) by a nano spray ion source as described previously (Hauck et al., 2010; Merl et al., 2012). Each sample was automatically injected and loaded onto the C18 trap column at a flow rate of 30 µL/min in 7% ACN/ 0.1% formic acid (FA). After 5 min, the peptides were eluted from the trap column and separated on the analytical column by a 135 min gradient from 7 to 32% ACN in 0.1% FA at 300 nL/min flow rate followed by a short gradient from 32 to 93% ACN in 0.1% FA in 5 min. Between each sample, the gradient was set back to 7% ACN in 0.1% FA and left to equilibrate for 20 min. The samples were analyzed with and without the addition of DMSO to the buffers.

Analyses without DMSO- Every sample was automatically injected and loaded onto the C18 trap column at a flow rate of 30 µL/min in 7% ACN/ 0.1% formic acid (FA). After 5 min, the peptides were eluted from the trap column and separated on the analytical column by a 135 min gradient from 7 to 32% ACN in 0.1% FA at 300 nL/min flow rate followed by a short

gradient from 32 to 93% ACN in 0.1% FA in 5 min. Between each sample, the gradient was set back to 7% ACN in 0.1% FA and left to equilibrate for 20 minutes.

Analyses with DMSO- The samples were automatically injected and loaded onto the trap column at a flow rate of 30 μ L/min in 3% buffer B (73% ACN/ 3% DMSO/ 0.1% formic acid (FA) in HPLC-grade water) and 97% buffer A (2% ACN/ 3% DMSO/ 0.1% FA) (Hahne et al., 2013). After 5 min, the peptides were eluted from the trap column and separated on the analytical column by a 135 min gradient from 3 to 35% of buffer B at 300 nL/min flow rate followed by a short gradient from 35 to 95% buffer B in 5 min. Between each sample, the gradient was set back to 3% buffer B and left to equilibrate for 20 minutes.

From the MS pre-scan, the 10 most abundant peptide ions were selected for fragmentation in the linear ion trap if they exceeded an intensity of at least 200 counts and if they were at least doubly charged. During fragment analysis a high-resolution (60,000 full-width half maximum) MS spectrum was acquired in the Orbitrap with a mass range from 300 to 1500 Da.

iii. Label-free quantitative analysis

The acquired raw data of each dataset to be compared was loaded in the Progenesis LC-MS software (version 2.5, Nonlinear) for label free quantification and analyzed as described previously (Hauck et al., 2010; Merl et al., 2012). Briefly, profile data of the MS scans were transformed to peak lists with respective peak m/z values, intensities, abundances (areas under the peaks) and m/z width. MS/MS spectra were treated similarly. After reference selection, the retention times of the other samples were aligned by automatic alignment to a maximal overlay of all features. Features with only one charge or more than seven charges were excluded from further analyses. After normalization and assignment of the samples to the respective groups, all MS/MS spectra were exported as Mascot generic file (mgf) and used for peptide identification with Mascot (version 2.4) in the N47 protein database (version 4, 1302846 residues, 5001 sequences). Search parameters used were: 10 ppm peptide mass tolerance and 0.6 Da fragment mass tolerance, one missed cleavage allowed, carbamidomethylation was set as fixed modification, methionine oxidation and asparagine or glutamine deamidation were allowed as variable modifications. Searches were performed with a Mascot ion score cut-off of 30 and an appropriate significance threshold p, in order to reach a maximum false discovery rate of 1%. Search results were re-imported into the Progenesis LC-MS software. The abundances of all peptides allocated to each protein were summed up and exported. The resulting normalized protein abundances were used for calculation of fold-changes of proteins and for calculation of significance using an unpaired both-sided Student's t-test in Excel.

2.7 Biochemical methods

2.7.1 Enzyme purification

i. GST purification

During heterologous expression of the gene *N47_K27540* by the plasmid 'pGEX-6P1_*N47K27540*' (and all other genes inserted into the expression vector 'pGEX-6P1'), the produced protein was fused to glutathione S-transferase (GST) on its N-terminus. The tag has a size of around 29 kDa and enables the fusion protein to bind to glutathione sepharose beads. GST-*N47_K27540* was purified in batch using Glutathione Sepharose 4B beads as recommended by the manufacturer with some modifications (GE Healthcare Europe, Freiburg, Germany).

The heterologously produced protein was purified from 5-10 g *E. coli* cells (see Materials and Methods 2.4.1). The stored pellet was resuspended in binding buffer (50 mM Tris/HCl, pH 7.5; 1 M NaCl; 1 mM EDTA) and the cells were disrupted by sonication (see Materials and Methods 2.4.3). After sonication, 1% IGEPAL[®] CA-630 (Sigma-Aldrich, St. Louis, MO) was added. For purification, 1 mL of Glutathione Sepharose 4B slurry was used. The beads were incubated with *E. coli* cell-free extract containing GST-*N47_K27540* on an end-over-end rotator at 4 °C for 2 h and subsequently 3 times washed with washing buffer (50 mM Tris/HCl, pH 7.5; 140 mM NaCl). The GST-*N47_K27540* coupled to the sepharose beads was used for subsequent pull-down experiments (see Materials and Methods 2.7.4). The purified protein was stored in 20 mM Tris/HCl, pH 7.5 with 50% glycerol at -20 °C.

ii. HIS purification

The recombinant, His-tagged proteins were purified using His SpinTrap TALON[®] columns filled with a cobalt-based immobilized metal affinity chromatography medium according to the manufacturer's protocol (GE Healthcare Europe, Freiburg, Germany). The N- or C-terminally tagged proteins were heterologously produced in *E. coli* (see Materials and Methods 2.4.1) using the expression vector pHAT or pET derivatives and purified from 5-10 g cells. Elution fractions were analyzed by SDS-PAGE (see Materials and Methods 2.7.2), if possible combined, desalted (see Materials and Methods 2.7.1, iii) to remove the imidazole (Carl Roth, Karlsruhe, Germany) and concentrated (see Materials and Methods 2.7.1, iii). Afterwards, the samples were mixed with 10% (w/v) glycerol and stored at -20 °C until further use.

iii. Desalting and concentration of proteins

Depending on the volume, PD-10 or illustra NAP-5 columns (GE Healthcare Europe, Freiburg, Germany) were used to decrease the concentration of salt within a protein sample. The samples were treated as described by the manufacture and eluted with low-salt buffers such as 10 mM Tris/HCl, pH 8.

Afterwards, the proteins were concentrated by ultrafiltration using Vivaspin® columns (Sartorius Stedim Biotech, Göttingen, Germany) as recommended by the manufacturer. The columns were centrifuged (4000 rpm, 4 °C) for several minutes depending on the concentration of the protein solution and the pore size of the used filter.

2.7.2 Polyacrylamide gel electrophoresis

i. SDS polyacrylamide gel electrophoresis

SDS polyacrylamide gel electrophoresis (SDS-PAGE) was performed in the Mini-PROTEAN Tetra Cell (Bio-Rad Laboratories, Hercules, CA) as described previously (Laemmli, 1970). The samples were mixed with SDS loading dye (20% (v/v) 0.5 M Tris/HCl, pH 6.8; 23% (v/v) glycerol; 40% (v/v) of a 10% (w/v) SDS solution; 10% (v/v) β -mercaptoethanol; ad 10 mL MilliQ water; addition of bromophenol blue until the characteristic blue color appears) and incubated for 10 min at 95 °C. The SDS polyacrylamide gels (15%) were divided into a stacking and a separation gel (Tab. 28).

Table 28: SDS polyacrylamide gel (15%).

	Separation gel (mL)	Stacking gel (mL)
1 M Tris-HCl pH 8.8	1.95	-
1 M Tris-HCl pH 6.8	-	0.235
MilliQ water	0.275	1.27
30% Acrylamide/Bis-acrylamide (29:1)	2.41	0.480
10% SDS	0.0545	0.02
100% TEMED	0.002725	0.001
10% APS	0.078	0.04

The SDS-PAGE was run in 1X SDS buffer (25 mM Tris, 192 mM glycine, 0.1 % SDS) at 80-200 V and RT. Generally, 25 μ g of protein were loaded to the PAGE and PageRuler™ prestained protein ladder (Thermo Fisher Scientific, Waltham, MA) was used as a marker.

For visualization of proteins, the gels were incubated in staining solution (0.25 % (w/v) Coomassie Blue R-250, 5% (v/v) acetic acid, 50% (v/v) ethanol) for 20 min and destained in water over night (covered with paper tissue to absorb the coomassie). The gels were stored in water.

ii. Blue native polyacrylamide gel electrophoresis

Blue native PAGEs (BNPs) were performed in a cold room under oxic conditions or in an anaerobic chamber with N₂-atmosphere using NativePAGE™ Novex® 4-16% Bis-Tris gels in the XCell SureLock® Mini Cell (Life Technologies, Carlsbad, CA). The anode and the dark blue cathode buffer were prepared as recommended by the NativePAGE™ Running Buffer kit. When the experiment was performed under strict anoxic conditions, all the buffers were previously flushed with N₂ gas and all steps excluding the staining process were done in an anaerobic chamber. If not indicated differently, 30 µg of total protein were loaded. The loaded samples were prepared according to the NativePAGE™ Sample Prep kit (Life Technologies, Carlsbad, CA). The cell pellets were resuspended in 1X NativePAGE™ sample buffer containing 1% (w/v) n-dodecyl-β-D-maltoside (DDM) (Life Technologies, Carlsbad, CA) following 3-4 cycles of sonication (see Materials and Methods 2.4.3). Moreover, the samples were supplemented with 0.25% of NativePAGE™ G-250 Sample Additive (Life Technologies, Carlsbad, CA). NativeMark™ Unstained Protein Standard (Life Technologies, Carlsbad, CA) served as marker. The electrophoresis ran for 1 h at 150 V, and 1 h at 250 V. For visualization of proteins, the gels were stained overnight using the Colloidal Blue Staining kit following the manufacturer's protocol (Life Technologies, Carlsbad, CA).

2.7.3 Extraction of proteins from BNPs

For a separation of native proteins from BNPs in SDS-PAGEs (see Materials and Methods 2.7.2), an established extraction method was performed (Tang et al., 2013). The extracted proteins were concentrated by an Amicon Ultra Centrifugal filter with a 3 kDa cutoff (Millipore, Billerica, MA).

2.7.4 *In vitro* protein interaction analysis (Pull-down experiment)

For the pull-down experiments, the purified GST-N47_K27540 (see Materials and Methods 2.7.1) was incubated with N47 cell-free extracts from cells either grown on naphthalene or 2-methylnaphthalene (see Materials and Methods 2.4.3).

The GST-N47_K27540 coupled to the Glutathione Sepharose beads stored at -20 °C was washed with 1X PBS buffer (140 mM NaCl, 2.7 mM KCl, 10 mM Na₂HPO₄, 1.8 mM KH₂PO₄, pH 7.3) and 120 µL of the slurry were incubated for 4 h at 4 °C with 500 µL of the respective cell-free extract on an end-over-end rotator. After three washing steps (1X PBS, 5 min, 4 °C), 30 µL beads were combined with 5X SDS-PAGE loading dye and analyzed via SDS-PAGE (see Materials and Methods 2.7.2). In control experiments, GST alone coupled to Glutathione Sepharose beads and the affinity chromatography matrix were used to check for false positive protein interactions.

2.8 Enzyme assays

2.8.1 Naphthalene carboxylase enzyme assays

The naphthalene carboxylase activity assay was performed as described previously by Mouttaki et al. (2012).

The naphthalene carboxylase activity assay was carried out at 30 °C, while shaking in a Thermomixer[®] (850 rpm; Eppendorf, Hamburg, Germany) under strictly anoxic conditions. The total assay volume of 220 µL contained: 110 µL saturated naphthalene solution or 2-naphthoic acid (exchange reaction; concentrations are indicated) and 25 mM freshly prepared ¹³C-labeled NaHCO₃ (optional: 2.5-5 mM ATP and 5-15 mM MgCl₂, 20 mM KCl) in 150 mM MOPS/KOH, pH 7.3. The reaction was started by the addition of 50 µL cell-free/crude-extracts or whole cells. At the indicated time points, 50 µL sample were taken and the reaction stopped by addition of 10 µL 10% formic acid (LC-MS/MS) or 100 µL methanol (UPLC analysis, see Materials and Methods 2.6.3). After centrifugation (14,000 rpm, 4 °C, 20 min), 45 µL supernatant were mixed with 90 µL MilliQ water and the formation of ¹³C-2-naphthoic acid was analyzed by LC-MS/MS. The LC-MS/MS analyses was carried out on an Agilent 1200 HPLC system coupled to an Applied Biosystems Q-Trap mass spectrometer equipped with a TurboSpray ionization source. The used method and parameters are given in Mouttaki et al. (2012).

2.8.2 Naphthoate-CoA ligase enzyme assay

The naphthoate-CoA ligase activity assay was carried out at 30 °C, while shaking in a Thermomixer[®] (850 rpm; Eppendorf, Hamburg, Germany) under strictly anoxic conditions. The total assay volume of 220 µL contained: 2.5-5 mM ATP, 5-15 mM MgCl₂, 0.2 mM 2-naphthoic acid and 0.5 mM CoASH in 100 mM MOPS/KOH, pH 7.3. The reaction was started by the addition of 50 µL cell-free extract from N47 cells. At the indicated time points,

50 μ L sample were taken and the reaction stopped by addition of 100 μ L methanol. The samples were analyzed by UPLC (for analysis and sample preparation see Materials and Methods 2.6.3).

3. Results

Project 1

Identification of naphthalene carboxylase subunits of N47

Polycyclic aromatic hydrocarbons are chemically very stable molecules. Whereas the functionalization of PAHs in presence of oxygen is catalyzed by oxygenases, anaerobic bacteria have to develop alternative strategies to overcome the high resonance energy of the aromatic ring system. The anaerobic activation of such chemically stable molecules is biochemically very challenging. However, sulfate-reducing bacteria have developed a strategy to activate the model compound naphthalene. Initial investigations have indicated a carboxylation reaction as the first step in the anaerobic degradation of naphthalene (Zhang and Young, 1997; Meckenstock et al., 2000; Musat et al., 2009). Recently, the carboxylation reaction was biochemically characterized in crude extracts of the sulfate-reducing culture N47 (Mouttaki et al., 2012). Moreover, previous proteogenomic studies on N47 and the marine naphthalene-degrading strain NaphS2 allowed the identification of a gene cluster which products were suggested to be carboxylase-like subunits, potentially involved in the initial reaction of naphthalene degradation (DiDonato et al., 2010; Bergmann et al., 2011b). The aim of the main project of the present study was to identify the subunits of the naphthalene carboxylase complex in the sulfate-reducing culture N47.

3.1 Native purification of naphthalene carboxylase of N47

3.1.1 Small scale purification using the 'ÄKTAmicro' system under strict anoxic conditions

In order to identify the naphthalene carboxylase, the enzyme should initially be purified from cell-free extracts of naphthalene-grown N47 cells using the chromatography system 'ÄKTAmicro' (GE Healthcare Europe, Freiburg, Germany). Due to the low biomass obtained by N47, it was important to use a system that can be operated using low flow rates and allowing the collection of elution fractions on a microliter scale. Moreover, a small total dead volume (e.g. within the UV cell and the capillaries) of the chromatography system was necessary to keep the loss of sample volume as low as possible. Due to the high sensitivity of the enzyme towards oxygen (Mouttaki et al., 2012), it was crucial to operate the system under strict anoxic conditions. The original setup of the chromatography system 'ÄKTAmicro' was therefore modified and adapted as follows (technical support was kindly provided by Dr. Lars Brise; GE Healthcare, München, Germany).

Initially, the 'ÄKTAmicro' was transferred into the anaerobic chamber (Coy Laboratory Products, Grass Lake, MI) as purchased from GE Healthcare Europe. However, due to an extreme temperature increase within the anaerobic chamber while running the system, it was decided to disassemble and to partially transfer the purification system.

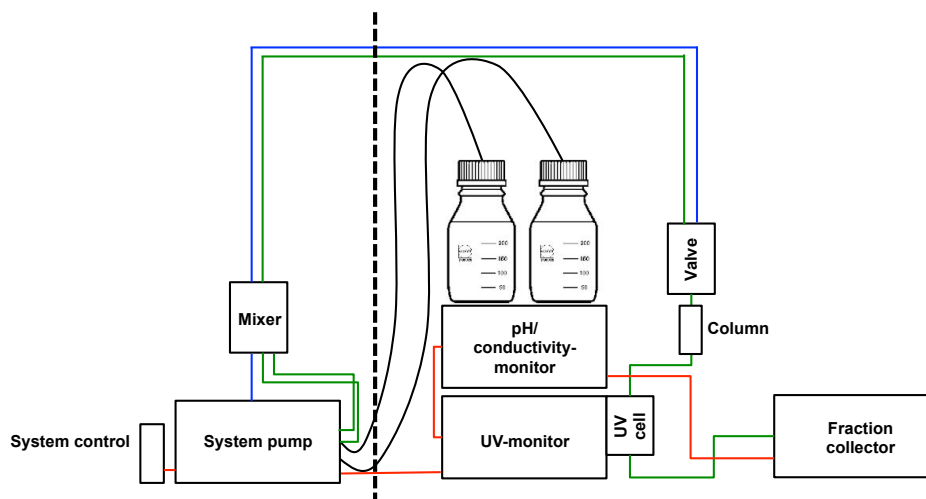


Figure 14: Schematic of the modified 'ÄKTAmicro' system for anaerobic purification. The dotted line represents the wall of the Coy anaerobic chamber (Coy Laboratory Products, Grass Lake, MI). The color code for the used tubing is as follows: red, UniNet1 (GE Healthcare Europe, Freiburg, Germany); blue, UniNet2 (GE Healthcare Europe, Freiburg, Germany); green, 1/16'' PEEK capillary; black, 1/8'' Teflon tubing. Further details are given in the text.

The main control unit, the system pump and the mixer remained outside, whereas the pH- and conductivity monitor, the UV-monitor and the fraction collector were transferred into the anaerobic chamber (Fig. 14, 15). Even though the pumps remained outside, the buffers were stored inside the anaerobic chamber and connected to the outside valves and the pump via Teflon tubings. However, to minimize the potential sites for oxygen penetration, the Teflon tubings were directly connected to the outlet of the valves bypassing the switch.

The two cables, two Teflon tubings and one capillary, connecting the system control, the system pump and the mixer with the elements in the anaerobic chamber, were inserted into a rubber stopper. The rubber stopper was plugged into the wall of the anaerobic chamber and tightly sealed with a two-component epoxy resin (UHU PLUS ENDFEST 300; UHU, Brühl, Germany) and hot glue (Fig. 15, B.).

The newly assembled 'ÄKTAmicro' allowed protein purification in small scale under strict anoxic conditions without a significant temperature increase in the anaerobic chamber.

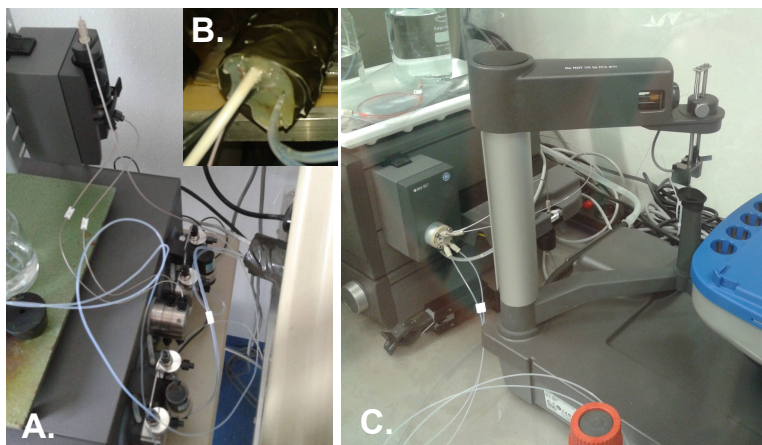


Figure 15: Modified 'ÄKTAmicro' system for anaerobic purification. A. The pump system and mixer outside of the glove box. B. The rubber stopper with the inserted tubings sealed with two-component epoxy resin. The rubber stopper was frozen in liquid nitrogen to permit accurate drilling. C. View inside the anaerobic chamber with the UV-monitor (plus UV cell), pH/ conductivity monitor, valve and fraction collector.

3.1.2 Storage of N47 and NaphS2 cells

In previous studies on naphthalene carboxylase, the enzyme activity could be measured only from freshly harvested N47 cells (Mouttaki et al., 2012). However, to allow the purification of the naphthalene carboxylase from cell-free extracts of naphthalene-grown N47 cells (native purification), high amounts of biomass were required. Due to the limited energy available for the sulfate-reducing enrichment culture N47 when growing with naphthalene as a carbon source, experiments were always limited by the biomass. Out of a 150 mL-culture containing exponentially grown N47 cells, only a few milligrams of biomass were harvested, corresponding to a total protein content of 1 up to 5 mg. Therefore, collection and storage of the cells would increase the available biomass for the purification process. Moreover, it would allow to grow N47 and NaphS2 cells in bigger batches, for example in a 200-liter fermenter, and to store viable material for further use.

To maintain the cell integrity and to protect the unstable naphthalene carboxylase, cryoprotectants were added before freezing the cells at $-80\text{ }^{\circ}\text{C}$. Exponentially grown N47 cells were harvested under anoxic conditions (see Material and Methods 2.4.3, ii.) and resuspended in buffer containing 2.5-7% DMSO or 10-12% glycerol. In parallel, the exponentially grown cells from another naphthalene degrader NaphS2 were treated the same way. In the control experiment, no cryoprotectant was added to the N47 and NaphS2 cells. After storage at $-80\text{ }^{\circ}\text{C}$, the naphthalene carboxylase activity (see Material and Methods 2.8.1) was not detectable in N47 or NaphS2 cell extracts. In the case of N47, the cells broke open during the freezing process and the cryoprotectant could therefore not be

removed from the cell-free extract. However, the naphthalene carboxylase activity could also not be detected in non-treated cells.

The cryoprotectants were added to reduce the freezing point of the mixture and thereby allowing a slower cooling rate. A slower cooling rate may avoid the formation of ice crystals, which can destroy cell membranes, proteins, and enzyme complexes. In a second experimental setup, the cells treated with cryoprotectant were frozen in a container filled with isopropanol (Nalgene® Mr. Frosty®) to provide a more controlled temperature decrease (1 °C/min). This method is commonly used in cell biology to freeze sensitive eukaryotic cells.

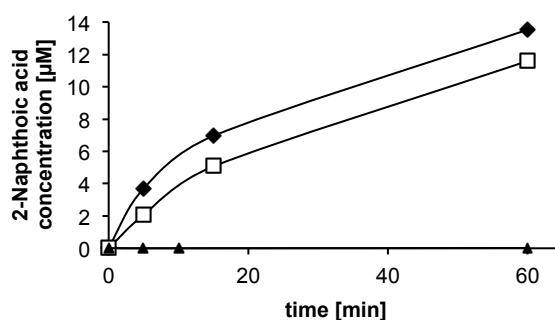


Figure 16: Time-resolved production of 2-[carboxyl- ^{13}C]naphthoic acid by whole NaphS2 cells before (◆) and after freezing (□) with 5% DMSO and without DMSO (▲) in an isopropanol-filled container. The activity of naphthalene carboxylase was determined within the first 5 min as a function of total protein added.

The isopropanol-filled container, including the treated and non-treated N47 and NaphS2 cells, was incubated at $-20\text{ }^{\circ}\text{C}$ for 12 h and then stored at $-80\text{ }^{\circ}\text{C}$ for a minimum of 8 h. After the freezing process, naphthalene carboxylase activity was only detected in NaphS2 cells frozen with 5% DMSO (Fig. 16). Specific naphthalene carboxylase activities of $0.66\text{ nmol min}^{-1}\text{ mg}^{-1}$ of protein and $0.28\text{ nmol min}^{-1}\text{ mg}^{-1}$ of protein were detected before and after freezing, respectively, indicating a recovery of 42% of the activity after freezing. In absence of cryoprotectant, naphthalene activity was completely lost from the NaphS2 cells (Fig. 16). Under the tested conditions mentioned above and unlike NaphS2, the naphthalene carboxylase activity could not be recovered in N47 cells after freezing with or without DMSO. Based on these results, all the experiments in the present study involving measurements of naphthalene carboxylase activity were performed using freshly harvested cells.

3.1.3 Cell lysis methods and naphthalene carboxylase activity

The naphthalene carboxylase reaction could recently be measured by Mouttaki et al. (2012). It was shown that the enzyme converts naphthalene and ^{13}C -labelled bicarbonate to 2-[carboxyl- ^{13}C]naphthoic acid at a rate of $0.12 \text{ nmol min}^{-1} \text{ mg}^{-1}$ of protein in crude cell extracts of N47. Additionally, it exhibits an isotopic exchange capability. The naphthalene carboxylase enzyme assay was measured in non-centrifuged cell extracts opened with lysozyme.

Even though naphthalene carboxylase activity was previously described as ATP-independent, all enzyme assays described in the following paragraph included ATP with a final concentration of 2-10 mM. In the following, crude extract is defined as a non-centrifuged solution after cell lysis whereas cell-free extract describes the supernatant of a crude extract after a centrifugation step. In contrast to cell-free extracts, crude extracts can potentially contain closed cells.

In order to purify the enzyme under native conditions from N47 cells (see Results 3.1.1), it was necessary to obtain clarified and active cell-free extracts. For this purpose, the cells were opened with lysozyme and centrifuged (see Material and Methods 2.4.3, ii.). After centrifugation, up to 96% of the naphthalene carboxylase activity was found in the non-soluble pellet fraction, however, the enzyme activity was not detectable in the supernatant. Different opening techniques such as sonication, bead beating or treatment with different detergents were tested to receive cell-free extracts and to preserve the naphthalene carboxylase activity in the meantime (see Material and Methods 2.4.3, ii.).

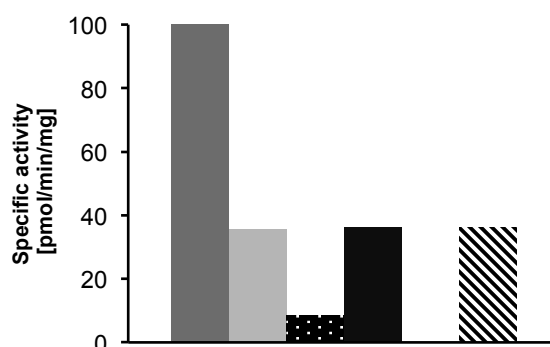


Figure 17: Naphthalene carboxylase activity in N47 after cell lysis using bead beating. The specific activity of naphthalene carboxylase was determined within the first 5 min as a function of total protein added. Different fractions during the cell lysis were used to measure the activity: dark grey, whole N47 cells before lysis (control); light grey, crude extract after bead beating at 20 m/s for 10 s; dotted, crude extract after two times bead beating at 20 m/s for 20 s; black, pellet after two times bead beating at 20 m/s for 20 s; grey, cell-free extract after two times bead beating at 20 m/s for 20 s (no activity); striped, pellet after two times bead beating at 20 m/s for 20 s and proteinase K treatment.

In sonicated samples, up to 80% of the enzyme activity could be measured in the pellet fraction, however, the activity was below the detection limit in the supernatant.

In samples which were opened by bead beating, up to 70% of the naphthalene carboxylase activity was lost after the first cycle (20 m/s, 10 s; Fig. 17). After two following cycles, the cells were completely lysed, however, only around 10% of the activity was preserved in the crude extract. The crude extract was centrifuged and approximately 30% of the initial specific activity was detected in the pellet fraction while the cell-free extract showed no naphthalene carboxylase activity. After treating the pellet fraction with proteinase K, a significant change in activity could not be observed.

In addition, when treating N47 with different types of detergents, naphthalene carboxylase activity could not be detected in the soluble fraction of any of the samples (see Material and Methods 2.4.3, ii.).

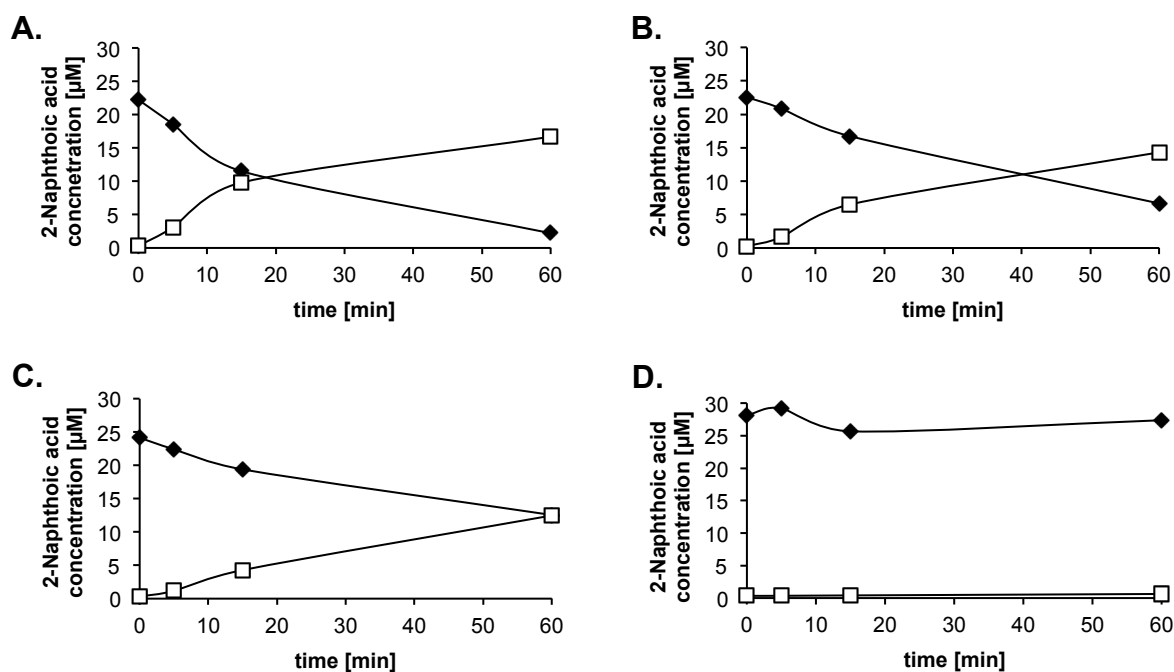


Figure 18: Isotope exchange reaction catalyzed by the naphthalene carboxylase of N47 cells after cell lysis by bead beating. The ¹²C-carboxyl moiety was exchanged with a labeled ¹³CO₂ originating from the H¹³CO₃⁻-containing buffer. Time-resolved decrease of 2-[carboxyl-¹²C]naphthoic acid (◆) with simultaneous stoichiometric production of 2-[carboxyl-¹³C]naphthoic acid (□). **A.** Isotopic exchange reaction in whole N47 cells. **B.** Isotopic exchange reaction in crude extract after bead beating at 20 m/s for 10 s. **C.** Isotopic exchange reaction in the pellet fraction after bead beating at 20 m/s for 10 s. **D.** Isotopic exchange reaction in cell-free extract after bead beating at 20 m/s for 10 s.

Also, the isotopic exchange reaction of naphthalene carboxylase (Mouttaki et al., 2012) could not be measured in the centrifuged supernatants of N47 cells opened by lysozyme, sonication, bead beating or various detergents, while it could still be detected within the pellet fraction. Figure 18 shows the loss of the isotopic exchange activity during cell lysis by bead beating.

Cell membrane and naphthalene carboxylase activity

After cell lysis, the naphthalene activity could only be detected in the pellet fraction (Fig. 17, 18) presumably due to the fact that entire cells remained in the extract. To investigate whether the naphthalene carboxylase may be a membrane-associated enzyme, the pellet fraction was incubated with NaCl of concentrations varying from 100 up to 500 mM after a bead beating treatment (20 m/s, 15 s). As previously established, membrane-associated enzymes can be released from the membrane by a treatment with high ionic strength buffers. However, after an additional centrifugation step, naphthalene carboxylase activities could not be detected in the supernatant fractions.

Additionally, the effect of sodium chloride on the naphthalene carboxylase activity was analyzed on whole cells of N47. Here, it could be shown that even comparatively low concentrations of sodium chloride inhibited the naphthalene carboxylase activity (Fig. 19).

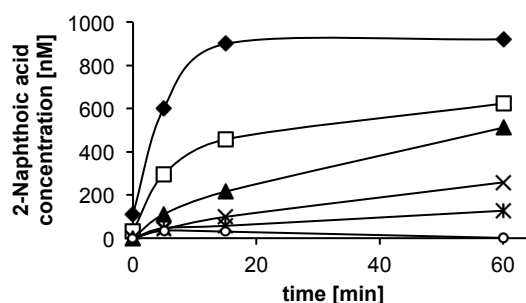


Figure 19: Effect of NaCl on the naphthalene carboxylase activity in whole N47 cells. Time-resolved production of 2-[carboxyl-¹³C]naphthoic acid with no additional (◆), 100 mM (□), 200 mM (▲), 300 mM (×), 400 mM (*) and 500 mM (○) NaCl in the assay buffer.

Moreover, it could not be excluded that naphthalene carboxylase activity detected in the pellet fraction was exclusively measured in intact cells. If indeed the naphthalene carboxylase activity could only be measured in whole cells, a correlation between the enzyme activity and the membrane potential would be possible. To test whether the membrane-integrity was essential for naphthalene carboxylase activity, the cells within the pellet, which showed naphthalene carboxylase activity, were stained with two dyes and

analyzed by flow cytometry. SYBR[®] Green was used to determine the total amount of N47 cells while propidium iodide, which cannot diffuse through intact membranes, was used to stain the DNA of dead cells only (cells without membrane potential). Subsequently, the loss of naphthalene carboxylase activity should be correlated with the amount of intact cells. Due to cell debris within the sample, a high background was detected during flow cytometry. Therefore, the method could not be used to determine whether naphthalene carboxylase activity located in the pellet fraction was based on whole-cell measurements.

Naphthalene carboxylase in cell-free extract generated by a French Press

A French Press treatment of cells represents the most efficient and gentle cell lysis method. However, this method was limited by the low available biomass and the opportunity to use the required equipment under strict anoxic conditions. As a consequence, alternative strategies were developed to identify the naphthalene carboxylase subunits of N47. Nevertheless, at the end of the present PhD project, in October of 2014, N47 cells from a 200L-fermenter were available in the group of Prof. Dr. Matthias Boll at the Albert-Ludwigs University Freiburg. N47 cells were harvested from the fermenter and opened by a French Press where the naphthalene carboxylase activity could be measured (Fig. 20, see Material and Methods 2.4.3, ii.). The used N47 cells were in the late-exponential phase of growth (personal communication, Sebastian Estelmann and Philip Weyrauch).

For the first time, naphthalene carboxylase activity could be detected in cell-free extracts (Fig. 20). Surprisingly, unlike what was observed earlier, the activity was 5-fold higher in the presence of 5 mM ATP. The assay buffer (100 mM MOPS/KOH, pH 7.3) contained K⁺, however, in the presence of additional 20 mM potassium chloride and 5 mM ATP activity could be enhanced from 2 (no additives) to 12 pmol min⁻¹ mg⁻¹ protein. The pellet fraction did not show any naphthalene carboxylase activity.

According to these results, naphthalene carboxylase is most likely an ATP-dependent soluble enzyme. Notwithstanding, the detected specific activity of 12 pmol min⁻¹ mg⁻¹ of protein in cell-free extracts in the presence of ATP and potassium chloride was low compared to the previously measured 120 pmol min⁻¹ mg⁻¹ of protein in crude extracts of N47 (Moultaki et al., 2012).

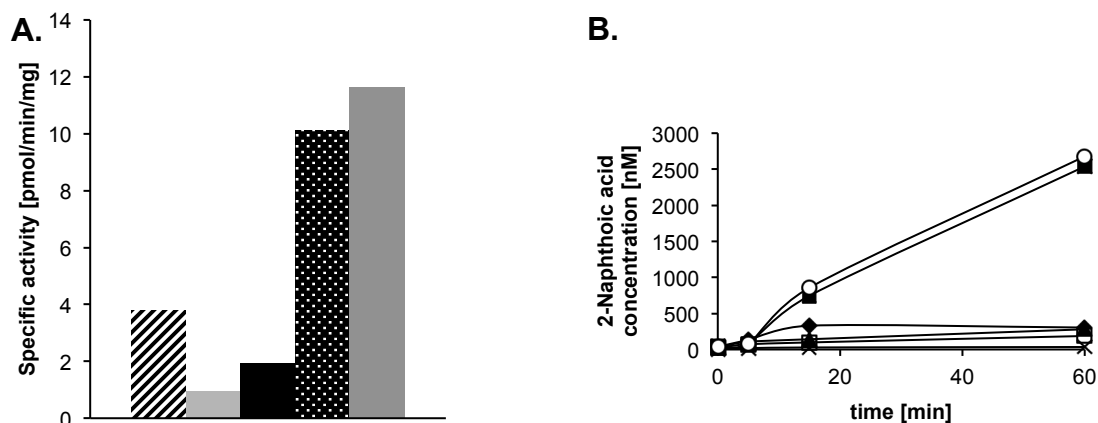


Figure 20: Naphthalene carboxylase activity after cell lysis using a French Press. **A.** The specific activity of naphthalene carboxylase was determined within the first 15 min as a function of cell extract added. Different fractions after the cell lysis were used to measure the activity: striped, whole N47 cells; light grey, crude extract after French Press; black, cell-free extract after 45K centrifugation; dotted, cell-free extract plus 5 mM ATP; dark grey, cell-free extract plus 5 mM ATP and 20 mM potassium chloride). **B.** Time-resolved production of 2-[carboxyl- ^{13}C]naphthoic acid in whole N47 cells (◆), crude extract after cell lysis using the French Press (□), the pellet fraction after 45K centrifugation (×), cell-free extract after 45K centrifugation (▲), cell-free extract plus 5 mM ATP (■), cell-free extract plus 5 mM ATP and 20 mM potassium chloride (○).

To determine naphthalene carboxylase activity, so far, the formation of 2-[carboxyl- ^{13}C]naphthoic acid was routinely analyzed by LC-MS/MS (see Material and Methods 2.8.1). In Prof. Boll's laboratory in Freiburg, the samples were additionally analyzed by UPLC (see Material and Methods 2.6.3). Using the UPLC, it was not possible to detect the low concentration of formed 2-naphthoic acid within the samples, however, a time-dependent formation of CoA esters was observed (Fig. 21). In naphthalene carboxylase activity assays containing 5 mM ATP but no additional free Coenzyme A (CoASH), NCoA was formed most likely by 2-naphthoate CoA-ligase and partially further converted by NCR and DHNCR to THNCoA (see Introduction 1.3.2; Fig. 21, A.; Fig. S1). A further reduction of THNCoA to HHNCoA was not observed. After 90 min of incubation (Fig 21, A.), the NCoA concentration within the sample decreased.

Coenzyme A within the cell is limited. Therefore, CoASH was added in the naphthalene carboxylase assay to stimulate the ligase activity (Fig. 21, B.). Due to the direct consumption of the formed 2-naphthoic acid, addition of CoASH might also enhance naphthalene carboxylase activity. Again, NCoA was formed but the concentration did not change compared to assays without CoASH, however, the concentration of NCoA stayed constant after 90 min.

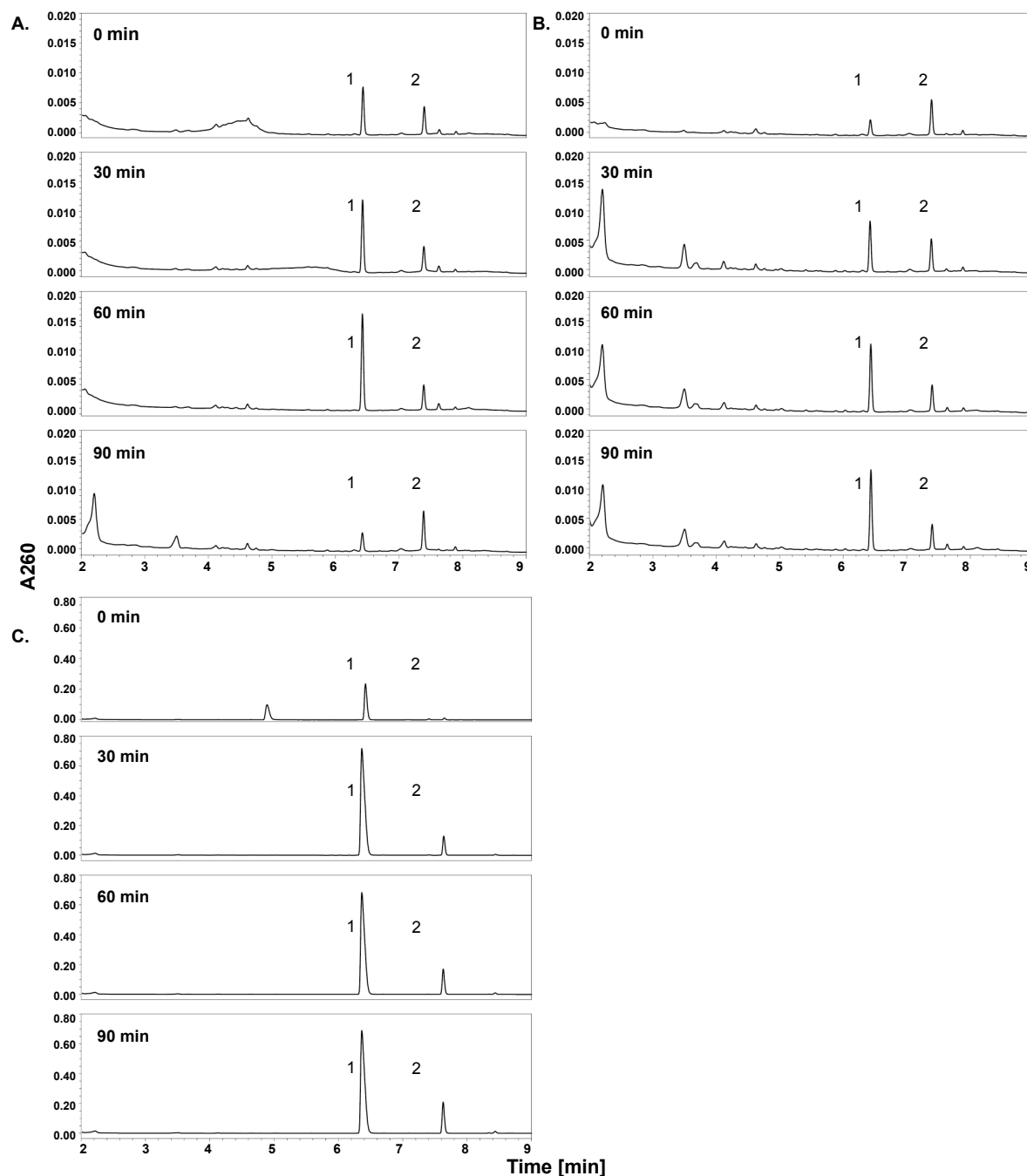


Figure 21: UPLC analyses of produced CoA-esters in the naphthalene carboxylase (A. and B.) and 2-naphthoate-CoA ligase (C.) enzyme assays. In the naphthalene carboxylase enzyme assay **A.** and **B.**, naphthalene was used as the substrate whereas in the 2-naphthoate-CoA ligase enzyme assay **C.** 2-naphthoic acid was added. Time-resolved formation of NCoA and THNCoA in the naphthalene carboxylase activity assay in the absence (**A.**) and in presence (**B.**) of CoASH. **C.** Time-resolved formation of NCoA and THNCoA in the 2-naphthoate-CoA ligase activity assay. All enzyme assays contained 5 mM ATP and 50 μ L of cell-free extract (identical batch). 1; NCoA. 2; THNCoA.

During the naphthalene carboxylase activity assays (Fig. 21, A./ B.), the increase of NCoA and THNCoA was negligible. To support that the CoA esters were produced due to additional enzyme activities in the same cell-free extract, a ligase assay containing 2-naphthoic acid rather than naphthalene as a substrate, ATP and free CoASH was conducted (see Material and Methods 2.8.2, Fig. 21, C.). Figure 21, C. shows the time-dependent formation of NCoA and THNCoA during the ligase assay (the compounds formed i.e. NCoA and THNCoA, have the same retention time than the observed compounds formed during the naphthalene carboxylase assay).

2-naphthoate CoA-ligase activity during the isotopic exchange reaction assay

When low concentrations of 2-[carboxyl- ^{12}C]naphthoic acid ($>5\ \mu\text{M}$) were used to investigate the isotopic exchange reaction of naphthalene carboxylase, an increase in the produced 2-[carboxyl- ^{13}C]naphthoic acid was observed until 5 min of incubation time of the assay mixture (Fig. 22). In contrast to the isotopic exchange reaction assays with higher concentrations of 2-[carboxyl- ^{12}C]naphthoic acid (Fig. 18), here the concentration of labeled 2-naphthoic acid did not stay constant but decreased again. Interestingly, simultaneous production of non-labeled 2-naphthoic acid could neither be detected. After 60 min of incubation, non-label and labeled 2-naphthoic acid were depleted.

This finding may indicate the potential decarboxylation reaction (back reaction of naphthalene carboxylase). However, naphthalene could not be detected in any of these samples (personal communication, Dr. H. Mouttaki). Considering the unidirectionality of naphthalene carboxylase and the formation of NCoA during the naphthalene carboxylase activity assay, the described loss of 2-naphthoic acid was potentially due to 2-naphthoate CoA-ligase activity in the N47 cells.

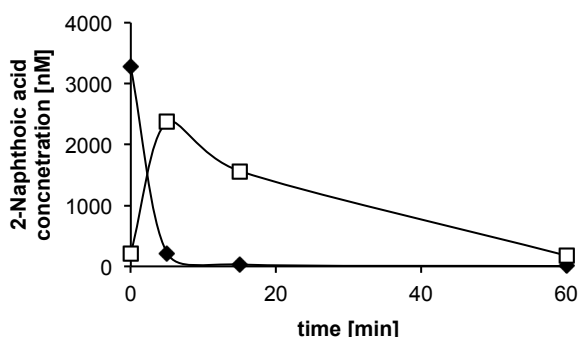


Figure 22: Isotope exchange reaction catalyzed by the naphthalene carboxylase on whole cells. Time-resolved decrease of 2-[carboxyl- ^{12}C]naphthoic acid (◆) and simultaneous production of 2-[carboxyl- ^{13}C]naphthoic acid (□).

3.2 Transcriptional analysis – Operon mapping by RT-PCR

Previous proteogenomic studies were carried out with N47 and NaphS2 and they allowed the identification of a gene cluster in which some of the products shared sequence similarity with carboxylase-like subunits and were therefore suggested to be potentially involved in the initial reaction of naphthalene degradation (DiDonato et al., 2010; Bergmann et al., 2011b) (see Introduction, Fig. 5). The gene products encoded within the putative naphthalene carboxylase gene clusters of N47 and NaphS2 shared sequence identities of up to 84% among each other (see Introduction, Fig. 5). In order to identify which genes within the cluster belong to a transcriptional unit, messenger RNA was extracted from naphthalene-grown N47 cells, retrotranscribed into cDNA and a PCR was conducted using primers covering genes and intergenic regions to identify the extent of the potential operon in N47.

3.2.1 RNA extraction and RT-PCR

The total RNA was extracted from 150 mL culture of N47 cells with naphthalene as substrate in the mid-exponential phase of growth (7 weeks) by two independent methods (see Material and Methods 2.5.6). In both described methods, mRNA was successfully extracted from N47 cells, however, the ‘classical’ hot phenol preparation was more efficient as higher RNA yields were obtained. After extraction, the RNA was treated with DNAase in order to remove residual genomic DNA (gDNA) and retrotranscribed into cDNA using random hexamer primers (see Material and Methods 2.5.7). To confirm a successful retrotranscription, the synthesized cDNA was used as a template to amplify a region of mRNA retrotranscribed within an open reading frame. The gene *N47_K27520* (921 bp) is part of the naphthalene carboxylase gene cluster in N47 and its gene product was shown to be up-regulated in naphthalene-grown N47 cell (Bergmann et al., 2011b). Figure 23 shows the results of the gene-specific PCRs targeting *N47_K27520*. When no reverse transcriptase was added to the RT-PCR reaction, no amplicon was produced during the subsequent gene-specific PCR (lane 1/2) indicating that the reactions were not contaminated with genomic DNA (gDNA). In reactions using synthesized cDNA as template, the expected amplicon with a size of around 1 kbp was amplified, suggesting a successful RT-PCR. The synthesized cDNA was used for the following operon mapping approach.

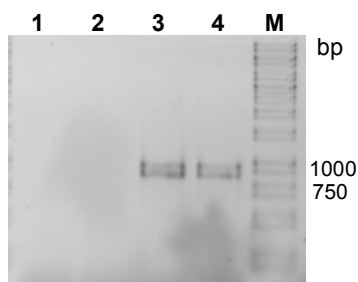


Figure 23: Results of gene-specific PCRs targeting *N47_K27520* used as a control to confirm successful RT-PCR. A 1.5% agarose gel stained with GelRed was used. Lane 1 and 2, controls for potential genomic DNA contamination in cDNA template (no addition of reverse transcriptase during RT-PCR, negative control); lane 3 and 4, gene-specific PCR (*N47_K27520*) on cDNA template (addition of reverse transcriptase during cDNA synthesis, positive control); M, DNA ladder. In the RT-PCR random hexamer primers were used.

The amplification of fragments with sizes superior to 1 kbp was not possible from cDNA templates which were synthesized using random hexamer primers. To produce longer and at the same time more specific cDNA, specific reverse primers targeting the naphthalene carboxylase gene cluster were used in the RT-PCR reaction (see Material and Methods, Tab. 7, reverse primer 1-4).

3.2.2 Operon mapping

In the last step of the transcriptional analyses, PCRs were done using primers covering genes and intergenic regions to identify the extent of a potential operon (see Material and Methods, Tab. 7). The gene cluster of N47 was compared to the one found in the other naphthalene degrader NaphS2 and the sequences for genes *N47_K27540* (see Appendix, Fig. A2), *N47_K27510*, and *N47_K27480* were changed (see Appendix, Fig. A10). For the molecular work performed in this study, the new sequences were used.

Amplicons were obtained between *N47_K27540* and *N47_K27520* (Fig. 24, 1), *N47_K27520* and *N47_K27500* (Fig. 24, 2), *N47_K27500* and *N47_K27480* (Fig. 24, 3) and between *N47_K27480* and *N47_K27460* (Fig. 24, 4). The two following genes namely *N47_K27450* and *N47_K27440* were as well identified within the naphthalene carboxylase gene cluster in NaphS2. However, no amplicons were obtained between *N47_K27460* and *N47_K27440* and between *N47_K27460* and *N47_K27450* (Fig. 24, 5/ 5.1).

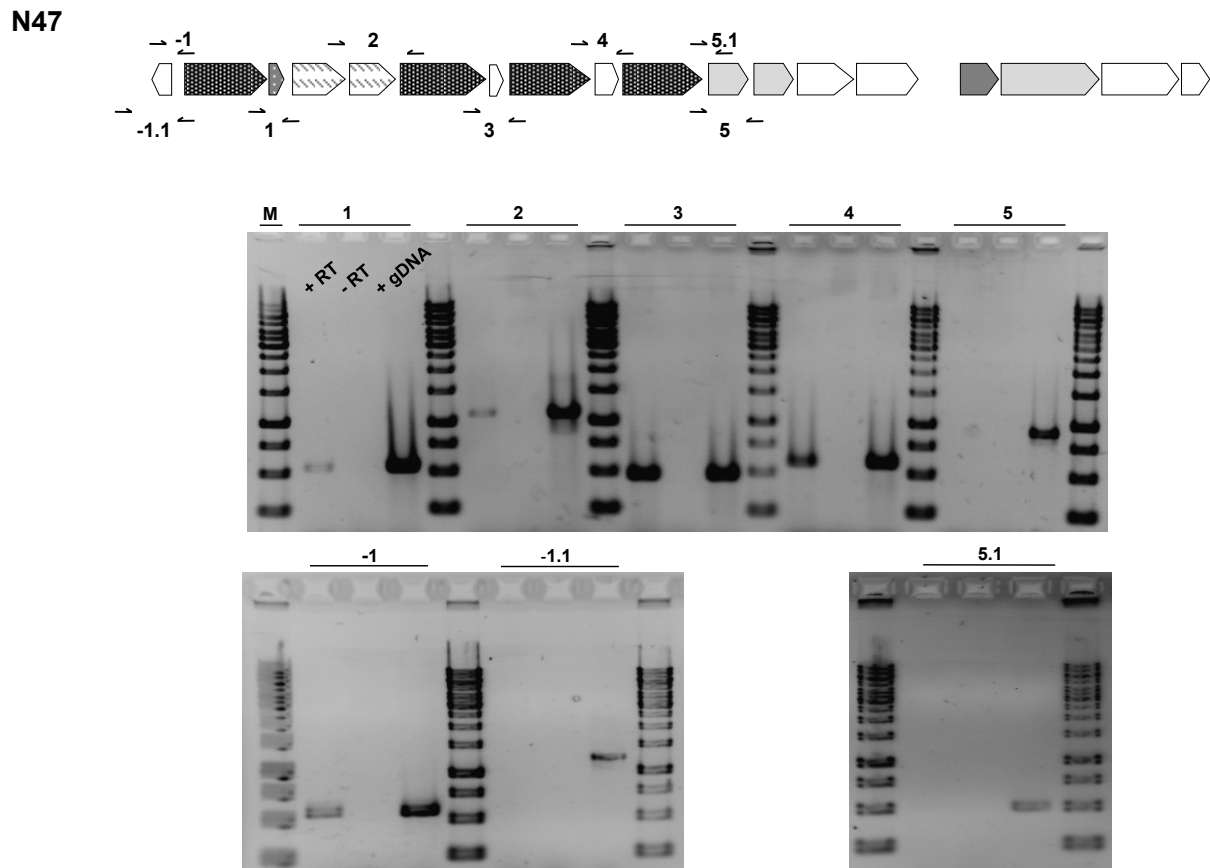


Figure 24: Transcriptional analysis by RT-PCR and subsequent gene-specific PCR. Top, organization of the gene cluster potentially involved in anaerobic degradation of naphthalene (*N47_K27550* to *N47_K27380*). The arrows represent the locations of the used primer sets. Open reading frames which products show similarity to UbiD-like carboxylases are filled in black, non-carboxylase-like subunits are shown in grey. Bottom, results of gene-specific PCRs using three different templates per primer set (+RT, gene-specific PCR on cDNA template (addition of reverse transcriptase during cDNA synthesis); -RT, control for potential genomic DNA contamination in cDNA template (no addition of reverse transcriptase during RT-PCR); + gDNA, gene-specific PCR on genomic DNA (positive control)). A 1.5% agarose gel stained with GelRed was used. M, DNA ladder; numbers, represent the used primer set. In the RT-PCR random hexamer primers were used.

The transcriptional analysis indicated that the genes potentially encoding the naphthalene carboxylase subunits were organized in the form of an operon within the putative naphthalene carboxylase gene cluster previously mentioned (Bergmann et al., 2011b). The operon coding for the genes involved in the carboxylation of naphthalene included genes from the carboxylase-like gene *N47_K27540* to the fourth carboxylase-like gene *N47_K27460* (Fig. 27) and covered around 8.9 kb including nine genes.

In this study, cDNA was used as a template to amplify intergenic regions to identify the size of the naphthalene carboxylase operon. However, the used primers should hybridize at the beginning of a gene to avoid false positive amplicons. Indeed, if the primer hybridized with a region within the regulatory region of the following gene (Fig. 25), a PCR product will be obtained, even though this particular gene does not belong to the operon. Therefore, we repeated the aforementioned experiment with new forward primers (see Material and Methods, Tab. 7, primer set 1A-4D). The obtained fragments (Fig. 26) confirmed the data of the initial transcriptional analysis (Fig. 24).

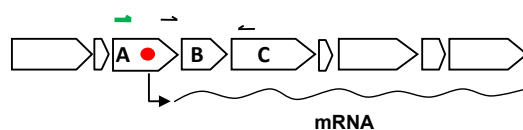


Figure 25: Potential false positive results during the operon mapping approach. The initially used forward primer is shown in black and the newly designed primer in green. The red dot represents the transcriptional start of the polycistronic mRNA obtained together from gene B and gene C. In contrast to the newly designed primer set, the initially used primer would bind to the regulatory region of the following gene leading to an amplicon even though gene A was not part of the polycistronic mRNA.

Furthermore, we tried to amplify the whole operon with its length of 8.9 kbp. The amplification of such a huge fragment worked already poorly with genomic DNA and could not be amplified in reactions with cDNA as template.

N47

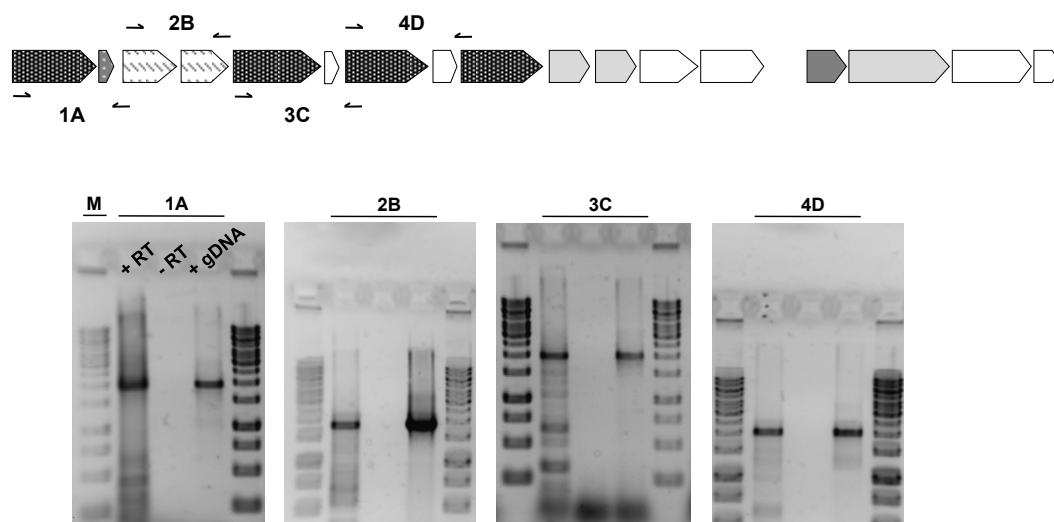


Figure 26: Transcriptional analysis by RT- and subsequent gene-specific PCR. Top, organization of the gene cluster potentially involved in anaerobic degradation of naphthalene (*N47_K27550* to *N47_K27380*). The arrows represent the locations of the used primer sets. Open reading frames which products show similarity to UbiD-like carboxylases are filled in black, non-carboxylase-like subunits are shown in grey. Bottom, results of gene-specific PCRs using three different templates per primer set (+RT, gene-specific PCR on cDNA template (addition of reverse transcriptase during cDNA synthesis); -RT, control for potential genomic DNA contamination in cDNA template (no addition of reverse transcriptase during RT-PCR); + gDNA, gene-specific PCR on genomic DNA (positive control)). A 1.5% agarose gel stained with GelRed was used. M, DNA ladder; numbers, represent the used primer set. In the RT-PCR gene-specific revers primers were used.

3.3 Blue native polyacrylamide gel electrophoresis

In 2D gel electrophoresis done by Bergmann et al. (2011b), the carboxylase-like proteins N47_K27540, N47_K27500, and N47_K27480 were differentially abundant in naphthalene-versus 2-methylnaphthalene-grown N47 cells with a ratio of up to 5.5 (Fig. 27).

Moreover, the naphthalene carboxylase activity could be measured in N47 cells grown with naphthalene but just hardly in 2-methylnaphthalene-grown cells suggesting transcriptional and/or translational regulation of the enzyme (Mouttaki et al, unpublished data). To gain new insights into the native conformation of the naphthalene carboxylase complex, Blue native PAGEs (BNPs) were performed and the native protein induction patterns of naphthalene-versus 2-methylnaphthalene-grown cells were compared.

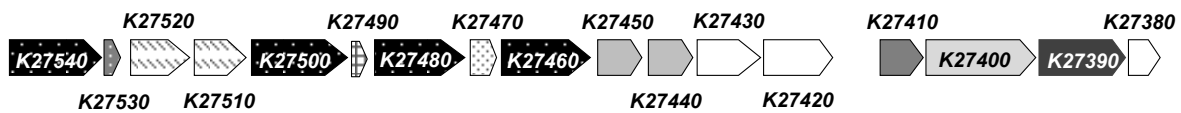


Figure 27: Putative naphthalene carboxylase gene cluster identified within the genome of the sulfate-reducing Deltaproteobacterium N47 (N47_K27540 to N47_K27380). Open reading frames which products show similarity to UbiD-like carboxylases are filled in black, non-carboxylase-like subunits are shown in grey. Genes which are co-transcribed are indicated by a pattern fill. Annotated function of the gene products: N47_K27540, putative phenylphosphate carboxylase, alpha subunit; N47_K27530, putative phenylphosphate carboxylase, gamma subunit; N47_K27520, MRP, Fer4_NifH superfamily; N47_K27510, ParA/MinD ATPase like, MRP, Fer4_NifH superfamily; N47_K27500, UbiD family decarboxylase; N47_K27490, conserved hypothetical protein; N47_K27480, UbiD family decarboxylase; N47_K27470, conserved hypothetical protein; N47_K27460, UbiD family decarboxylase; N47_K27450 & N47_K27440, HAD hydrolase; N47_K27430, membrane protein involved in aromatic hydrocarbon degradation; N47_K27420, IS4 transposase; N47_K27410, succinate dehydrogenase and fumarate reductase iron-sulfur protein; N47_K27400, putative succinate dehydrogenase flavoprotein subunit; N47_K27390, UbiD family decarboxylase; N47_K27380, pyridoxamine 5'-phosphate oxidase family protein.

Blue native PAGE- Method development

For a better resolution of the different protein complexes on Blue native PAGEs, soft detergents such as digitonin or DDM are usually added to the samples (in concentrations between 0.5 to 2%). To ensure that the pretreatment of the samples did not impair the native protein production pattern, different preparation of N47 cell-free extracts were loaded onto a BNP and compared (Fig. 28, see Material and Methods 2.7.1, i).

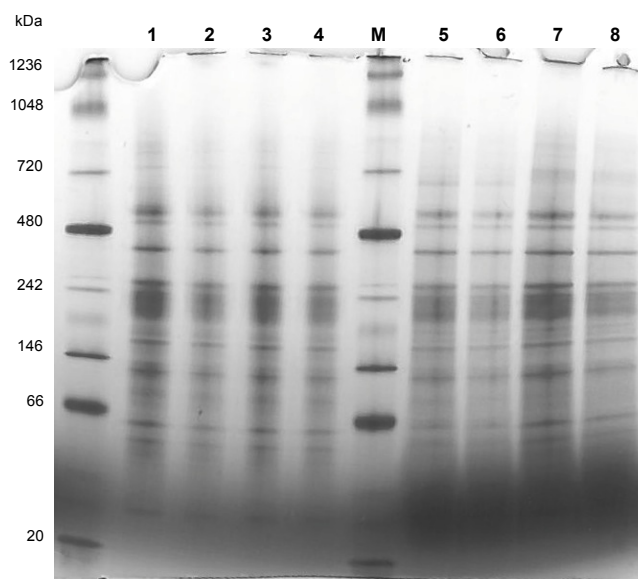


Figure 28: Blue native PAGE of cell-free extracts from N47 cells grown with naphthalene. A coomassie blue-stained Novex® 4-16% Bis-Tris gel was used. Lanes contained 15 µg (lane 2, 4, 6 and 8) or 30 µg (lane 1, 3, 5 and 7) of soluble protein. Prior to the BNP run, frozen N47 cells were not treated (lane 1, 2), sonicated (lane 3, 4) or additionally treated with detergents such as 1% DDM (lane 5, 6) or 1% digitonin (lane 7, 8).

The native protein pattern of samples treated with detergent showed additional protein bands compared to the non-treated control. The addition of detergent to the protein samples indeed increased the resolution. Unless stated otherwise, samples for the following BNPs were opened via sonication and treated with 1% DDM.

3.3.1 Blue native polyacrylamide gel electrophoresis using N47 cells

Proteins were extracted from N47 cells grown with naphthalene or 2-methylnaphthalene in the mid-exponential phase of growth. To make sure that oxygen did not impair the native conformation of the protein complex, the BNPs were ran and compared under oxic and anoxic conditions. The BNP gels ran under oxic versus anoxic conditions showed no visible differences (Fig. 29, B./ C.). Despite of it, all the following experiments were conducted in the absence of oxygen.

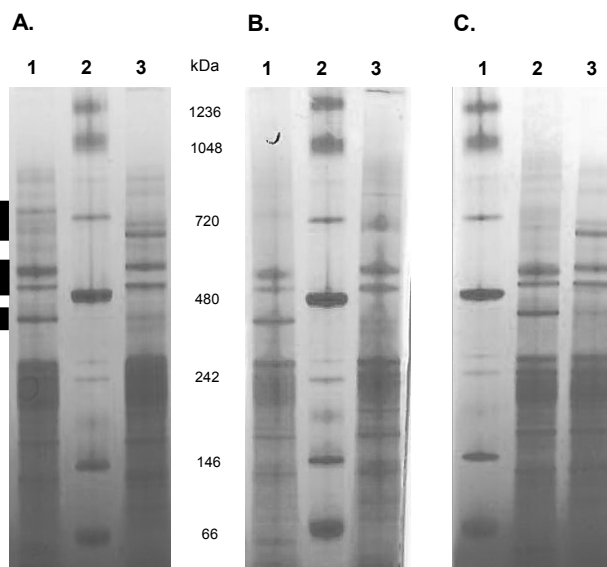


Figure 29: Differential protein induction analysis of N47 on Blue native PAGE (BNP). A coomassie blue-stained Novex® 4-16% Bis-Tris gel was used. Lanes contained 30 µg of soluble protein. Vertical bars indicate parts of the gel which were cut and send for proteomic analysis. **A.** BNP performed under anoxic conditions using non-frozen N47 cells. Lane 1, cell-free extract of naphthalene-grown N47 cells; lane 2, molecular mass standard (1236 – 66 kDa); lane 3, cell-free extract of 2-methylnaphthalene-grown N47 cells. **B.** BNP performed under oxic conditions using frozen N47 cells. Lane 1, cell-free extract of naphthalene-grown N47 cells; lane 2, molecular mass standard; lane 3, cell-free extract of 2-methylnaphthalene-grown N47 cells. **C.** BNP performed under anoxic conditions using frozen N47 cells. Lane 1, molecular mass standard; lane 2, cell-free extract of naphthalene-grown N47 cells; lane 3, cell-free extract of 2-methylnaphthalene-grown N47 cells.

The same amount of protein extracted from N47 cells grown with the two different substrates was applied to the BNP. However, a band with a size of 400 kDa was differentially induced in naphthalene-grown samples. Furthermore, a band of around 560 kDa, which was produced under both growth conditions, was more intense in naphthalene samples (Fig. 29).

The BNPs were run using cell-free extracts of N47 cells which were stored at -20 °C prior to protein extraction. Previous experiments have shown that the naphthalene carboxylase activity was lost after freezing the N47 cells (see Results 3.1.2). Therefore, the BNPs were carried out with freshly harvested cells only (Fig. 29, A.). Indeed, a protein band of around 750 kDa appeared differentially produced with an increased intensity on the BNP. The three regions of the gels with the differentially induced bands with sizes of about 750, 560, and 400 kDa were excised from the gel in extracts from both growing conditions and analyzed by proteomics (Table 29; see Appendix, Tab. A3-A4, A11-A13). Unless stated otherwise, the proteomic data mentioned in the following originated from BNP ran under anoxic conditions using non-frozen and fresh N47 cells (see Material and Methods 2.6.9).

Table 29: List of proteins identified on Blue native PAGE gel slices shown to be differentially induced in naphthalene-grown N47 cells (Naph) in comparison to 2-methylnaphthalene-grown cells (2MN). The proteins with a p-value ≤ 0.01 and an enrichment factor ≥ 2 are shown below. The proteins shown in bold letters correspond to the ones which are encoded in the naphthalene carboxylase gene cluster. **A.** BNP gel slice with a size of about 750 kDa; **B.** BNP gel slice with a size of about 560 kDa; and **C.** BNP gel slice with a size of about 400 kDa. C. score, confidence score; peptides used for quant., peptides used for quantification.

A.

UniProtKB entry name	Peptides used for quant.	C. score	Anova (p)	Description	Annotated function	Ratio Naph/2MN
E1YIW6_9DELTA	51	2872	0.001300	N47_K27500	UbiD family decarboxylase	13.6
E1YIW4_9DELTA	43	2426	0.002304	N47_K27480	UbiD family decarboxylase	13.7
E1YIX0_9DELTA	36	2249	0.002096	N47_K27540	Putative phenylphosphate carboxylase, alpha subunit	9.0
E1YMM1_9DELTA	38	2153	0.004875	N47_N26400	Formate dehydrogenase	4.8
E1YMM2_9DELTA	21	1028	0.004232	N47_N26410	Formate dehydrogenase	4.7
E1YMK9_9DELTA	17	783	0.003309	N47_N26280	NADH-quinone oxidoreductase subunit D (NuoD)	4.0
E1YIW8_9DELTA	12	697	0.000145	N47_K27520	MRP; Fer4_NifH superfamily	45.5
E1YIW7_9DELTA	17	694	0.003368	N47_K27510	ParA/MinD ATPase like, MRP; Fer4_NifH superfamily	23.6
E1YMJ0_9DELTA	13	577	0.004192	N47_N26090	Hypothetical protein	7.3
E1YIW3_9DELTA	12	549	0.005448	N47_K27470	Conserved hypothetical protein	155.7
E1Y9R5_9DELTA	9	526	0.001656	N47_H21310	Outer membrane protein (OprM)	2.2
E1YML1_9DELTA	10	468	0.007661	N47_N26300	NADH-quinone oxidoreductase subunit I (NuoI)	3.7
E1Y9R3_9DELTA	8	392	0.008104	N47_H21290	Multidrug resistance protein (MexA)	2.7
E1YML9_9DELTA	8	349	0.000245	N47_N26380	Putative NADH dehydrogenase	4.4
E1YH08_9DELTA	8	330	0.004488	N47_F15470	S-adenosyl-L-homocysteine hydrolase (AhcY)	10.5
E1YIW9_9DELTA	5	306	0.001724	N47_K27530	Putative phenylphosphate carboxylase, gamma subunit	7.8
E1YH23_9DELTA	4	169	0.001721	N47_F15620	KaiC-like protein 1	3.2
E1YJ15_9DELTA	3	124	0.007889	N47_E47810	Carbon monoxide dehydrogenase 1	2.9
E1YE11_9DELTA	3	121	0.003866	N47_P16800	Putative electron transfer flavoprotein subunit beta	2.2
E1YMK8_9DELTA	2	118	0.002801	N47_N26270	NADH-quinone oxidoreductase	3.9
E1YFV9_9DELTA	2	97	0.004174	N47_J04340	Heterodisulfide reductase	2.8
E1YIX6_9DELTA	2	75	0.001990	N47_K27600	MRP; Fer4_NifH superfamily	89.6
E1YFV8_9DELTA	1	60	0.009389	N47_J04330	Heterodisulfide reductase	2.3
E1YIC8_9DELTA	1	59	0.007554	N47_D32060	Hypothetical protein	4.2
E1YCB2_9DELTA	1	49	0.000753	N47_G35300	Segregation and condensation protein A	2.8
E1YMI9_9DELTA	1	44	0.005921	N47_N26080	Formate dehydrogenase	26.2
E1YDF8_9DELTA	1	42	0.002768	N47_G39260	Putative PAS/PAC sensor signal transduction histidine kinase	3.6
E1YCZ0_9DELTA	1	33	0.009488	N47_G37580	RNA polymerase sigma-54 factor	2.3
E1YD04_9DELTA	1	33	0.009531	N47_G37720	DsbA-like protein	4.6

LC-MS/MS run was performed using buffers with DMSO.

B.

UniProtKB entry name	Peptides used for quant.	C. score	Anova (p)	Description	Annotated function	Ratio Naph/2MN
E1YIX0_9DELTA	35	2162	0.000002	N47_K27540	Putative phenylphosphate carboxylase, alpha subunit	15.0
E1YIW6_9DELTA	18	950	0.000150	N47_K27500	UbiD family decarboxylase	9.0
E1YIW4_9DELTA	18	934	0.000005	N47_K27480	UbiD family decarboxylase	11.4
E1YIW9_9DELTA	6	376	0.000017	N47_K27530	Putative phenylphosphate carboxylase, gamma subunit	14.7
E1YD22_9DELTA	5	272	0.002796	N47_G37900	Tol-pal system protein	3.7
E1YFV8_9DELTA	3	184	0.000080	N47_J04330	Heterodisulfide reductase	13.4
E1YM45_9DELTA	3	126	0.000025	N47_E46900	K(+)-insensitive pyrophosphate-energized H ⁺ pump	13.5
E1YFV9_9DELTA	3	122	0.003161	N47_J04340	Heterodisulfide reductase	6.8
E1YL54_9DELTA	1	110	0.003247	N47_E43490	Heterodisulfide reductase	3.9
E1YDG6_9DELTA	2	103	0.003375	N47_G39340	Heterodisulfide reductase	10.1 ^a
E1YG28_9DELTA	2	80	0.003211	N47_J05030	Hypothetical protein	3.0
E1YFW0_9DELTA	2	73	0.000147	N47_J04350	Heterodisulfide reductase	12.7
E1YFY6_9DELTA	2	70	0.000423	N47_J04610	Integral membrane protein, putative response regulator	2.1
E1YB72_9DELTA	2	63	0.004478	N47_C18070	10 kDa chaperonin, GroS	2.3
E1YDG5_9DELTA	1	47	0.004723	N47_G39330	Heterodisulfide reductase	7.0
E1YKY7_9DELTA	1	38	0.003326	N47_E42820	Hypothetical protein	3.1
E1YBF4_9DELTA	1	34	0.000190	N47_G32220	Putative outer membrane protein, OmpA-like	16.7
E1YAH1_9DELTA	1	34	0.003316	N47_H23870	Putative outer membrane protein, OmpA-like	5.3
E1Y984_9DELTA	1	32	0.000279	N47_A11570	Electron transfer flavoprotein	3.5
E1YHR4_9DELTA	1	32	0.000084	N47_D29920	Protein-export membrane protein SecF	100.9
E1YJZ4_9DELTA	1	31	0.000201	N47_E51100	Hypothetical protein	18.1
E1YKW3_9DELTA	1	31	0.000052	N47_E42580	Putative Mo-binding, Fe-S-binding oxidoreductase	63.4
E1YDG9_9DELTA	1	30	0.000023	N47_G39370	Hypothetical protein, family of Fe/Mo cluster-binding protein	5.8

C.

UniProtKB entry name	Peptides used for quant.	C. score	Anova (p)	Description	Annotated function	Ratio Naph/2MN
E1YIW6_9DELTA	35	2424	0.000445	N47_K27500	UbiD family decarboxylase	26.1^a
E1YIW4_9DELTA	37	2305	0.000023	N47_K27480	UbiD family decarboxylase	18.2
E1YFV9_9DELTA	15	621	0.007925	N47_J04340	Heterodisulfide reductase	6.3
E1YFV8_9DELTA	13	612	0.002579	N47_J04330	Heterodisulfide reductase	5.3
E1YM45_9DELTA	6	269	0.003678	N47_E46900	K(+)-insensitive pyrophosphate-energized H ⁺ pump	4.9
E1YIW8_9DELTA	3	123	0.000912	N47_K27520	MRP; Fer4_NifH superfamily	23.0
E1YHR5_9DELTA	3	120	0.003953	N47_D29930	Protein-export membrane protein SecD	7.1
E1YFW0_9DELTA	3	118	0.001262	N47_J04350	Heterodisulfide reductase	12.1
E1Y983_9DELTA	2	90	0.004217	N47_A11560	Electron transfer flavoprotein (alpha subunit)	6.5

^a Coefficient of variation (CV%) \geq 50 in 2-methylnaphthalene samples.

i. Blue native PAGE band with a size of around 750 kDa

In the 750 kDa band, a total of 288 proteins were identified, 29 of which were differentially abundant with a ratio of ≥ 2 in naphthalene-grown cells compared to 2-methylnaphthalene (Tab. 29, A.; see Appendix, Tab. A11). The most abundant proteins in the band were the carboxylase-like subunits N47_K27540, N47_K27500 and N47_K27480, which were differentially produced in naphthalene-grown cells with a ratio of 9.0, 13.6 and 13.7, respectively. Another carboxylase-like protein, N47_K27530, encoded within the naphthalene carboxylase operon (see Results 3.2), was also differentially induced with a ratio of 7.8. Moreover, the ATPase-like proteins N47_K27520 and N47_K27510 and the hypothetical protein N47_K27470 were enriched with a ratio of 45.5 and 23.6 and 155.7, respectively.

Another ATPase-like protein N47_K27600, which shows 37% sequence identity with N47_K27520, was differentially abundant with a ratio of 89.6. The gene encoding N47_K27600 is located upstream of the naphthalene carboxylase operon. Moreover, N47_K27600 shares 75% of sequence identity with NPH_5849 from NaphS2. The gene *NPH_5849* was shown to be up-regulated in NaphS2 cells grown with naphthalene versus benzoate or pyruvate with a factor of 2.14 and 2.29, respectively (DiDonato et al., 2010).

In all three differentially produced bands of the three different sizes on BNP, heterodisulfide reductase-like subunits were identified. N47_J04340 and N47_J04330 were more abundant in naphthalene samples with a factor of 2.8 and 2.3, respectively. Furthermore, membrane proteins like N47_H21310 (an outer membrane protein) and a multidrug resistance protein (N47_H21290) were enriched with ratios of 2.2 and 2.4, respectively.

ii. Blue native PAGE band with a size of around 560 kDa

In an additional slice, which contained the band with a size of around 560 kDa, among the 133 detected proteins, 23 were enriched under naphthalene growing conditions compared to 2-methylnaphthalene growing conditions (Tab. 29, A.; see Appendix, Tab. A11). Within this band, the most abundant and differentially induced proteins with ratios of 15.0, 9.0, 11.4 and 14.7 were the carboxylase-like subunits N47_K27540, N47_K27500, N47_K27480, and N47_K27530, respectively. As seen with the band excised at a size of 750 kDa, some heterodisulfide reductase subunits (N47_J04330, N47_J04340, N47_J04350 and N47_G39330, N47_G39340) were enriched with a factor of up to 13.4. In addition, N47_E46900 a putative membrane protein annotated as K(+)-insensitive pyrophosphate-energized proton pump was detected and differentially produced with a factor of 13.5.

iii. Blue native PAGE band with a size of around 400 kDa

In the slice, which contained the band with a size of around 400 kDa, 125 proteins were identified in total and 10 proteins were enriched in naphthalene-grown samples (Tab. 29, A.; see Appendix, Tab. A11). The most abundant and at the same time differentially produced proteins were the carboxylase-like proteins N47_K27500 and N47_K27480 with a ratio of 26.1 and 18.2, respectively. The ATPase-like protein N47_K27520 was induced with a ratio of 23.0. As seen for the bands excised at a size of 750 kDa and 560 kDa, proteins annotated as heterodisulfide reductase subunits (N47_J04330, N47_J04340, N47J04350) with a differential induction ratio of up to 12.1 and the K(+)-insensitive pyrophosphate-energized proton pump N47_E46900 with a ratio of 4.9 were identified.

Some proteins within the 400 kDa band could only be identified in one replicate by proteomics. One of these proteins, the ATPase-like protein N47_K27510, was only detected and differentially produced with a ratio of 13.4 in another sample set using frozen N47 cells (Fig. 29, C.; see Appendix, Tab. A4, A13). Moreover, N47_K27490, a hypothetical protein, was enriched with a factor of 25.2. In the same sample, an UbiX-like protein N47_B20630/N47_H21380 was more abundant in naphthalene samples with a factor of 5.2. Interestingly, the protein N47_I06840 annotated as CoA ligase was differentially abundant with a ratio of 7.6 within this 400 kDa band.

In order to check the reproducibility of biological replicates, the normalized protein abundances of naphthalene-grown samples for the two most abundant proteins, N47_K27500 and N47_K27480, from frozen versus non-frozen N47 cells in the band with a size of 400 kDa were compared. The coefficient of variance (CV%) for N47_K27500 and N47_K27480 were 1.3 and 5.5, respectively, indicating high reproducibility. However, some low abundant proteins were only detected in one replicate.

Extraction of native proteins from a BNP and subsequent separation on a SDS-PAGE

The protein band of about 400 kDa that was differentially abundant in naphthalene-grown protein extract was excised from the BNP gel and the extracted proteins were submitted to a second dimension separation on a SDS-PAGE (see Material and Methods 2.7.3).

Here, two major bands with a size of approximately 55 and 57 kDa were detected (Fig. 30, B., lane 1,2). These bands most likely corresponded to the carboxylase-like proteins N47_K27500 (56.9 kDa) and N47_K27480 (54.5 kDa), which were the most abundant proteins detected in proteomic analyses.

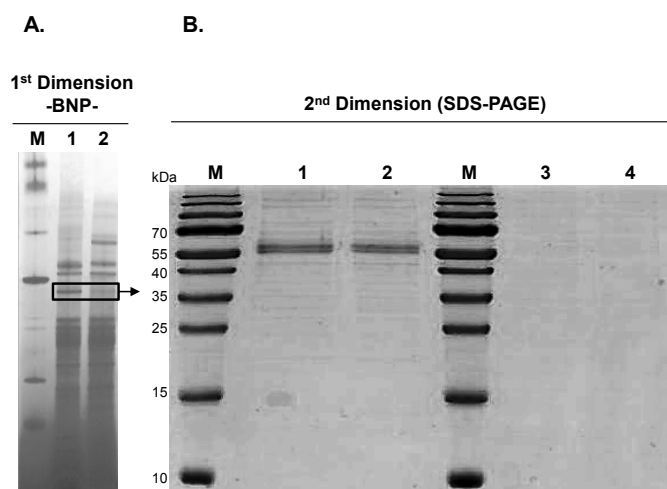


Figure 30: Analysis of the differentially induced 400 kDa protein band from a Blue native PAGE (A., 1st dimension) on a SDS-PAGE (B., 2nd dimension). A. The BNP was performed under anoxic conditions. A coomassie blue-stained Novex® 4-16% Bis-Tris gel was used. M, molecular mass standard (1236, 1048, 720, 480, 242, 146 and 66 kDa); lane 1, cell-free extract of naphthalene-grown N47 cells (30 µg); lane 2, cell-free extract of 2-methylnaphthalene-grown N47 cells (30 µg). Box, 400 kDa native protein band which was cut for protein extraction and analyzed on a SDS-PAGE B. SDS-PAGE with denatured proteins extracted from a native 400 kDa protein band. A coomassie blue-stained 15% SDS-PAGE gel was used. M, molecular mass standard (170 – 10 kDa); lane 1 and 2, extracted proteins from the naphthalene-induced 400 kDa band; lane 3 and 4, extracted proteins from the corresponding BNP gel region in 2-methylnaphthalene samples.

In summary, in comparative native proteomic studies on BNP, three naphthalene-induced bands with a size of around 750, 560 and 400 kDa were identified and analyzed. Within the 750 kDa band, almost all proteins which genes were encoded in the naphthalene carboxylase operon could be identified, whereas the number of identified subunits decreased within the naphthalene-induced bands smaller than 750 kDa (Fig. 31; Tab. 29). The 560 and 400 kDa bands were detected on BNP with proteins extracted from frozen naphthalene-grown N47 cells (Fig. 29, B./C.), while the 750 kDa band was more intense when the proteins were extracted from freshly harvested cells in mid-exponential phase of growth (Fig. 29, A.). Furthermore, the naphthalene-specific bands were not visible in 2-methylnaphthalene-grown N47 cells in which naphthalene carboxylase activity could hardly be detected. In the present PhD project, the interaction of the gene products encoded within this naphthalene carboxylase gene cluster was shown for the first time.

Based on these lines of evidence, it is proposed that the naphthalene carboxylase subunits form a complex of around 750 kDa in native conformation. However, it was only possible to indirectly correlate these findings with naphthalene carboxylase activity. In a next step, in-gel

activity assays were conducted (see Results 3.3.2).

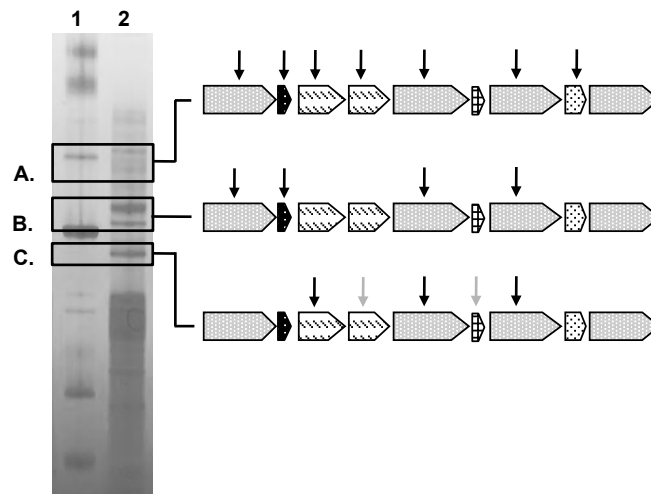


Figure 31: Native soluble protein pattern of non-frozen N47 cells on a Blue native PAGE and gene cluster encoding the proteins identified to be significantly up-regulated within the analyzed bands. The BNP was performed under anoxic conditions. A coomassie blue-stained Novex® 4-16% Bis-Tris gel was used. Lane 1, molecular mass standard (1236, 1048, 720, 480, 242, 146 and 66 kDA); lane 2, cell-free extract of naphthalene-grown N47 cells (30 µg). Boxes indicate the three parts of the gel which were cut and send for proteomic analysis. Right sight, organization of the operon involved in anaerobic degradation of naphthalene (*N47_K27540* to *N47_K27460*). Open reading frames which products show similarity to UbiD-like carboxylases are filled in grey. Arrows, genes encoding proteins which were significantly up-regulated during growth with naphthalene compared to 2-methylnaphthalene. Grey arrows, genes encoding proteins which were not reproducibly detected in MS run.

3.3.2 In-gel naphthalene carboxylase activity

Naphthalene carboxylase activity could exclusively be detected in cell-free extracts of N47 cells which were opened with a French Press. To correlate the putative naphthalene carboxylase complex with naphthalene carboxylase activity, a BNP using these cell-free extracts was performed. The three differentially induced native protein bands were cut from the BNP and used in a naphthalene carboxylase activity assay (Fig. 32; see Material and Methods 2.8.1). The gel pieces were incubated in the assay (containing 5 mM ATP). The production of ^{13}C -labeled 2-naphthoic acid was not detected in the samples.

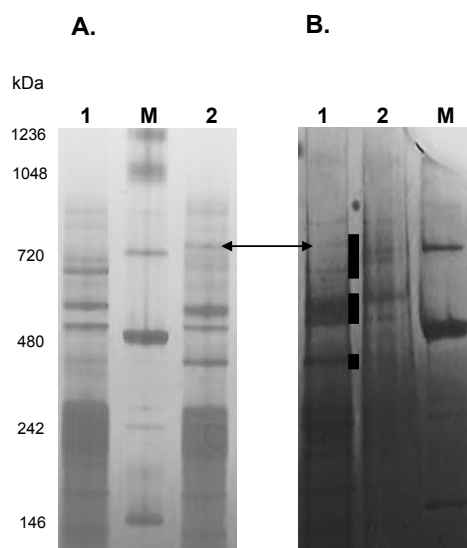


Figure 32: Blue native PAGEs with N47 cell-free extracts generated by sonication (A.) and French Press (B.). A coomassie blue-stained Novex® 4-16% Bis-Tris gel was used. Lanes contained 30 µg of soluble protein. The arrow indicates the naphthalene carboxylase complex. Vertical bars indicate parts of the gel, which were cut and used in the naphthalene carboxylase activity assay. **A.** BNP performed under anoxic conditions using non-frozen N47 cells in the mid exponential phase of growth. Lane 1, cell-free extract of 2-methylnaphthalene-grown N47 cells; M, molecular mass standard (1236 – 66 kDa); lane 2, cell-free extract of naphthalene-grown N47 cells. **B.** Blue native PAGE performed under anoxic conditions using non-frozen N47 cells of a fermenter in the late exponential phase of growth. Lane 1, cell-free extract of naphthalene-grown N47 cells; lane 2, cell-free extract of 2-methylnaphthalene-grown N47 cells; M, molecular mass standard.

3.3.3 Analysis of the 2-methylnaphthalene specific 220 kDa protein band

A differentially produced band of around 200 kDa was visible in cell-free extracts extracted from 2-methylnaphthalene samples (Fig. 29). The corresponding gel region in naphthalene and 2-methylnaphthalene samples was excised and analyzed by proteomics (Tab. 30; see Appendix, Tab. A14). The three subunits of the naphthyl-2-methyl-succinate synthase NmsABC could be identified as differentially produced in 2-methylnaphthalene versus naphthalene samples with a ratio of 3.3, 5.9 and 3.8, respectively. Analogous to the initial reaction in toluene degradation catalyzed by the benzylsuccinate synthase (Bss) in *Thauera aromatica*, the initial step in 2-methylnaphthalene degradation is catalyzed by the naphthyl-2-methyl-succinate synthase (Nms) (Leuthner et al., 1998; Safinowski and Meckenstock, 2004). The size of the band is in accordance with previous work done by Selesi et al. (2010) and Leuthner et al. (1998), where the apparent molecular masses of the Nms or the Bss are around 220 kDa.

Table 30: List of proteins identified on Blue native PAGE gel slices shown to be differentially induced in 2-methylnaphthalene-grown N47 cells (2MN) in comparison to naphthalene-grown cells (Naph). The gel slices contained proteins of around 200 kDa. The proteins with a p-value ≤ 0.035 and an enrichment factor ≥ 2 are shown below. The proteins shown in bold, black letters are known to form the naphthyl-2-methyl-succinate synthase (NmsABC). The proteins shown in bold, grey letters are encoded in the *bns* gene cluster. C. score, confidence score; peptides used for quant., peptides used for quantification. The LC-MS/MS run was performed using buffers with DMSO.

UniProtKB entry name	Peptides used for quant.	C. score	Anova (p)	Description	Annotated function	Ratio 2MN/Naph
E1YFR6_9DELTA	49	3074	0.001867	N47_J03910	Putative naphthyl-2-methyl-succinyl-CoA dehydrogenase (BnsG)	3.6
E1YFQ9_9DELTA	34	1928	0.006128	N47_J03840	Putative naphthyl-2-methyl-succinate synthase alpha subunit (NmsA)	3.3
E1YFR8_9DELTA	28	1773	0.004122	N47_J03930	Putative naphthyl-2-methyl-succinate CoA transferase subunit (BnsE)	4.9
E1YFR7_9DELTA	23	1334	0.002649	N47_J03920	Putative naphthyl-2-methyl-succinate CoA transferase subunit (BsnF)	6.3
E1YIY2_9DELTA	22	1184	0.005069	N47_K27660	Putative uncharacterized protein	5.8
E1YG28_9DELTA	17	1037	0.007610	N47_J05030	Putative cyclohexanecarboxylate-CoA ligase	3.0
E1Y9L9_9DELTA	12	745	0.012972	N47_I06830	Hypothetical protein	3.2
E1YFS0_9DELTA	9	448	0.005786	N47_J03950	Putative naphthyl-2-hydroxymethyl-succinyl-CoA dehydrogenase subunit (BnsD)	3.6
E1YFR5_9DELTA	8	360	0.008515	N47_J03900	Putative naphthyl-2-hydroxymethyl-succinyl-CoA hydratase (BnsH)	2.6
E1YMF3_9DELTA	6	357	0.009829	N47_N25720	Hypothetical protein	2.2
E1YFR2_9DELTA	7	331	0.010927	N47_J03870	Hypothetical protein	4.2
E1YFS2_9DELTA	5	297	0.014276	N47_J03970	Putative naphthyl-2-oxomethyl-succinyl-CoA thiolase subunit (BnsB)	3.5
E1YFS1_9DELTA	5	260	0.017553	N47_J03960	Putative naphthyl-2-hydroxymethyl-succinyl-CoA dehydrogenase subunit (BnsC)	3.6
E1YIS9_9DELTA	5	226	0.005423	N47_E52290	Putative membrane protein	2.8
E1YFQ7_9DELTA	4	203	0.034166	N47_J03820	Putative naphthyl-2-methyl-succinate synthase activating enzyme (NmsD)	2.3
E1Y8Y7_9DELTA	4	203	0.014738	N47_A10600	Hypothetical protein	18.6
E1YD04_9DELTA	3	133	0.003632	N47_G37720	Putative oxidoreduktase	2.3
E1YI73_9DELTA	2	100	0.015037	N47_D31510	Putative ABC transporter	3.6
E1YFS3_9DELTA	2	91	0.009045	N47_J03980	Putative naphthyl-2-oxomethyl-succinyl-CoA thiolase subunit (BnsA)	3.6
E1YFQ8_9DELTA	1	74	0.013813	N47_J03830	Putative naphthyl-2-methyl-succinate synthase beta subunit (NmsB)	5.9
E1YFR0_9DELTA	1	52	0.030595	N47_J03850	Putative naphthyl-2-methyl-succinate synthase gamma subunit (NmsC)	3.8
E1YA80_9DELTA	1	48	0.000201	N47_H22960	Putative Glutaconyl-CoA decarboxylase subunit beta	4.3

Additionally, peptides of the activating enzyme NmsD and peptides of the enzymes, which were reported to be involved in the beta-oxidation of naphthyl-2-methyl-succinate to 2-naphthoyl-CoA, were found to be more abundant in cell-free extracts of 2-methylnaphthalene-grown N47 cells (Selesi et al., 2010) (Tab. 30; see Appendix, Tab. A14). The naphthyl-2-methyl-succinyl-CoA dehydrogenase (BnsG) and the two naphthyl-2-methyl-succinate CoA transferase subunits, BnsE and BnsF, were the most abundant proteins within the 200 kDa band with a ratio of 3.6, 4.9 and 6.3, respectively. Furthermore, the naphthyl-2-methylene-succinyl-CoA hydratase BnsH, the naphthyl-2-hydroxymethylsuccinyl-CoA dehydrogenase subunits BnsC and BnsD as well as the naphthyl-2-oxomethyl-succinyl-CoA thiolase subunits BnsA and BnsB were more differentially produced in 2-methylnaphthalene-grown samples with ratios up to 6.3.

3.3.4 Blue native polyacrylamide gel electrophoresis using NaphS2 cell-free extracts

Knowing that NaphS2 carries a gene region (NPH_5855 to NPH_5880) which is similar to the naphthalene carboxylase gene cluster of N47 (see Introduction, Fig 5; Fig. 33; (DiDonato et al., 2010)), a comparative BNP was carried out with NaphS2 growing with naphthalene or 2-methylnaphthalene.

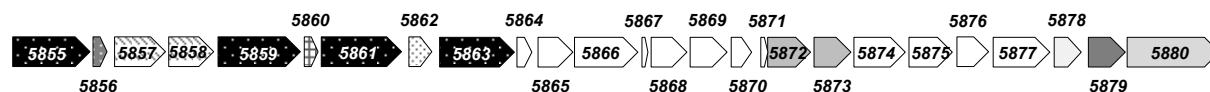


Figure 33: Putative naphthalene carboxylase gene cluster identified within the genome of the sulfate-reducing Deltaproteobacteria NaphS2 (NPH_5855 to NPH_5880). The numbers represent the names of the genes. Open reading frames which products show similarity to UbiD-like carboxylases are filled in black, non-carboxylase-like subunits are shown in grey. Genes which are co-transcribed are indicated by a pattern fill. Annotated function of the gene products: NPH_5855, putative phenylphosphate carboxylase, alpha subunit; NPH_5856, putative phenylphosphate carboxylase, gamma subunit; NPH_5857, uncharacterized protein; NPH_5858, ParA family protein; NPH_5859, 3-octaprenyl-4-hydroxybenzoate carboxylase; NPH_5860, hypothetical protein; NPH_5861, 3-octaprenyl-4-hydroxybenzoate carboxylase; NPH_5862, conserved domain protein; NPH_5863, UbiD family decarboxylase; NPH_5864, hypothetical protein; NPH_5865, putative phenolic acid decarboxylase subunit B (UbiX-like protein); NPH_5866, 3,4-dihydroxy-2-butanone 4-phosphate synthase; NPH_5867, uncharacterized protein; NPH_5868, putative phosphoglycolate phosphatase; NPH_5869 - NPH_5872, uncharacterized protein; NPH_5873, HAD hydrolase; NPH_5874, putative nodulation ATP-binding protein I, NPH_5875 - NPH_5879, hypothetical protein; NPH_5880, putative succinate dehydrogenase flavoprotein subunit.

The native proteins were extracted from NaphS2 cells grown with these two PAHs in the mid-exponential phase of growth and the BNPs were ran under anoxic conditions (Fig. 34). Protein bands of around 750, 440, and 400 kDa were differentially abundant in naphthalene compared to the 2-methylnaphthalene and 2-naphthoate-grown NaphS2 sample. However, the differences in the protein production pattern comparing the cell-free extracts obtained from the two different growth conditions were not as pronounced as in N47 (Fig. 29). Nevertheless, the gel regions with the differentially produced protein bands with sizes of about 750 kDa and 400-440 kDa were excised from the gel and analyzed by proteomics (see Appendix, Tab. A5, A15).

The calculated ratios were indeed lower than the ones observed in the proteomic analysis using N47 cells. Therefore, all identified proteins from the gel slices with a ratio of >1 and a confidence score of >30 were listed (see Appendix, Tab. A5, A15).

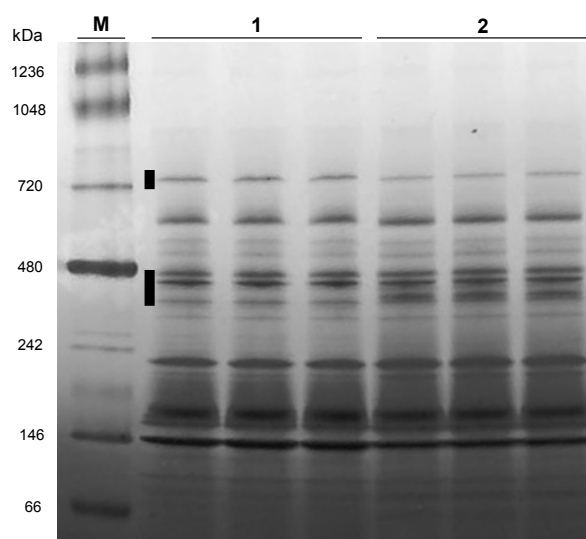


Figure 34: Blue native PAGE performed under anoxic conditions using non-frozen NaphS2 cells.

A coomassie blue-stained Novex® 4-16% Bis-Tris gel was used. The lanes contained 30 μ g of soluble protein. Vertical bars indicate parts of the gel which were cut and send for proteomic analysis. M, molecular mass standard (1236 – 66 kDa); lane 1, cell-free extract of naphthalene-grown NaphS2 cells; lane 2, cell-free extract of 2-methylnaphthalene-grown NaphS2 cells.

i. Blue native PAGE band with a size of around 750 kDa

In the slice, which contained the band with a size of about 750 kDa, 25 proteins were identified in total and 10 proteins were differentially abundant with a ratio of ≥ 2 in naphthalene-grown NaphS2 cells compared to 2-methylnaphthalene. The carboxylase-like NPH_5859 was the most abundant protein and it was differentially produced with a ratio of only 2.2 (Fig. 33, see Appendix, Tab. A5, A15). Additionally, other carboxylase-like proteins

of the cluster, such as NPH_5861, NPH_5856, and NPH_5855, were detected within the excised band of 750 kDa, however, these proteins were not differentially abundant in naphthalene-grown NaphS2 cells compared to other growth conditions.

The identified carboxylase-like proteins NPH_5855, NPH_5856, NPH_5859, and NPH_5861 show sequence identities of 84, 76, 80, and 77% to the putative naphthalene carboxylase subunits N47_K27540, N47_K27530, N47_K27500, and N47_K27480 of N47, respectively. In N47, these subunits were identified as differentially produced when naphthalene was used as a substrate compared to 2-methylnaphthalene growing conditions (Tab. 29).

ii. Blue native PAGE band with a size of around 400-450 kDa

In the gel region containing proteins with a size of about 400-450 kDa, 150 proteins were identified in total and 31 proteins were differentially produced in naphthalene compared to 2-methylnaphthalene-grown cells (see Appendix, Tab. A5, A15). The most abundant proteins were the carboxylase-like proteins NPH_5855 and NPH_5856 with ratios of 1.9 and 2.1, respectively. Moreover, the other two carboxylase-like proteins NPH_5859 and NPH_5861 were identified but were not differentially produced under the tested conditions.

Another carboxylase-like protein NPH_5865, showing similarities to UbiX an isoenzyme of UbiD, was differentially abundant with a ratio of 5.6. In the genome of NaphS2, the *ubiX* gene was located in close vicinity to the putative genes encoding the naphthalene carboxylase subunits from NaphS2. The gene *NPH_5865* was also described to be up-regulated in NaphS2 cells grown on naphthalene in another study (DiDonato et al., 2010).

Furthermore, the ATPase-like proteins NPH_5857 and NPH_5858, which genes belong to the naphthalene carboxylase gene cluster, were differentially produced with ratios of 2.4 and 4.4 in naphthalene-grown NaphS2 cells compared to 2-methylnaphthalene. The same proteins, namely N47_K27520 (sequence identity of 82% to NPH_5857) and N47_K27510 (sequence identity of 75% to NPH_5858) were shown to be differentially abundant in naphthalene-grown N47 cells (Tab. 29).

As seen in N47, within the excised band of 400 kDa, NPH_5477, a protein similar to a ligase was differentially produced in NaphS2 in naphthalene versus 2-methylnaphthalene extracts. These results confirm previous experiments carried out by DiDonato et al. (2010), where the same protein was identified and seen to be more abundant in NaphS2 cells grown with naphthalene compared to benzoate-grown cells. The protein was suggested to be a putative 2-naphthoate CoA-ligase. In the BNP, the putative ligase was enriched with a factor of 2.8.

NPH_5477 shares 77.1% sequence identities with N47_I06840 shown to be differentially produced in naphthalene-grown N47 cells (Tab. 29).

Moreover, subunits annotated as heterodisulfide reductase/ 4Fe-4S binding protein such as NPH_4205, NPH_6289, and NPH_1820 were identified with a ratio of up to 1.4 in naphthalene versus 2-methylnaphthalene samples. The putative heterodisulfide reductase/ 4Fe-4S binding protein NPH_4205 and NPH_6289 shared between 55 and 63% sequence identity with the putative heterodisulfide reductase subunits N47_G39340 and N47_E43490, which were identified as differentially produced in BNP using N47 cells (Tab. 29).

Differences in the protein production pattern on BNP comparing NaphS2 cells grown with naphthalene versus 2-methylnaphthalene were not as pronounced as in N47 (see Results 3.3.1). In N47, the naphthalene-specific protein band of 750 kDa was not visible in 2-methylnaphthalene-grown cells. In NaphS2, the corresponding protein band could be detected on BNP run with cell-free extracts from naphthalene and 2-methylnaphthalene cells indicating no transcriptional or translational regulation (Fig. 34, 1/2). However, in NaphS2, homologs of the subunits, which were proposed to represent subunits of the naphthalene carboxylase in N47 such as the carboxylase-like subunits NPH_5855 (N47_K27540), NPH_5859 (N47_K27500), NPH_5861 (N47_K27480) and NPH_5856 (N47_K27530) as well as the ATPase-like proteins NPH_5857 (N47_K27520) and NPH_5858 (N47_K27510), were identified on BNP of NaphS2 cell-free extracts grown with naphthalene.

3.4 *In vitro* protein interaction assays

For the *in vitro* protein interaction assays (Fig. 35), N47_K27540, encoded by the first gene of the naphthalene carboxylase operon, was chosen and heterologously produced in *E. coli*. After successful purification using Glutathione Sepharose beads, the GST-tagged protein was incubated with N47 cell-free extract grown with naphthalene. As shown in the differential protein induction studies on BNP, the putative naphthalene carboxylase subunits form a complex (see Results 3.3.1). The hypothesis was that the tagged protein N47_K27540 should be able to interact with the other subunits of the naphthalene carboxylase complex.

In the pull-down assay, the complex attached to the tagged protein should be separated from the rest of the proteins by centrifugation. The proteins in the pellet fraction were then separated on SDS-PAGE and the enriched bands, potentially including the co-purified interaction partners, were cut and send for proteomic analysis for identification.

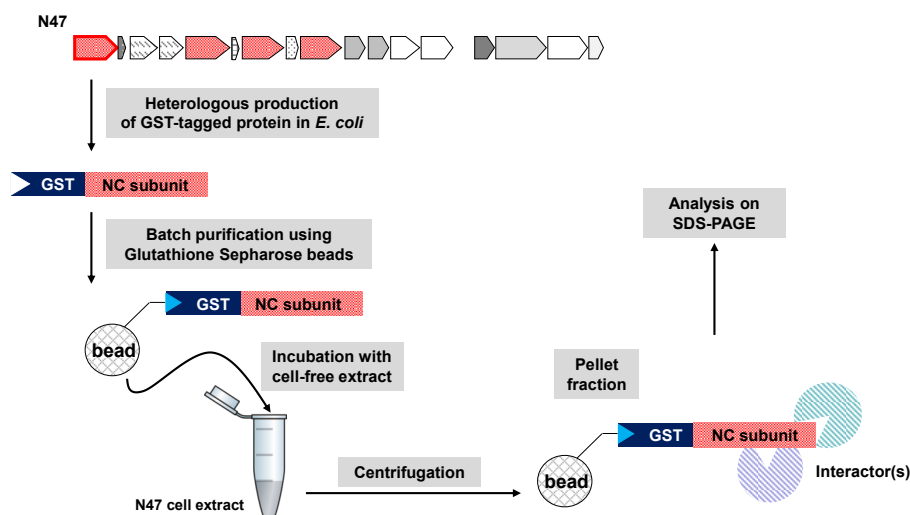


Figure 35: Experimental setup for the *in vitro* protein interaction assay. Further details are given in the text. NC, naphthalene carboxylase.

3.4.1 Heterologous production and purification of N47_K27540

For the *in vitro* protein interaction assays, N47_K27540 was heterologously produced with a HIS tag and as a GST-tagged fusion protein in *E. coli*.

i. Production and purification of His-tagged N47_K27540

The gene *N47_K27540* was cloned into different expression vectors, which were used to heterologously produce the His-tagged protein in *E. coli* (see Material and Methods 2.4.1; Tab. 3). However, soluble His-tagged protein could only be produced in *E. coli* Rosetta™ using the expression vector pHAT_*N47_K27540* but the solubility of the overproduced protein N47_K27540 was very low in all tested conditions. From 5 g (wet mass) of *E. coli* Rosetta™ cells, only 0.1 mg of purified protein was obtained (Fig. 36; see Material and Methods, Tab. 7; 2.7.1, ii).

N47_K27540 possesses an UbiD-like protein domain. In *E. coli*, UbiD catalyzes the decarboxylation of an isoprenylated 4-hydroxybenzoate derivative in ubiquinone biosynthesis and is associated to the membrane (Cox et al., 1969; Leppik et al., 1976; Meganathan, 2001). Due to the similarity of N47_K27540 to the UbiD present in *E. coli*, N47_K27540 may be attached to the membrane during the heterologous production in *E. coli*. Therefore, crude *E. coli* extracts were treated with 1% of the detergent deoxycholate or 1 M NaCl to destroy such potential membrane-interactions. After the treatment, the protein could not be purified from the cell-free extracts indicating the incorporation of N47_K27540 into inclusion bodies in *E. coli*.

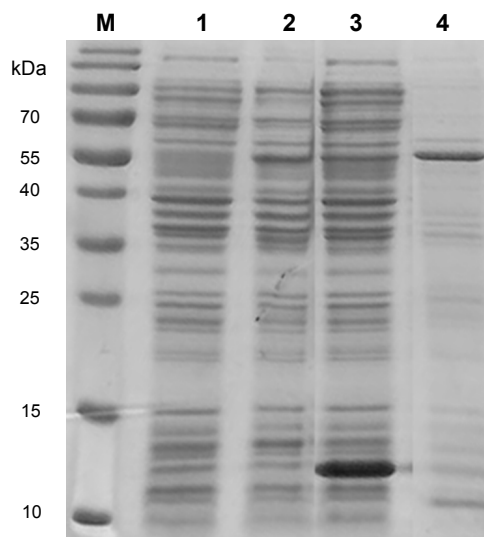


Figure 36: Purification of the His-tagged subunit N47_K27540 produced in *E. coli* Rosetta™ with the expression vector pHAT. A coomassie blue-stained 15% SDS-PAGE gel was used. Lanes contained 25 µg of protein. M, molecular mass standards; lane 1, *E. coli* Rosetta™ cells before induction; lane 2, *E. coli* Rosetta™ cells after induction with 0.5 mM IPTG for 3 h at 37 °C; lane 3, purified His-tagged protein N47_K27540 (55.2 kDa) (20 µL).

The attempts to produce higher amounts of the His-tagged carboxylase-like protein failed, unfortunately, since the production and purification of a soluble and His-tagged protein N47_K27540 could not be reproduced.

It has been reported that the fusion of a target protein to a soluble protein, which is already present in *E. coli*, might improve the solubility during heterologous production (Davis et al., 1999; Kapust and Waugh, 1999; Harper and Speicher, 2011). Therefore, N47_K27540 was fused to a Glutathione S-transferase (size of 220 amino acids) and produced as a fusion protein in *E. coli* (see Results 3.4.1, i).

ii. Production and purification of GST-tagged N47_K27540

The carboxylase-like protein N47_K27540 was used for heterologous production of a GST-tagged fusion protein in *E. coli* Rosetta™. The heterologously produced carboxylase-like protein was reproducibly soluble only when expressed as a GST fusion protein. However, the solubility was rather low and the protein was instable, which was indicated by additional bands on the SDS-PAGE corresponding to the degradation products of GST-N47_K27540 (Fig. 37; this was confirmed by the analysis of the sequences excised from the bands visible on the gel by LC/MS).

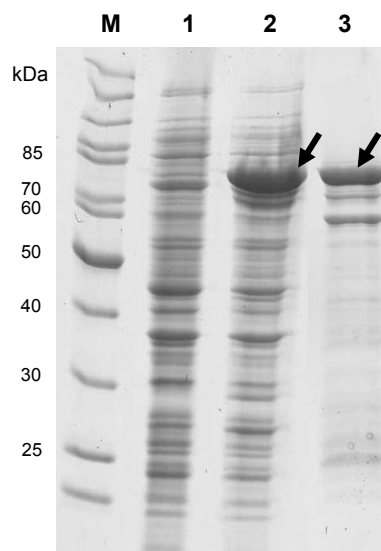


Figure 37: Production and purification of the GST-tagged N47_K27540 subunit in *E. coli* Rosetta. A coomassie blue-stained 15% SDS-PAGE gel was used. The fusion protein GST-N47_K27540 is indicated by the arrows. M, molecular mass standard; lane 1, *E. coli* Rosetta™ cells before induction (25 µg); lane 2, *E. coli* Rosetta™ cells after induction with 0.5 mM IPTG for 3 h at 37 °C (25 µg); lane 3, purified fusion protein GST-N47_K27540 (80 kDa) coupled to glutathione sepharose beads (10 µL beads). The two other abundant protein bands visible on the gel (70 kDa and 58 kDa) represent the degradation products of GST-N47_K27540.

After successful purification (Fig. 37; see Materials and Methods 2.7.1, i), the GST-N47_K27540 coupled to the sepharose beads was used for the follow-up pull-down experiment (Fig. 35).

3.4.2 Pull-down assay

The GST-tagged protein N47_K27540 coupled to the sepharose beads (see Results 3.4.1, ii) was incubated with N47 cell-free extract of cells grown with naphthalene. After incubation with the cell-free extracts, samples were applied and separated on a SDS-PAGE (Fig. 38).

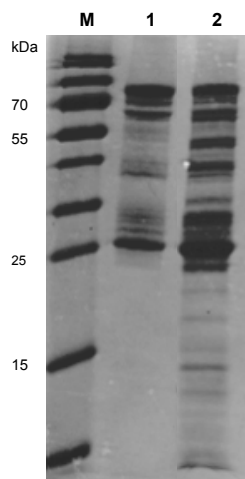


Figure 38: Protein interaction assay with GST-N47_27540 in cell-free extracts of N47 grown with naphthalene. A coomassie blue-stained 15% SDS-PAGE gel was used. M, molecular mass standard; lane 1, purified GST-N47_K27540 coupled to glutathione sepharose beads (input sample, 30 μ L); lane 2, purified GST-N47_K27540 coupled to glutathione sepharose after 4 h of incubation with cell-free extract of naphthalene-grown N47 cells (30 μ L).

On the SDS-PAGE, new bands were visible in samples which were incubated with N47 cell-free extracts compared to the control corresponding to the purified GST-tagged protein N47_K27540 overproduced in *E. coli* (Fig. 38).

To improve the specificity of the generated pull-down data, the experiment was repeated and the fusion protein GST-N47_K27540 was incubated with N47 cell extract of cells either grown with naphthalene or 2-methylnaphthalene. The enriched bands from naphthalene and 2-methylnaphthalene samples were excised from the SDS-PAGE and sent for proteomic analysis (Tab. 31; see Appendix, Tab. A16). In a second set of control experiments, GST alone (Fig. 39, 5/6) or the chromatography matrix (Glutathione Sepharose 4B slurry) without any bound protein were incubated with cell-free extract of N47. An unspecific interaction of N47 proteins with the controls could not be observed.

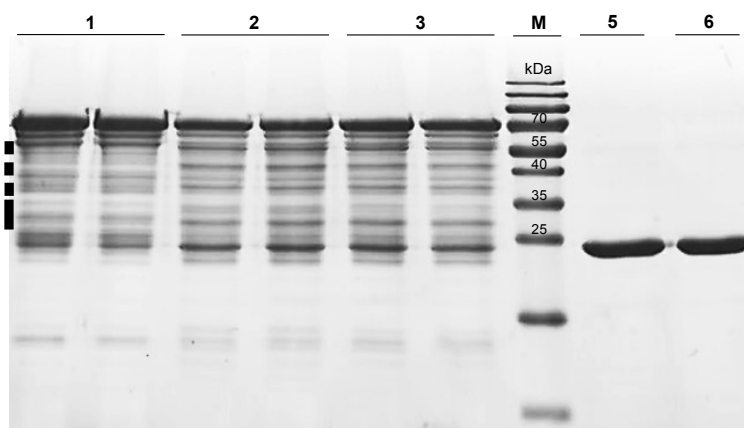


Figure 39: Protein interaction assay with GST-N47_K27540 in cell-free extracts of N47 grown with naphthalene and 2-methylnaphthalene. A coomassie blue-stained 15% SDS-PAGE gel was used. Lane 1, purified GST-N47_K27540 coupled to glutathione sepharose beads (input sample, 30 μ L); lane 2, purified GST-N47_K27540 coupled to glutathione sepharose (lane 1) after 4 h of incubation with cell-free extract of naphthalene-grown N47 cells (30 μ L); lane 3, purified GST-N47_K27540 coupled to glutathione sepharose beads (lane 1) after 4 h of incubation with cell-free extract of 2-methylnaphthalene-grown N47 cells (30 μ L); lane 4, molecular mass standard (170, 130, 100, 70, 55, 40, 35, 25, 15 and 10 kDa); lane 5, GST coupled to glutathione sepharose beads after 4 h of incubation in cell-free extracts of naphthalene-grown N47 cells; lane 6, GST coupled to glutathione sepharose beads after 4 h of incubation in cell-free extracts of 2-methylnaphthalene-grown N47 cells. Vertical bars indicate parts of the gel, which were cut and send for proteomic analysis.

The pull-down assay indicated an *in vitro* interaction of N47_K27540 with protein subunits, some of which are the ones belonging to the same operon of naphthalene carboxylase (see Results 3.3, Fig. 27). These proteins were also identified in the naphthalene carboxylase complex analyzed by BNP mentioned above (see Results 3.3.1, Tab. 29). The most abundant proteins interacting with the GST-N47_K27540 protein in naphthalene compared to 2-methylnaphthalene-grown samples were the carboxylase-like proteins N47_K27500 and N47_K27480 with enrichment factors of 23.6 and 31.0, respectively (Tab. 31, A./ B.) and the two ATPase-like proteins N47_K27520 and N47_K27510 with enrichment factors of 50.4 and 56.2 (Tab. 31, D.) all belonging to the naphthalene carboxylase operon.

The carboxylase-like protein N47_K27460, which is part of the naphthalene carboxylase operon, could not be detected in any of the BNP experiments. However, it appeared to interact with the GST-N47_K27540 protein.

In the interaction assay, additional proteins, which genes are not part of the identified gene cluster, were pulled-down indicating a possible interaction with the carboxylase like protein N47_K27540 (Tab. 31; see Appendix, Tab. A16). For example, N47_A07150, a FAD binding

domain protein which was also shown to be differentially abundant in 1D SDS-PAGEs, was enriched with a factor of 103.2 (Tab. 31, C.; Mouttaki et al., unpublished data). Moreover, the ATPase-like protein N47_K27600 was pulled-down with an enrichment factor of up to 84.9 (Tab. 31, C./ D.). N47_K27600 was also identified and differentially abundant within the 750 kDa band in BNP (see Results 3.3.1, Tab. 29). The *N47_K27600* gene is located in close vicinity to the naphthalene carboxylase gene cluster.

Additionally, N47_K27400, a succinate dehydrogenase-like flavoprotein, was identified with an enrichment factor of 44.6. The gene encoding this protein can be found downstream of the naphthalene carboxylase operon. Interestingly, a similar protein is encoded within the genome of NaphS2 (see Introduction, Fig. 5).

Furthermore, a sulfate adenylyltransferase (N47_J04360) showed an enrichment factor of 30.6 (Tab. 31, D.). This protein was not identified in BNP but it is encoded in close vicinity to the heterodisulfide reductase subunits N47_J04330, N47_J04340, and N47_J04350, which showed differential abundance in N47 naphthalene-grown samples in the BNP.

The data generated from the *in vitro* protein interaction assay supported the results from previously performed differential protein induction analysis on BNP (see Results 3.3.1). Again, the most abundant proteins interacting with GST-N47_K27540 in cell-free extracts of naphthalene-grown cells were the carboxylase-like proteins N47_K27500 and N47_K27480 and the two ATPase-like proteins N47_K27520 and N47_K27510 (see Results 3.3, Fig. 27). Moreover, some other proteins, which genes are encoded in close vicinity to the naphthalene carboxylase operon, such as the ATPase-like subunit N47_K27600 and the succinate dehydrogenase-like flavoprotein N47_K27400, were found to interact with the GST-tagged naphthalene carboxylase subunit N47_K27540. However, N47_K27400 and N47_K27600 were not detected in BNP. Additionally, the FAD binding protein N47_A07150 and a sulfate adenylyltransferase were shown to interact with the GST-tagged protein N47_K27540. Both proteins were not encoded by genes located in close vicinity of the naphthalene carboxylase operon and were not identified in the BNP experiments.

Table 31: List of GST-N45_K27540 interactors with an enrichment ≥ 15 and a p-value ≤ 0.01 detected in a pull-down assay and identified by LC-MS/MS. The proteins shown in bold letters, correspond to the ones which are encoded in the naphthalene carboxylase gene cluster. **A.** SDS gel region with a size of 60 – 50 kDa. **B.** SDS gel region with a size of 45 – 40 kDa. **C.** SDS gel region with a size of 38 – 35 kDa. **D.** SDS gel slice with protein size of 35 – 28 kDa. C. score, confidence score; peptides used for quant., peptides used for quantification.

A.

UniProtKB entry name	Peptides used for quant.	C. score	Anova (p)	Description	Annotated function	Ratio Naph/2MN
E1YIW4_9DELTA	18	1162	0.000633	N47_K27480	UbiD family decarboxylase	31.0
E1YIW6_9DELTA	13	819	0.000597	N47_K27500	UbiD family decarboxylase	23.6
E1YIV6_9DELTA	14	855	0.001726	N47_K27400	Putative succinate dehydrogenase flavoprotein	44.6
E1YAB2_9DELTA	4	217	0.000485	N47_H23280	Fumarate hydratase class I, anaerobic	28.0
E1YAB2_9DELTA	4	217	0.000485	N47_F14190	Uroporphyrin-III C-methyltransferase	155.1
E1YIW2_9DELTA	2	89	0.026798	N47_K27460	UbiD family decarboxylase	5171.5^a

B.

UniProtKB entry name	Peptides used for quant.	C. score	Anova (p)	Description	Annotated function	Ratio Naph/2MN
E1YKJ5_9DELTA	15	745	0.005969	N47_E41400	Acetyl-CoA acetyltransferase/Thiolase	17.1
E1YIW4_9DELTA	10	608	0.001111	N47_K27480	UbiD family decarboxylase	16.7

C.

UniProtKB entry name	Peptides used for quant.	C. score	Anova (p)	Description	Annotated function	Ratio Naph/2MN
E1YIX6_9DELTA	6	305	0.006848	N47_A07150	FAD binding domain protein	103.2 ^a
E1Y816_9DELTA	5	213	0.002488	N47_K27600	MinD ATPase like, Fer4_NifH superfamily	46.0
E1YFW1_9DELTA	2	65	0.009352	N47_F14520	CRISPR-associated protein	21.3

D.

UniProtKB entry name	Peptides used for quant.	C. score	Anova (p)	Description	Annotated function	Ratio Naph/2MN
E1YIW7_9DELTA	21	1147	0.00746	N47_K27510	MinD ATPase like, Fer4_NifH superfamily	56.2
E1YIW8_9DELTA	9	866	0.00195	N47_K27520	Fer4_NifH superfamily	50.4
E1YFW1_9DELTA	9	392	0.00015	N47_J04360	Sulfate adenylyltransferase	30.6
E1YIX6_9DELTA	7	323	0.00336	N47_K27600	MinD ATPase like, Fer4_NifH superfamily	84.9
E1YFR3_9DELTA	4	153	0.00014	N47_J03880	Putative electron transfer flavoprotein, FixB	25.8

^a Coefficient of variation (CV%) ≥ 50 in 2-methylnaphthalene samples.

Project 2

Characterization of *Cand. Treponema contaminophilus* sp. strain HM^T

The novel anaerobic bacterium *Cand. Treponema contaminophilus* sp. strain HM^T was isolated from the naphthalene-degrading enrichment culture N47 (Fig. 40). The enrichment culture N47 has been cultivated in the laboratory for almost two decades. The spirochete strain is the second most abundant organism beside the naphthalene-degrading Deltaproteobacterium (Fig. 40). Uncultivated members of the family *Spirochaetaceae* can usually be found in contaminated sites in the environment. Based on 16S rRNA gene sequences, they are closely related species with high similarity to the N47 spirochete. The ecological function of *Spirochaetaceae* within this niche is unknown. In the present PhD project, the anaerobic bacterium *Cand. Treponema contaminophilus* sp. strain HM^T was characterized with classical microbiological and molecular biological approaches.

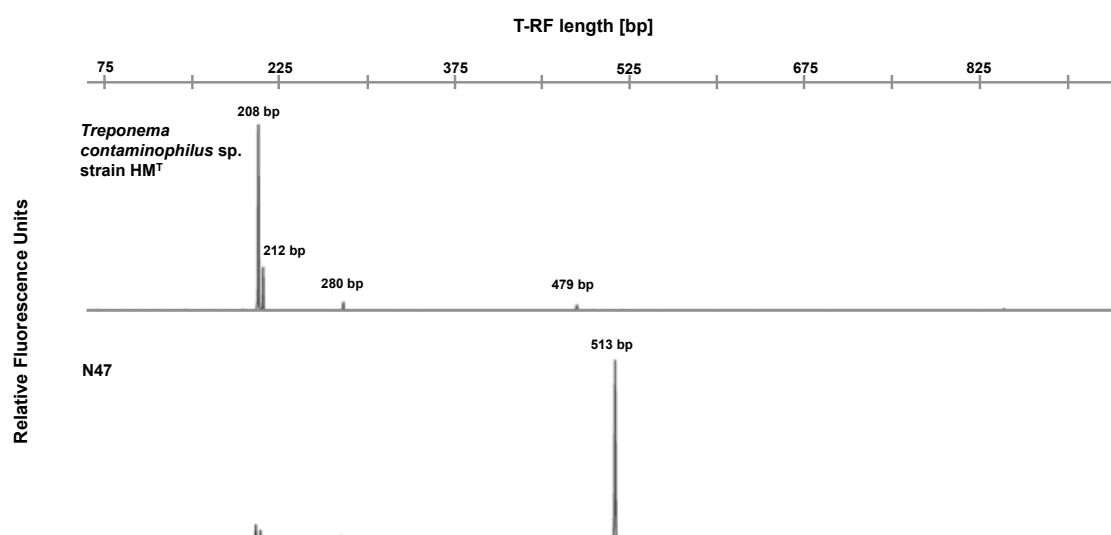


Figure 40: T-RFLP analyses of bacterial 16S rRNA gene sequence of the pure culture *Cand. T. contaminophilus* sp. strain HM^T grown with glucose plus yeast extract with rifampicin and T-RFs from the enrichment culture N47 grown with naphthalene. The length of major T-RFs is indicated.

3.5 Characterization of *Cand. Treponema contaminophilus* sp. strain HM^T

3.5.1 Morphology of *Cand. Treponema contaminophilus* sp. strain HM^T cells

In roll tubes, *Cand. Treponema contaminophilus* sp. strain HM^T formed circular, convex elevated, smooth colonies with a diameter of 0.5-1 mm on the agar surface. They lacked pigmentation but showed a white almost translucent color with a viscous consistency. The colonies became visible after five weeks of incubation.

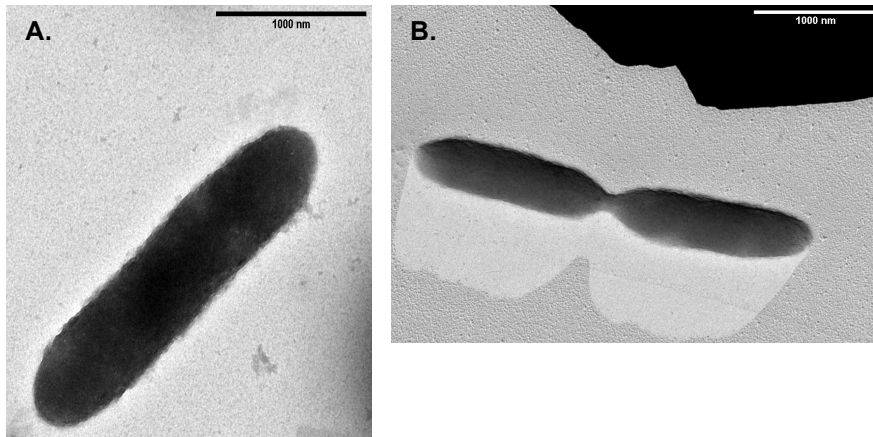


Figure 41: Electron micrograph of *Cand. T. contaminophilus* strain HM^T using a negative stain with uranyl acetate (A.) and platinum-carbon shadowed (B.) preparation. The cells are rod-shaped and non-motile. The electron micrograph of *Cand. T. contaminophilus* strain HM^T was provided by Dr. Carolin Meyer and Prof. Dr. Reinhard Rachel.

Interestingly, cells of *Cand. T. contaminophilus* sp. strain HM^T did not show the characteristic spiral morphology. During growth in liquid bicarbonate-buffered freshwater medium, the cells were rod-shaped with a size of 0.3-0.5 μm in diameter and 1-2.5 μm in length (Fig. 41, see Material and Methods 2.6.7, ii). They were resistant to rifampicin but sensitive to ampicillin, chloramphenicol, and kanamycin. The rifampicin resistance is typical of the family *Spirochaetaceae* and is probably due to a low affinity of spirochete RNA polymerase for the antibiotic (Stanton and Canale-Parola, 1979; Leschine and Canale-Parola, 1980; Leschine and Canale-Parola, 1986).

3.5.2 Physiology of strain HM^T

i. Substrate utilization

Growth of strain HM^T was dependent on the presence of yeast extract which could not be replaced by a richer vitamin solution, nor by 0.1% peptone or 0.1% casamino acids (Tab. 32). *Cand. T. contaminophilus* sp. strain HM^T was able to grow with glucose and 0.1% tryptone but growth was diminished compared to cultures grown with glucose and 0.1% yeast extract.

H₂ and acetate were detected during fermentation of glucose by strain HM^T (personal communication Alexander Schmidt, AG Prof. Dr. Schink, University of Konstanz; see Material and Methods 2.6.3). Lactate was not detectable as potential end product.

The isolate was able to grow in the presence of 0.1 up to 1% NaCl (optimum 0.1% NaCl). However, higher concentrations ($\geq 2\%$) of salt inhibited growth. D-glucose, D-fructose, L-fructose, D-galactose, D-lactose, lactulose, D-mannose, D-melezitose, D-melibiose, sucrose, and pyruvate supported growth whereas mannitol and glycerol were not metabolized (for more see Appendix, Fig. A6; Material and Methods 2.4.2, ii.). In addition, the isolate was able to use the amino acid L-valine as a substrate. The electron acceptor thiosulfate did neither support growth with benzoate nor with acetate. Homoacetogenic growth with H_2 and CO_2 as energy and C-source was not observed in mineral salt medium.

Table 32: Substrate utilization spectrum of strain HM^T.

Substrates tested	Growth	Substrates tested+ 0.1% YE	Growth
10 mM Glucose	-	5 mM Fructose	+
10 mM Glucose, 0.1% Yeast extract (YE)	+	5 mM Sucrose	-/+
10 mM Glucose, 0.1% Casamino acids	-	5 mM Mannitol	-
10 mM Glucose, 0.1% Tryptone	+/-	5 mM Glycerol	-
10 mM Glucose, 0.1% Peptone	-	5 mM Pyruvate	+
0.1% Yeast Extract	-		
0.1% Casamino Acids	-		
0.1% Tryptone	-	10 mM Glucose, 0.1% NaCl	+
0.1% Peptone	-	10 mM Glucose, 1% NaCl	+/-
10 mM Glucose, 7-vitamin solution (Widdel and Pfennig, 1981)	-	10 mM Glucose, 2% NaCl	-
10 mM Glucose, vitamin solution 141 (DSMZ)	-	10 mM Glucose, 5% NaCl	-
Naphthalene, SO_4^{2-}	-	5 mM L-Valine	+
5 mM Sodium Benzoate,	-		
10 mM Thiosulfate, 0.1% Yeast Extract	-		
5 mM Acetate	-		
10 mM Thiosulfate, 0.1% Yeast Extract	-	$H_2 + CO_2$	-

* +, growth. -, no growth. +/-, growth diminish compared to growth with 0.1% yeast extract and glucose.

Within the enrichment culture N47, the Deltaproteobacterium was reported to degrade polycyclic aromatic compounds (Selesi et al., 2010; Bergmann et al., 2011a; Bergmann et al., 2011b; Mouttaki et al., 2012). The pure culture of *Cand. T. contaminophilus* sp. strain HM^T did not grow in N47 medium supplied with naphthalene as sole carbon source and sulfate as electron acceptor. However, the spirochete is a stable member of the enrichment culture N47 (Fig. 40). This might indicate a so far unknown interaction between the spirochete and the Deltaproteobacterium during naphthalene degradation.

Within the enrichment culture, growth of *Cand. T. contaminophilus* sp. strain HM^T is probably dependent on a compound, which is released from the Deltaproteobacterium during degradation of naphthalene. To test for the putative compound, which might be soluble,

0.2 μm filtrated culture supernatant of an exponentially grown N47 culture was added to a fresh medium inoculated with strain HM^T in the absence of substrate and yeast extract. Growth of *Cand. T. contaminophilus* sp. strain HM^T could not be sustained from the soluble components released during concomitant growth of both microorganisms after six weeks of incubation. These findings might indicate that the unknown compound is unstable or present in low concentration and was immediately metabolized by the spirochetes already present from the enrichment.

ii. Temperature, pH and oxygen range of growth

Growth of strain HM^T occurred at a temperature range of 12-50 °C with an optimum at 37 °C (Fig. 42) and was not observed at 60 °C. Under optimal conditions (with 10 mM glucose and 0.1% yeast extract at 37 °C), the doubling time of the organism was 7.5 h. Routinely, cultures were stored at 4 °C and subcultures grew within seven days.

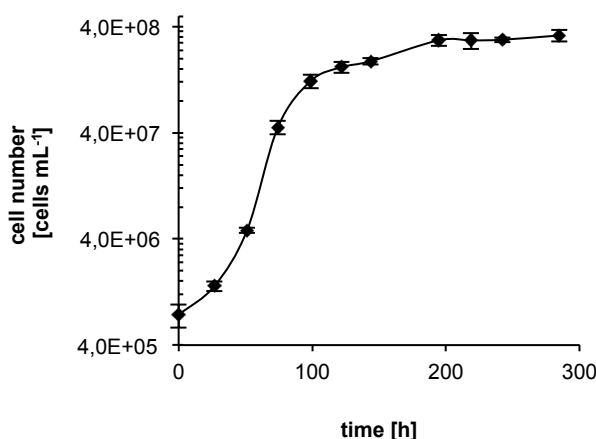


Figure 42: Growth curve of *Cand. T. contaminophilus* sp. strain HM^T with 0.1% yeast extract and 10 mM glucose at 37 °C. The cell numbers were measured by flow cytometry. The data points represent measurements of three independent biological replicates.

The pH optimum of strain HM^T was between pH 6-7 (see Material and Methods 2.3.4, Tab. 22). The cells were catalase- and oxidase negative, however, short-term exposure to air did not inhibit growth (see Material and Methods 2.6.6). Under micro-oxic conditions (up to 1.5% oxygen in the headspace), strain HM^T was still able to grow, however, growth was decreased compared to the control experiments under strict anoxic conditions. Tolerance to low amounts of oxygen was already described in other catalase-negative spirochetes such as *Spirochaeta perfilievii* sp., *Sphaerochaeta globosa* Buddy^T and *Sphaerochaeta pleomorpha* Grapes^T. (Dubinina et al., 2011; Ritalahti et al., 2012).

Experiments using thioglycollate broth indicated that *Cand. T. contaminophilus* sp. strain HM^T is aerotolerant (see Material and Methods 2.4.2, ii.). In thioglycollate medium, growth of strain HM^T occurred initially approximately 0.5 cm beneath the oxic part in form of a disc (Fig. 43). After longer incubation (more than two weeks), growth occurred in the whole anoxic part (beneath the initial disc).

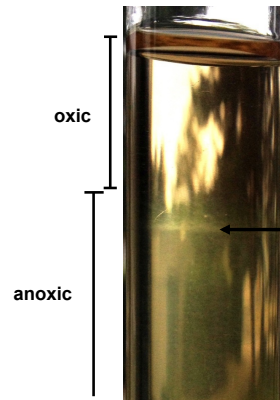


Figure 43: Growth of strain HM^T in thioglycollate medium. Growth of strain HM^T occurred approximately 0.5 cm beneath the oxic part in form of a disc (arrow). Turbidity indicating growth was also visible in the anoxic part beneath the initial disc.

Surprisingly, the new isolate does not need to grow at low redox potentials since growth was also observed in anaerobic bicarbonate-buffered freshwater medium without additional reduction. As bacterial impurities were excluded (Fig. 44), this supports again resistance of *Cand. T. contaminophilus* sp. strain HM^T to small amounts of oxygen and indicates that the strain was not dependent on a low redox potential in the medium which is usually observed for strict anaerobes.

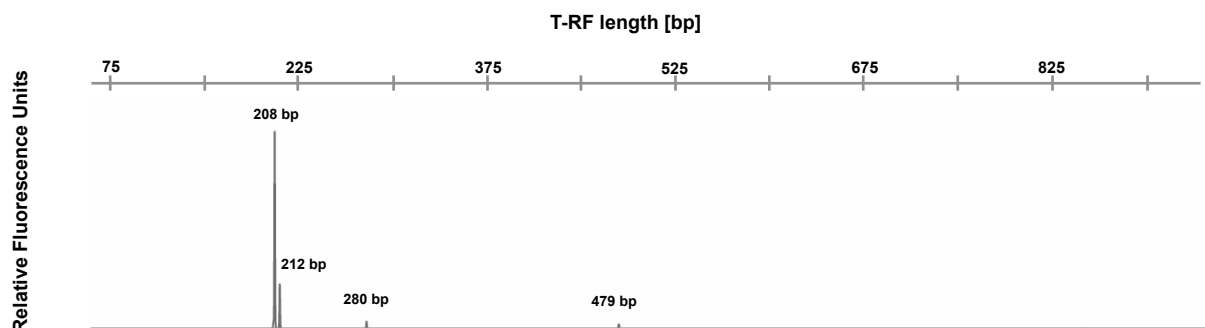


Figure 44: T-RFLP analysis of bacterial 16S rRNA gene sequence of the pure culture *Cand. T. contaminophilus* sp. strain HM^T grown with 0.5% peptone, 0.25% yeast extract and 0.1% glucose at pH 7. The length of major T-RFs is indicated.

3.5.3 Membrane

During the exponential phase of growth, the cells stained Gram-negative (see Material and Methods 2.6.6). The fatty acids composition of the strain was dominated by the mono-unsaturated fatty acids C_{16:1}ω9t (24.4%), C_{16:1}ω9c (11.4%), C_{16:1}ω11c (15.8%), and C_{18:1}ω13c (25%) (Tab. 33; Material and Methods 2.6.4). The major saturated fatty acid was C_{14:0} (11.2%). Branched fatty acids were not detected.

Table 33: Composition the detected FAMES of *Cand. T. contaminophilus* strain HM^T.

FAME	FAME (%)
C _{14:0}	11.2
C _{14:1C}	2.9
C _{16:0}	5.6
C _{16:1} ω9t	24.4
C _{16:1} ω9c	11.4
C _{16:1} ω11c	15.8
C _{18:0}	2.3
C _{18:1} ω11c	1.5
C _{18:1} ω13c	25.0
Sum	100

3.5.4 Motility of strain HM^T

Motility of strain HM^T was not observed in liquid or semi-solid (0.8% agar-agar) medium. Moreover, flagella were not detected microscopically. The major filament protein FlaB is well conserved between different spirochete species and *flaB*-mutants of *Borrelia burgdorferi* have been described as non-motile and rod-shaped whereas wildtype cells showed a flat-wave morphology (Li et al., 2000; Motaleb et al., 2000). Primers, which were originally designed to amplify the flagella genes *flaB2* and *flaB3* within a flagella gene cluster in *Treponema maltophilum* (Heuner et al., 2000), were used to screen the genome of our new isolate for potential flagella genes and in particular the subunit FlaB.

The positive control *Treponema maltophilum* generated two amplicons with a size of 1942 and 690 bp. However, for strain HM^T the tested primers generated amplicons which had different sizes (Fig. 45). The two unspecific amplicons with a size of 400 and 2250 bp were sequenced and a Blast search showed that these sequences were not specific to known motility genes. The best matches were with a phosphor-N-acetylmuramoyl-pentapeptide-transferase from *Spirocheata thermophila* for the 400 bp amplicon and with an ABC-type transporter from *Sphaerochaeta globosa* Buddy^T for the 2250 bp amplicon. These results might indicate that the used primers were not specific for strain HM^T and only genome sequencing will reveal if the genome of the new isolate encodes motility genes. Moreover, in batch experiments *Cand. T. contaminophilus* sp. strain HM^T showed no motility.

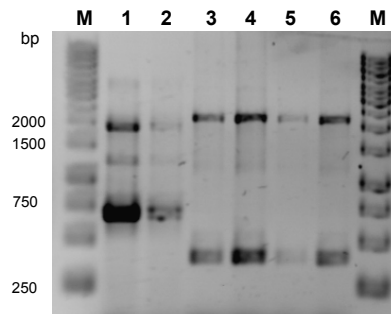


Figure 45: Analysis of PCR targeting the flagella genes *flaB2* and *flaB3* within a flagella gene cluster in *Treponema maltophilum*. A 1.5% agarose gel stained with GelRed was used. M, DNA ladder; lane 1 and 2, PCR with *Treponema maltophilum* gDNA (positive control); lane 3-6, PCR with *Cand. T. contaminophilus* strain HM^T gDNA isolated from different biological replicates.

3.5.5 DNA G+C base content

The DNA G+C base content of *Cand. T. contaminophilus* sp. strain HM^T was 51.5 mol% (see Material and Methods 2.6.5), which is comparable to detected values from other members of the genus *Treponema* typically ranging from 44 to 65 mol% (Pikuta et al., 2009).

3.5.6 16S rRNA gene sequence of *Cand. T. contaminophilus* sp. strain HM^T

T-RFLP analyses of the 16S rRNA genes within the enrichment culture N47 identified two major organisms- a Deltaproteobacterium (513 bp T-RF) and a spirochete (208/212 bp T-RF) (Fig. 40) (Selesi et al., 2010; Bergmann et al., 2011b). In the T-RFLP analyses of the pure isolate *Cand. Treponema contaminophilus* sp. strain HM^T, the 513 bp T-RF corresponding to the Deltaproteobacterium was absent. Two additional T-RFs with a size of 280 and 479 bp were obtained due to multiple *MspI* restriction sites within the 16S rRNA gene sequence of the isolated spirochete (Fig. 40). The GenBank accession number for the 16S rRNA gene sequences of strain HM^T is KP297860.

For the phylogenetic classification of the new isolate, the 16S rRNA gene was amplified and sequenced (see Appendix, Fig A17). A comparison with available sequences of cultivated bacteria showed that HM^T was similar to sequences of the genus *Treponema* (Fig. 46).

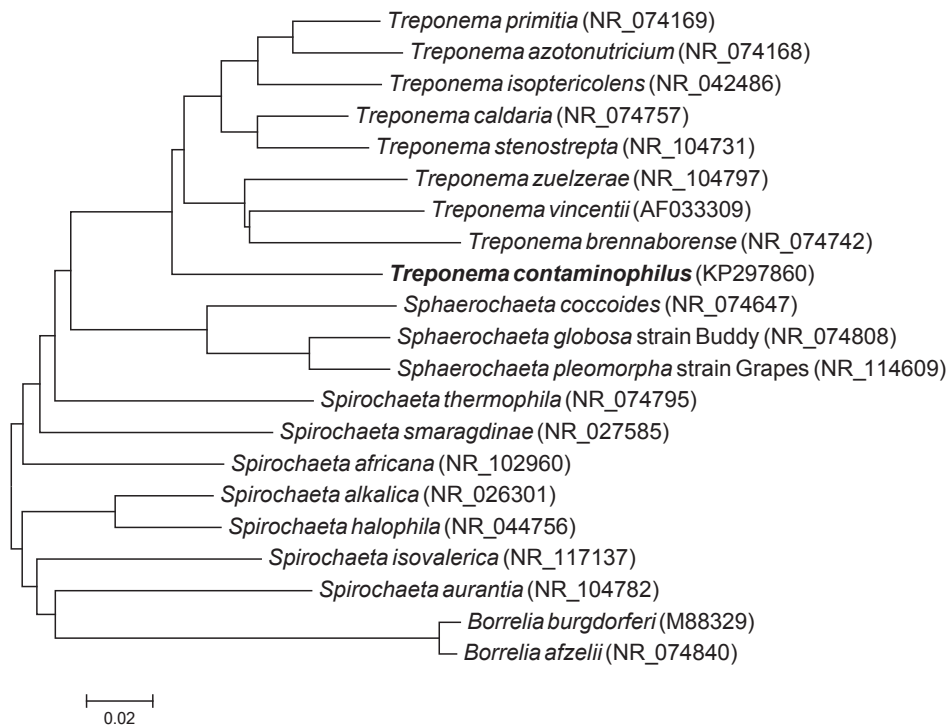


Figure 46: Phylogenetic tree based on 16S rRNA gene sequences. The phylogenetic tree was generated using the MEGA6 software (Tamura et al., 2013). The alignment algorithm utilized MUSCLE with the neighbor-joining method (1392 aligned bases).

The closest relative with spirochete-characteristic motility and spiral morphology is *Treponema caldaria* strain DSM 7334, a free-living, anaerobic, thermophilic carbohydrate-fermenter (Pohlschroeder et al., 1994), which exhibits 89.5% 16S rRNA gene sequence similarity to *Cand. Treponema contaminophilus* sp. strain HM^T. In the phylogenetic tree, *Cand. Treponema contaminophilus* sp. strain HM^T clustered together with endosymbiotic termite gut spirochetes and the free-living freshwater isolates *T. caldaria* and *T. stenostrepta*, which were recently reclassified from the genus *Spirochaeta* (Zuelzer, 1912; Pohlschroeder et al., 1994; Abt et al., 2013).

Project 3

Raman microspectroscopy of N47

3.6 Raman microspectroscopy of N47

Raman microscopy is a combination of Raman spectroscopy and optical microscopy. The method is non-invasive and with its spatial resolution in the μm range, it allows the chemical analysis of single microbial cells. During Raman microscopy, only little interference with water was observed. Thus, samples usually need no further preparation prior to analysis.

Raman scattering is based on the inelastic interaction of light with molecules and the spectra obtained by Raman spectroscopy correspond to the vibration of chemical bonds (Huang et al., 2004; Huang et al., 2009). Biologically relevant molecules such as nucleic acids, protein, lipids, and carbohydrates generate strong signals in the corresponding Raman spectra and can therefore be used to generate 'whole-organism fingerprints' of single cells. Raman microspectroscopy was, for example, used to discriminate between different species in a sample or to analyze the physiological state of single cells (Huang et al., 2004).

Huang et al. (2004) demonstrated that in the Raman spectra of *Pseudomonas fluorescens* cells, which were incubated with ^{13}C -labeled glucose, several characteristic Raman bands were shifted to a lower wavenumber compared to spectra of cells grown with non-labeled substrate. This isotopic or 'red shift' of bands in the obtained Raman spectra was observed for bands corresponding to proteins, lipids, nucleic acids, and carbohydrates of the cells which incorporated the label into their biomass.

In another study by Huang et al. (2007), in the Raman spectra of non-labeled *P. fluorescens* cells, a strong resonance band at 1003 cm^{-1} corresponding to the aromatic amino acid phenylalanine was observed to be red-shifted by about 36 wavenumbers to 967 cm^{-1} when the cells were incubated with ^{13}C -labeled glucose. Interestingly, the phenylalanine band showed only limited interference with other Raman bands and was already observed in several organisms (Huang et al., 2007; Li et al., 2012).

Based on the aforementioned studies, the phenylalanine Raman band can be used as a marker for ^{13}C -incorporation originating from a labeled substrate into the biomass of individual microbial cells.

Here, we investigated whether stable isotope Raman microspectroscopy is a suitable method to detect the incorporation of stable isotopes into the biomass of anaerobic cells. The analysis of ^{13}C -assimilation into microbial cells might be of relevance for the identification of

microbial key players in their natural habitats or in enrichment cultures in the laboratory as the isotope incorporation indicates the utilization of a specific substrate. However, in contrast to stable isotope probing (SIP) experiments, stable isotope Raman microspectroscopy allows the analysis on the single cell level. To establish a suitable protocol for stable isotope Raman microspectroscopy, the sulfate reducer N47 was used as the model organism and $^{13}\text{C}_{10}$ -labeled naphthalene as the model substrate.

Preliminary experiments for the Raman project in cooperation with Patrick Kubryk and Dr. Natalia P. Ivleva (Institute of Hydrochemistry, Chair for Analytical Chemistry, Technische Universität München) were performed by a former Master student in our group, Alejandra del Rocio Diaz Mejorada. In these experiments, the analyzed N47 cells were non-treated or fixed with 2.5% glutardialdehyde. Even though incorporation of $^{13}\text{C}_1$ -naphthalene into the biomass was shown (for non-fixed samples) by stable isotope Raman microspectroscopy, the spectra quality was low.

In the present PhD project, different fixation methods for N47 cells were tested to improve the quality of the generated Raman spectra. The Raman microspectroscopy was performed by Patrick Kubryk and Dr. Natalia P. Ivleva at the Institute of Hydrochemistry, TU München.

3.6.1 Preparation and analysis of N47 cells by stable isotope Raman

For method development, ^{12}C -naphthalene-grown N47 cells in the mid-exponential phase of growth were used. Two different sample preparation techniques were tested. The cells were either fixed with 1% paraformaldehyde and dehydrated in ethanol or fixed and dehydrated in a stepwise increased concentration of ethanol (see Materials and Methods 2.6.7, ii.).

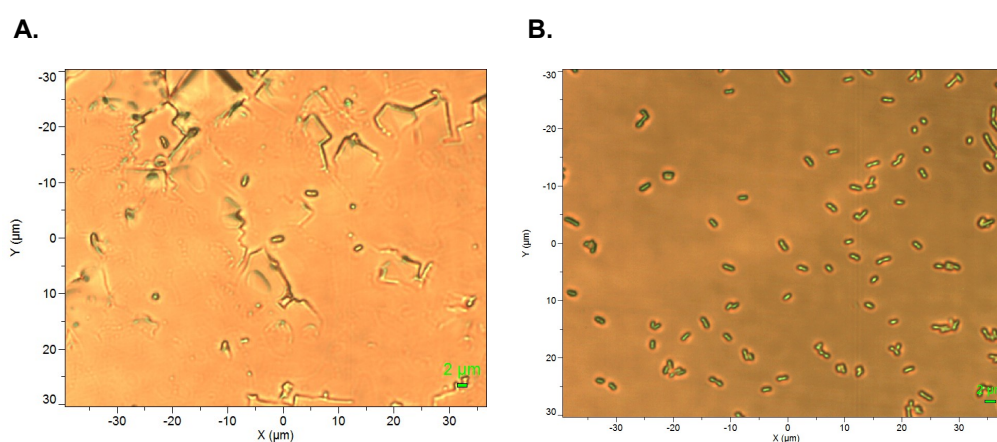


Figure 47: Optical microscope image of non-fixed (A.) or fixed with 1% paraformaldehyde (B.) N47 cells. Figure 47 A. was taken from del Rocio Diaz Mejorada (2013) and figure 47 B. was obtained in the present study and provided by Patrick Kubryk.

Figure 47 shows optical microscopic images of non-fixed (in PBS, (del Rocio Diaz Mejorada, 2013)) and fixed (with 1% paraformaldehyde) and subsequently dehydrated N47 cells. The newly established preparation method (Fig. 47, B.) led to clear microscopic images without any formation of crystals (Fig. 47, A.).

Subsequently, the fixed cells, which were prepared according to the new method mentioned above, were analyzed by Raman microspectroscopy. The two different preparation techniques resulted in similar spectra (Fig. 48). However, a lower background and a slightly better signal to noise ratio (28 vs. 30) was observed for fixed N47 cells, which were subsequently dehydrated in a stepwise increased concentration of ethanol compared to a one-step ethanol treatment.

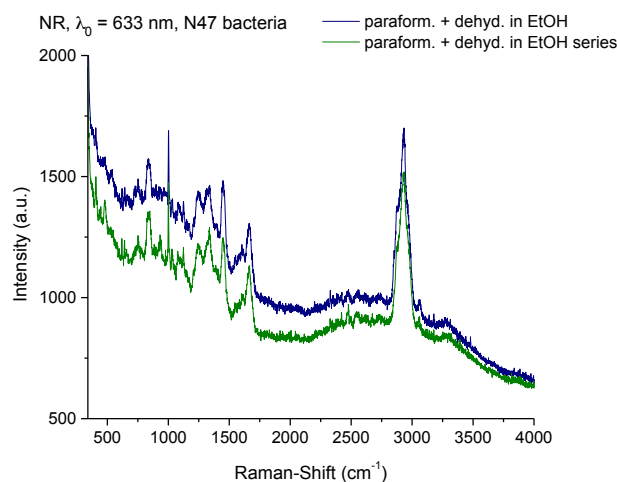


Figure 48: Raman spectra of N47 cells cultivated with ^{12}C -naphthalene. The Raman spectra obtained from paraformaldehyde fixed and dehydrated N47 cells are shown in blue whereas the spectra from fixed cells, which were dehydrated in a stepwise increased concentration of ethanol, are indicated by a green color. The figure was provided by Patrick Kubryk.

The quality of the Raman spectra from N47 cells grown with non-labeled naphthalene, which were obtained during the present PhD project, was highly increased compared to the previous experiments by del Rocio Diaz Mejorada (2013). Additionally, the spectra showed a high reproducibility.

For further analysis using stable isotope Raman microspectroscopy, the N47 cells were fixed with 1% paraformaldehyde and subsequently dehydrated in a stepwise increased concentration of ethanol to analyze the incorporation of $^{13}\text{C}_{10}$ -naphthalene into the biomass.

Stable isotope Raman microspectroscopy of N47

For stable isotope Raman microspectroscopy, N47 cells were cultivated in either unlabeled or fully ^{13}C -labeled naphthalene and unlabeled bicarbonate. In figure 49, the spectra of both cultivations were compared with special interest in the region of the characteristic phenylalanine marker band at 1001 cm^{-1} .

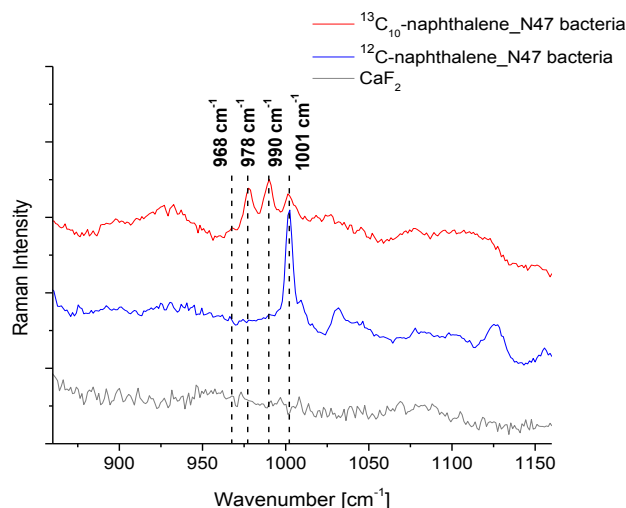


Figure 49: Raman spectra of N47 cells cultivated with ^{12}C -naphthalene or $^{13}\text{C}_{10}$ -naphthalene. The characteristic isotopic red shift of the phenylalanine marker band was clearly visible. The figure was provided by Patrick Kubryk.

The four Raman bands at 1001 cm^{-1} , 990 cm^{-1} , 978 cm^{-1} , and 968 cm^{-1} represented the different isotopologues of phenylalanine with 0, 2, 4 or 6 labeled ^{13}C -atoms in the aromatic ring (Li et al., 2012). The isotopic shift of the phenylalanine marker band to lower wavenumbers indicated the incorporation of ^{13}C -naphthalene into the biomass of N47. However, N47 cells containing fully labeled phenylalanine only were not detected.

Due to financial reasons, the pre-culture of the analyzed N47 cells was grown with ^{12}C -naphthalene. Therefore, N47 grew with a mixture of the remaining ^{12}C -naphthalene and ^{13}C -naphthalene. The degradation of naphthalene and other metabolic pathways in N47 include several carboxylation (such as the initial step catalyzed by naphthalene carboxylase) and decarboxylation steps, which result in the incorporation of $^{12}\text{CO}_2$ originating from the unlabeled bicarbonate buffer.

Flow cytometry using N47 cells

During cultivation of N47 for Raman microspectroscopy, the cells were counted by flow cytometry. Initially, the samples were fixed with 2.5% glutardialdehyde and stored at 4 °C prior to analysis. However, the flow cytometry results indicated that glutardialdehyde interacted with N47 cells creating some agglutination of the cells (see Appendix; A7, C.). The cells could neither be analyzed by flow cytometry nor by Raman microspectroscopy (del Rocio Diaz Mejorada, 2013). Therefore, N47 cells were not fixed prior to flow cytometry and needed to be measured within two days after sampling (see Appendix; A7, A./B.).

3.6.2 Scanning Electron Microscopy of N47

The prepared N47 cells, which were used for Raman microspectroscopy (fixed in 1% paraformaldehyde and subsequently dehydrated in ethanol), were additionally analyzed by Scanning Electron Microscopy (SEM). The N47 cells were rod-shaped with a size of 1-2 μm (Fig. 50). Interestingly, some chemical attachment on the surface of the cells was observed (Fig. 50, B.). These attachments might represent naphthalene or ferrous sulfide (FeS). However, an impact of the fixation agent paraformaldehyde, such as the formation of crystals, could also not be excluded. The SEM of N47 was kindly provided by Dr. Natalia P. Ivleva and was performed by Dr. Andreas Schertel (Carl Zeiss Microscopy GmbH).

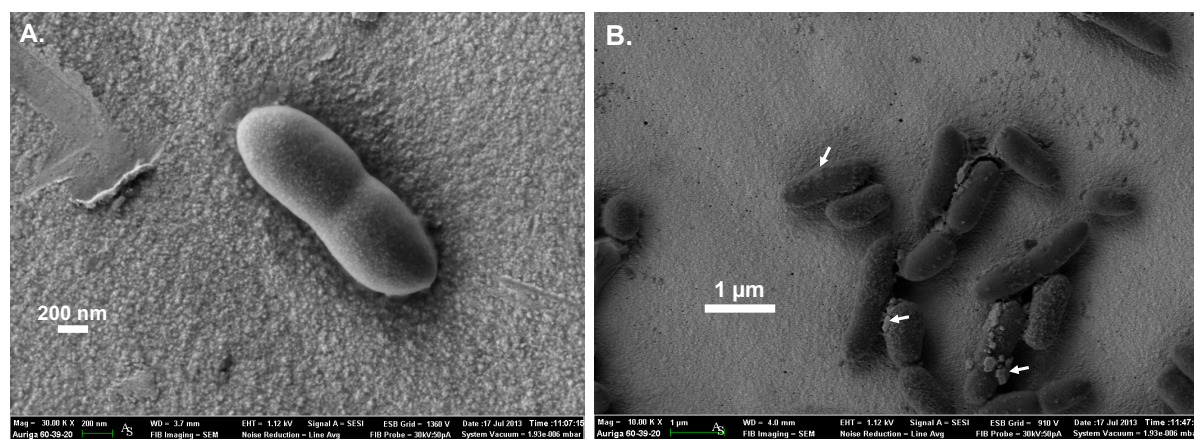


Figure 50: SEM image of N47 cells. A. Dividing N47 cell. **B.** N47 cells with chemicals attached to the cell surface indicated by arrows. The SEM images of N47 cells were provided by Dr. Natalia P. Ivleva and Dr. Andreas Schertel.

4. Discussion

Project 1

Identification of naphthalene carboxylase subunits of N47

The carboxylation of naphthalene is an unprecedented biochemical reaction and its activity could recently be measured in crude extracts of the sulfate-reducing culture N47 (Mouttaki et al., 2012). In proteogenomic studies in the two deltaproteobacterial strains N47 and NaphS2, similar gene clusters encoding carboxylase-like proteins were identified by 2D gel electrophoresis and gene expression analysis (DiDonato et al., 2010; Bergmann et al., 2011b). Interestingly, these two naphthalene-degrading strains are related only distantly (Selesi et al., 2010). Their 16S rRNA gene sequences shared sequence identity of 88.4%. Furthermore, they naturally occur in different habitats. Whereas N47 was isolated from a contaminated aquifer from a former coal gasification site near Stuttgart (Meckenstock et al., 2000), NaphS2 was found in anoxic marine sediments from a North Sea harbor near Wilhelmshaven (Galushko et al., 1999). Based on the conservation of the identified gene clusters within the two available genome sequences of naphthalene-degrading strains, the authors proposed the gene products to be involved in the carboxylation of naphthalene. In the present PhD project, the interaction of the gene products encoded within this naphthalene carboxylase gene cluster was shown for the first time. Based on the lines of evidence obtained in the present study, naphthalene carboxylase subunits were proposed to form a complex of around 750 kDa in native conformation.

4.1 Biochemistry of naphthalene carboxylase- Activity in cell-free extracts

To identify the enzyme catalyzing a reaction of interest, the enzyme is usually purified in its active state from cell-free extracts. Initially, it was planned to purify the naphthalene carboxylase complex under native conditions from N47 cells. Due to the slow growth and the little biomass obtained from N47, only limited material was available for the purification of this oxygen sensitive enzyme. Unfortunately, all initial attempts to purify the enzyme under native conditions failed as the generated cell-free extracts neither preserved the naphthalene carboxylase nor the isotopic exchange activity.

4.1.1 Naphthalene carboxylase activity located in the pellet fraction

After cell opening using various cell lysis techniques and a subsequent centrifugation step, naphthalene carboxylase activity was located in the pellet fraction indicating that naphthalene carboxylase might be attached to the membrane. However, a proteinase treatment of the

pellet fraction did not decrease the activity of the naphthalene carboxylase significantly. This observation might suggest that the enzyme could not be accessed by the proteinase, likely due to the following reasons:

i. Is the naphthalene carboxylase encapsulated in microcompartments?

Naphthalene carboxylase might have been encapsulated in a microcompartment comparable to a carboxysome. Carboxysomes were found in cyanobacteria and some chemoautotrophic bacteria (Cannon et al., 2001; Yeates et al., 2008). These proteinaceous polyhedral microcompartments are usually filled with ribulose-1,5-bisphosphate carboxylase/ oxygenase (RuBisCO), the key enzyme in CO₂ fixation and carbonic anhydrase which converts bicarbonate to CO₂. The encapsulation of these enzymes ensures a high local concentration of the reactants such as CO₂ and ribulose-1,5-bisphosphate. Additionally, it protects the enzyme RuBisCO from oxygen preventing the oxygenase site reaction (Marcus et al., 1992; Kinney et al., 2011). Due to these facts, the encapsulation of naphthalene carboxylase in a microcompartment could be advantageous as the enzyme was reported to be sensitive towards oxygen (Moultaki et al., 2012). However, the fast inactivation of the enzyme by exposure of the crude extracts to molecular oxygen might already indicate that it is not encapsulated.

All known carboxysome shell proteins contain a conserved bacterial microcompartment (BMC) domain (Pfam00936) (Yeates et al., 2008; Klein et al., 2009). Therefore, the genome of N47 was screened for genes potentially encoding carboxysome shell proteins such as *csoS1A-C* [α -type carboxysome] or *ccmK1-4* and *ccmO* [β -type carboxysome] (Badger and Bek, 2008; Kinney et al., 2011). In the genome of N47, no genes were detected that might encode proteins exhibiting a BMC domain. Due to missing candidate genes, encapsulation of the enzyme in microcompartments is rather unlikely.

ii. Is the activity in the pellet fraction detectable due to intact cells?

Crude bacterial extracts always contain intact cells. These cells are located in the pellet fraction after centrifugation. The naphthalene carboxylase activity detected in the pellet fraction might have occurred due to measurements made with whole N47 cells only. This assumption was strongly supported by the inability of proteinase K to inhibit naphthalene carboxylase activity in the pellet fraction. Moreover, incubation of the pellet fraction with high concentrations of salt did not transfer the naphthalene carboxylase activity from the pellet fraction to the supernatant, which would have been expected for membrane-associated proteins. It is also unlikely that an ordinary table centrifuge would be able to spin down membrane fragments, which were generated during cell lysis. Therefore, the activity of

membrane-associated enzyme would most likely be detectable in the soluble fraction after table centrifugation.

Furthermore, it seems unlikely that naphthalene carboxylase was dependent on the membrane potential since its activity was detected in cell-free extracts.

4.1.2 Naphthalene carboxylase activity in cell-free extracts in presence of ATP

Naphthalene carboxylase activity was detected in cell-free extracts of N47 cells, which were grown in a 200 L fermenter and disrupted by a French Press. Surprisingly, naphthalene carboxylase activity was increased 5-fold in the presence of ATP. In initial studies by Mouttaki et al. (2012) the enzyme was characterized as ATP-independent. In contrast to the initial characterization in which crude extract was added to the naphthalene carboxylase activity assay, in the present study cell-free extract was used. According to the new findings, naphthalene carboxylase might be ATP-dependent.

i. Is naphthalene carboxylase activity in cell-free extracts coupled to the direct esterification of 2-naphthoic acid?

The initial step in anaerobic catechol degradation by *Desulfobacterium* sp. strain Cat2 was demonstrated to be a carboxylation reaction to form protocatechuate (Gorny and Schink, 1994). Due to the equilibrium constant for the catechol carboxylation, the activity of the carboxylase could only be detected by coupling the carboxylation reaction to the esterification with CoASH followed by hydrolysis of pyrophosphate ensuring a direct removal of the product protocatechuate.

In the present study, we were able to show that the enzymes catalyzing the steps following the carboxylation reaction in anaerobic naphthalene degradation, such as 2-naphthoate-CoA ligase, 2-naphthoyl-CoA reductase, as well as the dihydro-2-naphthyl-CoA reductase were all active together in one assay (Fig. 51). The 2-naphthoate-CoA ligase activity most likely explains the comparatively low concentration of formed 2-naphthoic acid in cell-free extracts during the naphthalene carboxylase activity assay with ATP, as it might further convert the formed 2-naphthoic acid. However, the low detected activity for naphthalene carboxylase of $12 \text{ pmol min}^{-1} \text{ mg}^{-1}$ of protein might additionally reflect the physiological state of the N47 cells. The cells harvested from the fermenter were already in the late-exponential phase of growth and it is known that the naphthalene carboxylase activity decreases in this phase of growth (Dr. Housna Mouttaki, personal communication).

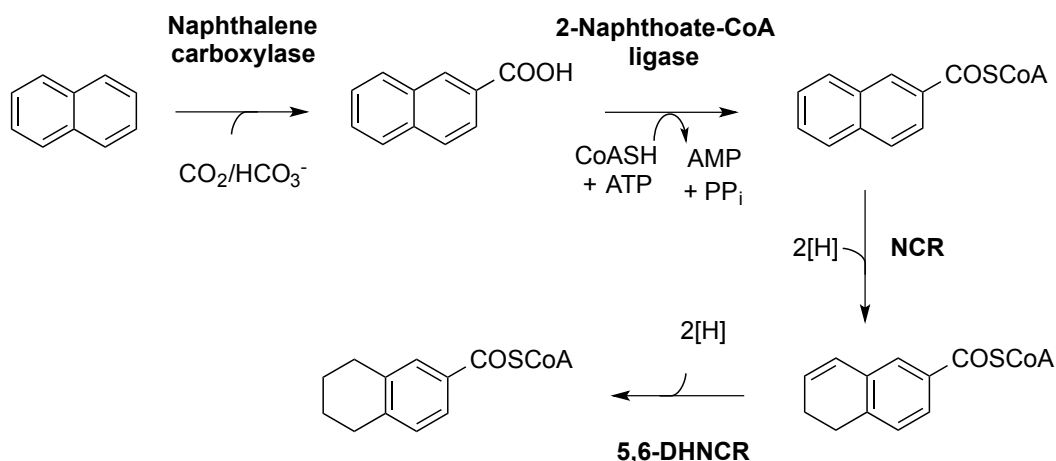


Figure 51: Initial steps in anaerobic degradation of naphthalene in the enrichment culture N47. NCR, 2-naphthoyl-CoA reductase; 5,6-DHNCR, 5,6-dihydro-2-naphthyl-CoA reductase.

If we would in fact deal with a scenario comparable to catechol carboxylation in strain Cat2, the addition of ATP to the naphthalene carboxylase activity assay would activate the 2-naphthoate-CoA ligase which would convert the newly formed 2-naphthoic acid produced by a putative ATP-independent naphthalene carboxylase. As a consequence, naphthalene carboxylase activity would be stimulated in the presence of ATP due to downstream reactions even though the enzyme would not be ATP-dependent.

In case of coupling between a carboxylation and a subsequent activation of the product by a ligase, one would not expect to detect the product of the first reaction as it would be converted immediately by the second enzyme catalyzing the exergonic reaction. Indeed, Gorny and Schink (1994) have not detected the free acid formed by catechol carboxylase in the activity assays without ATP and CoASH. In contrast, during naphthalene carboxylase activity assays in crude-extracts (without addition of ATP and CoASH) up to $1 \mu\text{M}$ of 2-naphthoic acid was detected (Mouttaki et al., 2012) and in activity assays of the naphthalene carboxylase in cell-free extracts in presence of ATP up to $2.5 \mu\text{M}$ 2-naphthoic acid were formed. Based on our results, a coupling of 2-naphthoate-CoA ligase and naphthalene carboxylase is rather unlikely.

The equilibrium of a reaction catalyzed by an AMP-forming ligase would only be shifted towards the product formation when the pyrophosphate is subsequently hydrolyzed by a pyrophosphatase (LeGall and Fauque, 1988; Schöcke and Schink, 1998). We have not tested whether a pyrophosphatase was active in cell-free extracts. N47 might use a membrane-bound pyrophosphatase to couple the hydrolysis of pyrophosphate to the membrane potential as described for other anaerobic bacteria (Nyren et al., 1991; Schöcke and Schink, 1998). In this case, pyrophosphatase activity would only occur in presence of the membrane fraction. Consequently, the 2-naphthoate-CoA ligase reaction in cell-free extracts

would not be exergonic enough to drive the reaction towards product formation. Naphthalene carboxylase would not be enhanced and the reactions would run into an equilibrium. However, our measurements showed that the naphthalene carboxylase activity is enhanced in the presence of ATP in cell-free extracts supporting that the carboxylation is not coupled to the 2-naphthoate-CoA ligase.

Based on the genome sequence, a gene encoding a putative membrane-bound phosphatase (*N47_E46900*) is present in N47, however, the activity needs to be measured in cell-free extracts to verify our assumption.

In activity assays with whole N47 cells, naphthalene carboxylase activity always leveled off after around 30 min with no novel formation of ^{13}C -labeled 2-naphthoic acid. This observation indicates that a specific compound, potentially a cofactor, was present within the cells and once fully consumed the reaction could not proceed any longer. The naphthalene carboxylase assay contained the educts of the reaction such as naphthalene and bicarbonate in excess, thus, a limitation of the substrates was rather unlikely. Notwithstanding, we suggest that the carboxylase was limited by a so far unknown compound such as ATP. If the missing compound would be CoASH or ATP for the ligase and the two enzymes would indeed be coupled, the free acid would first increase and then decrease as the accumulation of 2-naphthoic acid would shift the equilibrium towards the decarboxylation reaction. Without a coupling of the naphthalene carboxylase to an exergonic reaction such as hydrolysis of ATP, the enzyme would be theoretically fully reversible. However, the decarboxylation of 2-naphthoic acid to naphthalene could not be detected indicating that the enzyme is unidirectional (Dr. Housna Mouttaki, personal communication). The irreversibility of the naphthalene carboxylation might further support that the reaction is coupled to the hydrolysis of ATP.

In contrast to measurements with whole N47 cells, the concentration of 2-naphthoic acid formed by the naphthalene carboxylase in cell-free extracts in presence of ATP did not level off but further increased linearly. This result further supports that the naphthalene carboxylase activity might be limited in ATP during activity measurements with whole N47 cells and is not coupled to the subsequent activation by the ligase.

Due to the loss of 2-naphthoic acid by the downstream reactions, the detected specific activity of $12 \text{ pmol min}^{-1} \text{ mg}^{-1}$ of protein for the naphthalene carboxylase most likely did not represent the real activity of the enzyme. Only the purification of naphthalene carboxylase from cell-free extracts of N47 will allow to further analyze the kinetics of the enzyme and to investigate the impact of the following reactions on the carboxylation.

ii. Naphthalene carboxylase- an additional ATP-dependent enzyme in anaerobic degradation of naphthalene by the sulfate reducer N47?

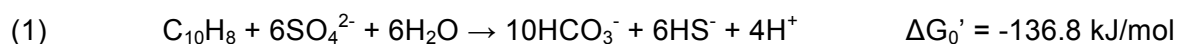
We do not have information about the endogenous ATP and CoASH pool within N47. However, it should be kept in mind that we are dealing with very low product concentrations (here 2-naphthoic acid) in a range of approximately 2 μM / mg of biomass. According to our data showing the formation of CoASH-esters in cell-free extracts of N47, it seems that the endogenous pool would allow ATP and CoASH-dependent reactions to a certain extent. Therefore, it might be possible to measure an ATP-dependent reaction such as naphthalene carboxylase with whole cells without further addition of ATP. Nevertheless, the available endogenous ATP will be limiting which might explain why naphthalene carboxylase activity with whole cells leveled off after a certain time. As aforementioned, in cell-free extracts with ATP the naphthalene carboxylase activity linearly increased supporting that ATP might be the limiting cofactor for the reaction.

Another question was whether an additional ATP-dependent step in the anaerobic degradation of naphthalene would be energetically conceivable for N47. To activate 2-naphthoic acid produced in the initial carboxylation step, the putative AMP-forming 2-naphthoate-CoA ligase (N47_I06840) potentially consumes two ATP equivalents. The tetrahydro-2-naphthoyl-CoA reductase was characterized as an ATP-dependent enzyme most likely consuming additional two ATP equivalents (Eberlein et al., 2013a; Eberlein et al., 2013b).

Due to its ten available carbon atoms, the oxidation of one molecule of naphthalene results in the formation of five molecules of acetyl-CoA, which can be used for energy conservation. Nevertheless, it must be taken into consideration that in dissimilatory sulfate-reducing bacteria the reductive half reaction is endergonic will therefore lower the available energy (Fuchs and Schlegel, 2006; Pereira et al., 2011; Grein et al., 2013). On the other hand, some other reactions might be coupled to the conservation of energy, especially in the downstream reactions of the anaerobic naphthalene degradation pathway. It was postulated that pimeloyl-CoA might be produced as an intermediate in the anaerobic degradation of naphthalene after the second ring-cleavage (Weyrauch et al., unpublished data). To link the further degradation of pimeloyl-CoA to the central metabolism of the cell, pimeloyl-CoA was suggested to be converted by several enzymatic steps to yield glutaryl-CoA. Weyrauch et al. proposed that in the following reactions, N47 might use a non-decarboxylating dehydrogenase forming glutaconyl-CoA, which is subsequently converted to crotonyl-CoA by an energy-conserving glutaconyl-CoA decarboxylase. This hypothesis was further supported by the genome sequence of N47 in which genes coding putative glutaconyl-CoA decarboxylases (N47_I06890 and N47_G40520) and putative acyl-CoA dehydrogenases (N47_I06870 and

N47_G40550) were identified and were in the close vicinity (Weyrauch et al., unpublished data). It was reported that the use of a non-decarboxylating glutaryl-CoA dehydrogenases enables anaerobic microorganisms to conserve energy by coupling the decarboxylation of glutaconyl-CoA with the translocation of sodium ions across the membrane (Buckel and Semmler, 1982, 1983; Bendrat and Buckel, 1993; Braune et al., 1999).

Under standard conditions, the oxidation of 1 mol naphthalene with sulfate as terminal electron acceptor theoretically efforts the conservation of around 1-2 mol ATP ($\Delta G_0' = -70$ kJ/mol ATP; equation 1 (Meckenstock and Mouttaki, 2011)).



Assuming that some so far uncharacterized reactions of the pathway might additionally conserve energy, an investment of the gained energy for an efficient ATP-dependent activation of naphthalene would theoretically be possible and, at the same time, still allow a total yield of about of 1-2 mol ATP per mol of naphthalene.

Most of the enzymes of the pathway were not biochemically characterized. Thus, their energy requirements are unknown and can only be estimated. A closer look at some reactions such as the activation of 2-naphthoic acid by the AMP-forming ligase might allow speculation on less energy-consuming alternative reactions. In the anaerobic degradation of toluene in *Thauera aromatica*, the anaerobic carnitine metabolism in *Escherichia coli* or *Proteus* sp., the anaerobic bile acid transformation in *Eubacterium* sp. and the anaerobic degradation of benzoate in *Geobacter metallireducens*, it has been reported that the activation of the respective compound could be catalyzed by an energetically less demanding CoA-transferase instead of a ligase (Leutwein and Heider, 1999; Heider, 2001; Oberender et al., 2012). The transferase would need the investment of one ATP equivalent rather than two as seen for the ligase.

In contrast to ligases, CoA-transferases are fully reversible which can be disadvantageous under low substrate concentration expected in nature compared to high substrate concentration during the cultivation of the microorganism in the laboratory (Oberender et al., 2012).

Furthermore, 2-naphthoate-CoA ligase might form ADP instead of AMP such as succinyl-CoA ligase (EC 6.2.1.5) or malate-CoA ligases (6.2.1.9). However, the identified candidate gene *N47_106840*, potentially encoding the 2-naphthoate-CoA ligase, exhibits an AMP-binding motif (Pfam00501) supporting the hydrolysis of ATP to AMP and pyrophosphate. Again, the ligase has neither been purified from N47 nor from NaphS2 cells but due to

previous studies N47_I06840 represents a likely candidate potentially catalyzing the activation of 2-naphthoic acid. Additionally, we could identify N47_I06840 as differentially abundant in one of the naphthalene-induced bands on BNP (see Discussion 4.4).

In BNP, a K^+ -insensitive pyrophosphate-energized proton pump N47_E46900 was differentially abundant in naphthalene growing N47 cells. We hypothesize that naphthalene carboxylase itself is coupled to the hydrolysis of one ATP to form AMP and 2 P_i as seen in *Aromatoleum aromaticum* strain EbN1 with acetone carboxylase (Schühle and Heider, 2011). Subsequently, the generated PP_i could be further hydrolyzed by the pyrophosphate-energized proton pump N47_E46900, which would be coupled to ATP formation by a membrane-bound ATPase. This would allow the formation of ATP coupled to PP_i cleavage to regain some of the invested energy from the carboxylation reaction. It was reported for a membrane-bound proton-translocating pyrophosphatase found in *Syntrophus gentianae*, a syntrophically benzoate-degrading fermenting bacterium, that one third of an ATP (which equals one proton pumped across the membrane) can be conserved per PP_i hydrolyzed (Schöcke and Schink, 1998).

On the other hand, we could identify the potential 2-naphthoate-CoA ligase in one of the naphthalene-induced bands on BNP indicating a close interaction of the naphthalene carboxylase complex with the ligase. Even though the naphthalene carboxylase and the 2-naphthoate-CoA ligase might interact closely, their reactions might be physiologically separated from each other. Putatively, instead of the naphthalene carboxylase, the ligase might interact with the identified membrane-bound pyrophosphatase hydrolyzing the produced PP_i , which would allow the conservation of energy coupled to a membrane potential.

In conclusion, according to our results, naphthalene carboxylase is most likely an ATP-dependent, soluble enzyme. The carboxylation of naphthalene is slightly endergonic under standard conditions ($\Delta G_0' = +14.2$ kJ/mol) (Meckenstock and Mouttaki, 2011). Initial studies on naphthalene carboxylase indicated that the reaction might be possible without ATP under the high concentrations of naphthalene and bicarbonate (Mouttaki et al., 2012). However, under the physiologically low substrate concentrations found in N47, it would be questionable if the degradation pathway of naphthalene could be initiated by an endergonic and theoretically reversible reaction as under these conditions the decarboxylation reaction would be favored. As mentioned earlier, an ATP-independent carboxylation of naphthalene would theoretically be reversible. In other organisms, efficient carboxylation reactions are energetically driven by exergonic reactions (Boll et al., 2014). These exergonic reactions

include the hydrolysis of an energy-rich bond as found for example in phosphoenolpyruvate (phosphoenolpyruvate carboxylase) or the hydrolysis of ATP in the carboxylation of acetophenone and acetone (Jobst et al., 2010; Schühle and Heider, 2011).

A potential ATP-dependency of naphthalene carboxylase would be unidirectional and shift the equilibrium towards the carboxylation even under low substrate concentration. Subsequent ATP-dependent (irreversible) esterification by a ligase would avoid the loss of the intermediate as CoA-ester are known to be membrane impermeable therefore allowing their accumulation within the cell (Fuchs et al., 2011). For a sulfate-reducing organism living at a contaminated site, ATP-dependency of the initial steps in the degradation pathway might result in very slow growth but it would allow efficient substrate utilization.

4.2 Molecular biological investigation on naphthalene carboxylase-Organization of the naphthalene carboxylase operon

Transcriptional analyses indicated that the genes encoding naphthalene carboxylase subunits were organized in form of an operon within the naphthalene carboxylase gene cluster. The operon from *N47_K27540* to *N47_K27460* covered 8.9 kbp including 9 genes. The two neighboring genes, which were not part of the operon, *N47_K27450* and *N47_K27460*, encoded HAD-like proteins (haloacid dehalogenase superfamily (HAD); cd01427; conserved domain database, National Center for Biotechnology Information). Among others, proteins belonging to the HAD-like hydrolase superfamily were reported to function as phosphatases (Koonin and Tatusov, 1994; Allen and Dunaway-Mariano, 2004; Kuznetsova et al., 2006). Another HAD-like protein, namely PpcC is part of the phenylphosphate carboxylase complex in *Thauera aromatica*, the key enzyme in anaerobic phenol degradation. Here, it was proposed to bind and dephosphorylate the substrate phenylphosphate before this intermediate is further carboxylated (Schühle and Fuchs, 2004). As there was so far no indication for such a phosphorylated intermediate in the carboxylation of naphthalene, a phosphatase-like subunit would not be required in the functional complex. However, genes encoding HAD-like proteins were conserved in the naphthalene carboxylase gene cluster within the genomes of N47 and NaphS2.

The gene clusters containing the naphthalene carboxylase genes were surrounded by viral genes in the genomes of N47 (*N47_K27300*, *N47_K27370*, *N47_K27640* putative transposases) and NaphS2 (*NPH_5851*, protein of IS4 family; *NPH_5852* putative transposase). Considering the high sequence identity of the gene clusters (up to 84%) and the presence of genetic elements, which are involved in DNA rearrangement, horizontal gene transfer could be suggested (Ochman et al., 2000; Frost et al., 2005; Wozniak and Waldor,

2010). The presence of transposases and IS elements in close vicinity of gene clusters involved in anaerobic degradation of (polycyclic)aromatic hydrocarbons was often observed and discussed as potential hint for putative horizontal gene transfer events in the evolution of aromatic hydrocarbon degradation (Rabus et al., 2005; Abu Laban et al., 2009; Carmona et al., 2009; Selesi et al., 2010).

4.3 Naphthalene carboxylase complex and its subunits

In comparative native proteomic studies on BNP, three naphthalene-induced bands with a size of around 750, 560, and 400 kDa were identified and analyzed. We could show that the naphthalene carboxylase subunits were included within all these induced bands. Seven out of nine proteins, which genes were encoded within the naphthalene carboxylase operon, were identified within the 750 kDa band, while the number of identified subunits decreased within the naphthalene-induced bands smaller than 750 kDa. This result indicated a disassociation of the complex. The 560 and 400 kDa bands were detected on BNP with proteins extracted from previously frozen naphthalene-grown N47 cells. We have shown in this study that the naphthalene carboxylase activity could not be detected in cells that were not freshly harvested. This was confirmed by the fact that the 750 kDa band was only visible using proteins extracted from freshly harvested cells in the mid-exponential phase of growth. Furthermore, the naphthalene-specific bands were not visible in 2-methylnaphthalene-grown N47 cells in which naphthalene carboxylase activity could hardly be detected. Therefore, it is likely that the 750 kDa band represented the active naphthalene carboxylase complex. However, at the present state we were not able to correlate the 750 kDa band with activity measurements.

In the following paragraph, the subunits encoded within the naphthalene carboxylase operon and their potential functions in the naphthalene carboxylase complex are discussed.

Various UbiD-like subunits, namely N47_K27540 (52.4 kDa), N47_K27500 (57 kDa), and N47_K27480 (54.5 kDa), are encoded within the naphthalene carboxylase operon. In *E. coli*, the 3-polyprenyl-4-hydroxybenzoate decarboxylase (UbiD) catalyzes the decarboxylation of an isoprenylated 4-hydroxybenzoate derivative in ubiquinone biosynthesis (Fig. 54) (Cox et al., 1969; Meganathan, 2001). The identified subunits in N47 showed up to 46% sequence identity to the alpha subunit of phenylphosphate carboxylase PpcA of *T. aromatica* and up to 48% to a putative benzene carboxylase AbcA of the iron-reducing enrichment culture BF (Schühle and Fuchs, 2004; Abu Laban et al., 2010).

The naphthalene carboxylase operon encodes as well ParA/MinD ATPase-like proteins, namely N47_K27510 (29.4 kDa) and N47_K27520 (33.6 kDa), which most likely represent

subunits of the complex. The presence of the ATPase-like subunits N47_K27510 and N47_K27520 within the complex correlates with our recent finding that naphthalene carboxylase might be ATP-dependent. Proteins of the ParA/MinD family include ATPases involved in a variety of cellular processes such as in chromosome segregation and cell division (Gerdes et al., 2000; Lutkenhaus, 2012).

Additionally, the subunits N47_K27530 (9.8 kDa), N47_K27490 (9.2 kDa), and N47_K27470 (16.6 kDa) annotated as hypothetical proteins, were encoded within the naphthalene carboxylase operon. Due to their small size and the fact that they do not contain any known conserved domain, one may speculate that these proteins might function as linker proteins in the naphthalene carboxylase complex.

The carboxylase-like subunit N47_K27460 could not be detected within the 750 kDa complex in BNP, neither could it be detected in 2D PAGE carried out by Bergmann et al. (2011b). However, this subunit interacted with the other carboxylase-like subunits (N47_K27540, N47_K27500 and N47_K27480) and the ATPase-like subunits (N47_K27520 and N47_K27510) in the *in vitro* pull-down assay. This might be due to the loss of the subunit N47_K27460 during sample preparation or the subunit does not belong to the active naphthalene carboxylase complex. Indeed, N47_K27460 showed high similarity to PpcX from *T. aromatica* and *A. aromaticum* strain EbN1. PpcX is a phenol-induced UbiD-like protein and its gene is encoded within the phenol gene cluster but it is not part of the phenylphosphate carboxylase complex (Schühle and Fuchs, 2004). Furthermore, a phylogenetic tree of UbiD/PpcA-like subunits, which were reported to be involved in anaerobic degradation of aromatic compounds, showed that both subunit, PpcX and N47_K27460, clustered together (Fig. 56). This supports the hypothesis that the carboxylase-like subunit N47_K27460 might not be part of the active naphthalene carboxylase.

With a size of at least 750 kDa, naphthalene carboxylase is a comparatively large complex. Moreover, our experiments showed that the complex was unstable. This might also explain why most of the initially tested opening techniques led to cell-free extracts without naphthalene carboxylase activity. The inhibitory effect of salt on the naphthalene carboxylase activity also confirms this hypothesis as high salt concentrations could disturb the interaction between the different subunits of the complex.

4.3.1 Potential regulation of the naphthalene carboxylase

i. Transcriptional regulation of the naphthalene carboxylase

The sulfate-reducing strain N47 is energetically limited when growing with naphthalene as a carbon source (see above). Therefore, it would be more reasonable to regulate the production of such a big complex at the transcriptional level and to minimize the energy need for protein production. The hypothesis of a transcriptional regulation could be supported by the presence of a putative regulator N47_K27610, which was identified up-stream of the naphthalene carboxylase operon. N47_K27610 showed sequence similarities to NifA, a transcriptional activator involved in nitrogen fixation (Buchanan-Wollaston et al., 1981). The putative regulator N47_K27610 contained a GAF (cGMP phospho-diesterase, Adenylate cyclase, FhlA domain) domain, a AAA⁺-domain (ATPases associated with a wide variety of cellular activities), and a helix-turn-helix (HTH_8) motif.

For promoter recognition and the initiation of transcription by the bacterial RNA polymerase, a sigma subunit is required to form a sigma-RNA polymerase holoenzyme (Fuchs and Schlegel, 2006). In the case of the sigma⁵⁴-RNA polymerase holoenzyme, the interaction with a transcriptional activator namely EBP (bacterial enhancer-binding protein) is needed to pursue initiation of the transcription (Buck et al., 2000; Zhang et al., 2002). The ATP-hydrolysis catalyzed by the transcriptional activator causes a conformational change of the closed sigma⁵⁴- RNA polymerase holoenzyme to an open and functional complex able to initiate transcription.

GAF domains were described as sensory modules of such bacterial enhancer-binding proteins (EBPs) activating the transcription by the RNA polymerase containing a sigma⁵⁴ factor (Studholme and Dixon, 2003). These domains were reported to bind various ligands such as formate to regulate the expression of genes encoding the formate hydrogenlyase components in *E. coli* (Hopper and Böck, 1995) or aromatic compounds such as dibenzofuran, dibenzo-*p*-dioxin, and biphenyl to regulate their degradation in actinomycetes (Iida et al., 2009). Furthermore, in *Azotobacter vinelandii* the GAF domain of NifA binds 2-oxoglutarate to regulate the expression of the nitrogenase (Little and Dixon, 2003).

A 'GAFTGA' motif, which is also conserved in the sequence of N47_K27610, was suggested to directly interact with the sigma factor (Zhang et al., 2002). Moreover, it was hypothesized that the C-terminal DNA helix-turn-helix motifs, such as the HTH_8 motif found in N47_K27610, might allow the binding of the EBPs to enhancer-like elements upstream of the sigma⁵⁴-dependent promoters (Studholme and Dixon, 2003).

GAF and PAS (named after homology to the period protein (PER) in *Drosophila*, the aryl hydrocarbon receptor nuclear translocator protein (ARNT) and single-minded protein (SIM) in

Drosophila (Hefti et al., 2004)) domains share similar structural properties (Ho et al., 2000). Interestingly, PAS domains were suggested to be involved in the regulation of toluene degradation in *Thauera aromatica* and in the regulation of ethylbenzene and acetophenone degradation in *Aromatoleum aromaticum* strain EbN1 (Leuthner and Heider, 1998; Rabus et al., 2002; Kube et al., 2004).

In summary, the GAF domain of N47_K27610 might bind naphthalene and thereby enhance the expression of genes encoded within the naphthalene carboxylase operon. However, the transcriptional regulation of naphthalene carboxylase has not been studied yet.

ii. Post-translational regulation of naphthalene carboxylase

In previous studies, cell-free extracts grown with different substrates showed no striking differences in the protein induction pattern on SDS-PAGE (Bergmann, 2010). However, by using BNP to study native protein complexes, naphthalene-induced protein bands were clearly visible on the gel. The subunits of naphthalene carboxylase were differentially abundant with ratios up to 155, unlike with SDS-PAGE where N47_K27540 showed an up-regulation of only up to 5.5 when comparing naphthalene versus 2-methylnaphthalene growing cells (Bergmann et al., 2011b).

Based on these data, it seems that the synthesis of the subunits of the naphthalene carboxylase complex might not be regulated at the transcription level, as they were probably produced constitutively in cells grown on naphthalene and 2-methylnaphthalene. However, the functional naphthalene carboxylase complex was only produced in naphthalene-grown cells. This indicates that there might be a post-translational regulation of the naphthalene carboxylase complex. Indeed, a regulation factor of unknown identity, such as a chaperon, might enable the assembly of the produced subunits into a functional naphthalene carboxylase complex. The assembly of RuBisCO for example is known to be depending on chaperons (Liu et al., 2010; Bracher et al., 2011).

4.4 Interaction of naphthalene carboxylase with other proteins

i. 2-naphthoate-CoA ligase N47_I06840

The interaction of the naphthalene carboxylase with a potential 2-naphthoate-CoA ligase (N47_I06840) was observed. N47_I06840 shared sequence identity of 35% to phenylacetate-CoA ligase of *Desulfobacula toluolica* Tol2. Phenylacetate-CoA ligase catalyzes the first step in the aerobic and anaerobic degradation of phenylacetate in various bacteria by the conversion of phenylacetate to phenylacetyl-CoA (Martínez-Blanco et al.,

1990; Mohamed and Fuchs, 1993; Mohamed, 2000). The ligases known to activate aromatic compounds were reported to function as monomers or homodimers in their active form (Mohamed and Fuchs, 1993; Gibson et al., 1994; Egland et al., 1995; Schühle et al., 2003; Wischgoll et al., 2005; Kawaguchi et al., 2006) leading to an expected size of around 50 or 100 kDa for N47_I06840 as a monomer or dimer, respectively. However, N47_I06840 was present and differentially abundant within the band of around 400 kDa on BNP suggesting a possible interaction of the naphthalene carboxylase complex with the potential 2-naphthoate-CoA ligase. Moreover, N47_I06840 shared 77.1% sequence identity with the protein NPH_5477 shown to be up-regulated under growth with naphthalene in NaphS2 (DiDonato et al., 2010). The gene encoding NPH_5477 shared 50% similarity with a ligase identified in *E. coli* and is part of a cluster containing reductases, which play a role in the initial ring dearomatization of naphthalene in anaerobic naphthalene degradation (DiDonato et al., 2010; Eberlein et al., 2013a). Therefore, it was suggested by the authors to be the 2-naphthoate CoA-ligase in NaphS2.

ii. Interaction of naphthalene carboxylase with membrane proteins

For naphthalene carboxylase, we have initially suggested that the enzyme could be membrane associated since the activity could only be measured in the pellet fraction of crude cell extracts. However, naphthalene carboxylase activity could finally be measured in cell-free extracts once the French Press could be used to disrupt the N47 cells. Since the naphthalene carboxylase was shown to be unstable, the dissociation of the complex after the opening techniques used previously was most likely the reason for its inactivity (see Discussion 4.3). The protein sequences of the naphthalene carboxylases subunits indicated that they were not membrane proteins. However, their interaction with membrane-bound or membrane-associated proteins could not be excluded. In BNP, a few membrane proteins were found that were differentially abundant in naphthalene-grown cells.

As mentioned above, an annotated K(+)-insensitive pyrophosphate-energized H⁺ pump, which is proposed to generate a proton motive force while coupled to the hydrolysis of newly formed pyrophosphate, was identified in the proteomic approach. An interaction with the naphthalene carboxylase to supply energy in the form of ATP could be possible and was discussed in section 4.1.2, i.

Proteins which are annotated as heterodisulfide reductases were identified within the naphthalene-induced bands on BNP. In methanogenic archaea, heterodisulfide reductases catalyze the reduction of a heterodisulfide of coenzyme M and coenzyme B (CoM-S-S-CoB).

This reduction is an exergonic process. In methanogens without cytochromes, heterodisulfide reductases and hydrogenases form a complex in which the endergonic reduction of ferredoxin with H₂ is coupled to the exergonic reduction of CoM-S-S-CoB with H₂ via a flavin-based electron bifurcation (Thauer et al., 2008; Costa et al., 2010; Buckel and Thauer, 2013). Furthermore, in class II benzoyl-CoA reductases a similar electron bifurcation process was proposed. Here, BamDE share sequence similarity to heterodisulfide reductases (Kung et al., 2009; Fuchs et al., 2011). For the carboxylation of naphthalene, a reduction step is not necessary and the presence of heterodisulfide reductases cannot be explained at the present state of knowledge.

iii. The FAD-binding protein N47_A07150

One interesting interaction with a putative FAD-binding protein N47_A07150 was observed in the pull-down assay but not in BNP. N47_A07150 was identified earlier on a 1D SDS-PAGE investigating the differential protein induction pattern of cells grown with naphthalene versus 2-methylnaphthalene. This protein was more abundant in naphthalene-grown cells with a ratio of 110 compared to 2-methylnaphthalene-grown cells (Moultaki et al., unpublished data). The protein shared sequence similarity to putative FAD-dependent oxidoreductases. N47_A07140 overlapped with N47_A07150 and showed a NAD-binding domain. Potentially, both proteins function together in one reaction. The adjacent genes encode proteins that show sequence similarity to viral genes acting in DNA rearrangement. The genes encoding the putative oxidoreductases flanked the edge of the contig, therefore, genes which were encoded up-stream could not be identified. As the putative oxidoreductases were not detected in BNP, they were not suggested of being part of the complex but they might be involved in the initial activation of naphthalene. At the current state of knowledge, we do not have experimental data supporting this hypothesis.

4.5 Complexes involved in anaerobic 2-methylnaphthalene degradation

On BNP, a differentially abundant band with a size of about 200 kDa was visible from protein samples of 2-methylnaphthalene-grown N47 cells. Proteomic analyses have shown that within this band, subunits of naphthyl-2-methyl-succinate synthase NmsABC and its activating enzyme NmsD were identified. Additionally, all the subunits involved in the β -oxidation of naphthoyl-2-methyl succinate to the formation of naphthoyl-CoA, which are encoded within the *bns* operon, were identified (Fig. 52).

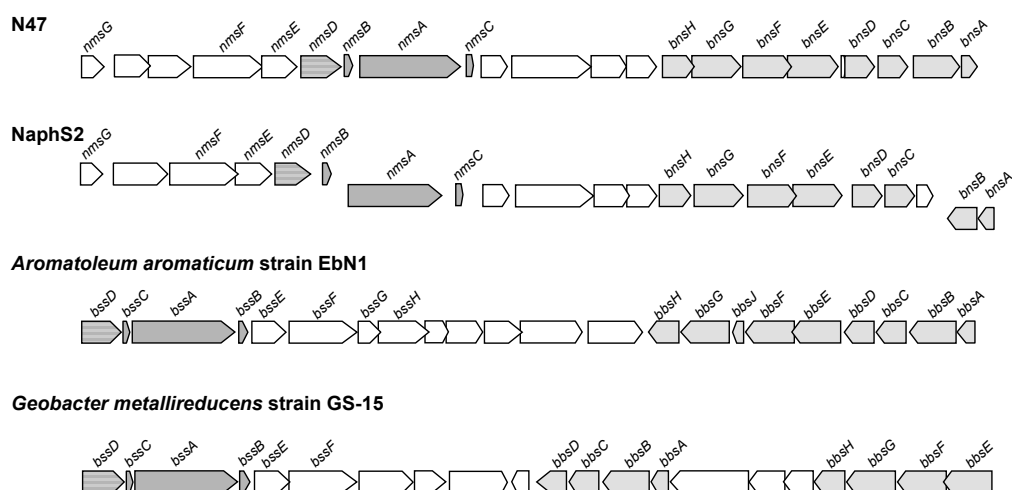


Figure 52: Organization of the *nms* and *bns* gene clusters involved in anaerobic degradation of 2-methylnaphthalene in the sulfate-reducing culture N47 (GI:308272792 to GI:308272813) and NaphS2 (GI:300445470 to GI:300445481; GI:493469349 to GI: 493469353; GI:493468260 to GI:493468261) compared to the organization of the *bss* and *bbs* genes encoding enzymes involved in anaerobic degradation of toluene in *Aromatoleum aromaticum* strain EbN1 (GI:499556099 to GI:499556120) and *Geobacter metallireducens* strain GS-15 (GI:404496403 to GI:404496383). In NaphS2, the genes of the *nms* and *bns* gene cluster are encoded on separate contigs in two distinct clusters. Open reading frames are represented by arrows. Genes of the *nms/bss-operon* are shown in dark grey, those of the *bns/bbs-operon* are indicated in light grey. Annotated function of gene products involved in anaerobic degradation of 2-methylnaphthalene: NmsABC and NmsD, naphthyl-2-methyl-succinate synthase and the activating enzyme; NmsE, putative chaperone; BnsH, naphthyl-2-methylene-succinyl-CoA hydratase; BnsG, naphthyl-2-methyl-succinyl-CoA dehydrogenase; BnsEF, naphthyl-2-methyl-succinate CoA transferase; BnsCD, naphthyl-2-hydroxymethylsuccinyl-CoA dehydrogenase; BnsAB, naphthyl-2-oxomethyl-succinyl-CoA thiolase; NmsG, NmsF and NmsE, hypothetical proteins. Annotated function of gene products involved in anaerobic degradation of toluene: BssABC and BssD, benzylsuccinate synthase and the activating enzyme; BssE, putative chaperone; BssH, putative transporter; BbsEF, succinyl-CoA:(R)-benzylsuccinate CoA-transferase; BbsG, (R)-benzylsuccinyl-CoA dehydrogenase; BbsH, phenylitaconyl-CoA hydratase; BbsCD, 2-[hydroxy(phenyl)methyl]-succinyl-CoA dehydrogenase; BbsAB, benzoylsuccinyl-CoA thiolase; BssF, BssG, BbsI, and BbsJ, hypothetical proteins.

According to previous data on β -oxidation enzymes involved in the anaerobic degradation of toluene and based on their molecular sizes, we could estimate the theoretical sizes of the different enzymes involved in the β -oxidation of naphthyl-2-methyl-succinate (Tab. 34).

The molecular masses experimentally determined by BNP for NmsABC, BnsEF, and BnsG match the expected sizes of around 200 kDa. However, based on previous studies the

respective sizes of BnsH, BnsCD, and BnsAB were suggested to be smaller (Tab. 34). This finding might be explained by a close interaction of the β -oxidation enzymes and the formation of supercomplexes. Since their intermediates are CoA-esters, which are known to be degraded easily by thioesterases in the cytosol, a close interaction of the enzymes might prevent them from further degradation. No biochemical studies were carried out on the enzymes involved in the degradation of 2-methylnaphthalene, therefore, the composition of the active enzymes and their resulting molecular weights remain unknown.

Table 34: Theoretically estimated molecular weights for the enzymes involved in the anaerobic 2-methylnaphthalene degradation in N47 based on characterized enzymes involved in the anaerobic degradation of toluene.

Enzyme	Theoretical apparent molecular weight	
Naphthyl-2-methyl-succinate synthase NmsABC	223.4 kDa ($\alpha_2\beta_2\gamma_2$)	(Selesi et al., 2010)
Naphthyl-2-methyl-succinate CoA transferase BnsEF	185.2 kDa ($\alpha_2\beta_2$)	(Leutwein and Heider, 2001)
Naphthyl-2-methyl-succinyl-CoA dehydrogenase BnsG	185.2 kDa (α_4)	(Leutwein and Heider, 2002)
Naphthyl-2-hydroxymethyl-succinyl-CoA hydratase BnsH	117.2 kDa (α_4)	(Lippert, 2009)
Naphthyl-2-hydroxymethylsuccinyl-CoA dehydrogenase BnsCD	53.8 kDa ($\alpha\beta$)	(Lippert, 2009)
Naphthyl-2-oxomethyl-succinyl-CoA thiolase BnsAB	113.2 kDa ($\alpha_2\beta_2$)	(Lippert, 2009)

Furthermore, proteomic analysis allowed the identification of NmsA, BnsEF, and BnsG with more peptides within the band. For NmsB and NmsC lower peptide numbers were identified, which was most likely due to their small protein sizes (around 7.9 and 6.8 kDa). From personal communication, we know that one of the limitations of proteomic analysis using a LC-MS/MS (especially without the addition of DMSO into the buffers (Hahne et al., 2013)) is that smaller peptides and/or hydrophobic peptides could be overlooked or remain undetected. As a consequence, the abundance of this particular protein would be underestimated and not be identified.

4.6 Naphthalene carboxylase in NaphS2

In contrast to N47, differences in the protein production pattern on BNPs when comparing NaphS2 cells grown with naphthalene versus 2-methylnaphthalene were not as obvious. However, to a lower extent, we could still see the same induction profile with NaphS2.

As mentioned earlier, a putative NifA-like transcriptional regulator was identified up-stream of the naphthalene carboxylase operon in N47 (see Discussion 4.3.1). Sequence analyses of genes up-stream of the naphthalene carboxylase cluster in the NaphS2 genome did not show similarities to any known transcriptional regulator suggesting a different or no regulation of the gene cluster. However, the possible existence of a regulation of the naphthalene carboxylase operon in N47, or NaphS2, has not been experimentally investigated yet.

4.7 UbiD-like (de)carboxylases involved in anaerobic degradation of aromatic compounds- A new class of enzymes with common properties?

To date, only limited biochemical data are available for members of the UbiD-like decarboxylase/ carboxylase enzyme family acting in the anaerobic degradation of (poly)aromatic compounds such as phenol, benzene, hydroxyarylic acids, terephthalate, and naphthalene. However, one may speculate that all members of this putative enzyme family might share common features in the reaction mechanism.

The first indications that UbiD-like subunits might be involved in the (de)carboxylation reaction of aromatic compounds were often derived from proteogenomic approaches. The analysis of the genomes of the microorganisms showed that *ubiD*-like genes, which might be involved in the (de)carboxylation reaction of the aromatic compounds, were organized in a similar structure (see Fig. 53). However, so far only some enzymes of the UbiD-like enzyme family such as the phenylphosphate carboxylase from *T. aromatica* and some non-oxidative decarboxylases have been purified and biochemically characterized.

In the following paragraph, we will discuss potential members of this new UbiD-like enzyme family which might be involved in the (de)carboxylation of aromatic compounds in the anaerobic degradation. Moreover, we will compare and discuss the available biochemical data for the naphthalene carboxylase with the phenylphosphate carboxylase.

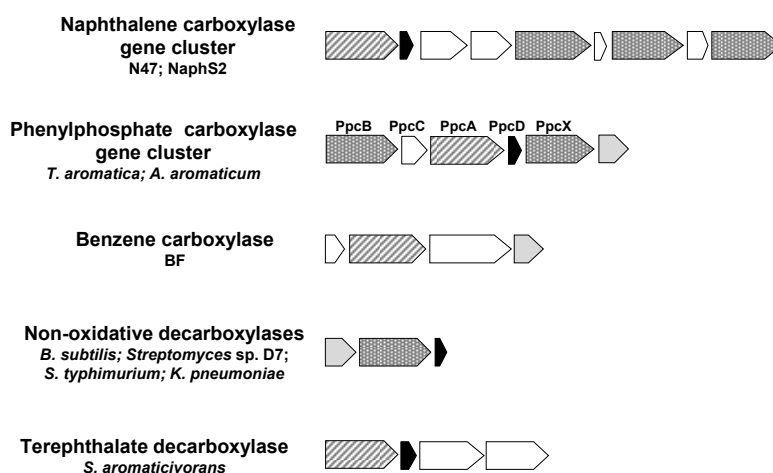


Figure 53: Organization of gene clusters encoding UbiD-like proteins catalyzing (de)carboxylation reactions potentially involved in anaerobic degradation of aromatic compounds. The naphthalene carboxylase gene cluster is encoded within the genome of the sulfate-reducing cultures N47 (GI:308273914 to GI:308273906) and NaphS2 (GI:300445470 to GI:300443511). The phenylphosphate carboxylase PpcABCD is encoded within the phenol gene cluster in the nitrate reducers *T. aromatica* (GI:10697121 to GI:10697125) and *A. aromaticum* strain EbN1 (GI:56475432 to GI:56475432). The putative benzene carboxylase gene cluster (GI:300245886 to GI:300245892) was identified within the genome of the iron-reducing culture BF. Moreover, in *B. subtilis* (GI:2632649 to GI:225184740), *Streptomyces* sp. D7 (GI:4741968 to GI:4741970), *S. typhimurium* (GI:16421470 to GI:16421472) and *K. pneumoniae* (GI:66932639 to GI:66866415) gene clusters for non-oxidative decarboxylases (subunits BCD) were identified. It should be noted that for the non-oxidative decarboxylases in *S. hydroxybenzoicus* (GI:5739200 to GI:67462197) the genes organization was different (subunits CDB). Recently, a putative terephthalate decarboxylase gene cluster was identified within the genome of *S. aromaticivorans* (GI:655512305 to GI:655512308). Open reading frames are represented by arrows. *UbiD*-like genes of are shown in a pattern fill, whereas striped arrows represent *PpcA*-like genes. *PpcD*-like genes are indicated by dark grey and *UbiX*-like genes in light grey. Further details are mentioned in the text.

4.7.1 UbiD in ubiquinone biosynthesis

The decarboxylase UbiD is involved in ubiquinone biosynthesis in *E. coli* (Fig. 54). The holoenzyme had an apparent molecular mass of 340 kDa and its activity required a metal ion preferably Mg^{2+} and an unidentified heat stable cofactor of about 10 kDa (Leppik et al., 1976). The presence of the reducing agent dithiothreitol increased the enzyme activity. Furthermore, the addition of membranes or phospholipids stimulated the activity indicating its physiological function in association with the membrane. However, Leppik et al. (1976) showed that the enzyme could be separated from the membrane by centrifugation.

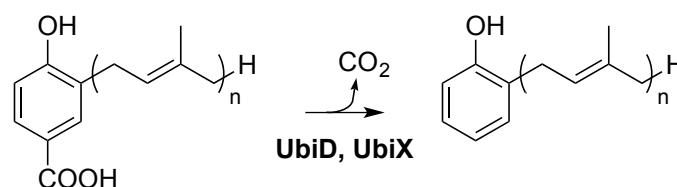


Figure 54: Decarboxylation catalyzed by UbiD during ubiquinone biosynthesis.

i. UbiX- An isoenzyme of UbiD in ubiquinone biosynthesis?

In the *E. coli* genome, another protein, UbiX a putative isoenzyme of UbiD, is encoded. It has not been established how the two proteins act together with one another (Zhang and Javor, 2003). It was hypothesized that UbiX could potentially be involved in substrate delivery to UbiD (Gulmezian et al., 2007).

In yeast, two enzymes PAD1 (UbiX homolog) and FDC1 (UbiD homolog) are required for the decarboxylation of antimicrobial aromatic acids. Interestingly, the two enzymes shared sequence similarities to UbiX (50% sequence similarity with PAD1) and UbiD (22% sequence similarity with FDC1) from *E. coli*. Very recently, Lin et al. (2015) demonstrated that PAD1, annotated as phenylacrylic acid decarboxylase, was a FMN-containing protein and did not function as a decarboxylase. The authors suggested that PAD1 catalyzed the formation of a novel cofactor required by FDC1, a ferulic acid decarboxylase, for its activity. The cofactor was very labile and could not be identified but most likely it was a modified form of a reduced FMN (Lin et al., 2015). Surprisingly, UbiX from *E. coli* could replace PAD1 in its function to activate FDC1 and vice versa, PAD1 could replace the function of UbiX in the biosynthesis of ubiquinone in *E. coli*. As a consequence, the authors hypothesized that UbiX might synthesize a FMN-related cofactor required by UbiD in the ubiquinone biosynthesis in *E. coli*.

ii. UbiX-like proteins in the anaerobic degradation of aromatic compounds

In *Thauera aromatica*, a protein which shared sequence similarities to UbiX, the aforementioned putative isoenzyme of UbiD in the ubiquinone biosynthesis in *E. coli*, was induced during the anaerobic degradation of phenol (Schühle and Fuchs, 2004). The genes encoding this UbiX-like protein, the subunits of phenylphosphate carboxylase (PpcBCAD) as well as the subunits of phenylphosphate synthetase (PpsABC) were all together present within the phenol gene cluster in the genome of *T. aromatica*. However, the UbiX-like protein was shown not to be part of the native phenylphosphate carboxylase enzyme complex. Therefore, the UbiX-like protein was suggested to be involved in the carboxylation of other phenolic compounds but its function remained unclear (Schühle and Fuchs, 2004).

In the N47 genome, an *ubiX*-like gene was not in the vicinity of the naphthalene carboxylase operon, but two identical copies *N47_B20630* and *N47_H21380* were encoded elsewhere within the N47 genome. The differentiation between these two proteins was not possible because both subunits shared 100% identity but one or both of them were more abundant in cells grown with naphthalene.

In NaphS2, an UbiX-like protein NPH_5865 was encoded within the cluster and was shown to be differentially abundant in naphthalene-grown cells. Previous work done by DiDonato et al. (2010) showed similar results confirming its probable role in naphthalene degradation.

As mentioned above, a recent publication might indicate that UbiX-like proteins synthesized a FMN-like cofactor required by the respective (de)carboxylase (Lin et al., 2015). All the UbiD-like subunits of naphthalene carboxylase showed putative FMN-binding sites and the UbiX-like subunits were differentially abundant in N47 and NaphS2 cells grown on naphthalene, which might support such a cofactor requirement. However, to biochemically demonstrate such a potential role of UbiX for naphthalene carboxylase more knowledge about the enzyme is required.

4.7.2 Comparison of naphthalene carboxylase with phenylphosphate carboxylase, the prototype of UbiD-like enzymes in anaerobic degradation of aromatic compounds

Phenylphosphate carboxylase represents the prototype of UbiD-like carboxylases and is a key enzyme in the anaerobic degradation of phenol. The purified enzyme from *T. aromatica* was composed of four subunits including two UbiD-like proteins ($\alpha\beta$, 54 and 53 kDa), a hypothetical protein (γ , 10 kDa) and a phosphatase-like protein (δ , 18 kDa) (Schühle and Fuchs, 2004).

Like the naphthalene carboxylase complex, the phenylphosphate carboxylase holoenzyme was unstable and during purification the enzyme dissociated into a core complex ($\alpha\beta\gamma$) and the phosphatase-like δ -subunit. The core complex ($\alpha\beta\gamma$) was able to catalyze the exchange reaction between $^{14}\text{CO}_2$ and the carboxyl group of 4-hydroxybenzoate but not the phenylphosphate carboxylation reaction itself. The holoenzyme and its activity could be reconstituted by the addition of the heterologously produced δ -subunit. For naphthalene carboxylase, both activities, the carboxylation and the exchange reaction, could not be detected in cell-free extracts generated by most of the cell lysis techniques utilized. Based on our current data, we cannot comment on the catalytic structure for none of the two reactions catalyzed by the naphthalene carboxylase.

The core complex of the phenylphosphate carboxylase had an apparent molecular weight of around 360 kDa and the heterologously produced δ -subunit of around 58 kDa. Therefore, the authors suggested a trimeric structure ($\alpha\beta\gamma\delta$)₃. The naphthalene carboxylase complex had a putative size of around 750 kDa in its native conformation. However, it is not possible to predict the stoichiometry of subunits within the complex based on proteomic data. Therefore, the stoichiometry remains speculative. If all the subunits of the operon would be involved in the complex, it would have a minimum size of around 314 kDa, without N47_K27460 around 263 kDa. Analogously to phenylphosphate carboxylase, a trimeric structure would result in a size of about 943 kDa or 787 kDa with or without N47_K27460, respectively. A size of around 787 kDa would match the molecular mass obtained on the BNP.

Phenylphosphate carboxylase required K^+ and divalent metal cations like Mg^{2+} or Mn^{2+} for its activity but no other cofactors were detected. In the present PhD project, we showed that naphthalene carboxylase might be ATP-dependent. At the present state of knowledge, the presence of other cofactors in naphthalene carboxylase remains elusive since we were not able to purify the protein so far. Based on the amino acid sequence, potential binding sites for FMN (GO0010181; UniProt-GO annotation database, European Bioinformatics Institute) and nucleotide-binding domains were identified in the carboxylase-like subunits N47_K27540, N47_K27500, N47_K27480, and N47_K27460 and in the ATPase-like proteins N47_K27510 and N47_K27520 (cd02037; conserved domain database, National Center for Biotechnology Information), respectively.

The phenylphosphate carboxylase was shown to be oxygen sensitive and reducing agents except for dithionite did not impair the enzyme activity. After inactivation of the enzyme with molecular oxygen, the phenylphosphate carboxylase activity could be completely recovered by subsequently anoxic incubation of the enzyme with the reducing agent 2-mercaptoethanol (Schühle and Fuchs, 2004). Naphthalene carboxylase was also inhibited by oxygen but in contrast to phenylphosphate carboxylase, its activity was inhibited by all tested reducing agents such as sodium dithionite, 2-mercaptoethanol, and Ti(III) citrate (Mouttaki et al., 2012).

4.7.3 UbiD-like (de)carboxylases involved in anaerobic degradation of aromatic compounds

i. Benzene carboxylase

Based on proteogenomic data, other UbiD-like carboxylases acting on non-substituted aromatic compounds were identified and suggested to be the putative benzene carboxylase

subunits. Genes encoding putative benzene carboxylases were identified in the genome of the iron-reducing enrichment culture BF (Abu Laban et al., 2010), the pure archaeal culture *Ferroglobus placidus* (Holmes et al., 2011) and recently in the metagenome of a benzene degrading, nitrate-reducing enrichment culture (Luo et al., 2014). Other putative benzene carboxylases from *F. placidus* and the *Peptococcaceae* in the nitrate-reducing enrichment culture shared between 31% and 90% sequence identity to the putative benzene carboxylase *AbcA* of BF, respectively (Holmes et al., 2011; Luo et al., 2014). Moreover, the organization of the genes seemed to be identical between the bacterial strains (Luo et al., 2014). In the putative benzene carboxylase gene cluster, genes were present encoding a phenylphosphate γ -subunit-like protein *AbcD*, an UbiD-like protein *AbcA*, a putative Benzoyl-CoA ligase *BziA*, and an UbiX-like protein (Fig. 53). However, in the archaeal genome of *F. placidus*, only an *abcA* homolog was identified (Holmes et al., 2011). Moreover, the *AbcA* from *F. placidus* showed higher sequence similarity to the UbiD from *E. coli* than to UbiD-like subunits, which are involved in aromatic compound carboxylation (Fig. 56). So far, biochemical data confirming the carboxylation of benzene are missing.

ii. Non-oxidative hydroxyarylic acid decarboxylases/ phenol carboxylases

Another group of UbiD-like enzymes acting in the anaerobic degradation of aromatic compounds are the reversible, non-oxidative, cofactor-independent hydroxyarylic acid decarboxylases/ phenol carboxylases (Lupa et al., 2005). All members of this enzyme family were encoded within a cluster of three genes *BCD*, where gene *B* shows similarity to *ubiX*, gene *C* to *ubiD* and gene *D* is unique. The organization of the genes can vary among different species. Characterized members of this enzyme family are a vanillate (4-hydroxy-3-methoxybenzoate)/ 4-hydroxybenzoate decarboxylase from *Bacillus subtilis* (BsdBCD) (Lupa et al., 2008), a vanillate decarboxylase from *Streptomyces* sp. D7 (Chow et al., 1999) (VdcBCD) and hydroxyarylic acid decarboxylases from *Salmonella typhimurium* (StdBCD) and *Klebsiella pneumoniae* (KpdBCD) (Lupa et al., 2005). These enzymes were predominantly found in facultative anaerobes and catalyze the (de)carboxylation under both oxic and anoxic conditions.

Another member of the family sharing common features is the oxygen-sensitive 4-hydroxybenzoate decarboxylase from *Sedimentibacter hydroxybenzoicus*. The enzyme was reported to form a complex of 350 kDa. Its activity did not require the presence of any cofactor e.g. metal ions or ATP (He and Wiegel, 1995; Breitenstein et al., 2002). The enzyme catalyzed as well the reverse reaction, the carboxylation of phenol but at much slower rates. Lupa et al. (2005) demonstrated that the heterologous production of the subunits C and D in

E. coli was sufficient for the 4-hydroxybenzoate decarboxylase activity. However, they suggested that the function of the subunit B could be replaced by the inherent UbiX in *E. coli*, which was over 50% similar to subunit B.

Likewise the 4-hydroxybenzoate decarboxylase from *S. hydroxybenzoicus*, the vanillate decarboxylase (Vdc) from *Streptomyces* sp. D7 belongs to the enzyme family of non-oxidative hydroxyarylic acid decarboxylases/ phenol carboxylases and is encoded by the three clustered genes *vdcBCD*. The heterologous production of different combinations of the subunits (each of the *vdc* genes separately or in combination of two) of the vanillate decarboxylase from *Streptomyces* sp. D7 in *Streptomyces lividans* resulted in a non-functional enzyme (Chow et al., 1999). UbiX-like proteins found in the genome of *S. lividans* showed 36% sequence identity to VdcB from *Streptomyces* sp. D7 and were obviously not able to replace the function. This result supported the aforementioned hypothesis that all three subunits B, C, and D were required for a functional non-oxidative hydroxyarylic acid decarboxylase/ phenol carboxylase.

iii. Terephthalate decarboxylase

Recently, the genome of an anaerobic, syntrophic organism *Syntrophorhabdus aromaticivorans* strain UI capable to grow with different aromatic compounds under methanogenic conditions was sequenced (Nobu et al., 2014). Within the genome, gene clusters were identified which were similar to the genes encoding phenylphosphate synthetase and phenylphosphate carboxylase from *T. aromatica* suggesting that phenol could be degraded in a homologous ATP-dependent reaction. Moreover, a gene cluster putatively encoding enzymes involved in the degradation of terephthalate was identified. A gene product of this cluster, namely SynarDRAFT_0373 showed similarity to the putative PpcA-like and UbiD-like decarboxylase Tadcc27178 which was suggested to be the terephthalate decarboxylase in a syntrophic *Pelotomaculum* strain (Lykidis et al., 2011; Wu et al., 2013). Therefore, analogously to the syntrophic, terephthalate degrading *Pelotomaculum* strain, the authors speculated that terephthalate is first activated by a ligase and subsequently decarboxylated by a complex of an UbiD-like protein and a phenylphosphate γ -subunit-like protein to produce benzoyl-CoA (Fig. 55). However, no biochemical data confirming these reactions are available yet.

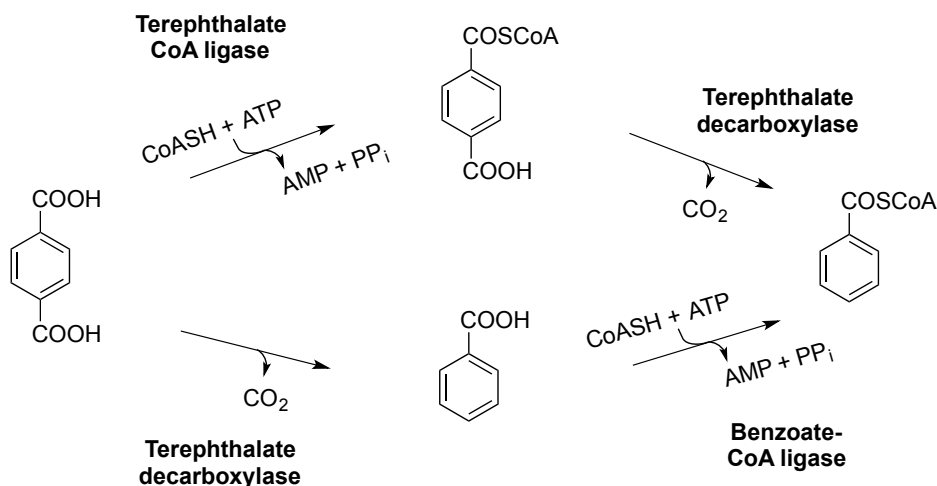


Figure 55: Synthrophic terephthalate degradation in *S. aromaticivorans* strain UI. Two possible routes were suggested. Terephthalate is first activated to its respective CoA-ester terephthalyl-CoA and subsequently decarboxylated to benzoyl-CoA or terephthalate is first decarboxylated to benzoate and then activated by the benzoate-CoA ligase (Nobu et al., 2014).

iv. Aniline carboxylase

In the sulfate-reducing bacterium, *Desulfatiglans anilini* strain Anil1, aniline was reported to be degraded via a reductive deamination of 4-aminobenzoyl-CoA (Schnell et al., 1989; Schnell and Schink, 1991). The degradation of aniline in cell suspension experiments was dependent on the presence of CO₂. Therefore, the initial step was hypothesized to be a carboxylation reaction followed by a CoA ligation. The genome of *Desulfatiglans anilini* strain Anil1 has been sequenced and we could identify two gene clusters containing genes encoding UbiD-like proteins (one *ubiD*-like gene per cluster), an UbiX-like protein (only encoded in one cluster; GI:654869198-GI:654869189), putative 4-hydroxybenzoyl-CoA reductase subunits (alpha and beta subunit, only encoded in one cluster; GI:654869198-GI:654869189), a putative ligase (only encoded in one cluster; GI:654869198-GI:654869189), and phenylphosphate synthase subunits (only PpsA) (GI:654870411-654870418; GI:654869198-GI:654869189). *Desulfatiglans anilini* strain Anil1 was reported to grow as well with phenol as substrate. Therefore, we do not know whether one of the two clusters might also be involved in the degradation of phenol.

Interestingly, a similar gene cluster was identified in *D. anilini* strain AK1 but its gene products were suggested to be involved in the anaerobic degradation of phenol as the strain was not able to grow with aniline (Ahn et al., 2009). The gene cluster identified in *D. anilini* strain AK1 contained genes putatively encoding an alpha subunit of the 4-hydroxybenzoyl-CoA reductase, the phenylphosphate synthase subunits PpsA and PpsB, a putative regulator, and a ligase (accession number EF127527) (Ahn et al., 2009). The whole genome

of *D. anilini* strain AK1 has not been sequenced so far and therefore it is unknown if it encodes a putative UbiD-like phenylphosphate carboxylase.

The enzyme activities of the carboxylases, which might be involved in the anaerobic degradation of aniline and phenol, have not been measured so far in none of the two strains. The hypothesis that UbiD-like enzymes might catalyze the aniline carboxylation reactions is highly speculative and would need to be experimentally verified using purified enzymes.

v. Carboxylases acting on higher molecular weight PAHs

In addition to naphthalene, phenanthrene, a three-ringed PAH, was proposed to be activated via a carboxylation reaction (Zhang and Young, 1997; Davidova et al., 2007). In growth experiments using either deuterated or ^{14}C -labeled phenanthrene the respectively labeled metabolite 2-phenanthroic acid was identified as a metabolite. Moreover, the incorporation of ^{13}C -labeled bicarbonate into 2-phenanthroic acid supported a direct carboxylation. So far, genomic data are not available for a phenanthrene degrading enrichment culture. It would be very interesting to see if a gene cluster encoding UbiD-like proteins, comparable to the one identified in N47 and NaphS2, can be found as well in these anaerobic microorganisms. The same holds true for the anaerobic degradation of biphenyl where the transient formation of the intermediate biphenyl-4-carboxylic acid indicated an initial carboxylation step (Selesi and Meckenstock, 2009).

4.7.4 Phylogenetic analysis of UbiD-like enzymes involved in the anaerobic degradation

In a phylogenetic tree based on UbiD/PpcA-like subunits found to be involved in anaerobic degradation of aromatic compounds (Fig. 56), a main branch is occupied by the alpha subunit of phenylphosphate carboxylase (PpcA) from *T. aromatica*, *A. aromaticum* strain EbN1 and *S. aromaticivorans*, which form a cluster with the PpcA-like proteins of the putative benzene carboxylase from the iron-reducing culture BF, naphthalene carboxylase from N47 and NaphS2 and the putative terephthalate decarboxylase from *S. aromaticivorans*. Two other distinct branches contain the beta subunit of phenylphosphate carboxylase (PpcB) and the two other UbiD-like subunits of naphthalene carboxylase. A different branch is occupied by non-oxidative decarboxylases. Furthermore, PpcX from *T. aromatica*, which was induced in cells grown with phenol but shown not to be part of the phenylphosphate carboxylase complex, builds a cluster with N47_K27460 from N47, which was not detected in the native naphthalene carboxylase complex on BNP, and its homolog in NaphS2 supporting that the protein is not part of the naphthalene carboxylase complex (see Discussion 4.3). Moreover,

UbiD from *E. coli* is located on the same branch as the putative benzene carboxylase from *F. placidus*.

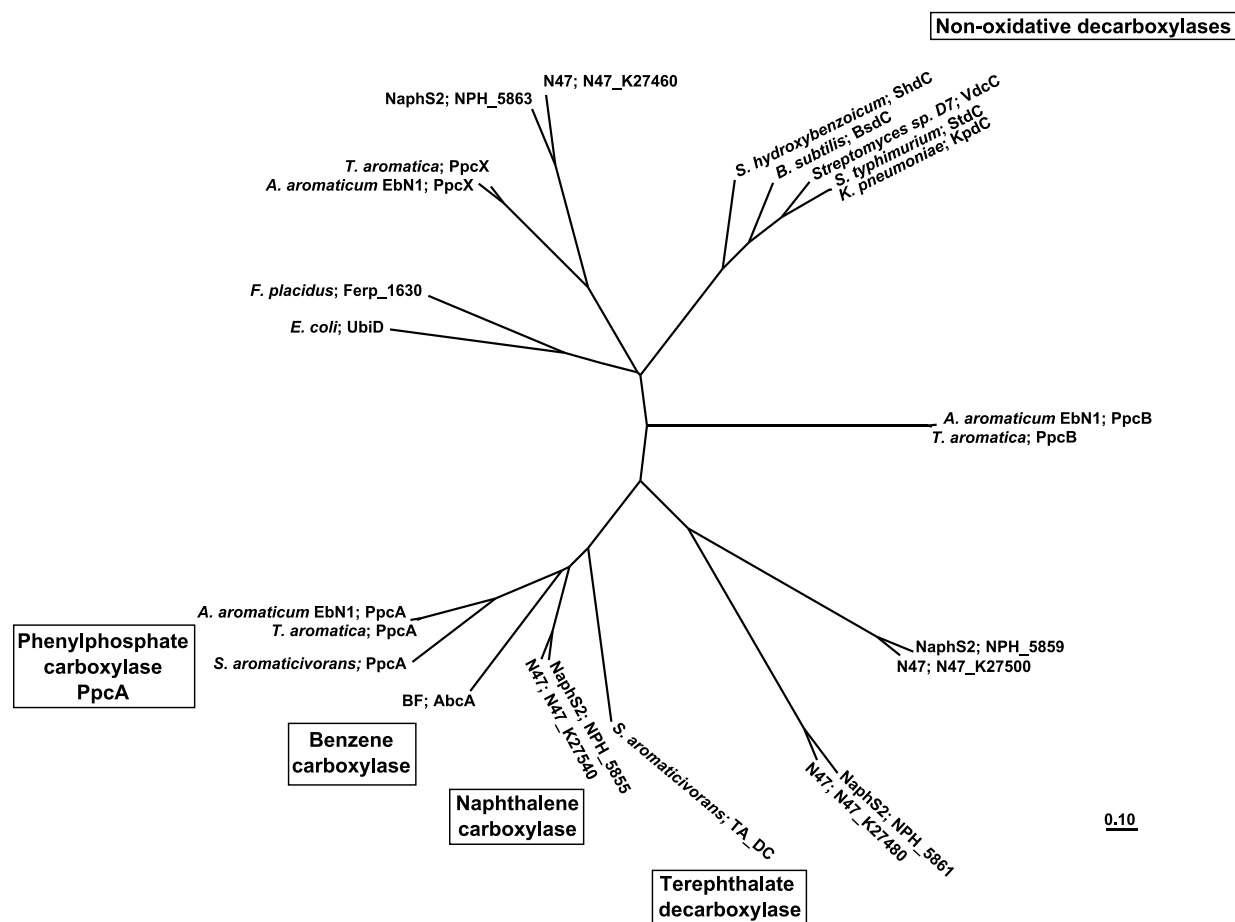


Figure 56: Phylogenetic tree of naphthalene, phenylphosphate, and benzene carboxylases and non-oxidative and terephthalate decarboxylases based on UbiD/PpcA-like subunits. For accession numbers, see Table A8 in the Appendix. The sequence alignment is shown in the Appendix in figure A9.

The high sequence similarity between the naphthalene carboxylase identified in N47 and NaphS2 and the fact that carboxylated metabolites can be identified also for other PAHs suggest that the initial carboxylation is a common strategy in the anaerobic degradation of PAHs. Therefore, the identification of the naphthalene carboxylase subunits can not only be used to develop molecular probes to study the potential ability of a community to degrade naphthalene in contaminated sites but also to identify carboxylases which might be involved in degradation of other PAHs.

4.8 Potential reaction mechanisms for naphthalene carboxylase

At present, only limited biochemical data are available for UbiD-like (de)carboxylases acting in the anaerobic degradation of (polycyclic)aromatic compounds. The high sensitivity of UbiD-like enzymes towards molecular oxygen and their instability so far hindered the investigations on their molecular reaction mechanisms. As seen in the present PhD project, the purification of UbiD-like enzymes from strictly anaerobic microorganisms can already present the bottleneck of studying the enzymes in detail. In the case of benzene carboxylase, the reaction could not yet be biochemically verified *in vitro*.

Based on the available data, we can only speculate on a putative reaction mechanism for naphthalene carboxylase. However, the ability of naphthalene carboxylase to catalyze an isotope exchange of the carboxyl-moiety might indicate that the enzyme follows a ping-pong mechanism in which an enzyme bound intermediate can reversibly be carboxylated (Schühle and Fuchs, 2004). The isotope exchange reaction also supports that naphthalene carboxylase is not biotin-dependent and therefore a reaction mechanism comparable to pyruvate, acetyl-CoA or propionyl-CoA carboxylase can be excluded (Knowles, 1989; Mouttaki et al., 2012).

It is generally accepted that a carboxylation reaction involves a negatively charged intermediate which attacks the CO₂ to form a C-C bond (see Introduction, Fig. 9) (O'Leary, 1992). For phenylphosphate carboxylase, which represents the best-studied UbiD-like enzyme, the enzyme-bound anionic phenolate intermediate, generated in an exergonic (and unidirectional) reaction from phenylphosphate, is carboxylated in the *para* position similar to the Kolbe-Schmitt reaction (Schühle and Fuchs, 2004). Naphthalene does not contain a hydroxyl group, which would allow the formation of such a negatively charged intermediate. However, the carbon atom in position 2 is the most electronegative of the ring, which might allow an electrophilic aromatic substitution reaction mechanism yielding 2-naphthoic acid (see Introduction, Fig. 4). This reaction mechanism would generate the formation of an unstable carbocation intermediate. Alternatively, a reaction mechanism involving a radical intermediate such as a naphthalene radical anion might be possible. In organic chemistry, it was observed that a reaction of sodium naphthalene with CO₂ always resulted in the formation of a dihydronaphthalene dicarboxylic acid (carbonation temperature -70 °C) (Walker and Scott, 1938; Lyssy, 1962). Moreover, the naphthalene radical anion was prepared from sodium and naphthalene in solvents such as 1,2-dimethoxyethane (DME) (Garst, 1971). It is questionable whether such harsh conditions can be simulated in an enzymatic environment.

In the present project, we showed that naphthalene carboxylase might be ATP-dependent. On one hand, ATP-hydrolysis could be only indirectly linked to catalysis and might induce

e.g. a conformational change of the enzyme allowing substrate binding. On the other hand, the activation of bicarbonate to a carbonic-phosphoric anhydride (carboxyphosphate) such as in phosphoenolpyruvate, acetophenone or acetone carboxylase might be possible. However, the involvement of a carboxyphosphate might not allow the isotopic exchange activity. Alternatively, the hydrolysis of ATP might lead to the phosphorylation of an amino acid residue within the active side of the enzyme or the formation a phosphorylated product (such as 2-naphthoyl phosphate). Such an intermediate was not detected in N47 and would also not be in accordance with the isotope exchange reaction. Nevertheless, a dephosphorylation of such an intermediate within the naphthalene carboxylase would be potentially possible as putative phosphatases (N47_K27450 and N47_K27440) were encoded within the naphthalene carboxylase gene cluster. These proteins were not identified as part of the naphthalene carboxylase in BNP nor as part of the naphthalene carboxylase operon. The phosphorylation and subsequent dephosphorylation of an amino acid residue would not necessarily have a function in the catalysis. Potentially, the only function of phosphorylation/hydrolysis would be to shift the equilibrium towards naphthalene carboxylation such as the phenylphosphate formation/hydrolysis in phenylphosphate carboxylase (Schühle and Fuchs, 2004; Boll et al., 2014).

Project 2

4.9 Characterization of *Cand. Treponema contaminophilus* sp. strain HM^T

The novel anaerobic bacterium *Cand. Treponema contaminophilus* sp. strain HM^T was isolated from the naphthalene-degrading enrichment culture N47 and characterized in pure culture. Strain HM^T is the second most abundant organism beside the naphthalene-degrading Deltaproteobacterium. In pure culture, the rod-shaped bacterium showed a fermentative lifestyle and its growth was dependent on the presence of yeast extract. In contrast to the majority of described spirochete species, *Cand. Treponema contaminophilus* sp. strain HM^T showed a rod-shaped morphology and was non-motile. The absence of the motility genes of the characteristic spiral spirochetes was recently described for other 'nonspiral spirochetes' belonging to the new genus *Sphaerochaeta* (Abt et al., 2012; Caro-Quintero et al., 2012).

Interestingly, strain HM^T shared high sequence similarity (99%) with 16S rRNA gene sequences of uncultured members of the family *Spirochaetaceae*, which were detected in contaminated sites and co-occurred with key degrader microorganisms such as *Dehalococcoides* sp. or Deltaproteobacteria (Tab. 35).

Table 35: 16S rRNA gene sequences of spirochetes, which were detected in contaminated sites. They co-occur with key players degrading the pollutants under anoxic conditions. All molecular clones share 99% sequence identity with *Cand. T. contaminophilus* strain HM^T.

Name of spirochete clone	Accession No. of 16S rRNA gene sequence	Relative abundance of spirochetal sequences	Co-occurring bacteria	Isolated from	Environmental contaminant present	Reference
Bacterial enrichment culture clone N47 isolate 2	GU080088	ND	<i>Deltaproteobacteria</i> (<i>Desulfobacteraceae</i>)	Soil material from a contaminated aquifer, Testfeld-Süd, Stuttgart, Germany	Poly- and monocyclic aromatic compounds	(Meckenstock et al., 2000)
Uncultured bacterium clone LHJB-126	JF741946	ND	ND	Oil reservoirs	Oil	
Uncultured bacterium clone LAC6	JQ004088	up to 4.3% within the enrichment culture	<i>Dehalococcoides</i> , <i>Pelosinus</i> , <i>Dendrosporobacter</i> , <i>Sporotalea</i> , <i>Clostridium</i> , <i>Desulfovibrio</i> , <i>Bacteroides</i>	Groundwater from a TCE-contaminated site, New Jersey, USA	TCE	(Zhao et al., 2012; Men et al., 2013)
Uncultured Spirochaetales bacterium clone D15_39	EU266876	ND	<i>Chloroflexi</i> , <i>Deltaproteobacteria</i> , <i>Actinobacteria</i> , others	Subsurface samples from a tar oil-contaminated former gasworks site, Düsseldorf-Flingern, Germany	Poly- and monocyclic aromatic compounds	(Winderl et al., 2008)
Uncultured bacterium clone NK-Q5 and NK-	JN685463, JN685488	up to 11.76% within the natural environment	<i>Alpha-, Delta- and Betaproteobacteria</i> , <i>Firmicutes</i> , <i>Methanomicrobia</i>	Water flooding oil reservoirs, China	Oil	(Zhao et al., 2012)
Spirochaetes bacterium enrichment culture clone DhR^2/LM-B02 M26	HQ012843	ND	<i>Dehalococcoides</i> , <i>Acetobacterium</i> , <i>Clostridium</i> , <i>Geobacter</i>	Sediment from a tributary of the Chesapeake Bay, Baltimore, Maryland, USA	Polychlorinated aromatics	(Ziv-El et al., 2011)
Uncultured spirochete clone KB-1	AY780558	ND	<i>Dehalococcoides</i>	Culture degrading chlorinated ethenes	Chlorinated ethenes	
Uncultured Spirochaetes bacterium	AB853925	ND	ND	Enrichment cultures anaerobically degrading phenols	Phenols	
Spirochaetes bacterium SA-8 and SA-10	AY695839, AY695841	ND	ND	Gold mine	ND	
Uncultured spirochete clone ccsIm209	AY133081	ND	ND	TCE-contaminated site	TCE	
Uncultured Spirochaetaceae bacterium	HE652872	ND	<i>Dehalococcoides</i> , <i>Bacteroidales</i> , <i>Sulfurospirillum</i>	Enrichment culture derived from contaminated groundwater, Bitterfeld, Germany	Poly- and monocyclic aromatic compounds, Chlorinated ethenes	(Motaleb et al., 2000)

The molecular clones were identified in sediment, ground-, and freshwater samples contaminated with poly- and monocyclic aromatic hydrocarbons or (poly)chlorinated ethenes. Those spirochetes were reported to build up to 11% of the bacterial community in some contaminated sites (Zhao et al., 2012). It was suggested that members of the family *Spirochaetaceae* might act as homoacetogens in these habitats (Duhamel and Edwards, 2006; Ziv-El et al., 2011). Acetogenesis from H₂ and CO₂ was described for spirochetes isolated from termite hindgut such as *Treponema primitia* ZAS-2^T. However, *T. isoptericolens* sp. strain SPIT5^T did not show growth with this energy and carbon sources (Leadbetter et al., 1999; Graber and Breznak, 2004; Graber et al., 2004). Additionally, homoacetogenic growth could not be demonstrated for *Cand. Treponema contaminophilus* HM^T, *Sphaerochaeta globosa* Buddy^T or *Sphaerochaeta pleomorpha* Grapes^T (Ritalahti et al., 2012).

The co-occurrence of spirochetes within enrichment cultures might also correlate with the presence of intermediates of the anaerobic degradation of the contaminants such as acetate, which could serve as carbon source for the spirochetes. Surprisingly, none of the so far characterized spirochetes isolated from these habitats, neither *Sphaerochaeta globosa* Buddy^T nor *S. pleomorpha* Grapes^T, were able to degrade acetate in presence of different electron acceptors including nitrate, nitrite, sulfate, fumarate or thiosulfate (Ritalahti et al., 2012).

Mutualistic interaction between a spirochete and another microorganism has been described before. Recently, syntrophic acetate oxidation was reported for spirochetes together with hydrogenotrophic methanogens in anaerobic digestion systems (Lee et al., 2013; Lee et al., 2015). Furthermore, *Treponema caldaria* was not able to grow on cellulose in pure culture, however, it was shown to enhance cellulose degradation by *Clostridium thermocellum* in coculture (Pohlschroeder et al., 1994). *C. thermocellum* was reported to produce an extracellular cellulase system hydrolyzing cellulose to cellobiose and other soluble sugars (Pohlschroeder et al., 1994). The authors suggested that *T. caldaria* might utilize these hydrolysis products from *C. thermocellum* as carbon and energy sources. This hypothesis was supported by the finding that extracellular cellulase preparation from *Clostridium papyrosolvens* strain C7 supported growth of *T. caldaria* strain H1, which was also not able to use cellulose as carbon and energy sources in pure culture (Cavedon et al., 1990b, a). The reason for the enhanced cellulose degradation in coculture remained unknown.

The isolation of spirochetes and their characterization might help to understand their putative role in the degradation of contaminants. The spherical spirochetes Buddy^T and Grapes^T were isolated from a reductively dechlorinating consortium along with a *Dehalococcoides* strain. It was initially suggested that they provided corrinoid as an essential co-factor for the reductive

dechlorination process (He et al., 2007). However, this hypothesis has been ruled out since the biosynthetic pathway for corrinoids was not identified within the *Sphaerochaeta* genomes (Caro-Quintero et al., 2012). For strain HM^T, it was initially hypothesized that it potentially releases a compound or a vitamin needed by the sulfate-reducing Deltaproteobacterium and thereby support the degradation of naphthalene or 2-methylnaphthalene (Selesi et al., 2010). However, based on the genome of the Deltaproteobacterium, Bergmann et al. (2011a) demonstrated the presence of all the biosynthetic pathways involved in vitamin formation. Furthermore, the Deltaproteobacterium was isolated in pure culture and it maintained its ability to degrade naphthalene even in the absence of the spirochete strain (Moultaki et al., unpublished data). Therefore, such hypothesis could be ruled out.

In pure culture, strain HM^T was shown to be a yeast extract-dependent carbohydrate degrader but in coculture with the sulfate-reducing Deltaproteobacterium these carbon/energy sources are not available. Therefore, the question arises about the carbon source that *Cand. T. contaminophilus* sp. strain HM^T utilizes within the enrichment culture.

When the enrichment culture N47 anaerobically metabolized naphthalene, which was dissolved in heptamethylnonane, emulsion of the carrier phase was observed after some weeks of incubation. This might indicate the production of a biosurfactant. The production of biosurfactants during aerobic and anaerobic degradation of aromatic hydrocarbons was described for some bacteria (La Riviere, 1955; Cooper et al., 1980; Javaheri et al., 1985; Déziel et al., 1996; Willumsen and Karlson, 1996; Pacwa-Płociniczak et al., 2011). Depending on the chemical composition and concentration, biosurfactants reduce the surface tension thus enhancing the mobilization, solubilization or emulsification of hydrophobic compounds (Pacwa-Płociniczak et al., 2011). Therefore, the production of a biosurfactant, usually as a secondary metabolite in the late exponential phase of growth, by a hydrocarbon-degrading microorganism increases the bioavailability of its substrate by increasing the surface of the contaminant. Furthermore, biosurfactants were shown to change the properties of the cell surface (Al-Tahhan et al., 2000; Sotirova et al., 2009; Pacwa-Płociniczak et al., 2011). The hydrophobicity of the cell surface is increased allowing the cell to interact with its hydrophobic substrate. Biosurfactants were divided into different groups such as glycolipids e.g. rhamnolipids and lipopeptides. Possibly, strain HM^T might use as a carbon source such a biosurfactant or another secondary metabolite potentially excreted by the Deltaproteobacterium.

Another possibility is that *Cand. T. contaminophilus* sp. strain HM^T receives all required substances to support its growth from dead biomass.

Project 3

4.10 Raman microspectroscopy of N47

In cooperation with Patrick Kubryk and Dr. Natalia P. Ivleva (Institute of Hydrochemistry, Chair for Analytical Chemistry, Technische Universität München), a protocol was established to analyze anaerobic cells such as N47 with stable isotope Raman microspectroscopy (SIRM). Raman microspectroscopy is a non-invasive method, which allows the chemical analysis of cells on the single cell level. The SIRM analysis of ^{13}C -labeled N47 cells confirmed the peak pattern of the different isotopologues of phenylalanine described by Li et al. (2012) for *E. coli* cells grown with $^{12}\text{C}/^{13}\text{C}$ -glucose.

Even though we used fully labeled ^{13}C -naphthalene, a fully labeled biomass was not detected. As mentioned earlier, due to cost reasons we were not able to cultivate the cells with ^{13}C -labeled naphthalene for several transfers. Therefore, the pre-culture was grown on ^{12}C -naphthalene and a contribution of carried over ^{12}C -naphthalene or its intermediates should be taken into consideration.

Based on the genome sequence, it was suggested that the naphthalene-degrading Deltaproteobacterium is able to synthesize all amino acids (Bergmann et al., 2011a) but the genes encoding the key enzymes of the biosynthesis of phenylalanine via shikimate such as 3-dehydroquinate dehydratase (DHQD) were not detected within the genome. However, only approximately 98% of the total genome sequence of N47 has been sequenced so far (Bergmann et al., 2011a). Therefore, it might be possible that the key enzymes of the biosynthesis of phenylalanine were encoded within the missing parts of the genome or they might vary from the sequences of the already described enzymes. The lack of fully labeled biomass could be explained by some (de)carboxylation steps within the pathway. Moreover, the analysis of N47 cells cultivated with ^{12}C -naphthalene and ^{13}C -bicarbonate showed a partial red-shift of the phenylalanine marker band from 1001 cm^{-1} to 990 cm^{-1} (del Rocio Diaz Mejorada, 2013). This finding suggested a contribution of bicarbonate from the medium to the biomass production during naphthalene degradation and would be consistent with the high ratio of heterotrophic CO_2 -fixation reported for other strict anaerobic aromatic hydrocarbon degraders detected via stable isotope probing approaches (Winderl et al., 2010; Taubert et al., 2012).

A surface enhanced Raman spectroscopy (SERS) (Fleischmann et al., 1974; Moskovits, 1985) was as well tested on N47 cells. For SERS, the cells were coated with colloidal silver nanoparticles to enhance the Raman scattering. However, for N47 SERS analysis was never reproducible and the obtained spectra varied between different cells, which was suggested to be a result of the heterogeneous coating of the cells surface with the nanoparticles. As

mentioned above (see Discussion 4.9), N47 potentially produces a biosurfactant to enhance the bioavailability of its hydrophobic substrate. The produced biosurfactants might change the cell surface to allow the interaction with the substrate as described for other bacteria (Al-Tahhan et al., 2000; Sotirova et al., 2009; Pacwa-Płociniczak et al., 2011). Furthermore, N47 medium contains heptamethylnonane, a branched alkane, which serves as a carrier phase for naphthalene and might as well prevent a proper coating of the cell. Interestingly, attachment of some structure on the cell surface of N47 was observed microscopically (see Results, Fig. 50). These attachments plus the higher hydrophobicity of the cell surface might disturb the coating with charged silver nanoparticles.

5. Conclusion and Outlook

Polycyclic aromatic hydrocarbons (PAHs) are recalcitrant pollutants in the environment. Their removal from contaminated systems such as groundwater is of great concern due to their high toxicity on living organisms. The degradation of aromatic hydrocarbons by aerobic bacteria has been extensively studied and is well understood. However, PAHs are very difficult to degrade in the absence of molecular oxygen and the underlying anaerobic biochemical reactions are only poorly understood. The first step in anaerobic degradation of the model compound naphthalene, which is catalyzed by naphthalene carboxylase, was initially biochemically characterized in crude extracts of the sulfate-reducing culture N47 (Mouttaki et al., 2012). In two independent proteogenomic studies in N47 and NaphS2, similar gene clusters encoding carboxylase-like proteins were identified and it was suggested by the authors that the gene products might be involved in the initial reaction on the anaerobic degradation of naphthalene (DiDonato et al., 2010; Bergmann et al., 2011). However, the subunit composition of the naphthalene carboxylase remained unknown. In the present PhD project, we demonstrate for the first time the native interactions of subunits which genes are encoded within the previously identified naphthalene carboxylase gene cluster. We hypothesize that these subunits represent the naphthalene carboxylase complex with a size of about 750 kDa. Moreover, the identified potential naphthalene carboxylase subunits are encoded in a single operon structure within the above mentioned gene cluster. The high sequence similarity between the naphthalene carboxylase identified in N47 and NaphS2, the measurements of the naphthalene carboxylase activity, and the fact that carboxylated metabolites can be detected also for other PAHs suggests that initial carboxylation is a common strategy in PAH degradation. Therefore, identification of the naphthalene carboxylase subunits can not only be used to monitor degradation in contaminated sites, but also to possibly identify potential carboxylases involved in the degradation of other PAHs.

Eventually, naphthalene carboxylase activity could be measured in cell-free extracts of N47 cells. The new data suggested that naphthalene carboxylase might be ATP-dependent, even though the specific activity was 10-times lower than naphthalene carboxylase activity detected in crude extracts by Mouttaki et al. (2012). We were able to show that the enzymes following the initial carboxylation in the anaerobic degradation of naphthalene such as naphthoate-CoA ligase, naphthoyl-CoA reductase, and dihydro-2-naphthyl-CoA reductase were active in the naphthalene carboxylase enzyme assay. This might explain the low detected activity of the naphthalene carboxylase as its product 2-naphthoic acid could directly be used as substrate by the following enzyme.

We were not able to finally clarify whether the carboxylation of naphthalene and the subsequent esterification of 2-naphthoic acid were coupled to shift the equilibrium of the initial reaction towards carboxylation. In future experiments, the ATP-dependency of naphthalene carboxylase should be studied in more detail. To test whether the carboxylase and the ligase are coupled and to avoid loss of 2-naphthoic acid formed during carboxylation, it would be important to have more biochemical data about the 2-naphthoate-CoA ligase. A purified and characterized 2-naphthoate-CoA ligase might additionally be used for the detection of naphthalene carboxylase activity during purification as it might have an impact on the reaction equilibrium (which cannot be ruled out at the current state of knowledge).

Due to the conversion of the produced 2-naphthoic acid by other enzymes, it would be challenging to characterize the naphthalene carboxylase in cell-free extracts. However, the inhibition of the ligase would allow determining kinetics of naphthalene carboxylase in cell-free extracts without interference of the following enzymes. In order to inhibit the following ligase activity, the free CoASH within the cell-free extract of N47 could be trapped. Ellman's reagent for example is known to interact with the sulfhydryl group of free CoASH, however, it might also affect other enzymes (e.g. naphthalene carboxylase) as it reacts unspecifically with thiol groups. Free CoASH might also be trapped via pre-incubation of the cell-free extracts with a known CoASH-dependent enzyme in order to deplete the free CoASH.

The ability to preserve naphthalene carboxylase activity in cell-free extracts and the gained knowledge about the subunits of the enzyme will allow future work on the native purification of naphthalene carboxylase from cell-free extracts of N47. It will be inevitable to purify the enzyme under native conditions from N47 cell-free extracts to verify the identified subunits of the complex and to determine potential co-factors or to elucidate its molecular reaction mechanism. A heterologously produced naphthalene carboxylase complex might also be suitable. However, in *E. coli*, the heterologous production of potential subunits resulted in low yields of soluble protein.

During analysis of the naphthalene carboxylase gene cluster, we identified a putative transcriptional regulator up-stream of the naphthalene carboxylase operon. The putative regulator N47_K27610 shared high sequence similarity with the transcriptional activator NifA involved in nitrogen fixation. For future studies, it would be very interesting to investigate potential regulation mechanisms of the naphthalene carboxylase operon.

The sulfate-reducing enrichment culture N47 contains two main organisms, the naphthalene-degrading Deltaproteobacterium and a spirochete. We were able to isolate and to characterize the novel anaerobic spirochete for which the name *Treponema contaminophilus* sp. strain HM^T was proposed. The rod-shaped and non-motile bacterium showed a

fermentative lifestyle and its growth was dependent on the presence of yeast extract in pure culture. Interestingly, *Cand. Treponema contaminophilus* sp. strain HM^T represented the first cultivated strain of a new phylogenetic branch of free-living spirochetes that co-occur with bacteria which anaerobically degrade (poly)aromatic hydrocarbons, (poly)chlorinated aromatics, and ethenes in contaminated soil, groundwater and sediments. The ecological function of *Spirochaetaceae* within this niche is so far unknown and needs to be defined in future studies. For members of the genus *Sphaerochaeta* it was hypothesized but not experimentally verified that they might interact with species of the genus *Dehalococcoides* (Caro-Quintero et al., 2012). The inability of *Cand. Treponema contaminophilus* sp. strain HM^T to degrade naphthalene and its dependency on yeast extract in pure culture might indicate an interaction between the Deltaproteobacterium and the spirochete during anaerobic degradation of naphthalene. It would be very interesting to determine which carbon source the spirochetes utilize within the N47 enrichment culture. It might be possible that *Cand. Treponema contaminophilus* sp. strain HM^T uses a so far unknown compound produced by the Deltaproteobacterium or that it lives on dead N47 cells. Its dependency on yeast extract might also indicate a potential auxotrophy of strain HM^T.

The new isolate and the Deltaproteobacterium N47 can be used as model organisms to analyze a potential interaction of comparable organisms in contaminated sites in the environment. To prove such an interaction in future experiments, the Deltaproteobacterium needs to be grown in absence and in presence of strain HM^T and the rate of naphthalene degradation as well as the growth behavior should be monitored and compared. Additionally, analysis of the sequenced genome of *Cand. Treponema contaminophilus* sp. strain HM^T might allow further speculation on its potential role in contaminated sites and might provide deeper insights into a potential interaction with the Deltaproteobacterium. The genome sequencing has been finished and the genome needs to be annotated and analyzed in future projects.

In the present PhD project, we used the naphthalene-degrading Deltaproteobacterium N47 as a model organism to develop a protocol to analyze anaerobic PAH-degrading microorganisms by stable isotope Raman microspectroscopy. N47 cells were cultivated with fully labeled ¹³C-naphthalene and the region of the phenylalanine marker band at 1001 cm⁻¹ was analyzed by stable isotope Raman microspectroscopy. The red shift of the marker band (990, 978 and 968 cm⁻¹) representing different isotopologues of phenylalanine indicated a successful incorporation of the label into the biomass of N47.

Huang et al. (2009) selectively isolated microbial cells by a combination of stable isotope Raman microspectroscopy and optical trapping. In this approach, individual cells were

captured by an infrared laser beam and by a co-aligned laser Raman spectra were recorded simultaneously. Thus, cells, which anaerobically degraded the labeled substrate, could be identified by the incorporation of ^{13}C -carbon into the biomass. The collected cells were used for single-cell genome amplification or further cultivation. This approach might also allow the identification and subsequent analysis of key players involved in the degradation of anaerobic (poly)aromatic hydrocarbons. However, it might technically be challenging to run the described experimental setup under anoxic conditions. Furthermore, the used intensity of the laser and the comparatively long acquisition time in our experiments might damage the microbial cells preventing further analysis. In future experiments, it should be tested whether a selective isolation of a PAH-degrading microorganism followed by single-cell genome amplification would be possible. One should moreover test whether a ^{13}C -labeled substrate can be replaced by a deuterated substrate and analyze the resulting shifts in the Raman profile. The used deuterated compounds would be a cheaper alternative over the use of ^{13}C -labeled compounds.

To conclude, our experiments demonstrated for the first time that stable isotope Raman microspectroscopy is applicable for slow growing, anaerobic microorganisms degrading complex substrates.

6. Literature

- Abt, B., Goker, M., Scheuner, C. & other authors (2013).** Genome sequence of the thermophilic fresh-water bacterium *Spirochaeta caldaria* type strain (H1(T)), reclassification of *Spirochaeta caldaria*, *Spirochaeta stenostrepta*, and *Spirochaeta zuelzeriae* in the genus *Treponema* as *Treponema caldaria* comb. nov., *Treponema stenostrepta* comb. nov., and *Treponema zuelzeriae* comb. nov., and emendation of the genus *Treponema*. *Standards in Genomic Sciences* **8**, 88-105.
- Abt, B., Han, C., Scheuner, C. & other authors (2012).** Complete genome sequence of the termite hindgut bacterium *Spirochaeta coccoides* type strain (SPN1(T)), reclassification in the genus *Sphaerochaeta* as *Sphaerochaeta coccoides* comb. nov. and emendations of the family *Spirochaetaceae* and the genus *Sphaerochaeta*. *Standards in Genomic Sciences* **6**, 194-209.
- Abu Laban, N., Selesi, D., Jobelius, C. & Meckenstock, R. U. (2009).** Anaerobic benzene degradation by Gram-positive sulfate-reducing bacteria. *FEMS Microbiology Ecology* **68**, 300-311.
- Abu Laban, N., Selesi, D., Rattei, T., Tischler, P. & Meckenstock, R. U. (2010).** Identification of enzymes involved in anaerobic benzene degradation by a strictly anaerobic iron-reducing enrichment culture. *Environmental Microbiology* **12**, 2783-2796.
- Ahn, Y.-B., Chae, J.-C., Zylstra, G. J. & Häggblom, M. M. (2009).** Degradation of phenol via phenylphosphate and carboxylation to 4-hydroxybenzoate by a newly isolated strain of the sulfate-reducing bacterium *Desulfobacterium anilini*. *Applied and Environmental Microbiology* **75**, 4248-4253.
- Aksenova, H. Y., Rainey, F. A., Janssen, P. H., Zavarzin, G. A. & Morgan, H. W. (1992).** *Spirochaeta thermophila* sp. nov., an obligately anaerobic, polysaccharolytic, extremely thermophilic bacterium. *International Journal of Systematic Bacteriology* **42**, 175-177.
- Al-Tahhan, R. A., Sandrin, T. R., Bodour, A. A. & Maier, R. M. (2000).** Rhamnolipid-induced removal of lipopolysaccharide from *Pseudomonas aeruginosa*: Effect on cell surface properties and interaction with hydrophobic substrates. *Applied and Environmental Microbiology* **66**, 3262-3268.
- Allen, K. N. & Dunaway-Mariano, D. (2004).** Phosphoryl group transfer: evolution of a catalytic scaffold. *Trends in Biochemical Sciences* **29**, 495-503.
- Amann, R. I., Binder, B. J., Olson, R. J., Chisholm, S. W., Devereux, R. & Stahl, D. A. (1990).** Combination of 16S rRNA-targeted oligonucleotide probes with flow cytometry for analyzing mixed microbial populations. *Applied and Environmental Microbiology* **56**, 1919-1925.
- Ambrosoli, R., Petruzzelli, L., Luis Minati, J. & Ajmone Marsan, F. (2005).** Anaerobic PAH degradation in soil by a mixed bacterial consortium under denitrifying conditions. *Chemosphere* **60**, 1231-1236.
- Andersson, I. & Backlund, A. (2008).** Structure and function of RuBisCo. *Plant Physiology and Biochemistry* **46**, 275-291.
- Anneser, B., Einsiedl, F., Meckenstock, R. U., Richters, L., Wisotzky, F. & Griebler, C. (2008).** High-resolution monitoring of biogeochemical gradients in a tar oil-contaminated aquifer. *Applied Geochemistry* **23**, 1715-1730.

- Annweiler, E., Materna, A., Safinowski, M., Kappler, A., Richnow, H. H., Michaelis, W. & Meckenstock, R. U. (2000).** Anaerobic degradation of 2-methylnaphthalene by a sulfate-reducing enrichment culture. *Applied and Environmental Microbiology* **66**, 5329-5333.
- Annweiler, E., Michaelis, W. & Meckenstock, R. U. (2002).** Identical ring cleavage products during anaerobic degradation of naphthalene, 2-methylnaphthalene, and tetralin indicate a new metabolic pathway. *Applied and Environmental Microbiology* **68**, 852-858.
- Aresta, M. & Dibenedetto, A. (2007).** Utilisation of CO₂ as a chemical feedstock: opportunities and challenges. *Dalton Transactions* **28**, 2975-2992.
- Azuma, H., Toyota, M., Asakawa, Y. & Kawano, S. (1996).** Naphthalene - a constituent of Magnolia flowers. *Phytochemistry* **42**, 999-1004.
- Badger, M. R. & Bek, E. J. (2008).** Multiple Rubisco forms in proteobacteria: their functional significance in relation to CO₂ acquisition by the CBB cycle. *Journal of Experimental Botany* **59**, 1525-1541.
- Bassham, J. A., Benson, A. A. & Calvin, M. (1950).** The path of carbon in photosynthesis *Journal of Biological Chemistry* **185**, 781-787.
- Bauer, R. D., Maloszewski, P., Zhang, Y., Meckenstock, R. U. & Griebler, C. (2008).** Mixing-controlled biodegradation in a toluene plume — Results from two-dimensional laboratory experiments. *Journal of Contaminant Hydrology* **96**, 150-168.
- Bauer, R. D., Rolle, M., Bauer, S., Eberhardt, C., Grathwohl, P., Kolditz, O., Meckenstock, R. U. & Griebler, C. (2009).** Enhanced biodegradation by hydraulic heterogeneities in petroleum hydrocarbon plumes. *Journal of Contaminant Hydrology* **105**, 56-68.
- Bedessem, M. E., Swoboda-Colberg, N. G. & Colberg, P. J. S. (1997).** Naphthalene mineralization coupled to sulfate reduction in aquifer-derived enrichments. *FEMS Microbiology Letters* **152**, 213-218.
- Beller, H. R. & Spormann, A. M. (1999).** Substrate range of benzylsuccinate synthase from *Azoarcus* sp. strain T. *FEMS Microbiology Letters* **268**, 147-153.
- Bendrat, K. & Buckel, W. (1993).** Cloning, sequencing and expression of the gene encoding the carboxytransferase subunit of the biotin-dependent Na⁺ pump glutaconyl-CoA decarboxylase from *Acidaminococcus fermentans* in *Escherichia coli*. *European Journal of Biochemistry* **211**, 697-702.
- Berg, I. A., Kockelkorn, D., Buckel, W. & Fuchs, G. (2007).** A 3-hydroxypropionate/4-hydroxybutyrate autotrophic carbon dioxide assimilation pathway in archaea. *Science* **318**, 1782-1786.
- Berg, J. M., Tymoczko, J. L. & Stryer, L. (2003).** *Biochemie*. Heidelberg: Spektrum Akademischer Verlag.
- Bergmann, F., Selesi, D., Weinmaier, T., Tischler, P., Rattei, T. & Meckenstock, R. U. (2011).** Genomic insights into the metabolic potential of the polycyclic aromatic hydrocarbon degrading sulfate-reducing Deltaproteobacterium N47. *Environmental Microbiology* **13**, 1125-1137.
- Bergmann, F. D. (2010).** Physiological potential of the anaerobic naphthalene-degrading enrichment culture N47: Genomic, proteomic and stable isotope studies. PhD thesis. In: Technische Universität München.
- Bergmann, F. D., Selesi, D. & Meckenstock, R. U. (2011).** Identification of new enzymes potentially involved in anaerobic naphthalene degradation by the sulfate-reducing enrichment culture N47. *Archives of Microbiology* **193**, 241-250.

- Berlendis, S., Lascourreges, J.-F., Schraauwers, B., Sivadon, P. & Magot, M. (2010).** Anaerobic biodegradation of BTEX by original bacterial communities from an underground gas storage aquifer. *Environmental Science & Technology* **44**, 3621-3628.
- Biegert, T., Fuchs, G. & Johann, H. (1996).** Evidence that anaerobic oxidation of toluene in the denitrifying bacterium *Thauera aromatica* is initiated by formation of benzylsuccinate from toluene and fumarate. *European Journal of Biochemistry* **238**, 661-668.
- Bligh, E. G. & Dyer, W. J. (1959).** A rapid method of total lipid extraction and purification. *Canadian Journal of Biochemistry and Physiology* **37**, 911-917.
- Boll, M. & Fuchs, G. (1995).** Benzoyl-Coenzyme A reductase (dearomatizing), a key enzyme of anaerobic aromatic metabolism. *European Journal of Biochemistry* **234**, 921-933.
- Boll, M., Fuchs, G. & Heider, J. (2002).** Anaerobic oxidation of aromatic compounds and hydrocarbons. *Current Opinion in Chemical Biology* **6**, 604-611.
- Boll, M., Löffler, C., Morris, B. E. L. & Kung, J. W. (2014).** Anaerobic degradation of homocyclic aromatic compounds via arylcarboxyl-coenzyme A esters: organisms, strategies and key enzymes. *Environmental Microbiology* **16**, 612-627.
- Botton, S. & Parson, J. R. (2006).** Degradation of BTEX compounds under iron-reducing conditions in contaminated aquifer microcosms. *Environmental Toxicology and Chemistry* **25**, 2630-2638.
- Botton, S., Van Harmelen, M., Braster, M., Parsons, J. R. & Röling, W. F. M. (2007).** Dominance of *Geobacteraceae* in BTX-degrading enrichments from an iron-reducing aquifer. *FEMS Microbiology Ecology* **62**, 118-130.
- Bracher, A., Starling-Windhof, A., Hartl, F. U. & Hayer-Hartl, M. (2011).** Crystal structure of a chaperone-bound assembly intermediate of form I Rubisco. *Nature Structural and Molecular Biology* **18**, 875-880.
- Bradford, M. M. (1976).** A rapid and sensitive method for the quantitation of microgram quantities of protein utilizing the principle of protein-dye binding. *Analytical Biochemistry* **72**, 248-254.
- Braune, A., Bendrat, K., Rospert, S. & Buckel, W. (1999).** The sodium ion translocating glutaconyl-CoA decarboxylase from *Acidaminococcus fermentans*: cloning and function of the genes forming a second operon. *Molecular Microbiology* **31**, 473-487.
- Breitenstein, A., Wiegel, J., Haertig, C., Weiss, N., Andreesen, J. R. & Lechner, U. (2002).** Reclassification of *Clostridium hydroxybenzoicum* as *Sedimentibacter hydroxybenzoicus* gen. nov., comb. nov., and description of *Sedimentibacter saalensis* sp. nov. *International Journal of Systematic and Evolutionary Microbiology* **52**, 801-807.
- Buchanan-Wollaston, V., Cannon, M. C., Beynon, J. L. & Cannon, F. C. (1981).** Role of the *nifA* gene product in the regulation of *nif* expression in *Klebsiella pneumoniae*. *Nature* **294**, 776-778.
- Buck, M., Gallegos, M.-T., Studholme, D. J., Guo, Y. & Gralla, J. D. (2000).** The bacterial enhancer-dependent sigma(54) (sigma(N)) transcription factor. *Journal of Bacteriology* **182**, 4129-4136.
- Buckel, W. & Semmler, R. (1982).** A biotin-dependent sodium pump: glutaconyl-CoA decarboxylase from *Acidaminococcus fermentans*. *FEBS Letters* **148**, 35-38.
- Buckel, W. & Semmler, R. (1983).** Purification, characterisation and reconstitution of glutaconyl-CoA decarboxylase, a biotin-dependent sodium pump from anaerobic bacteria. *European Journal of Biochemistry* **136**, 427-434.

- Buckel, W. & Thauer, R. K. (2013).** Energy conservation via electron bifurcating ferredoxin reduction and proton/Na⁺ translocating ferredoxin oxidation. *Biochimica et Biophysica Acta (BBA) - Bioenergetics* **1827**, 94-113.
- Burland, S. M. & Edwards, E. A. (1999).** Anaerobic benzene biodegradation linked to nitrate reduction. *Applied and Environmental Microbiology* **65**, 529-533.
- Caldwell, M. E. & Suflita, J. M. (2000).** Detection of phenol and benzoate as intermediates of anaerobic benzene biodegradation under different terminal electron-accepting conditions. *Environmental Science & Technology* **34**, 1216-1220.
- Canale-Parola, E. (1984).** Order I: Spirochaetales. In *Bergey's Manual of Systematic Bacteriology*, pp. 38–39. Edited by N. R. a. H. Krieg, J. G. Baltimore, MD: The Williams & Wilkins Co.
- Cannon, G. C., Bradburne, C. E., Aldrich, H. C., Baker, S. H., Heinhorst, S. & Shively, J. M. (2001).** Microcompartments in prokaryotes: Carboxysomes and related polyhedra. *Applied and Environmental Microbiology* **67**, 5351-5361.
- Carmona, M., Zamarro, M. T., Blázquez, B., Durante-Rodríguez, G., Juárez, J. F., Valderrama, J. A., Barragán, M. J. L., García, J. L. & Díaz, E. (2009).** Anaerobic catabolism of aromatic compounds: a genetic and genomic view. *Microbiology and Molecular Biology Reviews* **73**, 71-131.
- Caro-Quintero, A., Ritalahti, K. M., Cusick, K. D., Löffler, F. E. & Konstantinidis, K. T. (2012).** The chimeric genome of *Sphaerochaeta*: Nonspiral spirochetes that break with the prevalent dogma in spirochete biology. *mBio* **3**, e00025-00012.
- Cavedon, K., Leschine, S. B. & Canale-Parola, E. (1990).** Characterization of the extracellular cellulase from a mesophilic clostridium (strain C7). *Journal of Bacteriology* **172**, 4231-4237.
- Cavedon, K., Leschine, S. B. & Canale-Parola, E. (1990).** Cellulase system of a free-living, mesophilic clostridium (strain C7). *Journal of Bacteriology* **172**, 4222-4230.
- Cerniglia, C. E. (1993).** Biodegradation of polycyclic aromatic hydrocarbons. *Current Opinion in Biotechnology* **4**, 331-338.
- Chakraborty, R. & Coates, J. D. (2005).** Hydroxylation and carboxylation—Two crucial steps of anaerobic benzene degradation by *Dechloromonas* strain RCB. *Applied and Environmental Microbiology* **71**, 5427-5432.
- Chang, W., Um, Y. & Pulliam Holoman, T. R. (2006).** Polycyclic aromatic hydrocarbon (PAH) degradation coupled to methanogenesis. *Biotechnology Letters* **28**, 425–430.
- Charon, N. W. & Goldstein, S. F. (2002).** Genetics of motility and chemotaxis of a fascinating group of bacteria: The *Spirochetes*. *Annual Review of Genetics* **36**, 47-73.
- Chen, J., Henderson, G., Grimm, C. C., Lloyd, S. W. & Laine, R. A. (1998).** Termites fumigate their nests with naphthalene. *Nature* **392**, 558-559.
- Chow, K. T., Pope, M. K. & Davies, J. (1999).** Characterization of a vanillic acid non-oxidative decarboxylation gene cluster from *Streptomyces* sp. D7. *Microbiology* **145**, 2393-2403.
- Christensen, T. H., Bjerg, P. L., Banwart, S. A., Jakobsen, R., Heron, G. & Albrechtsen, H.-J. (2000).** Characterization of redox conditions in groundwater contaminant plumes. *Journal of Contaminant Hydrology* **45**, 165-241.
- Christensen, T. H., Kjeldsen, P., Bjerg, P. L., Jensen, D. L., Christensen, J. B., Baun, A., Albrechtsen, H.-J. & Heron, G. (2001).** Biogeochemistry of landfill leachate plumes. *Applied Geochemistry* **16**, 659-718.
- Cline, J. D. (1969).** Spectrophotometric determination of hydrogen sulfide in natural waters. *Limnology and Oceanography* **14**, 454–458.

- Coates, J. D., Anderson, R. & Lovley, D. R. (1996).** Oxidation of polycyclic aromatic hydrocarbons under sulfate-reducing conditions. *Applied and Environmental Microbiology* **62**, 1099–1101.
- Coates, J. D., Chakraborty, R., Lack, J. G., O'Connor, S. M., Cole, K. A., Bender, K. S. & Achenbach, L. A. (2001).** Anaerobic benzene oxidation coupled to nitrate reduction in pure culture by two strains of *Dechloromonas*. *Nature* **411**, 1039-1043.
- Coates, J. D., Chakraborty, R. & McInerney, M. J. (2002).** Anaerobic benzene biodegradation—a new era. *Research in Microbiology* **153**, 621-628.
- Coates, J. D., Woodward, J., Allen, J., Philp, P. & Lovley, D. R. (1997).** Anaerobic degradation of polycyclic aromatic hydrocarbons and alkanes in petroleum-contaminated marine harbor sediments. *Applied and Environmental Microbiology* **63**, 3589-3593.
- Cooper, D. G., Zajic, J. E., Gerson, D. F. & Manninen, K. I. (1980).** Isolation and identification of biosurfactants produced during anaerobic growth of *Clostridium pasteurianum*. *Journal of Fermentation Technology* **58**, 83-86.
- Cooper, T. G. & Wood, H. G. (1971).** The carboxylation of phosphoenolpyruvate and pyruvate: II. THE ACTIVE SPECIES OF "CO₂" UTILIZED BY PHOSPHOENOLPYRUVATE CARBOXYLASE AND PYRUVATE CARBOXYLASE. *Journal of Biological Chemistry* **246**, 5488-5490.
- Costa, K. C., Wong, P. M., Wang, T., Lie, T. J., Dodsworth, J. A., Swanson, I., Burn, J. A., Hackett, M. & Leigh, J. A. (2010).** Protein complexing in a methanogen suggests electron bifurcation and electron delivery from formate to heterodisulfide reductase. *Proceedings of the National Academy of Sciences* **107**, 11050-11055.
- Cox, G. B., Young, I. G., McCann, L. M. & Gibson, F. (1969).** Biosynthesis of ubiquinone in *Escherichia coli* K-12: Location of genes affecting the metabolism of 3-octaprenyl-4-hydroxybenzoic acid and 2-octaprenylphenol. *Journal of Bacteriology* **99**, 450-458.
- Cunha Tarouco, P., Mouttaki, H. & Meckenstock, R. U. (2013).** Carboxylation is a common biochemical strategy to activate naphthalene in several anaerobic bacteria. Conference number FTV007. In Annual Conference of the Association for General and Applied Microbiology (VAAM) in collaboration with the Royal Netherlands Society for Microbiology (KNVM). Bremen.
- Daisy, B. H., Strobel, G. A., Castillo, U., Ezra, D., Sears, J., Weaver, D. K. & Runyon, J. B. (2002).** Naphthalene, an insect repellent, is produced by *Muscodor vitigenus*, a novel endophytic fungus. *Microbiology* **148**, 3737–3741.
- Davidova, I. A., Gieg, L. M., Duncan, K. E. & Suflita, J. M. (2007).** Anaerobic phenanthrene mineralization by a carboxylating sulfate-reducing bacterial enrichment. *The ISME Journal* **1**, 436-442.
- Davis, G. D., Elisee, C., Newham, D. M. & Harrison, R. G. (1999).** New fusion protein systems designed to give soluble expression in *Escherichia coli*. *Biotechnology and Bioengineering* **65**, 382-388.
- del Rocio Diaz Mejorada, A. (2013).** Anaerobic biodegradation of naphthalene. Master thesis. In: Technische Universität Dresden.
- Déziel, É., Paquette, G., Villemur, R., Lepine, F. & Bisailon, J. (1996).** Biosurfactant production by a soil pseudomonas strain growing on polycyclic aromatic hydrocarbons. *Applied and Environmental Microbiology* **62**, 1908-1912.
- DiDonato, R. J., Young, N. D., Butler, J. E., Chin, K. J., Hixson, K. K., Mouser, P., Lipton, M. S., DeBoy, R. & Methe, B. A. (2010).** Genome sequence of the deltaproteobacterial strain NaphS2 and analysis of differential gene expression during anaerobic growth on naphthalene. *Plos One* **5**, e14072.

- Ding, B., Schmeling, S. & Fuchs, G. (2008).** Anaerobic metabolism of catechol by the denitrifying bacterium *Thauera aromatica* - a result of promiscuous enzymes and regulators? *Journal of Bacteriology* **190**, 1620-1630.
- Dröge, S., Fröhlich, J., Radek, R. & König, H. (2006).** *Spirochaeta coccoides* sp. nov., a novel coccoid *Spirochete* from the hindgut of the termite *Neotermes castaneus*. *Applied and Environmental Microbiology* **72**, 392-397.
- Dröge, S., Rachel, R., Radek, R. & König, H. (2008).** *Treponema isopterocolens* sp. nov., a novel spirochaete from the hindgut of the termite *Incisitermes tabogae*. *International Journal of Systematic and Evolutionary Microbiology* **58**, 1079-1083.
- Dubinina, G., Grabovich, M., Leshcheva, N., Rainey, F. A. & Gavrish, E. (2011).** *Spirochaeta perfilievii* sp. nov., an oxygen-tolerant, sulfide-oxidizing, sulfur- and thiosulfate-reducing spirochaete isolated from a saline spring. *International Journal of Systematic and Evolutionary Microbiology* **61**, 110-117.
- Duhamel, M. & Edwards, E. A. (2006).** Microbial composition of chlorinated ethene-degrading cultures dominated by *Dehalococcoides*. *FEMS Microbiology Ecology* **58**, 538-549.
- Eberlein, C., Estelmann, S., Seifert, J., von Bergen, M., Müller, M., Meckenstock, R. U. & Boll, M. (2013).** Identification and characterization of 2-naphthoyl-coenzyme A reductase, the prototype of a novel class of dearomatizing reductases. *Molecular Microbiology* **88**, 1032-1039.
- Eberlein, C., Johannes, J., Mouttaki, H., Sadeghi, M., Golding, B. T., Boll, M. & Meckenstock, R. U. (2013).** ATP-dependent/-independent enzymatic ring reductions involved in the anaerobic catabolism of naphthalene. *Environmental Microbiology* **15**, 1832-1841.
- Egland, P. G., Gibson, J. & Harwood, C. S. (1995).** Benzoate-coenzyme A ligase, encoded by *badA*, is one of three ligases able to catalyze benzoyl-coenzyme A formation during anaerobic growth of *Rhodopseudomonas palustris* on benzoate. *Journal of Bacteriology* **177**, 6545-6551.
- Ellis, R. J. (1979).** The most abundant protein in the world. *Trends in Biochemical Sciences* **4**, 241-244.
- Erb, T. J. (2011).** Carboxylases in natural and synthetic microbial pathways. *Applied Environmental Microbiology*.
- Estelmann, S., Blank, I., Feldmann, A. & Boll, M. (2015).** Two distinct old yellow enzymes are involved in naphthyl ring reduction during anaerobic naphthalene degradation. *Molecular Microbiology*.
- Ettwig, K. F., Butler, M. K., Le Paslier, D. & other authors (2010).** Nitrite-driven anaerobic methane oxidation by oxygenic bacteria. *Nature* **464**, 543-548.
- Evans, M. C., Buchanan, B. B. & Arnon, D. I. (1966).** A new ferredoxin-dependent carbon reduction cycle in a photosynthetic bacterium. *Proceedings of the National Academy of Sciences of the United States of America* **55**, 928-934.
- Evans, W.C. & Fuchs, G. (1988).** Anaerobic degradation of aromatic compounds. *Annual Review of Microbiology* **42**, 289-317.
- Field, C. B., Behrenfeld, M. J., Randerson, J. T. & Falkowski, P. (1998).** Primary production of the biosphere: integrating terrestrial and oceanic components. *Science* **281**, 237-240.
- Fischer, E. (1924).** Bildung von Methylenblau als Reaktion auf Schwefelwasserstoff. In *Untersuchungen aus Verschiedenen Gebieten*, pp. 117-119. Edited by M. Bergmann: Springer Berlin Heidelberg.

- Fleischmann, M., Hendra, P. J. & McQuillan, A. J. (1974).** Raman spectra of pyridine adsorbed at a silver electrode. *Chemical Physics Letters* **26**, 163-166.
- Foght, J. (2008).** Anaerobic biodegradation of aromatic hydrocarbons: Pathways and prospects. *Journal of Molecular Microbiology and Biotechnology* **15**, 93-120.
- Formica, J. V. & Brady, R. O. (1959).** The enzymatic carboxylation of acetyl coenzyme A. *Journal of the American Chemical Society* **81**, 752-752.
- Frey, P. A. & Hegeman, A. D. (2006).** *Enzymatic reaction mechanisms*. Oxford: Oxford University Press.
- Frost, L. S., Leplae, R., Summers, A. O. & Toussaint, A. (2005).** Mobile genetic elements: the agents of open source evolution. *Nature Review Microbiology* **3**, 722-732.
- Fuchs, G., Boll, M. & Heider, J. (2011).** Microbial degradation of aromatic compounds — from one strategy to four. *Nature Reviews Microbiology* **9**, 803-816.
- Fuchs, G. & Schlegel, H. G. (2006).** *Allgemeine Mikrobiologie*. Stuttgart: Thieme.
- Gabor, E. M., de Vries, E. J. & Janssen, D. B. (2003).** Efficient recovery of environmental DNA for expression cloning by indirect extraction methods. *FEMS Microbiology Ecology* **44**, 153-163.
- Galushko, A., Minz, D., Schink, B. & Widdel, F. (1999).** Anaerobic degradation of naphthalene by a pure culture of a novel type of marine sulphate-reducing bacterium. *Environmental Microbiology* **1**, 415-420.
- Garst, J. F. (1971).** Electron transfer, naphthalene radical anion, and alkyl halides. *Accounts of Chemical Research* **4**, 400-406.
- Gassett, J. W., Wiesler, D. P., Baker, A. G., Osborn, D. A., Miller, K. V., Marchinton, R. L. & Novotny, M. (1997).** Volatile compounds from the forehead region of male white-tailed deer (*Odocoileus virginianus*). *Journal of Chemical Ecology* **23**, 569-578
- Gerdes, K., Møller-Jensen, J. & Jensen, R. B. (2000).** Plasmid and chromosome partitioning: surprises from phylogeny. *Molecular Microbiology* **37**, 455-466.
- GESTIS-Stoffdatenbank.** In: Institut für Arbeitsschutz der Deutschen Gesetzlichen Unfallversicherung (IFA).
- Gibson, J., Dispensa, M., Fogg, G. C., Evans, D. T. & Harwood, C. S. (1994).** 4-Hydroxybenzoate-coenzyme A ligase from *Rhodospseudomonas palustris*: purification, gene sequence, and role in anaerobic degradation. *Journal of Bacteriology* **176**, 634-641.
- Giovannoni, S. J., DeLong, E. F., Olsen, G. J. & Pace, N. R. (1988).** Phylogenetic group-specific oligodeoxynucleotide probes for identification of single microbial cells. *Journal of Bacteriology* **170**, 720-726.
- Glueck, S. M., Gumus, S., Fabian, W. M. F. & Faber, K. (2010).** Biocatalytic carboxylation. *Chemical Society Reviews* **39**, 313-328.
- Gorny, N. & Schink, B. (1994).** Anaerobic degradation of catechol by *Desulfobacterium* sp. strain Cat2 proceeds via carboxylation to protocatechuate. *Applied and Environmental Microbiology* **60**, 3396-3400.
- Graber, J. R. & Breznak, J. A. (2004).** Physiology and nutrition of *Treponema primitia*, an H₂/CO₂-acetogenic spirochete from termite hindguts. *Applied and Environmental Microbiology* **70**, 1307-1314.
- Graber, J. R., Leadbetter, J. R. & Breznak, J. A. (2004).** Description of *Treponema azotonutricium* sp. nov. and *Treponema primitia* sp. nov., the first *Spirochetes* isolated from termite guts. *Applied and Environmental Microbiology* **70**, 1315-1320.
- Grbić-Galić, D. & Vogel, T. M. (1987).** Transformation of toluene and benzene by mixed methanogenic cultures. *Applied and Environmental Microbiology* **53**, 254-260.

- Greenberg, E. P. & Canale-Parola, E. (1976).** *Spirochaeta halophila* sp. n., a facultative anaerobe from a high-salinity pond. *Archives of Microbiology* **110**, 185-194.
- Griebler, C., Safinowski, M., Vieth, A., Richnow, H. H. & Meckenstock, R. U. (2004).** Combined application of stable carbon isotope analysis and specific metabolites determination for assessing *in situ* degradation of aromatic hydrocarbons in a tar oil-contaminated aquifer. *Environmental Science & Technology* **38**, 617-631.
- Griffiths, S. K. (2012).** Oil release from Macondo Well MC252 following the Deepwater Horizon accident. *Environmental Science & Technology* **46**, 5616-5622.
- Gulmezian, M., Hyman, K. R., Marbois, B. N., Clarke, C. F. & Javor, G. T. (2007).** The role of UbiX in *Escherichia coli* coenzyme Q biosynthesis. *Archives of Biochemistry and Biophysics* **467**, 144-153.
- Gutiérrez Acosta, O. B., Hardt, N., Hacker, S. M., Strittmatter, T., Schink, B. & Marx, A. (2014).** Thiamine pyrophosphate stimulates acetone activation by *Desulfococcus biacutus* as monitored by a fluorogenic ATP analogue. *ACS Chemical Biology* **9**, 1263-1266.
- Gutiérrez Acosta, O. B., Hardt, N. & Schink, B. (2013).** Carbonylation as a key reaction in anaerobic acetone activation by *Desulfococcus biacutus*. *Applied and Environmental Microbiology* **79**, 6228-6235.
- Guyard, C., Raffel, S. J., Schruppf, M. E. & authors (2013).** Periplasmic flagellar export apparatus protein, FliH, is involved in post-transcriptional regulation of FlaB, motility and virulence of the relapsing fever spirochete *borrelia hermsii*. *PLoS ONE* **8**, e72550.
- Habe, H. & Omori, T. (2003).** Genetics of polycyclic aromatic hydrocarbon metabolism in diverse aerobic bacteria. *Bioscience, Biotechnology, and Biochemistry* **67**, 225-243.
- Hahne, H., Pachi, F., Ruprecht, B., Maier, S. K., Klaeger, S., Helm, D., Medard, G., Wilm, M., Lemeer, S. & Kuster, B. (2013).** DMSO enhances electrospray response, boosting sensitivity of proteomic experiments. *Nature Methods* **10**, 989-991.
- Harper, S. & Speicher, D. (2011).** Purification of proteins fused to Glutathione S-transferase. In *Protein Chromatography*, pp. 259-280. Edited by D. Walls and S. T. Loughran: Humana Press.
- Harwood, C. S. & Canale-Parola, E. (1983).** *Spirochaeta isovalerica* sp. nov., a marine anaerobe that forms branched-chain fatty acids as fermentation products. *International Journal of Systematic Bacteriology* **33**, 573-579.
- Harwood, C. S., Jannasch, H. W. & Canale-Parola, E. (1982).** Anaerobic spirochete from a deep-sea hydrothermal vent. *Applied and Environmental Microbiology* **44**, 234-237.
- Hauck, S. M., Dietter, J., Kramer, R. L., Hofmaier, F., Zipplies, J. K., Amann, B., Feuchtinger, A., Deeg, C. A. & Ueffing, M. (2010).** Deciphering membrane-associated molecular processes in target tissue of autoimmune uveitis by label-free quantitative Mass Spectrometry. *Molecular & Cellular Proteomics* **9**, 2292-2305.
- He, J., Holmes, V. F., Lee, P. K. H. & Alvarez-Cohen, L. (2007).** Influence of vitamin B12 and cocultures on the growth of *Dehalococcoides* isolates in defined medium. *Applied and Environmental Microbiology* **73**, 2847-2853.
- He, J., Sung, Y., Krajmalnik-Brown, R., Ritalahti, K. M. & Löffler, F. E. (2005).** Isolation and characterization of *Dehalococcoides* sp. strain FL2, a trichloroethene (TCE)- and 1,2-dichloroethene-respiring anaerobe. *Environmental Microbiology* **7**, 1442-1450.
- He, Z. & Wiegel, J. (1995).** Purification and characterization of an oxygen-sensitive reversible 4-hydroxybenzoate decarboxylase from *Clostridium hydroxybenzoicum*. *European Journal of Biochemistry* **229**, 77-82.

- Hefti, M. H., François, K.-J., de Vries, S. C., Dixon, R. & Vervoort, J. (2004).** The PAS fold- a redefinition of the PAS domain based upon structural prediction. *European Journal of Biochemistry* **271**, 1198-1208.
- Heider, J. (2001).** A new family of CoA-transferases. *FEBS Letters* **509**, 345-349.
- Hespell, R. B. & Canale-Parola, E. (1970).** *Spirochaeta litoralis* sp. n., a strictly anaerobic marine spirochete. *Archives of Microbiology* **74**, 1-18.
- Heuner, K., Große, K., Schade, R. & Göbel, U. B. (2000).** A flagellar gene cluster from the oral spirochaete *Treponema maltophilum*. *Microbiology* **146**, 497-507.
- Ho, Y.-S. J., Burden, L. M. & Hurley, J. H. (2000).** Structure of the GAF domain, a ubiquitous signaling motif and a new class of cyclic GMP receptor. *The EMBO Journal* **19**, 5288-5299.
- Holmes, D. E., Risso, C., Smith, J. A. & Lovley, D. R. (2011).** Anaerobic oxidation of benzene by the hyperthermophilic archaeon *Ferroglobus placidus*. *Applied and Environmental Microbiology* **77**, 5926-5933.
- Holmes, D. E., Risso, C., Smith, J. A. & Lovley, D. R. (2012).** Genome-scale analysis of anaerobic benzoate and phenol metabolism in the hyperthermophilic archaeon *Ferroglobus placidus*. *The ISME Journal* **6**, 146-157.
- Hopper, S. & Böck, A. (1995).** Effector-mediated stimulation of ATPase activity by the sigma 54-dependent transcriptional activator FHLA from *Escherichia coli*. *Journal of Bacteriology* **177**, 2798-2803.
- Huang, W. E., Griffiths, R. I., Thompson, I. P., Bailey, M. J. & Whiteley, A. S. (2004).** Raman microscopic analysis of single microbial cells. *Analytical Chemistry* **76**, 4452-4458.
- Huang, W. E., Stoecker, K., Griffiths, R., Newbold, L., Daims, H., Whiteley, A. S. & Wagner, M. (2007).** Raman-FISH: combining stable-isotope Raman spectroscopy and fluorescence *in situ* hybridization for the single cell analysis of identity and function. *Environmental Microbiology* **9**, 1878-1889.
- Huang, W. E., Ward, A. D. & Whiteley, A. S. (2009).** Raman tweezers sorting of single microbial cells. *Environmental Microbiology Reports* **1**, 44-49.
- Huber, H., Gallenberger, M., Jahn, U., Eylert, E., Berg, I. A., Kockelkorn, D., Eisenreich, W. & Fuchs, G. (2008).** A dicarboxylate/4-hydroxybutyrate autotrophic carbon assimilation cycle in the hyperthermophilic Archaeum *Ignicoccus hospitalis*. *Proceedings of the National Academy of Sciences* **105**, 7851-7856.
- Iida, T., Waki, T., Nakamura, K., Mukouzaka, Y. & Kudo, T. (2009).** The GAF-like-domain-containing transcriptional regulator DfdR is a sensor protein for dibenzofuran and several hydrophobic aromatic compounds. *Journal of Bacteriology* **191**, 123-134.
- Imachi, H., Sakai, S., Hirayama, H., Nakagawa, S., Nunoura, T., Takai, K. & Horikoshi, K. (2008).** *Exilispira thermophila* gen. nov., sp. nov., an anaerobic, thermophilic spirochaete isolated from a deep-sea hydrothermal vent chimney. *International Journal of Systematic and Evolutionary Microbiology* **58**, 2258-2265.
- Inoue, H., Nojima, H. & Okayama, H. (1990).** High efficiency transformation of *Escherichia coli* with plasmids. *Gene* **96**, 23-28.
- Inoue, S. & Yamazaki, N. (1982).** *Organic and bio-organic chemistry of carbon dioxide*: Halsted Press.
- Jahn, M. K., Haderlein, S. B. & Meckenstock, R. U. (2005).** Anaerobic degradation of benzene, toluene, ethylbenzene, and o-xylene in sediment-free iron-reducing enrichment cultures. *Applied and Environmental Microbiology* **71**, 3355-3358.

- Javaheri, M., Jenneman, G. E., McInerney, M. J. & Knapp, R. M. (1985).** Anaerobic production of a biosurfactant by *Bacillus licheniformis* JF-2. *Applied and Environmental Microbiology* **50**, 698-700.
- Jencks, W. P. (1975).** Binding Energy, Specificity, and Enzymic Catalysis: The Circe Effect. In *Advances in Enzymology and Related Areas of Molecular Biology*, pp. 219-410: John Wiley & Sons, Inc.
- Jobst, B., Schühle, K., Linne, U. & Heider, J. (2010).** ATP-dependent carboxylation of acetophenone by a novel type of carboxylase. *Journal of Bacteriology* **192**, 1387-1394.
- Johnsen, A. R., Wick, L. Y. & Harms, H. (2005).** Principles of microbial PAH-degradation in soil. *Environmental Pollution* **133**, 71-84.
- Kapust, R. B. & Waugh, D. S. (1999).** *Escherichia coli* maltose-binding protein is uncommonly effective at promoting the solubility of polypeptides to which it is fused. *Protein Science* **8**, 1668-1674.
- Karlsson, A., Parales, J. V., Parales, R. E., Gibson, D. T., Eklund, H. & Ramaswamy, S. (2003).** Crystal structure of naphthalene dioxygenase: Side-on binding of dioxygen to iron. *Science* **299**, 1039-1042.
- Kasai, Y., Takahata, Y., Manefield, M. & Watanabe, K. (2006).** RNA-based stable isotope probing and isolation of anaerobic benzene-degrading bacteria from gasoline-contaminated groundwater. *Applied and Environmental Microbiology* **72**, 3586-3592.
- Kawaguchi, K., Shinoda, Y., Yurimoto, H., Sakai, Y. & Kato, N. (2006).** Purification and characterization of benzoate-CoA ligase from *Magnetospirillum* sp. strain TS-6 capable of aerobic and anaerobic degradation of aromatic compounds. *Fems Microbiology Letters* **257**, 208-213.
- Kazumi, J., Caldwell, M. E., Suflita, J. M., Lovley, D. R. & Young, L. Y. (1997).** Anaerobic degradation of benzene in diverse anoxic environments. *Environmental Science & Technology* **31**, 813-818.
- Kimes, N. E., Callaghan, A. V., Aktas, D. F., Smith, W. L., Sunner, J., Golding, B. T., Drozdowska, M., Hazen, T. C., Suflita, J. M. & Morris, P. J. (2013).** Metagenomic analysis and metabolite profiling of deep-sea sediments from the Gulf of Mexico following the Deepwater Horizon oil spill. *Frontiers in Microbiology* **4**.
- Kinney, J. N., Axen, S. D. & Kerfeld, C. A. (2011).** Comparative analysis of carboxysome shell proteins. *Photosynth Res* **109**, 21-32.
- Klein, M. G., Zwart, P., Bagby, S. C., Cai, F., Chisholm, S. W., Heinhorst, S., Cannon, G. C. & Kerfeld, C. A. (2009).** Identification and structural analysis of a novel carboxysome shell protein with implications for metabolite transport. *Journal of Molecular Biology* **392**, 319-333.
- Knowles, J. (1989).** The mechanism of biotin-dependent enzymes. *Annual Review of Biochemistry* **58**, 195-221.
- Koch, H. R., Doldi, K. & Hockwin, O. (1976).** Naphthalene cataract development. *Doc Ophthalmol* **3**, 323-332.
- Koonin, E. V. & Tatusov, R. L. (1994).** Computer analysis of bacterial haloacid dehalogenases defines a large superfamily of hydrolases with diverse specificity: Application of an iterative approach to database search. *Journal of Molecular Biology* **244**, 125-132.
- Kube, M., Heider, J., Amann, J., Hufnagel, P., Kühner, S., Beck, A., Reinhardt, R. & Rabus, R. (2004).** Genes involved in the anaerobic degradation of toluene in a denitrifying bacterium, strain EbN1. *Archives of Microbiology* **181**, 182-194.

- Kunapuli, U., Griebler, C., Beller, H. R. & Meckenstock, R. U. (2008).** Identification of intermediates formed during anaerobic benzene degradation by an iron-reducing enrichment culture. *Environmental Microbiology* **10**, 1703-1712.
- Kunapuli, U., Lueders, T. & Meckenstock, R. U. (2007).** The use of stable isotope probing to identify key iron-reducing microorganisms involved in anaerobic benzene degradation. *The ISME Journal* **1**, 643-653.
- Kung, J. W., Löffler, C., Dörner, K., Heintz, D., Gallien, S., Van Dorsseleer, A., Friedrich, T. & Boll, M. (2009).** Identification and characterization of the tungsten-containing class of benzoyl-coenzyme A reductases. *Proceedings of the National Academy of Sciences* **106**, 17687-17692.
- Kuznetsova, E., Proudfoot, M., Gonzalez, C. F. & other authors (2006).** Genome-wide analysis of substrate specificities of the *Escherichia coli* haloacid dehalogenase-like phosphatase family. *Journal of Biological Chemistry* **281**, 36149-36161.
- La Riviere, J. W. (1955).** The production of surface active compounds by microorganisms and its possible significance in oil recovery. I. Some general observations on the change of surface tension in microbial cultures. *Antonie Van Leeuwenhoek* **21**, 1-8.
- Lack, A. & Fuchs, G. (1992).** Carboxylation of phenylphosphate by phenol carboxylase, an enzyme system of anaerobic phenol metabolism. *Journal of Bacteriology* **174**, 3629-3636.
- Laemmli, U. K. (1970).** Cleavage of structural proteins during the assembly of the head of bacteriophage T4. *Nature* **227**, 680-685.
- Lambert, A., Picardeau, M., Haake, D. A., Sermswan, R. W., Srikram, A., Adler, B. & Murray, G. A. (2012).** FlaA proteins in *Leptospira interrogans* are essential for motility and virulence but are not required for formation of the flagellum sheath. *Infection and Immunity* **80**, 2019-2025.
- Leadbetter, J. R., Schmidt, T. M., Graber, J. R. & Breznak, J. A. (1999).** Acetogenesis from H₂ plus CO₂ by spirochetes from termite guts. *Science* **283**, 686-689.
- Lee, S.-H., Park, J.-H., Kang, H.-J., Lee, Y. H., Lee, T. J. & Park, H.-D. (2013).** Distribution and abundance of *Spirochaetes* in full-scale anaerobic digesters. *Bioresource Technology* **145**, 25-32.
- Lee, S.-H., Park, J.-H., Kim, S.-H., Yu, B. J., Yoon, J.-J. & Park, H.-D. (2015).** Evidence of syntrophic acetate oxidation by *Spirochaetes* during anaerobic methane production. *Bioresource Technology*.
- LeGall, J. & Fauque, G. (1988).** Dissimilatory reduction of sulfur compounds. In *Biology of anaerobic microorganisms*, pp. 587-639. Edited by A. J. B. Zehnder. New York: Wiley.
- Leppik, R. A., Young, I. G. & Gibson, F. (1976).** Membrane-associated reactions in ubiquinone biosynthesis in *Escherichia coli*. 3-octaprenyl-4-hydroxybenzoate carboxylase. *Biochimica et Biophysica Acta (BBA) - Biomembranes* **436**, 800-810.
- Leschine, S. & Canale-Parola, E. (1980).** Rifampin as a selective agent for isolation of oral spirochetes. *Journal of clinical microbiology* **12**, 792.
- Leschine, S. B. & Canale-Parola, E. (1986).** Rifampin-resistant RNA polymerase in spirochetes. *FEMS Microbiology Letters* **35**, 199-204.
- Leuthner, B. & Heider, J. (1998).** A two-component system involved in regulation of anaerobic toluene metabolism in *Thauera aromatica*.
- Leuthner, B. & Heider, J. (1999).** Anaerobic toluene catabolism of *Thauera aromatica*: the *bbs* operon codes for enzymes of β -oxidation of the intermediate benzylsuccinate. *Journal of Bacteriology* **182**, 272-277.

- Leuthner, B., Leutwein, C., Schulz, H., Hörth, P., Haehnel, W., Schiltz, E., Schägger, H. & Heider, J. (1998).** Biochemical and genetic characterization of benzylsuccinate synthase from *Thauera aromatica*: a new glycyl radical enzyme catalysing the first step in anaerobic toluene metabolism. *Molecular Microbiology* **28**, 615-628.
- Leutwein, C. & Heider, J. (1999).** Anaerobic toluene-catabolic pathway in denitrifying *Thauera aromatica*: activation and β -oxidation of the first intermediate, (R)-(+)-benzylsuccinate. *Microbiology* **145**, 3265-3271.
- Leutwein, C. & Heider, J. (2001).** Succinyl-CoA:(R)-benzylsuccinate CoA-transferase: an enzyme of the anaerobic toluene catabolic pathway in denitrifying bacteria. *Journal of Bacteriology* **183**, 4288-4295.
- Leutwein, C. & Heider, J. (2002).** (R)-Benzylsuccinyl-CoA dehydrogenase of *Thauera aromatica*, an enzyme of the anaerobic toluene catabolic pathway. *Archives of Microbiology* **178**, 517-524.
- Li, C., Motaleb, A., Sal, M., Goldstein, S. F. & Charon, N. W. (2000).** Spirochete periplasmic flagella and motility. *Journal of molecular microbiology and biotechnology* **2**, 345-354.
- Li, M., Huang, W. E., Gibson, C. M., Fowler, P. W. & Jousset, A. (2012).** Stable Isotope Probing and Raman Spectroscopy for Monitoring Carbon Flow in a Food Chain and Revealing Metabolic Pathway. *Analytical Chemistry* **85**, 1642-1649.
- Lin, F., Ferguson, K. L., Boyer, D. R., Lin, X. N. & Marsh, E. N. G. (2015).** Isofunctional enzymes PAD1 and UbiX catalyze formation of a novel cofactor required by ferulic acid decarboxylase and 4-hydroxy-3-polyprenylbenzoic acid decarboxylase. *ACS Chemical Biology*.
- Lippert, M.-L. (2009).** Biochemie von Enzymen des anaeroben Stoffwechsels von Toluol in *Thauera aromatica*. PhD thesis. In: Technischen Universität Darmstadt.
- Little, R. & Dixon, R. (2003).** The Amino-terminal GAF domain of *Azotobacter vinelandii* NifA binds 2-oxoglutarate to resist inhibition by NifL under nitrogen-limiting conditions. *Journal of Biological Chemistry* **278**, 28711-28718.
- Liu, C., Young, A. L., Starling-Windhof, A. & other authors (2010).** Coupled chaperone action in folding and assembly of hexadecameric Rubisco. *Nature* **463**, 197-202.
- Löffler, C., Kuntze, K., Vazquez, J. R., Rugor, A., Kung, J. W., Böttcher, A. & Boll, M. (2011).** Occurrence, genes and expression of the W/Se-containing class II benzoyl-coenzyme A reductases in anaerobic bacteria. *Environmental Microbiology* **13**, 696-709.
- Löffler, G., Petrides, P. E. & Heinrich, P. C. (2006).** *Biochemie und Pathobiochemie*. Berlin Heidelberg: Springer.
- Lorimer, G. H., Badger, M. R. & Andrews, T. J. (1976).** The activation of ribulose-1,5-bisphosphate carboxylase by carbon dioxide and magnesium ions. Equilibria, kinetics, a suggested mechanism, and physiological implications. *Biochemistry* **14**, 529-536.
- Lovley, D. R. (1991).** Dissimilatory Fe(III) and Mn(IV) reduction. *Microbiological Reviews* **55**, 259-287.
- Lovley, D. R., Coates, J. D., Woodward, J. C. & Phillips, E. (1995).** Benzene oxidation coupled to sulfate reduction. *Applied and Environmental Microbiology* **61**, 953-958.
- Lovley, D. R., Woodward, J. C. & Chappelle, F. H. (1994).** Stimulated anoxic biodegradation of aromatic hydrocarbons using Fe(III) ligands. *Nature* **370**, 128-131.
- Lueders, T., Manefield, M. & Friedrich, M. W. (2004).** Enhanced sensitivity of DNA- and rRNA-based stable isotope probing by fractionation and quantitative analysis of isopycnic centrifugation gradients. *Environmental Microbiology* **6**, 73-78.

- Luo, F., Gitiafroz, R., Devine, C. E., Gong, Y., Hug, L. A., Raskin, L. & Edwards, E. A. (2014). Metatranscriptome of an anaerobic benzene-degrading nitrate-reducing enrichment culture reveals involvement of carboxylation in benzene ring activation. *Applied and Environmental Microbiology*.
- Lupa, B., Lyon, D., Gibbs, M. D., Reeves, R. A. & Wiegel, J. (2005). Distribution of genes encoding the microbial non-oxidative reversible hydroxyarylic acid decarboxylases/phenol carboxylases. *Genomics* **86**, 342-351.
- Lupa, B., Lyon, D., Shaw, L. N., Sieprawska-Lupa, M. & Wiegel, J. (2008). Properties of the reversible nonoxidative vanillate / 4-hydroxybenzoate decarboxylase from *Bacillus subtilis*. *Canadian Journal of Microbiology* **54**, 75-81.
- Lutkenhaus, J. (2012). The ParA/MinD family puts things in their place. *Trends in microbiology* **20**, 411-418.
- Lux, R., Miller, J. N., Park, N.-H. & Shi, W. (2001). Motility and chemotaxis in tissue penetration of oral epithelial cell layers by *Treponema denticola*. *Infection and Immunity* **69**, 6276-6283.
- Lykidis, A., Chen, C.-L., Tringe, S. G. & other authors (2011). Multiple syntrophic interactions in a terephthalate-degrading methanogenic consortium. *The ISME Journal* **5**, 122-130.
- Lyssy, T. M. (1962). Reaction of metallic sodium with naphthalene.1 dihydronaphthalenedicarboxylic acids-1,4 and -1,2 and related compounds. *The Journal of Organic Chemistry* **27**, 5-13.
- Magot, M., Fardeau, M.-L., Arnauld, O., Lanau, C., Ollivier, B., Thomas, P. & Patel, B. K. C. (1997). *Spirochaeta smaragdinae* sp. nov., a new mesophilic strictly anaerobic spirochete from an oil field. *Fems Microbiology Letters* **155**, 185-191.
- Maillacheruvu, K. Y. & Pathan, I. A. (2009). Biodegradation of naphthalene, phenanthrene, and pyrene under anaerobic conditions. *Journal of Environmental Science and Health, Part A* **44**, 1315-1326.
- Major, D. W., Mayfield, C. I. & Barker, J. F. (1988). Biotransformation of benzene by denitrification in aquifer sand. *Ground Water* **26**, 8-14.
- Mancini, S. A., Devine, C. E., Elsner, M., Nandi, M. E., Ulrich, A. C., Edwards, E. A. & Sherwood Lollar, B. (2008). Isotopic evidence suggests different Initial reaction mechanisms for anaerobic benzene biodegradation. *Environmental Science & Technology* **42**, 8290-8296.
- Marcus, Y., Berry, J. & Pierce, J. (1992). Photosynthesis and photorespiration in a mutant of the cyanobacterium *Synechocystis* PCC 6803 lacking carboxysomes. *Planta* **187**, 511-516.
- Marmur, J. (1961). A procedure for the isolation of deoxyribonucleic acid from micro-organisms. *Journal of Molecular Biology* **3**, 208-IN201.
- Marozava, S. V. (2013). Insights into the microbial physiology of bacteria capable of degrading pollutants in contaminated groundwater ecosystems. PhD thesis. In: Technische Universität München.
- Martínez-Blanco, H., Reglero, A., Rodríguez-Aparicio, L. B. & Luengo, J. M. (1990). Purification and biochemical characterization of phenylacetyl-CoA ligase from *Pseudomonas putida*. A specific enzyme for the catabolism of phenylacetic acid. *Journal of Biological Chemistry* **265**, 7084-7090.
- Maruyama, H., Easterday, R. L., Chang, H.-C. & Lane, M. D. (1966). The enzymatic carboxylation of phosphoenolpyruvate: I. PURIFICATION AND PROPERTIES OF PHOSPHOENOLPYRUVATE CARBOXYLASE. *Journal of Biological Chemistry* **241**, 2405-2412.

- Mason, O. U., Scott, N. M., Gonzalez, A. & other authors (2014).** Metagenomics reveals sediment microbial community response to Deepwater Horizon oil spill. *The ISME Journal* **8**, 1464-1475.
- Mazelis, M. & Vennesland, B. (1957).** Carbon dioxide fixation into oxalacetate in higher plants. *Plant Physiology* **32**, 591-600.
- Meckenstock, R. U., Annweiler, E., Michaelis, W., Richnow, H. H. & Schink, B. (2000).** Anaerobic naphthalene degradation by a sulfate-reducing enrichment culture. *Applied and Environmental Microbiology* **66**, 2743-2747.
- Meckenstock, R. U. & Mouttaki, H. (2011).** Anaerobic degradation of non-substituted aromatic hydrocarbons. *Current Opinion in Biotechnology* **22**, 406-414.
- Meganathan, R. (2001).** Ubiquinone biosynthesis in microorganisms. *FEMS Microbiology Letters* **203**, 131-139.
- Men, Y., Lee, P. H., Harding, K. & Alvarez-Cohen, L. (2013).** Characterization of four TCE-dechlorinating microbial enrichments grown with different cobalamin stress and methanogenic conditions. *Appl Microbiol Biotechnol* **97**, 6439-6450.
- Merl, J., Ueffing, M., Hauck, S. M. & von Toerne, C. (2012).** Direct comparison of MS-based label-free and SILAC quantitative proteome profiling strategies in primary retinal Müller cells. *PROTEOMICS* **12**, 1902-1911.
- Mesbah, M., Premachandran, U. & Whitman, W. B. (1989).** Precise measurement of the G+C content of deoxyribonucleic acid by High-Performance Liquid Chromatography. *International Journal of Systematic Bacteriology* **39**, 159-167.
- Mihelcic, J. R. & Luthy, R. G. (1988).** Degradation of polycyclic aromatic hydrocarbon compounds under various redox conditions in soil-water systems. *Applied and Environmental Microbiology* **54**, 1182-1187.
- Mohamed, M. E.-S. (2000).** Biochemical and molecular characterization of phenylacetate-coenzyme A ligase, an enzyme catalyzing the first step in aerobic metabolism of phenylacetic acid in *Azoarcus evansii*. *Journal of Bacteriology* **182**, 286-294.
- Mohamed, M. E.-S. & Fuchs, G. (1993).** Purification and characterization of phenylacetate-coenzyme A ligase from a denitrifying *Pseudomonas sp.*, an enzyme involved in the anaerobic degradation of phenylacetate. *Archives of Microbiology* **159**, 554-562.
- Morrison, W. R. & Smith, L. M. (1964).** Preparation of fatty acid methyl esters and dimethylacetals from lipids with boron fluoride-methanol. *Journal of Lipid Research* **5**, 600-608.
- Moskovits, M. (1985).** Surface-enhanced spectroscopy. *Reviews of Modern Physics* **57**, 783-826.
- Motaleb, M. A., Corum, L., Bono, J. L., Elias, A. F., Rosa, P., Samuels, D. S. & Charon, N. W. (2000).** *Borrelia burgdorferi* periplasmic flagella have both skeletal and motility functions. *PNAS* **97**, 10899-10904.
- Mouttaki, H., Johannes, J. & Meckenstock, R. U. (2012).** Identification of naphthalene carboxylase as a prototype for the anaerobic activation of non-substituted aromatic hydrocarbons. *Environmental Microbiology* **14**, 2770-2774.
- Musat, F., Galushko, A., Jacob, J., Widdel, F., Kube, M., Reinhardt, R., Wilkes, H., Schink, B. & Rabus, R. (2009).** Anaerobic degradation of naphthalene and 2-methylnaphthalene by strains of marine sulfate-reducing bacteria. *Environmental Microbiology* **11**, 209-219.
- Musat, F. & Widdel, F. (2008).** Anaerobic degradation of benzene by a marine sulfate-reducing enrichment culture, and cell hybridization of the dominant phylotype. *Environmental Microbiology* **10**, 10-19.

- Nales, M., Butler, B. J. & Edwards, E. A. (1998).** Anaerobic benzene biodegradation: A microcosm survey. *Bioremediation Journal* **2**, 125-144.
- National Toxicology Program (2000).** Draft technical report on the toxicology and carcinogenesis studies of naphthalene (CAS no. 91-20-3) in F344/N rats (inhalation studies). National Toxicology Program, U.S. Department of Health and Human Services, National Institutes of Health, Rockville, MD. Technical report series No. 500. NIH Publication No. 00-4434. In.
- Nelson, D. L. & Cox, M. M. (2008).** Lehninger Principles of Biochemistry. In: W.H. Freeman and Company, New York, NY, USA.
- Nobu, M. K., Narihiro, T., Hideyuki, T., Qiu, Y.-L., Sekiguchi, Y., Woyke, T., Goodwin, L., Davenport, K. W., Kamagata, Y. & Liu, W.-T. (2014).** The genome of *Syntrophorhabdus aromaticivorans* strain UI provides new insights for syntrophic aromatic compound metabolism and electron flow. *Environmental Microbiology*, n/a-n/a.
- Nyren, P., Nore, B. F. & Strid, A. (1991).** Proton-pumping N,N'-dicyclohexylcarbodiimide-sensitive inorganic pyrophosphate synthase from *Rhodospirillum rubrum*: purification, characterization, and reconstitution. *Biochemistry* **30**, 2883-2887.
- O'Leary, M. H. (1992).** 6 Catalytic Strategies in Enzymic Carboxylation and Decarboxylation. In *The Enzymes*, pp. 235-269. Edited by S. S. David: Academic Press.
- O'Leary, M. H., Rife, J. E. & Slater, J. D. (1981).** Kinetic and isotope effect studies of maize phosphoenolpyruvate carboxylase. *Biochemistry* **20**, 7308-7314.
- Oberender, J., Kung, J. W., Seifert, J., von Bergen, M. & Boll, M. (2012).** Identification and characterization of a succinyl-Coenzyme A (CoA):benzoate CoA transferase in *Geobacter metallireducens*. *Journal of Bacteriology* **194**, 2501-2508.
- Ochman, H., Lawrence, J. G. & Groisman, E. A. (2000).** Lateral gene transfer and the nature of bacterial innovation. *Nature* **405**, 299-304.
- Pacwa-Płociniczak, M., Płaza, G. A., Piotrowska-Seget, Z. & Cameotra, S. S. (2011).** Environmental applications of biosurfactants: Recent advances. *International Journal of Molecular Sciences* **12**, 633-654.
- Passow, U., Ziervogel, K., Asper, V. & Diercks, A. (2012).** Marine snow formation in the aftermath of the Deepwater Horizon oil spill in the Gulf of Mexico. *Environmental Research Letters* **7**, 035301.
- Paster, B. J. & Canale-Parola, E. (1980).** Involvement of periplasmic fibrils in motility of spirochetes. *Journal of Bacteriology* **141**, 359-364.
- Paster, B. J. & Dewhirst, F. E. (2000).** Phylogenetic foundation of spirochetes. *Journal of Molecular Microbiology and Biotechnology* **2**, 341-344.
- Peränen, J., Rikkonen, M., Hyvönen, M. & Kääriäinen, L. (1996).** T7 vectors with a modified T7lacPromoter for expression of proteins in *Escherichia coli*. *Analytical Biochemistry* **236**, 371-373.
- Pfennig, N. (1978).** *Rhodocyclus purpureus* gen. nov. and sp. nov., a ring-shaped, vitamin B12-requiring member of the family *Rhodospirillaceae*. *International Journal of Systematic Bacteriology* **28**, 283-288.
- Phelps, C. D., Kazumi, J. & Young, L. Y. (1996).** Anaerobic degradation of benzene in BTX mixtures dependent on sulfate reduction. *FEMS Microbiology Letters* **145**, 433-437.
- Pikuta, E. V., Hoover, R. B., Bej, A. K., Marsic, D., Whitman, W. B. & Krader, P. (2009).** *Spirochaeta dissipatitropha* sp. nov., an alkaliphilic, obligately anaerobic bacterium, and emended description of the genus *Spirochaeta* Ehrenberg 1835. *International Journal of Systematic and Evolutionary Microbiology* **59**, 1798-1804.

- Pilloni, G., von Netzer, F., Engel, M. & Lueders, T. (2011).** Electron acceptor-dependent identification of key anaerobic toluene degraders at a tar-oil-contaminated aquifer by Pyro-SIP. *FEMS Microbiology Ecology* **78**, 165-175.
- Pohlschroeder, M., Leschine, S. B. & Canale-Parola, E. (1994).** *Spirochaeta caldaria* sp. nov., a thermophilic bacterium that enhances cellulose degradation by *Clostridium thermocellum*. *Archives of Microbiology* **161**, 17-24.
- Preuss, R., Angerer, J. & Drexler, H. (2003).** Naphthalene—an environmental and occupational toxicant. *Int Arch Occup Environ Health* **76**, 556-576.
- Rabus, R., Kube, M., Beck, A., Widdel, F. & Reinhardt, R. (2002).** Genes involved in the anaerobic degradation of ethylbenzene in a denitrifying bacterium, strain EbN1. *Archives of Microbiology* **178**, 506-516.
- Rabus, R., Kube, M., Heider, J., Beck, A., Heitmann, K., Widdel, F. & Reinhardt, R. (2005).** The genome sequence of an anaerobic aromatic-degrading denitrifying bacterium, strain EbN1. *Archives of Microbiology* **183**, 27-36.
- Ragsdale, S. W. & Pierce, E. (2008).** Acetogenesis and the Wood–Ljungdahl pathway of CO₂ fixation. *Biochimica et Biophysica Acta* **1784**, 1873-1898.
- Ramseur, J. L. (2010).** Deepwater Horizon Oil Spill: The Fate of the Oil. Congressional Research Service; 1-20, 7-5700, R41531. In.
- Reddy, S. V., Aspana, S., Tushar, D. L., Sasikala, C. & Ramana, C. V. (2013).** *Spirochaeta sphaeroplastigenens* sp. nov., a halo-alkaliphilic, obligately anaerobic spirochaete isolated from soda lake Lonar. *International Journal of Systematic and Evolutionary Microbiology* **63**, 2223-2228.
- Ritalahti, K. M., Justicia-Leon, S. D., Cusick, K. D., Ramos-Hernandez, N., Rubin, M., Dornbush, J. & Löffler, F. E. (2012).** *Sphaerochaeta globosa* gen. nov., sp. nov. and *Sphaerochaeta pleomorpha* sp. nov., free-living, spherical spirochaetes. *International Journal of Systematic and Evolutionary Microbiology* **62**, 210-216.
- Ritalahti, K. M. & Löffler, F. E. (2004).** Populations implicated in anaerobic reductive dechlorination of 1,2-dichloropropane in highly enriched bacterial communities. *Applied and Environmental Microbiology* **70**, 4088-4095.
- Rockne, K. J., Chee-Sanford, J. C., Sanford, R. A., Hedlund, B. P., Staley, J. T. & Strand, S. E. (2000).** Anaerobic naphthalene degradation by microbial pure cultures under nitrate-reducing conditions. *Applied and Environmental Microbiology* **66**, 1595-1601.
- Rockne, K. J. & Strand, S. E. (1998).** Biodegradation of bicyclic and polycyclic aromatic hydrocarbons in anaerobic enrichments. *Environmental Science & Technology* **32**, 3962-3967.
- Rockne, K. J. & Strand, S. E. (2001).** Anaerobic biodegradation of naphthalene, phenanthrene, and biphenyl by a denitrifying enrichment culture. *Water Research* **35**, 291-299.
- Rosey, E. L., Kennedy, M. J. & Yancey, R. J. (1996).** Dual flaA1 flaB1 mutant of *Serpulina hyodysenteriae* expressing periplasmic flagella is severely attenuated in a murine model of swine dysentery. *Infection and Immunity* **64**, 4154-4162.
- Safinowski, M. & Meckenstock, R. U. (2004).** Enzymatic reactions in anaerobic 2-methylnaphthalene degradation by the sulphate-reducing enrichment culture N47. *FEMS Microbiology Letters* **240**, 99-104.
- Safinowski, M. & Meckenstock, R. U. (2006).** Methylation is the initial reaction in anaerobic naphthalene degradation by a sulfate-reducing enrichment culture. *Environmental Microbiology* **8**, 347-352.

- Sakai, N., Kurisu, F., Yagi, O., Nakajima, F. & Yamamoto, K. (2009).** Identification of putative benzene-degrading bacteria in methanogenic enrichment cultures. *Journal of Bioscience and Bioengineering* **108**, 501-507.
- Salinero, K., Keller, K., Feil, W., Feil, H., Trong, S., Bartolo, G. & Lapidus, A. (2009).** Metabolic analysis of the soil microbe *Dechloromonas aromatica* str. RCB: indications of a surprisingly complex life-style and cryptic anaerobic pathways for aromatic degradation. *BMC Genomics* **10**, 1-23.
- Sawers, G. & Watson, G. (1998).** A glycol radical solution: oxygen-dependent interconversion of pyruvate formate-lyase. *Molecular Microbiology* **29**, 945-954.
- Schleinitz, K. M., Schmeling, S., Jehmlich, N., von Bergen, M., Harms, H., Kleinsteuber, S., Vogt, C. & Fuchs, G. (2009).** Phenol degradation in the strictly anaerobic iron-reducing bacterium *Geobacter metallireducens* GS-15. *Applied and Environmental Microbiology* **75**, 3912-3919.
- Schmeling, S. & Fuchs, G. (2009).** Anaerobic metabolism of phenol in proteobacteria and further studies of phenylphosphate carboxylase. *Archives of Microbiology* **191**, 869-878.
- Schmeling, S., Narmandakh, A., Schmitt, O., Gad'on, N., Schühle, K. & Fuchs, G. (2004).** Phenylphosphate synthase: a new phosphotransferase catalyzing the first step in anaerobic phenol metabolism in *Thauera aromatica*. *Journal of Bacteriology* **186**, 8044-8057.
- Schmitt, M. E., Brown, T. A. & Trumpower, B. L. (1990).** A rapid and simple method for preparation of RNA from *Saccharomyces cerevisiae*. *Oxford University Press* **18**, 3091-3092.
- Schnell, S., Bak, F. & Pfennig, N. (1989).** Anaerobic degradation of aniline and dihydroxybenzenes by newly isolated sulfate-reducing bacteria and description of *Desulfobacterium anilini*. *Archives of Microbiology* **152**, 556-563.
- Schnell, S. & Schink, B. (1991).** Anaerobic aniline degradation via reductive deamination of 4-aminobenzoyl-CoA in *Desulfobacterium anilini*. *Archives of Microbiology* **155**, 183-190.
- Schöcke, L. & Schink, B. (1998).** Membrane-bound proton-translocating pyrophosphatase of *Syntrophus gentianae*, a syntrophically benzoate-degrading fermenting bacterium. *European Journal of Biochemistry* **256**, 589-594.
- Schrope, M. (2013).** Dirty blizzard buried Deepwater Horizon oil. Nature News; doi:10.1038/nature.2013.12304. In: Nature News.
- Schühle, K. & Fuchs, G. (2004).** Phenylphosphate carboxylase: a new C-C lyase involved in anaerobic in phenol metabolism in *Thauera aromatica*. *Journal of Bacteriology* **186**, 4556-4567.
- Schühle, K., Gescher, J., Feil, U., Paul, M., Jahn, M., Schägger, H. & Fuchs, G. (2003).** Benzoate-Coenzyme a ligase from *Thauera aromatica*: an enzyme acting in anaerobic and aerobic pathways. *Journal of Bacteriology* **185**, 4920-4929.
- Schühle, K. & Heider, J. (2011).** Acetone and butanone metabolism of the denitrifying bacterium "*Aromatoleum aromaticum*": novel biochemical properties of an ATP-dependent aliphatic ketone carboxylase. *Journal of Bacteriology*.
- Selesi, D., Jehmlich, N., von Bergen, M., Schmidt, F., Rattei, T., Tischler, P., Lueders, T. & Meckenstock, R. U. (2010).** Combined genomic and proteomic approaches identify gene clusters involved in anaerobic 2-methylnaphthalene degradation in the sulfate-reducing enrichment culture N47. *Journal of Bacteriology* **192**, 295-306.

- Selesi, D. & Meckenstock, R. U. (2009).** Anaerobic degradation of the aromatic hydrocarbon biphenyl by a sulfate-reducing enrichment culture. *FEMS Microbiology Ecology* **68**, 86-93.
- Selmer, T. & Andrei, P. I. (2001).** *p*-Hydroxyphenylacetate decarboxylase from *Clostridium difficile*. A novel glyceryl radical enzyme catalysing the formation of *p*-cresol. *European Journal of Biochemistry* **268**, 1363-1372.
- Söhngen, N. L. (1913).** Benzin, Petroleum, Paraffinöl und Paraffin als Kohlenstoff- und Energiequellen für Mikroben. *Zentralblatt fuer Bakteriologie, Parasitenkunde, Infektionskrankheiten und Hygiene, Abt II* **37**, 595–609.
- Sotirova, A., Spasova, D., Vasileva-Tonkova, E. & Galabova, D. (2009).** Effects of rhamnolipid-biosurfactant on cell surface of *Pseudomonas aeruginosa*. *Microbiological Research* **164**, 297-303.
- Stanton, T. B. & Canale-Parola, E. (1979).** Enumeration and selective isolation of rumen spirochetes. *Applied and Environmental Microbiology* **38**, 965-973.
- Studholme, D. J. & Dixon, R. (2003).** Domain architectures of σ^{54} -dependent transcriptional activators. *Journal of Bacteriology* **185**, 1757-1767.
- Studier, F. W. & Moffatt, B. A. (1986).** Use of bacteriophage T7 RNA polymerase to direct selective high-level expression of cloned genes. *Journal of Molecular Biology* **189**, 113-130.
- Suzuki, D., Li, Z., Cui, X., Zhang, C. & Katayama, A. (2014).** Reclassification of *Desulfobacterium anilini* as *Desulfatiglans anilini* comb. nov. within *Desulfatiglans* gen. nov., and description of a 4-chlorophenol-degrading sulfate-reducing bacterium, *Desulfatiglans parachlorophenolica* sp. nov. *International Journal of Systematic and Evolutionary Microbiology* **64**, 3081-3086.
- Tamaoka, J. & Komagata, K. (1984).** Determination of DNA base composition by reversed-phase high-performance liquid chromatography. *FEMS Microbiology Letters* **25**, 125-128.
- Tamura, K., Stecher, G., Peterson, D., Filipowski, A., & Kumar, S. (2013).** MEGA6: Molecular Evolutionary Genetics Analysis Version 6.0. *Molecular Biology and Evolution* **30**, 2725-2729.
- Tang, S., Chan, W. W. M., Fletcher, K. E., Seifert, J., Liang, X., Löffler, F. E., Edwards, E. A. & Adrian, L. (2013).** Functional characterization of reductive dehalogenases by using Blue Native Polyacrylamide Gel Electrophoresis. *Applied and Environmental Microbiology* **79**, 974-981.
- Taş, N., Van Eekert, M. H. A., De Vos, W. M. & Smidt, H. (2010).** The little bacteria that can – diversity, genomics and ecophysiology of ‘*Dehalococcoides*’ spp. in contaminated environments. *Microbial biotechnology* **3**, 389-402.
- Taubert, M., Vogt, C., Wubet, T., Kleinstaub, S., Tarkka, M. T., Harms, H., Buscot, F., Richnow, H.-H., von Bergen, M. & Seifert, J. (2012).** Protein-SIP enables time-resolved analysis of the carbon flux in a sulfate-reducing, benzene-degrading microbial consortium. *The ISME Journal* **6**, 2291-2301.
- Thauer, R. K., Kaster, A.-K., Seedorf, H., Buckel, W. & Hedderich, R. (2008).** Methanogenic archaea: ecologically relevant differences in energy conservation. *Nature Review Microbiology* **6**, 579-591.
- Thauer, R. K. & Shima, S. (2008).** Methane as fuel for anaerobic microorganisms. *Annals of the New York Academy of Sciences* **1125**, 158-170.
- Thierrin, J., Davis, G. B., Barber, C., Patterson, B. M., Pribac, F., Power, T. R. & Lambert, M. (1993).** Natural degradation rates of BTEX compounds and naphthalene in a sulphate reducing groundwater environment. *Hydrological Sciences* **38**, 309-322.

- U.S. Department of Health & Human Services (2005).** A toxicological profile for naphthalene, 1-methylnaphthalene, and 2-methylnaphthalene.
- Ulrich, A. C., Beller, H. R. & Edwards, E. A. (2005).** Metabolites detected during biodegradation of 13C6-benzene in nitrate-reducing and methanogenic enrichment cultures. *Environmental Science & Technology* **39**, 6681-6691.
- Ulrich, A. C. & Edwards, E. A. (2003).** Physiological and molecular characterization of anaerobic benzene-degrading mixed cultures. *Environmental Microbiology* **5**, 92-102.
- Unites States Environmental Protection Agency (2003).** Health effects support document for naphthalene. U.S. Environmental Protection Agency Office of Water (4304T) Health and Ecological Criteria Division Washington, DC 20460. EPA 822-R-03-005. In.
- Veldkamp, H. (1960).** Isolation and characteristics of *Treponema zuelzeriae* nov. spec., an anaerobic, free-living spirochete. *Antonie van Leeuwenhoek* **26**, 103-125.
- Villatoro-Monzón, W., Mesta-Howard, A. & Razo-Flores, E. (2003).** Anaerobic biodegradation of BTEX using Mn(IV) and Fe(III) as alternative electron acceptors. *Water science & technology* **48**, 125-131.
- Villatoro-Monzón, W., Morales-Ibarria, M., Velázquez, E., Ramírez-Saad, H. & Razo-Flores, E. (2008).** Benzene biodegradation under anaerobic conditions coupled with metal oxides reduction. *Water Air Soil Pollut* **192**, 165-172.
- Vogel, T. M. & Grbic-Galic, D. (1986).** Incorporation of oxygen from water into toluene and benzene during anaerobic fermentative transformation. *Applied and Environmental Microbiology* **52**, 200-202.
- Vogt, C., Gödeke, S., Treutler, H.-C., Weiß, H., Schirmer, M. & Richnow, H.-H. (2007).** Benzene oxidation under sulfate-reducing conditions in columns simulating in situ conditions. *Biodegradation* **18**, 625-636.
- Vogt, C., Kleinstuber, S. & Richnow, H.-H. (2011).** Anaerobic benzene degradation by bacteria. *Microbial Biotechnology* **4**, 710-724.
- Walker, J. F. & Scott, N. D. (1938).** Sodium naphthalene. II. Preparation and properties of dihydronaphthalene dicarboxylic acids. *Journal of the American Chemical Society* **60**, 951-955.
- Weelink, S. A. B., Tan, N. C. G., ten Broeke, H., van den Kieboom, C., van Doesburg, W., Langenhoff, A. A. M., Gerritse, J., Junca, H. & Stams, A. J. M. (2008).** Isolation and characterization of *Alicyclophilus denitrificans* strain BC, which grows on benzene with chlorate as the electron acceptor. *Applied and Environmental Microbiology* **74**, 6672-6681.
- Weelink, S. A. B., van Eekert, M. H. A. & Stams, A. J. M. (2010).** Degradation of BTEX by anaerobic bacteria: physiology and application. *Rev Environ Sci Biotechnol* **9**, 359-385.
- Weiner, J. M. & Lovley, D. R. (1998).** Rapid benzene degradation in methanogenic sediments from a petroleum-contaminated aquifer. *Applied and Environmental Microbiology* **64**, 1937-1939.
- Weisburg, W. G., Barns, S. M., Pelletier, D. A. & Lane, D. J. (1991).** 16S ribosomal DNA amplification for phylogenetic study. *Journal of Bacteriology* **173**, 697-703.
- Widdel, F., Kohring, G.-W. & Mayer, F. (1983).** Studies on dissimilatory sulfate-reducing bacteria that decompose fatty acids III. Characterization of the filamentous gliding *Desulfonema limicola* gen. nov. sp. nov., and *Desulfonema magnum* sp. nov. *Archives of Microbiology* **134**, 286-294.

- Widdel, F. & Pfennig, N. (1981).** Studies on dissimilatory sulfate-reducing bacteria that decompose fatty acids I. Isolation of new sulfate-reducing bacteria enriched with acetate from saline environments. Description of *Desulfobacter postgatei* gen. nov., sp. nov. *Archives of Microbiology* **129**, 395-400.
- Willumsen, P. A. & Karlson, U. (1996).** Screening of bacteria, isolated from PAH-contaminated soils, for production of biosurfactants and bioemulsifiers. *Biodegradation* **7**, 415-423.
- Wilson, B. H., Smith, G. B. & Rees, J. F. (1986).** Biotransformations of selected alkylbenzenes and halogenated aliphatic hydrocarbons in methanogenic aquifer material: a microcosm study. *Environmental Science & Technology* **20**, 997-1002.
- Winderl, C., Anneser, B., Griebler, C., Meckenstock, R. U. & Lueders, T. (2008).** Depth-Resolved Quantification of Anaerobic Toluene Degraders and Aquifer Microbial Community Patterns in Distinct Redox Zones of a Tar Oil Contaminant Plume. *Applied and Environmental Microbiology* **74**, 792-801.
- Winderl, C., Penning, H., Netzer, F. v., Meckenstock, R. U. & Lueders, T. (2010).** DNA-SIP identifies sulfate-reducing *Clostridia* as important toluene degraders in tar-oil-contaminated aquifer sediment. *The ISME Journal* **4**, 1314-1325.
- Wischgoll, S., Heintz, D., Peters, F., Erxleben, A., Sarnighausen, E., Reski, R., Van Dorselaer, A. & Boll, M. (2005).** Gene clusters involved in anaerobic benzoate degradation of *Geobacter metallireducens*. *Molecular Microbiology* **58**, 1238-1252.
- Woodcock, D. M., Crowther, P. J., Doherty, J., Jefferson, S., DeCruz, E., Noyer-Weidner, M., Smith, S. S., Michael, M. Z. & Graham, M. W. (1989).** Quantitative evaluation of *Escherichia coli* host strains for tolerance to cytosine methylation in plasmid and phage recombinants. *Nucleic Acids Research* **17**, 3469-3478.
- Wozniak, R. A. F. & Waldor, M. K. (2010).** Integrative and conjugative elements: mosaic mobile genetic elements enabling dynamic lateral gene flow. *Nature Review Microbiology* **8**, 552-563.
- Wu, J.-H., Wu, F.-Y., Chuang, H.-P., Chen, W.-Y., Huang, H.-J., Chen, S.-H. & Liu, W.-T. (2013).** Community and proteomic analysis of methanogenic consortia degrading terephthalate. *Applied and Environmental Microbiology* **79**, 105-112.
- Yang, S., Yoshida, N., Baba, D. & Katayama, A. (2008).** Anaerobic biodegradation of biphenyl in various paddy soils and river sediment. *Chemosphere* **71**, 328-336.
- Yeates, T. O., Kerfeld, C. A., Heinhorst, S., Cannon, G. C. & Shively, J. M. (2008).** Protein-based organelles in bacteria: carboxysomes and related microcompartments. *Nature Review Microbiology* **6**, 681-691.
- Zamfirescu, D. & Grathwohl, P. (2001).** Occurrence and attenuation of specific organic compounds in the groundwater plume at a former gasworks site. *Journal of Contaminant Hydrology* **53**, 407-427.
- Zarzycki, J., Brecht, V., Müller, M. & Fuchs, G. (2009).** Identifying the missing steps of the autotrophic 3-hydroxypropionate CO₂ fixation cycle in *Chloroflexus aurantiacus*. *Proceedings of the National Academy of Sciences* **106**, 21317-21322.
- Zhang, H. & Javor, G. T. (2003).** Regulation of the isofunctional genes *ubiD* and *ubiX* of the ubiquinone biosynthetic pathway of *Escherichia coli*. *FEMS Microbiology Letters* **223**, 67-72.
- Zhang, S., Wang, Q. & Xie, S. (2012).** Stable isotope probing identifies anthracene degraders under methanogenic conditions. *Biodegradation* **23**, 221-230.
- Zhang, T., Bain, T. S., Nevin, K. P., Barlett, M. A. & Lovley, D. R. (2012).** Anaerobic benzene oxidation by *Geobacter* species. *Applied and Environmental Microbiology* **78**, 8304-8310.

- Zhang, T., Tremblay, P.-L., Chaurasia, A. K., Smith, J. A., Bain, T. S. & Lovley, D. R. (2013). Anaerobic benzene oxidation via phenol in *Geobacter metallireducens*. *Applied and Environmental Microbiology*.
- Zhang, T., Tremblay, P.-L., Chaurasia, A. K., Smith, J. A., Bain, T. S. & Lovley, D. R. (2014). Identification of genes specifically required for the anaerobic metabolism of benzene in *Geobacter metallireducens*. *Frontiers in Microbiology* 5.
- Zhang, X., Chaney, M., Wigneshweraraj, S. R., Schumacher, J., Bordes, P., Cannon, W. & Buck, M. (2002). Mechanochemical ATPases and transcriptional activation. *Molecular Microbiology* 45, 895-903.
- Zhang, X. & Young, L. Y. (1997). Carboxylation as an initial reaction in the anaerobic metabolism of naphthalene and phenanthrene by sulfidogenic consortia. *Applied and Environmental Microbiology* 63, 4759–4764.
- Zhao, L., Ma, T., Gao, M., Gao, P., Cao, M., Zhu, X. & Li, G. (2012). Characterization of microbial diversity and community in water flooding oil reservoirs in China. *World J Microbiol Biotechnol* 28, 3039-3052.
- Zhilina, T. N., Zavarzin, G. A., Rainey, F., Kevbrin, V. V., Kostrikina, N. A. & Lysenko, A. M. (1996). *Spirochaeta alkalica* sp. nov., *Spirochaeta africana* sp. nov., and *Spirochaeta asiatica* sp. nov., alkaliphilic anaerobes from the continental soda lakes in Central Asia and the East African Rift. *International Journal of Systematic Bacteriology* 46, 305-312.
- Ziv-El, M., Delgado, A., Yao, Y., Kang, D.-W., Nelson, K., Halden, R. & Krajmalnik-Brown, R. (2011). Development and characterization of DehaloR², a novel anaerobic microbial consortium performing rapid dechlorination of TCE to ethene. *Appl Microbiol Biotechnol* 92, 1063-1071.
- Zuelzer, M. (1912). Über *Spirochaeta plicatilis* Ehrenberg und deren Verwandtschaftsbeziehungen. *Arch Protistenkd* 24, 1-59.

Publication and authorship clarifications

Published

1. Kubryk, P., Kölschbach, J. S., Marozava, S., Lueders, T., Meckenstock, R. U., Niessner, R. and Ivleva, N. P. (2015) Exploring the potential of stable isotope (resonance) Raman microspectroscopy and Surface-Enhanced Raman Scattering for the analysis of microorganisms at single cell level. *Analytical Chemistry*, DOI: 10.1021/acs.analchem.5b00673.

In Press

2. Meckenstock, R. U., Boll, M., Mouttaki, H., Koelschbach, J. S., Cunha Tarouco, P., Weyrauch, P., Dong, X. and Himmelberg, A. (2015) Anaerobic degradation of polycyclic aromatic hydrocarbons and benzene. *Submitted*, *Journal of Molecular Microbiology and Biotechnology*.

Pending manuscripts

3. Koelschbach, J. S., Mouttaki, H., Meyer, C., Heipieper, H. J., Rachel R., Lawson, P. A. and Meckenstock, R. U. (2015) *Treponema contaminophilus* sp. nov., a rode-shaped spirochete isolated from the anaerobic naphthalene-degrading enrichment culture N47. *In preparation*, *International Journal of Systematic and Evolutionary Microbiology (IJSEM)*.
4. Koelschbach, J. S., Mouttaki, H., Merl-Pham, J. and Meckenstock, R. U. (2015) Identification of naphthalene carboxylase subunits of the sulfate-reducing culture N47. *In preparation*, *Environmental Microbiology*.

1. Parts of the publication are based on the cooperation project 'Raman microspectroscopy of N47' which was described in the last chapter of the present PhD project. The experiments were planned by Rainer U. Meckenstock and Natalia P. Ivleva together with the PhD students Patrick Kubryk and Janina Kölschbach. Janina Kölschbach prepared the bacterial cells for Raman microspectroscopy. For flow cytometry, technical assistance and method development was provided by Nina Weber (Institute of Groundwater Ecology, Group of Microbial Ecology, Helmholtz Zentrum München). Raman microspectroscopy was performed by Patrick Kubryk and Dr. Natalia P. Ivleva at the Institute of Hydrochemistry, TU München. The manuscript draft was developed by Patrick Kubryk and

Dr. Natalia P. Ivleva. Parts dealing with N47 were complemented or added by Janina Kölschbach. All mentioned co-authors revised and edited the manuscript.

2. The review article will be part of a special issue of the journal JMMB. All invited authors of the special issue are members of the DFG priority program 'Biologische Umsetzungen von Kohlenwasserstoffen in Abwesenheit von Sauerstoff: Von molekularer zu globaler Ebene'. The outline of the review article was developed by Rainer U. Meckenstock. The PhD candidate Janina Kölschbach wrote the paragraph 'UbiD-like (de)carboxylases in anaerobic degradation of non-substituted (polycyclic)aromatic compounds', which is also part of the introduction and the discussion of the current PhD thesis. The used figure was designed by the PhD candidate. The manuscript draft was revised and edited by Rainer U. Meckenstock.
3. The manuscript is based on the side project 'Characterization of *Treponema contaminophilus* sp. strain HM^T'. The project was developed by Housna Mouttaki and planned together with the PhD student. The strain was isolated by Housna Mouttaki and characterized by Janina Kölschbach. Fatty acid methyl ester analysis was done by Janina Kölschbach in cooperation with Hermann J. Heipiper (Department Umweltbiotechnologie, Helmholtz Zentrum für Umweltforschung Leipzig). Electron microscopy was done at the University of Regensburg in collaboration with Carolin Meyer (former member of the Institute of Groundwater Ecology, Group of Anaerobic Degradation, Helmholtz Zentrum München) and Reinhard Rachel (Zentrum für Elektronenmikroskopie der Fakultät für Biologie und Vorklinische Medizin). The DNA G+C content of the strain HM^T was measured at the DSMZ in Braunschweig. Figures representing the results were designed by the PhD candidate. The manuscript draft was developed by Janina Kölschbach and Housna Mouttaki. Housna Mouttaki and Rainer U. Meckenstock revised and edited the manuscript.
4. The manuscript is based on the main project 'Identification of naphthalene carboxylase subunits of N47' of the present PhD project. The project was developed by Rainer U. Meckenstock. Housna Mouttaki supervised the project. The experiments were planned, conducted and analyzed by Janina Kölschbach. All proteomic analyses were done by Juliane Merl-Pham (Research Unit Protein Science, Helmholtz Zentrum München). Figures representing the results were designed by the PhD candidate. The manuscript draft was developed by Janina Kölschbach and Housna Mouttaki and revised and edited by Housna Mouttaki and Rainer U. Meckenstock.

Acknowledgements - Danksagung

Mein persönlicher Dank gilt meinem Doktorvater Herrn Prof. Dr. Rainer U. Meckenstock für die Bereitstellung dieses sehr interessanten und herausfordernden Themas sowie für seine stetige Hilfsbereitschaft. Außerdem möchte ich Dir für die Möglichkeit der Teilnahme an verschiedenen wissenschaftlichen Tagungen danken. Herrn PD Dr. Tillmann Lüders danke herzlich ich für die kurzfristige Übernahme des Erstgutachters meiner Arbeit. A special thanks goes to my second supervisor Dr. Housna Mouttaki. I thank you for your enormous support- all the helpful discussions and ideas for experiments and the correction of my talks, reports and my thesis. You gave me the confidence to realize my own ideas!

Mein ganz besonderer Dank gilt zudem Herrn Prof. Dr. Johann Heider für seine fortwährende Diskussionsbereitschaft und Unterstützung sowie die Teilnahme an meinen „Thesis Committee Meetings“ mit vielen hilfreichen Anmerkungen. Herrn Dr. Martin Elsner möchte ich für die kurze und freundliche Aufnahme in seiner Arbeitsgruppe danken. Für den sehr erkenntnisreichen Aufenthalt in seinem Labor möchte ich Herrn Prof. Dr. Matthias Boll (Universität Freiburg) sowie seiner Arbeitsgruppe herzlich danken! Für die Finanzielle Unterstützung danke ich der Deutschen Forschungsgemeinschaft, Schwerpunktprogramm SPP1319.

Unseren Kooperationspartnern Frau Dr. Juliane Merl-Pham (Research Unit Protein Science, Helmholtz Zentrum München) danke ich für die Durchführung der Proteomics-Analysen und ihrer stetigen Diskussionsbereitschaft sowie Herrn Patrick Kubryk und Frau Dr. Natalia P. Ivleva (TU München) für die Durchführung der Raman Mikroskopie und die gute Zusammenarbeit. Ebenso danke ich Herrn Prof. Dr. Reinhard Rachel (Universität Regensburg) und Frau Dr. Carolin Meyer für Ihre Hilfe bei der Elektronenmikroskopie sowie Herrn Dr. Hermann J. Heipiper für die Fettsäureanalyse (UFZ Leipzig).

Meinen Kolleginnen und Kollegen am IGOE (Helmholtz Zentrum München) danke ich für die freundliche Arbeitsatmosphäre und die Hilfsbereitschaft. Besonders danken möchte ich meinem Labormitbewohner Philip Weyrauch für die vielen biochemischen Diskussionen, Ideen und aufbauenden Gespräche! Ebenso danke ich meinen Kolleginnen und Kollegen aus Büro 142: Dr. Clemens Karwautz, Heide Schürner, Katrin Hörmann und Roland Hofmann. Vielen Dank für die vielen wissenschaftlichen Diskussionen und Gedankenanstöße, die Unterstützung bei Labormethoden, Softwareproblemen und mentaler Verzweiflung! Es war eine tolle Zeit mich euch! ☺ Herrn Dr. Frederick von Netzer, meiner Kummer-Nummer, danke ich für seine vielfältige Hilfe in allen wissenschaftlichen Anliegen und seine unglaubliche Geduld! Dem „IGOE-Laufteam“ (Dr. Doreen Franke, Heide Schürner, Dr. Kerstin Nicolaisen, Roland Hofmann und Tina Höche) danke ich für den perfekten Ausgleich zum Laboralltag! Dr. Franziska Rühle und Ben Gralher danke ich für die motivierende Busfreundschaft!

Ein ganz besonderes Dankschön gilt meiner Familie. Meinen Eltern und Schwestern danke ich von ganzem Herzen für Eure fortwährende Unterstützung und den familiären Zusammenhalt. Meinem Freund Maximilian Reuter danke dir für seine Unterstützung während des gesamten Studiums und der Promotion. Ohne Euch wäre das alles nicht möglich gewesen!!!

Lebenslauf

Janina Stephanie Kölschbach, geboren am 02.12.1986 in Waldbröl, NRW.

Schulbildung

08/1997-07/2003	Realschule der Stadt Wiehl, NRW
09/2003-06/2006	Dietrich-Bonhoeffer-Gymnasium Wiehl, NRW

Hochschulbildung

10/2006-06/2009	Bachelor-Studium im Studiengang „Biology“ an der Philipps-Universität Marburg, Hessen
10/2008-06/2009	Bachelorarbeit an der Philipps-Universität Marburg unter der Leitung von Prof. Dr. Johann Heider mit dem Thema „Biochemische Charakterisierung der Benzoylsuccinyl-CoA Thiolase, eines Enzyms des anaeroben Toluolabbaus“
10/2009-08/2011	Master-Studium im Studiengang „Molecular and Cellular Biology“ an der Philipps-Universität Marburg, Hessen
10/2010-08/2011	Masterarbeit an der Philipps-Universität Marburg unter der Leitung von Prof. Dr. Johann Heider mit dem Thema „Untersuchung eines potentiell neuen Stickstofffixierungsweges in <i>Paracoccus denitrificans</i> und Biochemie der Benzoylsuccinyl-CoA Thiolase“

Stipendium

06/2009-09/2011	Stipendium der Studienstiftung des deutschen Volkes
-----------------	---

Promotion

09/2011-03/2015	Promotion am Helmholtz Zentrum München, Institut für Grundwasserökologie in der Arbeitsgruppe Anaerober Schadstoffabbau unter der Leitung von Prof. Dr. Rainer U. Meckenstock mit dem Thema „Identification of naphthalene carboxylase subunits of the sulfate-reducing enrichment culture N47“
-----------------	---

Appendix

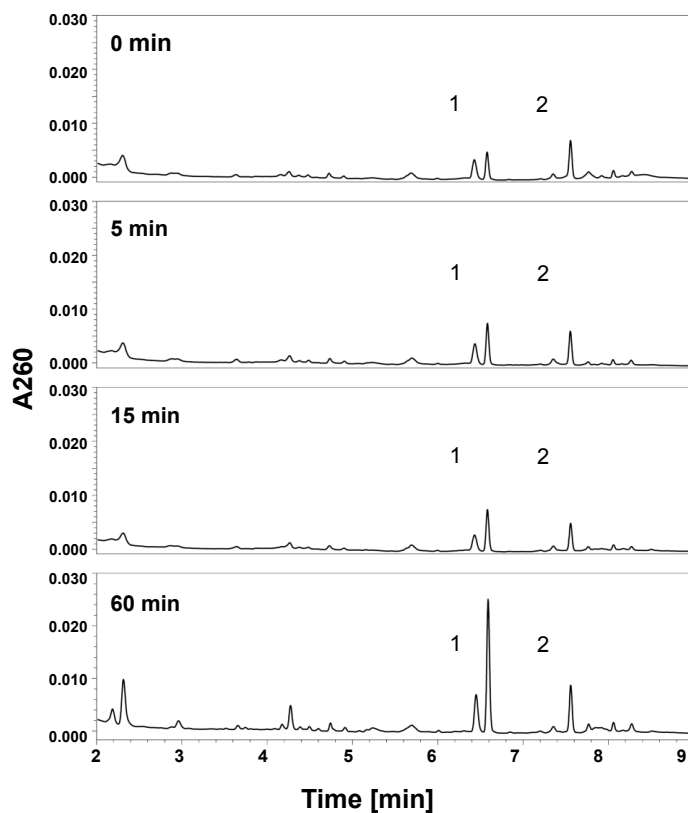


Figure A1: UPLC analyses of produced CoA-esters in the naphthalene carboxylase enzyme assays. Time-resolved formation of NCoA and THNCoA in naphthalene carboxylase activity assay in absence of additional CoASH. The enzyme assay contained 5 mM ATP. 1; NCoA. 2; THNCoA.

Table A3: Biological replicate of proteins identified on Blue native PAGE gel slices with a size of about 750 kDa which were shown to be differentially induced in naphthalene-grown N47 cells (Naph) in comparison to 2-methylnaphthalene-grown cells (2MN). The proteins with a p-value ≤ 0.01 and an enrichment factor ≥ 2 are shown below. The proteins shown in bold letters correspond to the ones which are encoded in the naphthalene carboxylase gene cluster. C. score, confidence score; peptides used for quant., peptides used for quantification.

UniProtKB entry name	Peptides used for quant.	C.score	Anova (p)	Description	Annotated function	Ratio Naph/2MN
E1YIW4_9DEL	21	1181	0.000008	N47_K27480	UbiD family decarboxylase	40.0
E1YIW6_9DEL	21	1091	0.000007	N47_K27500	UbiD family decarboxylase	29.9
E1YIX0_9DEL	13	675	0.000748	N47_K27540	Putative phenylphosphate carboxylase, alpha subunit Conserved hypothetical protein	16.3
E1YIW3_9DEL	3	129	0.000654	N47_K27470	Putative phenylphosphate carboxylase, gamma subunit	753.1^a
E1YD22_9DEL	3	121	0.005537	N47_G37900	Tol-pal system protein	3.0
E1YIW9_9DEL	1	81	0.006151	N47_K27530	Putative phenylphosphate carboxylase, gamma subunit	11.4^a
E1YJZ3_9DEL	1	60	0.000736	N47_E51090	Outer membrane protein, OmpA-like	8.4
E1YJZ4_9DEL	1	40	0.001023	N47_E51100	Hypothetical protein	9.8
E1YM45_9DEL	1	39	0.012367	N47_E46900	K(+)-insensitive pyrophosphate-energized H ⁺ pump	4.1
E1YBS7_9DEL	1	38	0.000442	N47_G33450	Hypothetical protein (dodecin superfamily)	5.8
E1YDG9_9DEL	1	35	0.001714	N47_G39370	Hypothetical protein, family of Fe/Mo cluster-binding protein	5.0
E1YIW8_9DEL	1	35	0.000711	N47_K27520	MRP; Fer4_NifH superfamily	18.2

^a Coefficient of variation (CV%) ≥ 50 ; in 2-methylnaphthalene samples.

Table A4: Proteins identified on Blue native PAGE gel slices with a size of about 400 kDa which were shown to be differentially induced in naphthalene-grown N47 cells (Naph) in comparison to 2-methylnaphthalene-grown cells (2MN). The Blue native PAGE was run under anoxic conditions using frozen N47 cells. The proteins with a p-value ≤ 0.01 and an enrichment factor ≥ 2 are shown below. The proteins shown in bold letters correspond to the ones which are encoded in the naphthalene carboxylase gene cluster. C. score, confidence score; peptides used for quant., peptides used for quantification.

UniProtKB entry name	Peptides used for quant.	C. score	Anova (p)	Description	Annotated function	Ratio Naph/2MN
E1YIW6_9DEL	52	3201	0.000003	N47_K27500	UbiD family decarboxylase	29.0
E1YIW4_9DEL	47	2736	0.000000	N47_K27480	UbiD family decarboxylase	25.7
E1YFV9_9DEL	26	1074	0.000176	N47_J04340	Heterodisulfide reductase	2.0
E1YIW8_9DEL	11	468	0.000000	N47_K27520	MRP; Fer4_NifH superfamily	15.9

UniProtKB entry name	Peptides used for quant.	C. score	Anova (p)	Description	Annotated function	Ratio Naph/2MN
E1YM45_9DELTA	7	370	0.001922	N47_E46900	K(+)-insensitive pyrophosphate-energized proton pump	5.7
E1YHR5_9DELTA	8	329	0.000087	N47_D29930	Protein-export membrane protein SecD	2.9
E1Y9M0_9DELTA	7	323	0.000596	N47_I06840	2-naphthoate-CoA-ligase	7.6
E1Y9S2_9DELTA	3	231	0.001834	N47_H21380 / N47_B20630	Probable aromatic acid decarboxylase, UbiX, Flavoprotein	5.2 ^b
E1YFW0_9DELTA	4	180	0.001097	N47_J04350	Heterodisulfide reductase	2.5
E1YIW7_9DELTA	4	166	0.000001	N47_K27510	ParA/MinD ATPase like, MRP; Fer4_NifH superfamily Unknown function (transmembran domain, signal peptide)	13.4
E1Y8M1_9DELTA	4	157	0.006159	N47_A09440	Protein-export membrane protein SecF	3.4
E1YHR4_9DELTA	3	135	0.009904	N47_D29920	Putative Lipoprotein (signal peptide)	7.7
E1Y8H6_9DELTA	3	127	0.010405	N47_A08990	General secretion pathway protein G	3.2
E1YBH2_9DELTA	1	52	0.006033	N47_G32400		5.3
E1YLQ7_9DELTA	1	37	0.000403	N47_E45520	Glycine cleavage H-protein	4.6
E1YIW5_9DELTA	1	34	0.000011	N47_K27490	Conserved hypothetical protein	25.2
E1YCI0_9DELTA	1	31	0.001641	N47_G35980	Hydrogenase subunit	4.2

^b Coefficient of variation (CV%) \geq 50; in naphthalene samples.

LC-MS/MS run was performed using buffers with DMSO.

Table A5: Proteins identified on Blue native PAGE gel slices from NaphS2 cells grown with naphthalene (Naph) and 2-methylnaphthalene (2MN). A confidence score (C. score) $>$ 30 was required for a protein to be considered as identified. The proteins shown in bold letters, correspond to the ones which are encoded in the naphthalene carboxylase gene cluster. **A.** BNP gel slice with a size of about 750 kDa; **B.** BNP gel slice with a size of about 400-440 kDa. Peptides used for quant., peptides used for quantification.

A.

Peptides used for quant.	C. score	Description NaphS2	Corresponding match in N47	Annotated function	Ratio Naph/2MN
56	4094	NPH_7198		Chaperonin GroL	3.0
23	1416	NPH_5861	N47_K27480	3-octaprenyl-4-hydroxybenzoate carboxylase	1.7
22	1274	NPH_5859	N47_K27500	3-octaprenyl-4-hydroxybenzoate carboxylase	2.2
28	1272	NPH_2828		Glutamate synthase (NADPH) small chain	2.6
14	797	NPH_2300		Cytochrome c Hsc	5.2
13	595	NPH_1561		ATP synthase F1, alpha subunit	1.3
8	494	NPH_1563		ATP synthase F1, beta subunit	1.3
10	375	NPH_5644		DNA-directed RNA polymerase, beta subunit	2.2
8	352	NPH_1886		V-type ATP synthase beta chain	1.0

Peptides used for quant.	C. score	Description NaphS2	Corresponding match in N47	Annotated function	Ratio Naph/2MN
5	223	NPH_3399		ATP-dependent protease La	1.1
4	143	NPH_2223		Carbon monoxide dehydrogenase/acetyl CoA	3.3
3	114	NPH_6203		Chain length determinant protein	3.3
3	112	NPH_2827		Aldehyde oxidase and xanthine dehydrogenase	3.7
2	90	NPH_5856	N47_K27530	Putative phenylphosphate carboxylase, gamma subunit	1.6^b
1	65	NPH_1562		ATP synthase F1, gamma subunit	1.7
1	59	NPH_5855	N47_K27540	Putative phenylphosphate carboxylase, alpha subunit	0.9
1	56	NPH_2826		Carbon monoxide dehydrogenase small chain	4.7
1	40	NPH_4833		TrkA-N domain protein	3.5

^b Coefficient of variation (CV%) ≥ 50 ; in naphthalene samples.

B.

Peptides used for quant.	C. score	Description NaphS2	Corresponding match in N47	Annotated function	Ratio Naph/2MN
18	5040	NPH_5476 NPH_5957		NADH oxidase	1.7
47	4305	NPH_5855	N47_K27540	Putative phenylphosphate carboxylase, alpha subunit	1.9
45	3215	NPH_4912		Uncharacterized protein	1.7
42	3142	NPH_5859	N47_K27500	3-octaprenyl-4-hydroxybenzoate carboxylase	1.0
39	2615	NPH_5861	N47_K27480	3-octaprenyl-4-hydroxybenzoate carboxylase	1.0
31	2070	NPH_4205	N47_G39340 N47_E43490	4Fe-4S binding domain protein	0.8
30	2017	NPH_2223		CO dehydrogenase/CO-methylating acetyl-CoA synthase complex	3.3
23	1876	NPH_5475 NPH_1621 NPH_2988		NADH oxidase	1.1
28	1762	NPH_1634		Related to alpha-subunit of acetone carboxylase	1.3
27	1576	NPH_2689		Carbon-monoxide dehydrogenase	1.3
22	1551	NPH_6237		Phosphate butyryltransferase	1.0
23	1403	NPH_1631		Related to beta-subunit of acetone carboxylase	1.0
16	1207	NPH_2657		Conserved hypothetical protein	1.0
18	1131	NPH_3005		Electron transport complex subunit G	1.1
17	1051	NPH_2224		Carbon-monoxide dehydrogenase, catalytic	1.0
17	979	NPH_1633 NPH_6293		Hydantoinase/oxoprolinase	2.4
17	979	NPH_3552		Oxidoreductase NAD-binding domain protein	1.1
15	944	NPH_6289	N47_G39340 N47_E43490	Heterodisulfide reductase	1.4
13	926	NPH_5856	N47_K27530	Putative phenylphosphate carboxylase, gamma subunit	2.1
10	845	NPH_3401		ATP-dependent Clp protease proteolytic subunit	2.9
13	844	NPH_2222		Acetyl-CoA decarbonylase/synthase complex	1.5
14	834	NPH_2656		Methyl-viologen-reducing hydrogenase, delta subunit	1.0
14	805	NPH_1638		Uncharacterized protein	1.5
11	723	NPH_1692		Alkyl hydroperoxide reductase subunit C	4.0

Peptides used for quant.	C. score	Description NaphS2	Corresponding match in N47	Annotated function	Ratio Naph/2MN
13	682	NPH_7178		Molybdopterin oxidoreductase, molybdopterin	1.1
9	629	NPH_0950		Hypothetical protein	1.0
10	595	NPH_1821		4Fe-4S binding domain protein	1.3
9	572	NPH_5978		Adenylosuccinate lyase	1.1
11	564	NPH_3996		Molybdopterin oxidoreductase	1.7
10	506	NPH_5569		Formate dehydrogenase alpha chain	1.3
9	463	NPH_2560		Corrinoid/iron-sulfur protein, small subunit	1.5
8	454	NPH_2690		Iron-sulfur cluster-binding protein	1.2
9	450	NPH_5480		DNA gyrase, A subunit	1.5
9	442	NPH_5477	N47_I06840	Phenylacetate-CoA ligase	2.8
9	434	NPH_4520		Delta-aminolevulinic acid dehydratase	1.1
7	419	NPH_3151		Pyrophosphate-energized proton pump	1.9
6	414	NPH_5857	N47_K27520	ParA type ATPase	2.4
8	412	NPH_2691		Nitrite reductase	1.6
7	409	NPH_6696		Acyl-CoA dehydrogenase	1.1
7	399	NPH_6970		3-methyl-2-oxobutanoate hydroxymethyltransferase	1.0
6	396	NPH_1875		5-oxoprolinase, putative	1.8
9	364	NPH_4724		Translation elongation factor G	1.5
7	364	NPH_3842		Phenylalanyl-tRNA synthetase, beta subunit	1.3
6	333	NPH_6822		Glutamate dehydrogenase	1.1
6	311	NPH_7070		Formate--tetrahydrofolate ligase	1.0
5	295	NPH_2877		Electron transfer flavoprotein FAD-binding domain protein	1.4
6	294	NPH_6370		Related to beta-subunit of acetone carboxylase	2.0
5	287	NPH_4572		Citrate synthase I	2.9
6	277	NPH_1874		Hydantoinase/oxoprolinase	1.9
4	271	NPH_5231		ATPase, AAA family	1.4
5	268	NPH_3917		Arylsulfatase	2.7
5	264	NPH_5865	N47_J00960	Putative Phenolic acid decarboxylase subunit B, UbiX	5.6
5	259	NPH_4798		Chaperone protein DnaK	1.2
5	257	NPH_1693		Uncharacterized protein	4.0
2	239	NPH_1558		ATP synthase B/B' CF(0)	1.8
4	230	NPH_3997		Hdr-like menaquinol oxidoreductase iron-sulfur, subunit 1	1.3
4	230	NPH_4095		Cysteine-rich domain protein	1.0
5	226	NPH_2292		Aldehyde oxidase and xanthine dehydrogenase	7.3
4	223	NPH_1820		CoB--CoM heterodisulfide reductase	1.4
5	223	NPH_6221		Hydantoinase/oxoprolinase	1.7
4	197	NPH_6299		Glutamate synthase (NADPH) small chain	1.1
3	196	NPH_2998		Inosine-5'-monophosphate dehydrogenase	1.0
4	190	NPH_1613		Hypothetical protein	3.2
4	187	NPH_5825		Glucose-1-phosphate adenylyltransferase	9.0
4	183	NPH_6563 NPH_0260		Toxin-antitoxin system, toxin component, PIN family	1.1
4	178	NPH_5423		Cysteine-rich domain protein	1.5
3	177	NPH_6762		Conserved hypothetical protein	3.2

Peptides used for quant.	C. score	Description NaphS2	Corresponding match in N47	Annotated function	Ratio Naph/2MN
4	169	NPH_5424		Uncharacterized protein	1.5
4	166	NPH_3340		Putative mechanosensitive channel protein	1.2
3	164	NPH_6672		Hypothetical protein	1.2
3	163	NPH_1115		Undecaprenyl-phosphate 4-deoxy-4-formamido-L-arabinose transferase	1.0
3	157	NPH_3826		Helicase, Snf2 family	6.4
3	149	NPH_5570		Formate dehydrogenase alpha chain	1.6
2	144	NPH_5320		Putative Nitric oxide reductase	4.7
3	142	NPH_5230		Conserved hypothetical protein	2.0
3	141	NPH_3006		Electron transport complex subunit E	1.1
2	131	NPH_4847		Pyrraline-5-carboxylate reductase	1.7
3	128	NPH_3995		Conserved hypothetical protein	1.5
3	127	NPH_5576		F420-non-reducing hydrogenase iron-sulfur subunit D family protein	1.4
2	114	NPH_2628		Conserved hypothetical protein	1.5
2	113	NPH_0973		Iron-sulfur cluster-binding protein	1.4
3	112	NPH_2876		Electron transfer flavoprotein beta-subunit	1.3
3	111	NPH_1116		Bifunctional UDP-glucuronic acid decarboxylase, UDP-4-amino-4-deoxy-L-arabinose formyltransferase	3.2
2	108	NPH_6194		Putative xanthine dehydrogenase accessory factor	1.3
3	101	NPH_1573		Long-chain fatty-acid-CoA ligase	2.0
2	100	NPH_2174		Conserved protein	1.2
2	99	NPH_6290		Methyl-viologen-reducing hydrogenase, delta subunit	1.1
2	99	NPH_5858	N47_K27510	ParA family protein	4.4
2	91	NPH_5579		Uncharacterized protein	1.5
2	90	NPH_7006		Bacterial group 1 Ig-like protein	1.0
2	84	NPH_3228		Elongation factor Tu	1.5
2	80	NPH_2826		Carbon monoxide dehydrogenase small chain	1.6
1	80	NPH_6398		Radical SAM domain protein	4.6
2	79	NPH_3423		Tetratricopeptide repeat domain protein	1.3
1	76	NPH_5512		Putative small-conductance mechanosensitive channel	1.2
2	70	NPH_3107		Hypothetical protein	5.8
2	68	NPH_3013		ABC-type multidrug/protein/lipid transporter	1.7
2	67	NPH_4090		Conserved hypothetical protein	1.3
1	63	NPH_4203		Uncharacterized protein	1.5
1	60	NPH_6213		SufB/sufD domain protein	1.6
1	59	NPH_2503		Electron transfer flavoprotein	1.1
1	55	NPH_0385		Conserved hypothetical protein	2.0
1	54	NPH_1716		Ribonuclease, Rne/Rng family	1.0
1	53	NPH_2290		FAD binding domain in molybdopterin dehydrogenase	9.4
1	49	NPH_3002		Cytochrome c family protein	1.3
1	43	NPH_0948		Hypothetical protein	1.5
1	42	NPH_6862		Adenylate and Guanylate cyclase catalytic	1.1

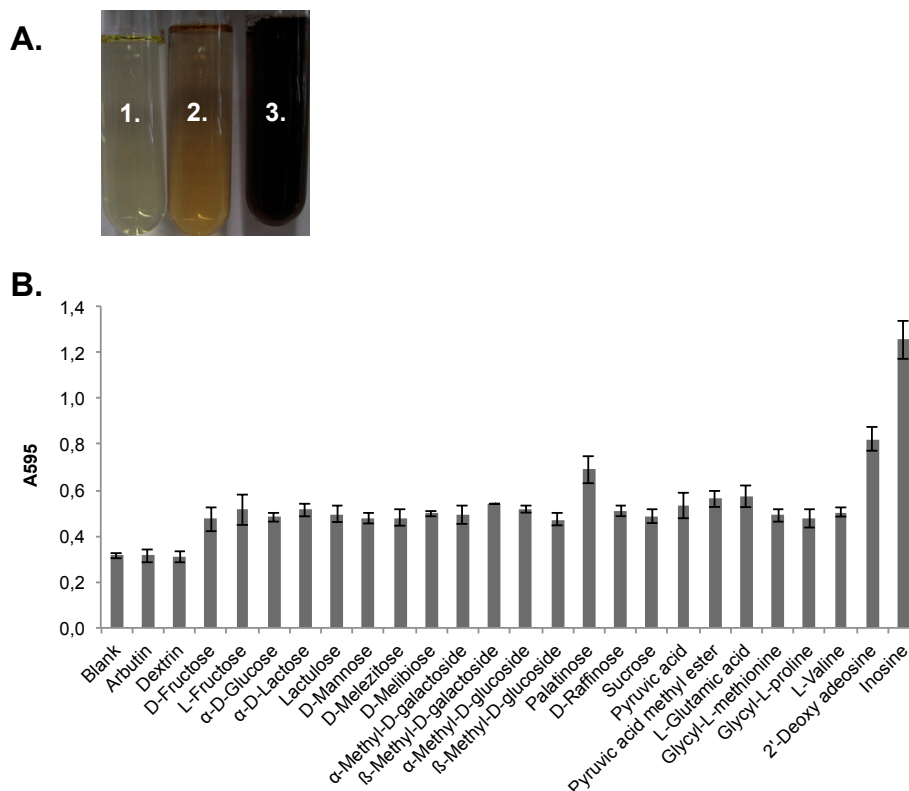


Figure A6: Substrate utilization test using BIOLOG AN MicroPlate™. **A.** Pretests with the modified medium used for BIOLOG AN MicroPlate™. 1., medium with tetrazolium salt and 0.1% yeast extract but without cells and carbon source; 2., medium with tetrazolium salt, 0.1% yeast extract and 5 mM glucose but without cells; 3., medium with tetrazolium salt, 0.1% yeast extract and 5 mM glucose inoculated with *Cand. T. contaminophilus* sp. strain HM^T after 1 week of incubation at 30°C. **B.** Analysis of the BIOLOG AN MicroPlate™ inoculated with *Cand. T. contaminophilus* sp. strain HM^T incubated at 30°C. The experiment was done in triplicates.

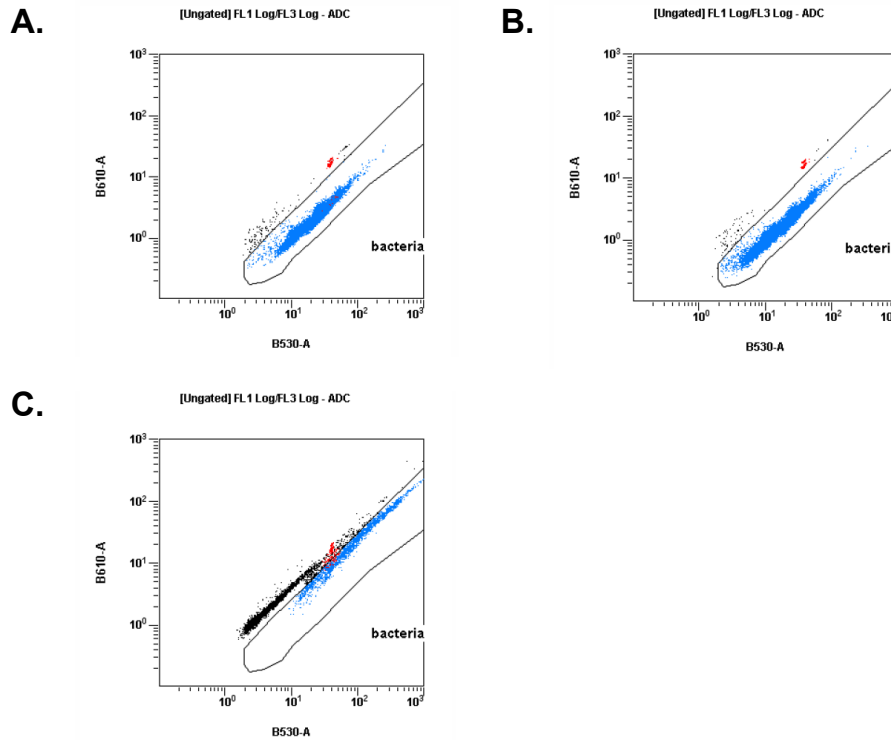


Figure A7: Flow cytometry using freshly harvested and non-fixed (A.), stored (2 days at 4 °C) and non-fixed (B.) and glutaraldehyde (2.5%) fixed N47 cells. Red, control beats; blue, individual N47 cells, which were counted; black, particles in the medium (no cells).

Table A8: UbiD-like proteins used to construct the phylogenetic tree Fig. 56.

UniProtKB entry name	Protein name	Annotated function	Organism
E1YIX0_9DELTA	N47_K27540	Putative uncharacterized protein	Uncultured Desulfobacterium sp. N47
E1YIW6_9DELTA	N47_K27500	Putative uncharacterized protein	Uncultured Desulfobacterium sp. N47
E1YIW4_9DELTA	N47_K27480	Putative uncharacterized protein	Uncultured Desulfobacterium sp. N47
E1YIW2_9DELTA	N47_K27460	Putative uncharacterized protein	Uncultured Desulfobacterium sp. N47
D8F9D7_9DELTA	NPH_5855	Putative phenylphosphate carboxylase, alpha subunit	Delta proteobacterium NaphS2
D8F9E1_9DELTA	NPH_5859	3-octaprenyl-4-hydroxybenzoate carboxylase	Delta proteobacterium NaphS2
D8F9E3_9DELTA	NPH_5861	3-octaprenyl-4-hydroxybenzoate carboxylase	Delta proteobacterium NaphS2
D8F9E5_9DELTA	NPH_5863	UbiD family decarboxylase	Delta proteobacterium NaphS2
D8WWP8_9FIRM	AbcA	Putative anaerobic benzene carboxylase AbcA	Clostridia bacterium enrichment culture clone BF
D3RZ65_FERPA	Ferp_1630	UbiD family decarboxylase	<i>Ferroglobus placidus</i> (strain DSM 10642 / AEDI112DO)
Q5P480_AROAE	PpcA	Alpha subunit of phenylphosphate carboxylase	<i>Aromatoleum aromaticum</i> (strain EbN1)
Q5P478_AROAE	PpcB	Beta subunit of phenylphosphate carboxylase	<i>Aromatoleum aromaticum</i> (strain EbN1)
Q5P482_AROAE	PpcX	Probable UbiD-like carboxylase subunit encoded in anaerobic phenol operon	<i>Aromatoleum aromaticum</i> (strain EbN1)
Q9F2B4_THAAR	PpcA, ORF6	Alpha subunit of phenylphosphate	<i>Thauera aromatica</i>

UniProtKB entry name	Protein name	Annotated function	Organism
Q9F2B6_THAAR	PpcB, ORF4	carboxylase Beta subunit of phenylphosphate carboxylase	<i>Thauera aromatica</i>
Q9F2B3_THAAR	PpcX, ORF7	3-octaprenyl-4-hydroxybenzoate carboxylase	<i>Thauera aromatica</i>
UBID_ECOLI	UbiD	3-octaprenyl-4-hydroxybenzoate carboxylase	<i>Escherichia coli</i> (strain K12)
BSDC_BACSU	BsdC	Phenolic acid decarboxylase subunit C	<i>Bacillus subtilis</i> (strain 168)
Q9S4M7_SEDHY	ShdC	4-hydroxybenzoate decarboxylase subunit C	<i>Sedimentibacter hydroxybenzoicus</i> (<i>Clostridium hydroxybenzoicum</i>)
Q462H3_KLEPN	KpdC	4-hydroxybenzoate decarboxylase subunit C	<i>Klebsiella pneumoniae</i>
Q8ZMG0_SALTY	StdC	Putative 3-polyprenyl-4-hydroxybenzoate decarboxylase	<i>Salmonella typhimurium</i> (strain LT2 / SGSC1412 / ATCC 700720)
VDCC_STRD7	VdcC	Protein VdcC	<i>Streptomyces</i> sp. (strain D7)
	WP_028893368	3-octaprenyl-4-hydroxybenzoate carboxylase	<i>Syntrophorhabdus aromaticivorans</i>
	WP_028895343	Alpha subunit of phenylphosphate carboxylase	<i>Syntrophorhabdus aromaticivorans</i>

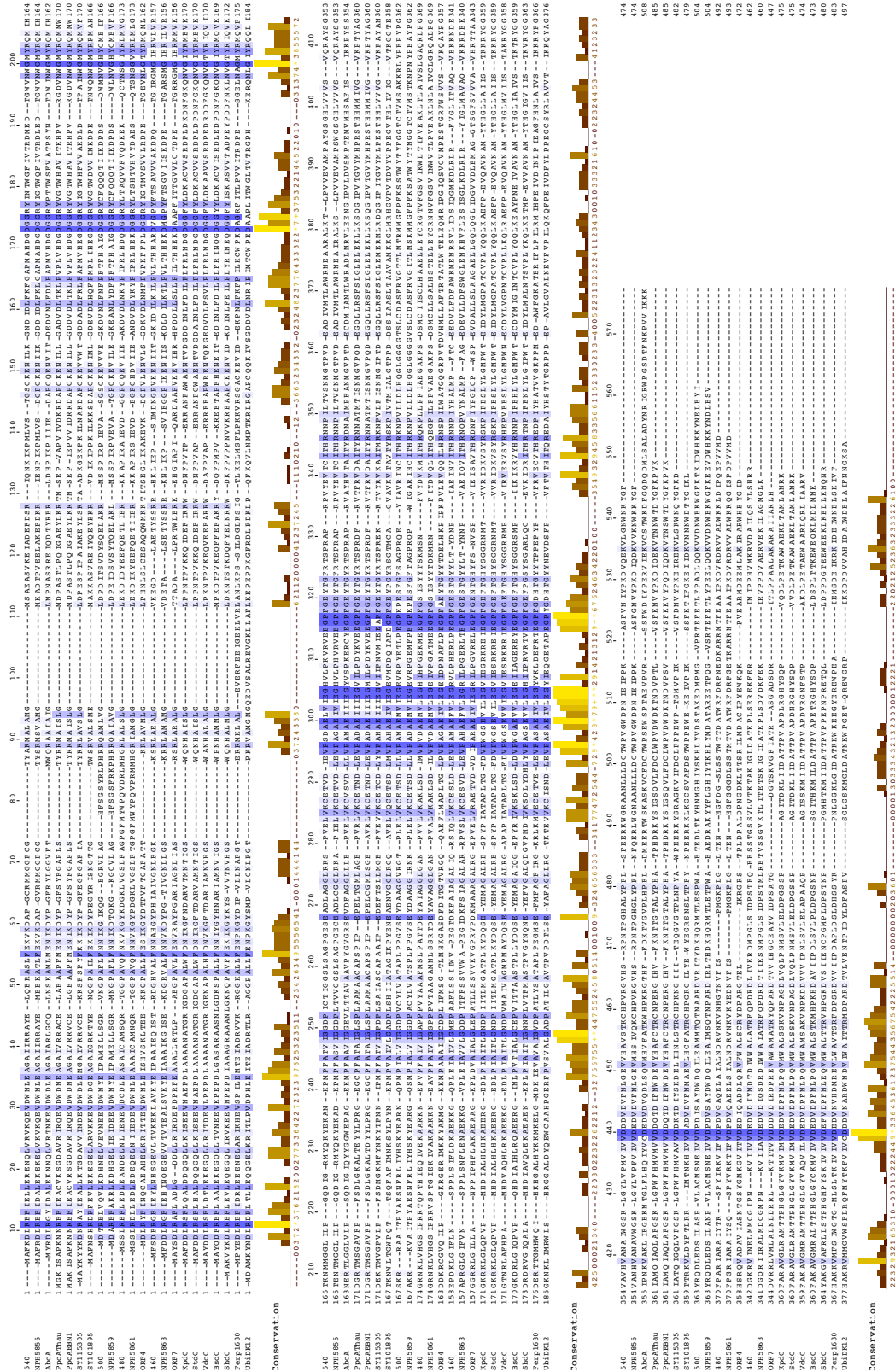


Figure A9: Sequence alignment of UbiD-like proteins. For accession numbers, see table A8. The shade of the blue color indicates the degree of conservation. The alignment was constructed using the Jalview software (<http://www.jalview.org/>).

tgaaattgaaatctcatagagaatgaggtggattgtgatttggagccagcgctatctgtgccaatgtcgcaaggacgggtggaccggctgtccag
ttaaacaaggtaaaaggataaaggacggaaaactggctggcagctcttggcggctcctgggtttatgtattggccgaggtggatcgtctga
tgcacggcgctcgcgctctctggggctcgagaaggacatagattatgaggaattccaggagacactcagcagcggaacaaaggccccat
cagagccattgaagtggatggcggctcctctgcaggaagtgatcatcgaggccaaagatgtggaccttaataaatacctatccccaggctacat
gatcaggatggcggcaggtatctcaccgcccaggtcgttttggccaagcaaggaaaaacagtgccaacattccgggtatttacagattgatgg
tggggggaaggaataagcttgcaccggctccataccacgcccactcaacccacgcataatgaacagatagtgaggaaagggcccgtaaaaa
tgaaccggtcccccttggcattgtcatttggcgctccaccaccccttaccctttagcggcggttttatgagtttgcggctgacaaacagcaatagcc
atcggggtggactggggccaaacctgttgtgctggcaggccaaattgagcgatcatcaggttctctgtagatgggaaaatgggtgctcgaag
gcatatccatccgggggagaaaatggaggaaggtccttccggatcgatccttattacacgccaagatgagcaattttgtctatgatgttaa
gatgattaccatcggaacacggctccttccctttatggcggggcgccaaacggatgacagcatgtgtattatcctgctcgtcagtg
gcgaattgctgggaattgtctcggcggcactgttccgggtcggatcataaaatggattgacgatcccggtggcgaattgcaacttggcagct
ttctttggggcgcaacgtttccgggcttcccgcgcatcgccaggcgattatacccgtagtctctataccgcaaagtaatttctg
ggatcctgacgttgggctcaagaactggcgatcgcgttgaatgacagatgaaataaagtgaatcatggaaccaatgtttcctatccccatg
ggcaaacactggcctgacggaataacaggttggatggtagctgtcaccacatggacgactgacgcaacttggaggttggacagacca
atgaaacgcaaaaggagaacttgaagcggcttgaagcggcttgaagcggcttagagatcctcaagcgttagagatcgtgtggttggcattcc
cgaggaaccagtggttatggactgaagaagcgtcatggaggaatacaatagaaaacttatacagattttgttccctatgagaaaaaggaa
gatgcatttaataccttaaggagatgagatgctgagtaaaactctcaggatgaggaacaggggaacagtttaaggctaagataaagat
ctgatagccccgggaagatgctgatattacatattcagttgagatccgggttatattggcgagggatggatgttcagatattacaagaga
agaagatgaggagagatgcttttgaatcgaagattggagcggatgaaagaggaacatattgctacgttccatgaggttggcagtaact
gaagatgcagagaaaaacgggtaatggaagaagcgtgaaacagcggcttcaatggaagaaaaagattgttaagaagatttctggaagattaa
gacgggggaagggcgtcattttagtgattttcggcgctttagcaatacctcaatcattcaggcgaagtattgacagtaaggaaaagcctg
tgaataaacgaaattccggcggaatcgaacaaatccacacgggacggctcagtcgctctttcaacaatgcccacggatctcctcat
gctatttggcgaaccttgggaaaaagagcaggttggcagcgttaggttgggtttaaagaagggatctgggaaacacatcagctcgt
ggcacaaccttattgaaccatcatcagataacggcgcggttaaggaaaatcctcaccgggaagatcgatattggaagatcttgcctgt
ttgacgcatcagccgggatgttggccttatttacaacagcggtagttgtggcgaagatccccagaccggatcagggtatgggtatc
cacagatttcttgcggagcctgacaactggggattttctaaactcggcgcctcttcaattttctggcaaggcggaaaaagaaaggcc
aacctatagaatagccttgggcaaaagagcaggttggcagcctccttctcaataatctgggttccggaaaggaacataaattgctat
tgcggcgctttgatacagcgttccatccagcgtggtgaaatgcgaatcttggatctggaagttcctgcgaatgcgaatttgttttagaggc
agagtattacctatgaacgattaccgaagggcatttggcgaatccacgggctactacctcactatgataatcctatggcgagattatg
ttattactcaccgcaacaacctatatacatgctttagcctttactctgcgaagaagatgtgctctcagatttggatggaagatgaaa
caggagcgtttttagatgattcaatccaggcattgaagattacgctctcgttttgggttggattaccggtggaagtaaaaaaa
gacgaagcggaaaaagatttcaacgaactgatgtgctgcacatccgaataaagtaatttgcgtagacgaggttggacatttaca
atgataccgatatctggtgggctttggccacacgcttccagccggaccgtgatttgatcgtgaaagagatgcccaggccttccattgacc
atcgacagagcaggagagattccaccgggagctcagttctcgttacaagaacggcagaataggcttggatggaccacagccttggatgaa
cgggaaaaatttggacggatataatctcccacgctgatgaagcgggtggatggcctatttgcagctcttatttgaagcctcggagatgggaa
aggtgtagagcctttgaaatgatacagattttaggtttagctgtcatttggacttggacggtacgctcatagattccataggtgctatt
ttgggctgggtggaagaagttgttgcacttgcctttagatccctcccatgaggtaatttggaggtcggcagaagtgagatttgcataa
gatattcgggaggaataatcggcggaaggttaggttaatagatcaacgggtgacgataatcagggaacattccacagatctcaggtat
aatctgcctgttctcggcggcccaactctcgaacgctcactgcccaggatgaaataggcaattgtaacctgacaccatcggcagat
ttattgacggtaaatagccttaagaagggcgtgctgacgctgattgcatcogtgatttgcacgaaatggtgaggtcaggtttaaagcc
tgacctgatccgctgctcgaatgcccggctcagacttggcgtgacagcggcaggagcgtatatacggcgattctacatgcacataaaagca
ggcaaacggcagggatgaaacgggtggcgttataccgggttggacagtttagagatgaaaggagaaacactgatcgtgctgggca
gtgcagggaatcaacggacagataatacaagacagggcaaggtgacaggcggcgttggcctatggcggatagcaacagatgctgattaca
agaaacgggataatcagggttattcctggacatagcggaaactttatagattcccttcccaatccatgaatccttcaatcggcgttggg
ggaattcggcctgtcctcggcgcccagagattattatcgaatgctcgggagtgggcattgggttggcgggataattgcgcccggtaacttcc
agcaaacctggagatagtttgcgataagatagcgaatggatactggcggaattcgtgaaagtggaatggatgttctcttgttggccgggg
tggtagagcgttgaatttttaaaggcggagggggcagataggcttggcaacgggaaagggcaagcggcggtgctatgaaatgggaaagact
cgagcgttagcagcgttctcagatttatttcaacggcgggtggaggtggcgaacccgaaacccggctgatcgtgattgctcagatgc
gcccggggaatggctgttgcctcgggatgtatagctgtggcgataccgtggcggaatatttgcggcagagcggccggagcaattccga
tagcctgatgacggggtagatggcgtgagaagctgaaacaggggttgcggcggggtttagaccggctgagcagataatggccttgtt
ccaaagcaacgggtcagtaggagggcgtgacagaagaagttgctaaacctgcttttgcatttgggttttcttctcgtggg
atggatggctatctgggtggcggcttaccggctcagcactaatgcaatcgaataatgctgggaacagggggcgtcgttagcattgggggg
gtggatcggcattgcccacgatacctccggcattgtagcaatcccggcattaccagataaaaggaggcggagtcgattcggcaacg
gtctattttccatgggtgagattgaaaacaggaataatcgtttgacagttccgacatggtcgtgactatgagcgtttttcttctact
tccgagtgggatgggtaaaacaccttctcagagccctttagctgggggtcggatatttgcgtaggaggggagggcaggggttcaa
ttgaaaaaacagtttctcggagggcaaaagtagagctcaaaactgccttatacaatttactcctactgttgcctatacaaacgccc
tgcttccggcaggtcttgccttataatattatctccctctgaagcttaaaggactcttggcctgtttatctgggtgttgataaagccga
tgcttggggggaggatagcgtgggagtagttatcaacctaccgaaggtgaaatggggatggcctatacctcgaatcgatgctcga
gactacgaacagacaaggataatacagatagcgggacagcaatcagcggcgcctgccaaggtgttgacttacagttgcccgaagaa
tccgctcgggacagttaccaggttactcctaaacttggcgggtttgacgctgaaatggcaggattactccatgcttgcgttaagatcgt
cgtagaatggaggggttccccatcccgccctgcaatctcgaatggaaagattcctaccacttggcgtcggggcagaataaagattactcct
gaggtaatttcaaaagctcgcattgaccgatatttttataaaaagcagttgaaataccaaataacatattgatttaataaagagaatgctc
tattatcttctaaattgcgcaattcaagaaggatgataatagcactccttggacatttgggaataccatacaaaagcaactttttccag
cattagaaaaatgaacttggcccaatttccgcaaggataaggaattcgaataaagattgtctctcgtggatttggaggcattgaaataaatt
caggtggcaggggtcggggcgtaaaagaaaagatcgcatagattgcaaaagccttgggtgcaaaagatggatcaagttgaccacacagat
actcttattgaaatctgaagaaatcgatgataccagacggctatcggtatgggaaaatgcatccaaataccatccaaggcaacttctoca
gggttcaaggatctgcggatagcaggttgcgcgaaatattcagagccatggtaaaagatattgtggtcaaaagcttgcgtgctacat
aagcgcgagctcagcggcattgaagcggcgtgaaacggcgtgaaagacgaaagaaagatgaagtaacccctggcccaaacgtaacgtgagc
ccagtaaaaggtgaagtctaccttccaaacggaaaaacgtgtggatctccaggccaccaggagttggaagacaatttaaatgatttggcga
ccactgtaacgtcggcaccaaaagaaacagcaagggctataaaggaaacctggatcggctataaacttcaacttgcattgatggggat
tccgataagggcattctcagcggcctcattgcatgattcaggttgcgatacctctgcaacagatgagttcaagcgggttgcacactt
tatgatttaagtagcggccttatgattcaccgcaaatctaatgaaatcagtaactcagggaacatagggcagatggttgataataacggagat
gtggggaaaaggttctgatggatcctgcaacaaaaatctcgttttggcgaagaacaggcggagccacaaaagtcattggccactctgatgtcgg
gataatcogatacagcattcagatatttccgattgcttcaatgacaagaacgaataagcttctgtttataataacgttttcaaaaacgat
cgggacggtattgtcaaaaactcggcatttattgcttgggttctcactgaaatcggagcccttaagtcgctctatggccggatttca
actgttgcctttaaacaagcgcctttaaactgcttgaatagctctccagccttacttaccggcaggtatgctatacaagcga
gtgtaacccggacagatggagatttctctacatccctctactacaggggattcccacaactctactgcccgttttggatatttgggagga
tttcttatcagatttggctgctcaccacctggatgtagaggaacaaacgggacaatccggatggggaagactacgaaaaatccacccctg

gggtttgagataaccttttctgataacctttacctggacctggccgggatgagactgacgttccatggagtttaaaggtggaatgtaaga^{aa}
^{ttgacgaggagaaaa}acatgaaaaagatcagggtaaaaatttccggcatgatccagaggaacagataagaacgggtggcaagagtttgc
 ggttgatgtggaagaaaagagcacgggtctggaggctctgatgaggattatgacacacaggattcttcccttagctttcaatcatggatgcaga
 gccggcaactgcccctttgtgacgataataaaatggacatccccgctatgctgaccagcaagataactgccaatgcagacatactcctc
 tccggcatctccctttaataaaaagatattggtcttcgacccggccgctttttccgtgaattggaaaagttaggccttatatagtaagaaaaa
 tgagccggaggcagagcctgagatattatgcaacccctggagcatgacccggtgatgagctgcccgtgaaatgtttgctgcttcttctctgc
 ctagatacgaactacagggataagctcttggggggccgctctgcttttctcaagcttgcccagcttcaactatgatgctccgtgattccctggatc
 gggtttcccagctctcgcgagttgggaattcttaattgtgcccactgcccgggttggcctgtatctccggcatccctattaaaagaattgttat
 cggccctttttggcattgcttgggaaacattaa^{taatttataaaggagcagcacaatggtggaatgagttgcgatgttttgtgtatcggggg}
 aggaggcgcggggttacccgcccagataacggccagcgaagggcaccgatgtcattctgctttccaaggaccatcggctacggcaacacc
 aggattatcggcggatcatgcccagggcaggttgtagacagacaggaagggagaaaaattttccgggacatggtcgtgggtggggttact
 tgaacaatcagaagctatgcccgtatggcccaggaggcctataatgcccgatcctgctggaacgttttggcggatggtaaaaagggacgg
 caagggataatttcccggaaatgctgctccaagtgggggacatacctctcccgcagcctgattctccctcagccggccgggggtggga
 caggggttgtgctacggggtggcccggaggaaaaaacattagaacctagaaaaaacatagtggtttgacctcttaaggaaggggggaaagt
 tggggcagctctgctatgacatcaccctcgggaaattatgttgcctcaagctcggcaaaagacaatttttagccaccggcctgaaatggtt
 ttatcctcacacagatacctcacgggttgcaccggcgatgggtttgcccctggccctgcatgcccggccaggctgatcgatattggagcagggt
 caatatactccttcacacttaaccatccttgggcatgtcggcattgttgcggggaacctttacagccgctcctcggggcgtatataaaaa
 acgtgaatggccgtgatactcccaggggtggcctcaagaccagggcgcaagtggcgaaatgctattatcctggaagttagaagggcaatgg
 acaaaaatcagcggctgtctgctggaatcttaaggcctaaagatcactcccaggggagcattctttatcctgcaatcagggaggggtctt
 aagccttttaccgacctgtcaggattgcttatggaaaggcagcggcggaaatgggaagaaacctgggacgtctatcccagggccattttttta
 tgggcccggattgtcataaatgaaatggtgcaagtgcaggggtgtgaaaacctctatgctgcccggagacagcagggcggcatcccaggggaaa
 ccgcttgggatcgggtggcagatgacagaattgtttgttttggtaaacggcggggtgaaaagggccggcagggacattagtacatgctgcccag
 cgagcagagtgactgattgacatggtgagaaatgagaaatgagaaactcaagcagggcttgagatttttctgctcatagaagaaaa
 agttgcaaaaaacctatgggaaaaggtaggccctgcccgggaagaagaaaaactcaagcagggcttgagatttttctgctcatagaagaaaa
 atttaaggatataaacctctcggggcgtgcaaatataactgaactgctcagatgcccctggaattgaggtttatggttgcgggttgaaggagt
 gtgactgtgagcgcctcgcaggaagaatcgcgggggacacatgttaggatagattatcccgaacgggatgacccggtcatggtgaaaaata
 tcgttggtaaaaaatgagaaaggaataatttggccgacacagggcagtagagttgttcttctcctgctgaaagcaatcttaagtagt
 taggtgttttacagaataactaataataaagaaggagtgaatatgggatatcgggatttaagggaactttctgcaaaaggctcaaacaggaaggtga
 acttatcgaattgaggaggaattggaccocaaatataagatgacggcaatattggaaaaattaggcaagcaggaatcggccgctgactctt
 aaaaacgttaagggttataatattcctgctcgcgggaaatttgcgggaagcaggaagcggctggctttaatacttgaacaacagtggaaggtc
 tgcaacaggagtagaagagaaagctcgcggaattctcccactggtatcccagctcgggtaaaagacatagtagtccgggacaat
 agacattatgctgcttttctgctttaaacaaccatgaactggatgcccgtccttatattaccaggggctcgtattcatgagagacctgct
 tcaggaagagtaacggtaggagtcaccgggttacagggttaagggtaaaaatggctgtgtattcaactgtgagccgcactccacggaaat
 atagacatgcccgaagaaaaaacgaaccctggaagtatgctatttggagtgtatccggcctgtgtgctgacggctgttacttggttcc
 ttcggcgacaaaaatagaattggcaggaggattcgcgtggagctcctctggaactggtgaaaggggaaacagtagggctgagatcctcgcgat
 gcgatgattgtgctggagaggaatccccccttttggcgggaaaccgatggaccttttggggaaagtccgggtattatacaaccgctccaga
 gccgggtggtggaatccaggccgtttgctgcaaaaaagatcccattatgctgtcttcaaacctggctctatcgaagatgatttaattctcaa
 ttttctcgggggagaggggttcaaaaaacttaagaacgatctcctgctcctgagggcttaaggtcaagttggaatgcttccacggcgatt
 atctccatcaagaaaaagaaacagggggagggcagaagggcagatttctgctgcttgatgaataatcttatcaagcagggcaattgtgtctg
 atgatgattggtatataataatcccagagaagtagaattggggcagtcgcaacgggttccagcctgacagggatttagtggttaatcccgaatgt
 agaagcaaaccccttgatcctctgtgagggatgggattatggctcacaatttgggtattgatgccacgaaacccctgggagaagaggataga
 ttcaaaaagattgggtgctcccgcctgttgcggaaagcaagcagaaagatctggaacgggtataatttataagcgggtgagcaaaaatagggt
 ccgggtctgataatacaacaattcttaaaaaataggctaaatggaagcagcgaatataaaaaaatcatttaaattatttggaaagccatc
 atactctcctcctggcaacgggttgggaaaggcttacggcagcgcactgcttttctatgtgaaatcgggcttgatctgtatttttaagcag
 cccgaccagccgcccagcattaatatgtctcactgtgcccaggtgtcggcaaccataaacgaagactatgcccagtgccgctcatcaagggg
 attcagctggagggcttggtaagacagtgagcggaaatctgggaaacggacggctggccatcgctttataaagaagtttctgagtggtgag
 atttttttcacccggaagctgggggaaaaaatttagcaaaagttgaaaggtgaaaaatattgaacttactcccaccagaatataatttcat
 caataatggaaattgggttggccatcgagaggaattgattctgcccattctcggccctgagtaaccccggcccagcagcattctcaacggat
 tttcggccaccagactgtgtcaca

Figure A10: DNA sequence of the naphthalene carboxylase gene cluster. Open reading frames are highlighted. The primers used for the operon mapping approach are indicated in red and a putative transcriptional start (*in silico* analysis) in blue. The first open reading frame marked in dark grey is not part of the naphthalene carboxylase gene cluster and encoded on the complementary DNA strand. The shown sequence was taken from the GenBank accession number FR695876 (53761 to 39601).

Table A11: Whole proteomic dataset for Tab. 29.

A.

Peptides used for quantitation	Confidence score	Anova (p)	Description	Normalized abundance 2MN				Normalized abundance Naph				Ratio Naphi/2MN		
				MOH6863A8 MA2_008-2MN_B1_2	MOH6863A9 MA2_009-2MN_B2_2	MOH6863A11 MA2_011-Naph_A1_2	MOH6863A12 MA2_012-Naph_A2_2	SD	CV%	SD	CV%			
51	2872	1,30E-03	N47_K27500	6350054	6102461	6226258	175074	3	92733612	77140168	84936890	11026230	13	13,6
43	2426	2,30E-03	N47_K27480	5695869	5164852	5430361	375485	7	83227230	66016470	74621850	12169845	16	13,7
36	2249	2,10E-03	N47_K27540	3251375	2660341	2955858	417924	14	26225345	26743421	26484383	366335	1	9,0
38	2153	4,88E-03	N47_N26400	1427307	1343608	1385457	59184	4	7277253	5902766	6590010	971909	15	4,8
21	1028	4,23E-03	N47_N26410	852741	864764	858753	8502	1	4465040	3650069	4057554	576271	14	4,7
17	783	3,31E-03	N47_N26280	1077065	1078431	1077748	966	0	4644349	3960481	4302415	483568	11	4,0
12	697	1,45E-04	N47_K27520	80424	77559	78992	2026	3	3748173	3444598	3596386	214660	6	45,5
17	694	3,37E-03	N47_K27510	110425	84800	97613	18119	19	2598882	2011119	2304901	415469	18	23,6
13	577	4,19E-03	N47_N26090	55532	51414	53473	2912	5	435237	340760	387999	66806	17	7,3
12	549	5,45E-03	N47_K27470	15276	9325	12301	4208	34	2438298	1391843	1915071	739955	39	155,7
9	526	1,66E-03	N47_H21310	324107	342199	333153	12794	4	710394	733493	721944	16333	2	2,2
10	468	7,66E-03	N47_N26300	166877	133771	150324	23410	16	536289	573046	554668	25991	5	3,7
8	392	8,10E-03	N47_H21290	268087	304668	286378	25867	9	821808	724180	772994	69034	9	2,7
8	349	2,45E-04	N47_N26380	332717	330501	331609	1567	0	1490549	1423782	1457165	47212	3	4,4
8	330	4,49E-03	N47_F15470	32432	44005	38219	8184	21	384050	419509	401780	25074	6	10,5
5	306	1,72E-03	N47_K27530	834999	763583	799291	50498	6	5751084	6647143	6199113	633609	10	7,8
4	169	1,72E-03	N47_F15620	52561	50794	51677	1250	2	170552	156002	163277	10289	6	3,2
3	124	7,89E-03	N47_E47810	23264	25764	24514	1768	7	77796	66114	71955	8260	11	2,9
3	121	3,87E-03	N47_P16800	19165	17671	18418	1056	6	41109	38985	40047	1501	4	2,2
2	118	2,80E-03	N47_N26270	318757	297123	307940	15297	5	1129288	1281428	1205358	107579	9	3,9
2	97	4,17E-03	N47_J04340	9751	10973	10362	865	8	29876	28078	28977	1271	4	2,8
2	75	1,99E-03	N47_K27600	681	640	661	29	4	47685	70800	59243	16344	28	89,6
1	60	9,39E-03	N47_J04330	9480	9752	9616	192	2	24065	20488	22277	2529	11	2,3
1	59	7,55E-03	N47_D32060	15695	14919	15307	549	4	56959	72852	64905	11239	17	4,2
1	49	7,53E-04	N47_G35300	908	886	897	16	2	2558	2432	2495	89	4	2,8
1	44	5,92E-03	N47_N26080	769	1170	969	284	29	28982	21822	25402	5063	20	26,2
1	42	2,77E-03	N47_G39260	2181	1914	2047	189	9	7261	7537	7399	195	3	3,6
1	33	9,49E-03	N47_G37580	9195	10513	9854	931	9	24087	21829	22958	1596	7	2,3
1	33	9,53E-03	N47_G37720	2013	2353	2183	241	11	11343	8785	10064	1809	18	4,6

B.

Peptides used for quantitation	Confidence score	Anova (p)	Description	Normalized abundance 2MN						Normalized abundance Naph						Ratio Naph/2MN
				MOH669 4A18MA 8_018-2MN_C1	MOH6694 A19MA8 019-2MN_C2	MOH6694 A20MA8 020-2MN_C3	MOH6694 A21MA8 021-2MN_C4	MOH6694 A22MA8 022-Naph_C4	MOH6694 A23MA8 023-Naph_C5	MOH6694 A24MA8 024-Naph_C6	σ	SD	CV%	σ	SD	
35	2162	1,72E-06	N47_K27540	2386011	2786931	2522240	2565061	203861	35605150	41342829	38158887	383668955	2874602	7	15,0	
6	376	1,73E-05	N47_K27530	612986	571526	561947	582153	27128	7151305	10333738	8202867	8562636	1621433	19	14,7	
18	950	1,50E-04	N47_K27500	395445	279769	371619	348944	61081	2568219	3814906	3044320	3142482	629114	20	9,0	
18	934	4,85E-06	N47_K27480	250787	297492	235991	261423	32100	2907502	2898278	3113547	2973109	121711	4	11,4	
2	63	4,48E-03	N47_C18070	100351	82669	70932	84651	14809	214898	156927	214655	195494	33400	17	2,3	
3	126	2,53E-05	N47_E46900	14334	16736	11584	14218	2578	184936	179483	212773	192397	17855	9	13,5	
5	272	2,80E-03	N47_G37900	20956	25760	24720	23812	2528	113897	60491	90499	88295	26771	30	3,7	
3	122	3,16E-03	N47_J04340	9783	6307	8017	8036	1738	30225	65999	68459	54894	21400	39	6,8	
2	73	1,47E-04	N47_J04350	3835	2945	2429	3069	711	47815	31389	37357	38854	8315	21	12,7	
3	184	7,98E-05	N47_J04330	2809	2041	2072	2307	435	38489	26297	27934	30907	6617	21	13,4	
2	80	3,21E-03	N47_J05030	4611	6157	3948	4905	1134	17004	11615	16146	14922	2896	19	3,0	
1	32	8,35E-05	N47_D29920	97	68	170	112	53	13702	10091	9948	11247	2127	19	100,9	
1	31	2,01E-04	N47_E51100	439	549	286	425	132	7545	6204	9274	7674	1539	20	18,1	
1	31	5,23E-05	N47_E42580	159	83	118	120	38	6289	6954	9557	7600	1727	23	63,4	
2	103	3,37E-03	N47_G39340	1052	466	310	609	391	7965	5531	4890	6129	1622	26	10,1	
1	32	2,79E-04	N47_A11570	1426	1939	1686	1683	257	6550	5382	5849	5927	588	10	3,5	
1	38	3,33E-03	N47_E42820	1475	1911	1150	1512	382	5481	3817	4553	4617	834	18	3,1	
1	34	1,90E-04	N47_G32220	351	270	193	271	79	5707	3795	4101	4535	1027	23	16,7	
1	30	2,34E-05	N47_G39370	827	726	720	758	60	4999	4049	4220	4423	507	11	5,8	
2	70	4,23E-04	N47_J04610	1913	1870	1701	1828	112	3406	4146	3784	3779	370	10	2,1	
1	47	4,72E-03	N47_G39330	667	459	230	452	219	4083	2320	3037	3147	887	28	7,0	
1	110	3,25E-03	N47_E43490	891	496	485	624	231	2945	2110	2311	2455	436	18	3,9	
1	34	3,32E-03	N47_H23870	594	420	307	440	145	3075	1618	2276	2323	729	31	5,3	

C.

Peptides used for quantitation	Confidence score	Anova (p)	Description	Normalized abundance 2MN				Normalized abundance Naph				Ratio Naph/2MN				
				MOH6694 A2MA8_02-02-2MN_A1	MOH6694 A3MA8_03-03-2MN_A2	MOH6694 A4MA8_04-04-2MN_A3	MOH6694 A6MA8_06-06-2MN_A4	MOH6694 A7MA8_07-07-2MN_A5	MOH6694 A8MA8_08-08-2MN_A6	MOH6694 A6MA8_06-06-2MN_A4	MOH6694 A7MA8_07-07-2MN_A5		MOH6694 A8MA8_08-08-2MN_A6	CV%	SD	CV%
37	2305	2,28E-05	N47_K27480	4110840	3980470	3755544	3948951	179733	5	64162364	90523750	60704597	71796904	16309817	23	18,2
35	2424	4,45E-04	N47_K27500	4070493	1730978	1604468	2468646	1388681	56	55266288	77397891	60411559	64358579	11581718	18	26,1
15	621	7,93E-03	N47_J04340	189226	85799	148883	141302	52128	37	470530	1014067	1188736	891111	374558	42	6,3
13	612	2,58E-03	N47_J04330	122913	95317	157802	125344	31313	25	431585	809894	756120	665866	204667	31	5,3
6	269	3,68E-03	N47_E46900	46345	61312	93238	66965	23953	36	239488	425096	312907	325830	93476	29	4,9
3	118	1,26E-03	N47_J04350	18700	12090	32794	21194	10575	50	276231	295785	195676	255897	53062	21	12,1
3	120	3,95E-03	N47_D29930	14259	13529	16737	14842	1682	11	53240	116358	148150	105916	48309	46	7,1
2	90	4,22E-03	N47_A11560	2628	2023	3716	2789	858	31	10234	19958	24038	18077	7092	39	6,5
3	123	9,12E-04	N47_K27520	335	838	723	632	263	42	9381	20001	14287	14556	5315	37	23,0

Table A12: Whole proteomic dataset for Tab. A3.

Peptides used for quantitation	Confidence score	Anova (p)	Description	Normalized abundance 2MN				Normalized abundance Naph				Ratio Naph/2MN				
				MOH669 MOH669 4A10MA 8_010-2MN_B1	MOH669 MOH669 4A11MA 8_011-2MN_B2	MOH669 MOH669 4A12MA 8_012-2MN_B3	MOH669 MOH669 A14MA8_014-Naph_B4	MOH669 MOH669 A15MA8_015-Naph_B5	MOH669 MOH669 A16MA8_016-Naph_B6	MOH669 MOH669 A14MA8_014-Naph_B4	MOH669 MOH669 A15MA8_015-Naph_B5		MOH669 MOH669 A16MA8_016-Naph_B6	CV%	SD	CV%
21	1181	8,40E-06	N47_K27480	364734	256417	345858	322336	57863	18	11695381	14556544	12474801	12908909	1479156	11	40,0
21	1091	6,99E-06	N47_K27500	438396	302060	344368	361608	69784	19	10473593	10561859	11368665	10801372	493268	5	29,9
13	675	7,48E-04	N47_K27540	118873	51870	122681	97808	39829	41	1242333	1854415	1679052	1591933	315204	20	16,3
1	81	6,15E-03	N47_K27530	36786	9208	16972	20989	14221	68	168919	372803	174953	238892	116010	49	11,4
3	129	6,54E-04	N47_K27470	211	36	413	220	189	86	164573	172498	159744	165605	6439	4	753,1
1	39	1,24E-02	N47_E46900	9740	7664	17755	11720	5329	45	32096	44523	67778	48132	18113	38	4,1
2	91	1,34E-02	N47_J05030	10476	6757	13181	10138	3225	32	30642	21266	37680	29863	8235	28	2,9
1	38	4,42E-04	N47_G33450	5056	3351	4853	4420	931	21	23276	30756	22301	25445	4626	18	5,8
3	121	5,54E-03	N47_G37900	6399	4569	7487	6152	1475	24	14178	17748	22789	18238	4327	24	3,0
3	129	1,54E-02	N47_H21220	6771	4603	8290	6555	1853	28	13352	20182	13663	15732	3857	25	2,4
1	35	7,11E-04	N47_K27520	799	575	957	777	192	25	14170	8107	20104	14127	5999	42	18,2

Peptides used for quantification	Confidence score	Anova (p)	Description	Normalized abundance 2MN				Normalized abundance Naph				Ratio Naph/2MN				
				MOH669 4A10MA 8_010-2MN_B1	MOH669 4A11MA 8_011-2MN_B2	MOH669 4A12MA 8_012-2MN_B3	MOH669 4A13MA 8_013-2MN_B4	MOH669 4A14MA 8_014-2MN_B5	MOH669 4A15MA 8_015-2MN_B6	MOH669 4A16MA 8_016-2MN_B7	MOH669 4A17MA 8_017-2MN_B8					
1	40	1,02E-03	N47_E51100	840	1064	899	934	116	12	6112	14015	7443	9190	4231	46	9,8
1	31	1,31E-02	N47_E42420	1928	2050	2849	2275	500	22	8108	4679	11352	8046	3337	41	3,5
1	35	1,71E-03	N47_G39370	1093	759	1359	1070	300	28	4426	4722	6787	5312	1286	24	5,0
1	60	7,36E-04	N47_E51090	479	422	696	532	144	27	4105	3315	5941	4454	1347	30	8,4
1	37	1,12E-03	N47_J03540	40	27	137	68	60	88	3088	2908	3659	3218	392	12	47,2

Table A13: Whole proteomic dataset for Tab. A4.

Peptides used for quantification	C. score	Anova (p)	Description	Normalized abundance 2MN				Normalized abundance Naph				Ratio Naph/2MN				
				MOH6651 A2MA3_0 02-2MN_1	MOH6651 A3MA3_0 03-2MN_2	MOH6651 A4MA3_0 04-2MN_3	MOH6651 A5MA3_0 05-2MN_4	MOH6651 A6MA3_0 06-2MN_5	MOH6651 A7MA3_0 07-2MN_6	MOH6651 A8MA3_0 08-2MN_7	MOH6651 A9MA3_0 09-2MN_8					
47	2736	4,39E-08	N47_K27480	3836235	2776929	2567227	2905204	3021399	560802	19	76960669	78176038	775668353	859396	1	25,7
52	3201	2,90E-06	N47_K27500	3095122	2894607	1479818	1563332	2258220	855214	38	69658690	61408445	66533567	5833804	9	29,0
26	1074	1,76E-04	N47_J04340	291986	300141	216665	248538	264332	39024	15	525769	534027	529898	5840	1	2,0
7	370	1,92E-03	N47_E46900 N47_H21380/	61506	35588	59105	60712	54228	12466	23	294086	328755	311420	24515	8	5,7
3	231	1,83E-03	N47_B20630	24336	19754	28960	17582	22658	5057	22	71763	162233	116998	63972	55	5,2
11	468	4,35E-07	N47_K27520	9800	6676	6292	6437	7301	1673	23	108423	123632	116027	10755	9	15,9
4	180	1,10E-03	N47_J04350	48576	32407	44378	57050	45603	10255	22	106269	122153	114211	11232	10	2,5
8	329	8,72E-05	N47_D29930	31488	21535	23792	27269	26021	4342	17	79693	73630	76661	4287	6	2,9
3	135	9,90E-03	N47_D29920	8366	9286	10958	5723	8584	2188	25	66971	64740	65856	1577	2	7,7
4	166	9,32E-07	N47_K27510	3749	4101	3558	4526	3983	426	11	50100	56361	53230	4427	8	13,4
7	323	5,96E-04	N47_I06840	3548	1930	1927	2451	2464	764	31	20475	17158	18817	2346	12	7,6
4	157	6,16E-03	N47_A09440	1773	1772	1504	1201	1563	272	17	5388	5165	5277	158	3	3,4
1	34	1,09E-05	N47_K27490	140	235	201	83	165	67	41	3971	4340	4155	261	6	25,2
1	37	4,03E-04	N47_E45520	798	706	736	554	698	104	15	2340	4017	3178	1186	37	4,6
1	31	1,64E-03	N47_G35980	815	774	602	409	650	185	28	1824	3573	2698	1237	46	4,2

Peptides used for quantitation	C. score	Anova (p)	Description	Normalized abundance 2MN			Normalized abundance Naph			Ratio Naph/2MN						
				MOH6651 A2MA3_0 02-2MN_1	MOH6651 A3MA3_0 03-2MN_2	MOH6651 A4MA3_0 04-2MN_3	MOH6651 A5MA3_0 05-2MN_4	MOH6651 A7MA3_0 07-Naph_5	MOH6651 A8MA3_008-Naph_6		Ratio 2MN/Naph					
3	127	1.04E-02	N47_A08990	737	815	927	638	779	122	16	2227	2764	2496	380	15	3.2
1	52	6.03E-03	N47_G32400	35	61	39	72	52	18	34	275	273	274	2	1	5.3

Table A14: Whole proteomic dataset for Tab. 30.

Peptides used for quantitation	Confidence score	Anova (p)	Description	Normalized abundance 2MN			Normalized abundance Naph			Ratio 2MN/Naph				
				MOH6863A1 MA2_014-2MN_B1_5	MOH6863A1 MA2_015-2MN_B2_5	MOH6863A1 MA2_017-8MA2_018-Naph_A1_5	MOH6863A1 MA2_017-8MA2_018-Naph_A2_5	MOH6863A1 MA2_017-8MA2_018-Naph_A1_5	MOH6863A1 MA2_017-8MA2_018-Naph_A2_5		Ratio 2MN/Naph			
49	3074	1,87E-03	N47_J03910	473415273	484264650	478839961	7671668	2	139022574	124609958	131816266	10191259	8	3.6
34	1928	6,13E-03	N47_J03840	6431054	7000558	6715806	402700	6	1859860	2200969	2030414	241201	12	3.3
28	1773	4,12E-03	N47_J03930	48691234	52237867	50464550	2507848	5	11259495	9281569	10270532	1398605	14	4.9
23	1334	2,65E-03	N47_J03920	14616173	16917342	15766758	1627172	10	2644968	2342246	2493607	214057	9	6.3
22	1184	5,07E-03	N47_K27660	11692734	11748203	11720468	39223	0	2288490	1779759	2034125	359728	18	5.8
17	1037	7,61E-03	N47_J05030	9378516	11044238	10211377	1177843	12	3578271	3233732	3406002	243626	7	3.0
12	745	1,30E-02	N47_I06830	8695596	10100926	9398261	993718	11	3278336	2628118	2953227	459774	16	3.2
9	448	5,79E-03	N47_J03950	1064712	1086664	1075688	15523	1	329789	271519	300654	41203	14	3.6
8	360	8,52E-03	N47_J03900	1023344	1050471	1036908	19182	2	432198	362066	397132	49590	12	2.6
6	357	9,83E-03	N47_N25720	882507	832722	857614	35203	4	410592	352897	381745	40797	11	2.2
7	331	1,09E-02	N47_J03870	542186	614060	578123	50823	9	156288	118351	137320	26825	20	4.2
5	297	1,43E-02	N47_J03970	319745	360539	340142	28846	8	83692	110714	97203	19108	20	3.5
5	260	1,76E-02	N47_J03960	439951	470207	455079	21394	5	148689	105904	127296	30254	24	3.6
5	226	5,42E-03	N47_E52290	1107895	984665	1046280	87137	8	353463	389670	371566	25602	7	2.8
4	203	3,42E-02	N47_J03820	2236678	166495	195086	40434	21	88862	79563	84213	6576	8	2.3
4	203	1,47E-02	N47_A10600	202843	226798	214821	16939	8	15574	7548	11561	5675	49	18.6
3	133	3,63E-03	N47_G37720	242241	229220	235731	9207	4	107837	99275	103556	6054	6	2.3
2	100	1,50E-02	N47_D31510	34929	39127	37028	2968	8	11828	8771	10299	2161	21	3.6
2	91	9,05E-03	N47_J03980	109757	86371	98064	16537	17	27686	26155	26920	1083	4	3.6

Peptides used for quantitation	Confidence score	Anova (p)	Description	Normalized abundance 2MN				Normalized abundance Naph				Ratio 2MN/Naph		
				MOH6863A14 MA2_014-2MN_B1_5	MOH6863A1 5MA2_015-2MN_B2_5	MOH6863A1 MA2_017-8MA2_018-Naph_A1_5	MOH6863A1 MA2_015-2MN_B2_5	MOH6863A1 MA2_017-8MA2_018-Naph_A2_5	MOH6863A1 MA2_015-2MN_B2_5	MOH6863A1 MA2_017-8MA2_018-Naph_A2_5				
1	74	1,38E-02	N47_J03830	50165	72540	61352	15822	26	11436	9384	10410	1451	14	5,9
1	52	3,06E-02	N47_J03850	63533	74733	69133	7920	11	22088	13908	17998	5784	32	3,8
1	48	2,01E-04	N47_H22960	13390	12874	13132	365	3	3064	3101	3082	26	1	4,3

Table A15: Proteomic dataset for Tab. A5.

A.

Peptides used for quant.	C. score	Description NaphS2	Normalized abundance 2MN				Normalized abundance Naph				Ratio Naph/2MN		
			MOH6861A5MA 3_005-2MN_B1_1	MOH6861A6 MA3_006-2MN_B2_1	MOH6861A8 MA3_008-Naph_A1_1	MOH6861A9 MA3_009-Naph_A2_1	MOH6861A8 MA3_008-Naph_A1_1	MOH6861A9 MA3_009-Naph_A2_1	MOH6861A8 MA3_008-Naph_A1_1	MOH6861A9 MA3_009-Naph_A2_1			
56	4094	NPH_7198	55688318	40814618	48251468	10517295	22	146646654	138913680	142780167	5468038	4	2,96
23	1416	NPH_5861	12571204	8246855	10409030	3057777	29	19737069	16130134	17933601	2550488	14	1,72
22	1274	NPH_5859	8402382	6514813	7458597	1334713	18	18087628	15050253	16568941	2147748	13	2,22
28	1272	NPH_2828	805758	579779	692768	159791	23	1752744	1840871	1796808	62315	3	2,59
14	797	NPH_2300	1514063	1309771	1411917	144457	10	8355525	6322687	7339106	1437433	20	5,20
13	595	NPH_1561	946999	673613	810306	193313	24	1351023	829840	1090431	368532	34	1,35
8	494	NPH_1563	335446	263414	299430	50934	17	450693	337097	393895	80324	20	1,32
10	375	NPH_5644	41028	45023	43026	2825	7	91808	100557	96182	6186	6	2,24
8	352	NPH_1886	357805	282920	320363	52952	17	379962	260358	320160	84573	26	1,00
7	329	NPH_3406	134035	129826	131931	2976	2	63706	45869	54787	12613	23	0,42
6	271	NPH_4054	661040	664723	662881	2604	0	224413	254058	239236	20962	9	0,36
4	259	NPH_4055	156944	108147	132545	34505	26	75178	77061	76119	1331	2	0,57
5	223	NPH_3399	52497	44260	48379	5825	12	52885	54544	53714	1173	2	1,11
4	170	NPH_5475/NPH_1621	191677	167228	179452	17288	10	75040	45898	60469	20606	34	0,34
4	169	NPH_2224	105688	93392	99540	8694	9	68725	43539	56132	17809	32	0,56

Peptides used for quant.	C. score	Description	Normalized abundance 2MN				Normalized abundance Naph				Ratio Naph/2MN
			2MN_B1_1	MOH6861A6 3_005-2MN_B2_1	MA3_006-2MN_B2_1	2MN_B1_1	MOH6861A8 Naph_A1_1	MA3_009-MA3_009-Naph_A2_1	MOH6861A9 Naph_A1_1	MA3_009-Naph_A2_1	
			ø	SD	CV%	ø	SD	CV%	ø	SD	CV%
4	143	NPH_2223	27829	21118	19	24473	4746	19	80934	23516	29
2	114	NPH_4056	191103	128698	28	159900	44127	28	68891	8921	12
3	114	NPH_6203	25546	19945	17	22746	3961	17	73894	1864	2
3	112	NPH_2827	22275	12007	42	17141	7261	42	64172	1837	3
2	90	NPH_5856	27330	13647	47	20489	9676	47	55971	31373	93
1	65	NPH_1562	18237	12965	24	15601	3728	24	33164	20988	32
2	64	NPH_0481	766	940	14	853	123	14	0	0	0
1	59	NPH_5855	23461	30008	17	26735	4629	17	30197	17316	38
1	56	NPH_2826	10900	6416	37	8658	3170	37	41583	39444	4
1	48	NPH_2548	427	238	40	332	133	40	0	0	0
1	40	NPH_4833	4373	4788	6	4581	293	6	15569	16362	4

B.

Peptides used for quant.	C. score	Description	Normalized abundance 2MN				Normalized abundance Naph				Ratio Naph/2MN
			2MN_B1_2	MOH6861A1 5MA3_015-2MN_B2_2	MA3_018-7MA3_017-8MA3_018-Naph_A1_2	MOH6861A1 Naph_A1_2	MOH6861A1 7MA3_017-8MA3_018-Naph_A2_2	MA3_018-Naph_A2_2			
			ø	SD	CV%	ø	SD	CV%	ø	SD	CV%
65	5391	NPH_7198	107261172	76280170	24	91770671	21906876	24	52083333	52049483	0
18	5040	NPH_5476/NPH_5957	34547671	20189858	37	27368764	10152507	37	47383433	47448239	0
59	4863	NPH_2655	89289754	60970740	27	75130247	20024567	27	70096495	66732186	7
21	4718	NPH_5426	15537189	9032187	37	12284688	4599731	37	10939868	12011929	7
14	4465	NPH_1622	3646058	4846941	20	4246500	849152	20	2660292	2817948	4
47	4305	NPH_5855	354994467	217177698	34	286086082	97451172	34	534717496	534665437	0
14	4285	NPH_4883	19078384	11061580	38	15069982	5668736	38	7649158	8775969	10
47	4037	NPH_4697	72118906	51596218	23	61857562	14511732	23	1985570	1651342	13
45	3215	NPH_4912	36428691	20262369	40	28345530	11431316	40	48491835	47611567	1
42	3142	NPH_5859	58212681	37986807	30	48099744	14301853	30	49040171	47649841	2
43	2623	NmsA	17714570	14531033	14	16122801	2251100	14	1282947	906288	24

Peptides used for quant.	C. score	Description	Normalized abundance 2MN					Normalized abundance Naph					Ratio Naph/2MN	
			MA3_014-2MN_B1_2	MOH6861A1 5MA3_015-2MN_B2_2	MA3_014-2MN_B1_2	MOH6861A1 5MA3_015-2MN_B2_2	CV%	SD	σ	MOH6861A1 7MA3_017-Naph_A1_2	MOH6861A1 8MA3_018-Naph_A2_2	CV%		SD
39	2615	NPH_5861	44567674	33149110	38858392	8074145	21	42346617	38908100	40627359	2431399	6	1,05	
43	2594	NPH_6979	5457413	4628540	5042976	586101	12	4754241	3429901	4092071	936450	23	0,81	
39	2494	NPH_3003	19132774	12680910	15906842	4562157	29	15101581	13850122	14475851	884915	6	0,91	
32	2378	NPH_4698	116026235	76731825	96379030	27786343	29	3832377	3063242	3447809	543860	16	0,04	
32	2313	NPH_2658	38543922	26627692	32585807	8426047	26	31136016	29325003	30230509	1280580	4	0,93	
31	2070	NPH_4205	5601092	3723567	4662330	1327611	28	4129021	3634769	3881895	349488	9	0,83	
30	2017	NPH_2223	4371873	2469805	3420839	1344965	39	13000534	9706646	11353590	2329130	21	3,32	
		NPH_5475,												
		NPH_1621,												
23	1876	NPH_2988	2872018	2312930	2592474	395335	15	3212372	2479178	2845775	518447	18	1,10	
28	1762	NPH_1634	196291	102159	149225	66561	45	198995	196333	197664	1883	1	1,32	
27	1576	NPH_2689	4559549	3106818	3833184	1027236	27	5454300	4475402	4964851	692185	14	1,30	
22	1551	NPH_6237	8722152	6325280	7523716	1694844	23	8475999	5915611	7195805	1810468	25	0,96	
23	1403	NPH_1631	711919	461445	586682	177112	30	585204	583657	584431	1095	0	1,00	
20	1375	NPH_1563	5206226	3682145	4444186	1077687	24	3839378	3923574	3881476	59536	2	0,87	
12	1208	NPH_2102	1564186	1031328	1297757	376787	29	1021860	945101	983481	54277	6	0,76	
16	1207	NPH_2657	20750380	12397551	16573966	5906342	36	16939753	14912931	15926342	1433180	9	0,96	
22	1158	NPH_0481	497693	419451	458572	55326	12	164842	114641	139741	35498	25	0,30	
18	1131	NPH_3005	6200451	3789623	4995037	1704713	34	6229595	5207905	5718750	722444	13	1,14	
17	1051	NPH_2224	1950164	1420944	1685554	374215	22	2048255	1387819	1718037	466999	27	1,02	
17	979	NPH_1633	80202	44710	62456	25097	40	146117	148700	147408	1826	1	2,36	
		NPH_6293,												
17	979	NPH_3552	3476264	2224406	2850335	885197	31	3170801	2874058	3022429	209829	7	1,06	
16	961	NPH_1561	4537563	2939518	3738541	1129988	30	3395282	3185192	3290237	148556	5	0,88	
15	944	NPH_6289	839322	551005	695163	203871	29	1028423	928296	978359	70800	7	1,41	
13	926	NPH_5856	117990250	74165767	96078008	30988589	32	212837197	183038674	197937936	21070738	11	2,06	
10	904	NPH_4487	1561507	759144	1160325	567356	49	1068727	1112268	1090498	30789	3	0,94	
10	845	NPH_3401	696162	590445	643303	74753	12	2271542	1449305	1860423	581409	31	2,89	
13	844	NPH_2222	661712	421787	541749	169653	31	835615	766447	801031	48910	6	1,48	
14	834	NPH_2656	7182922	4796594	5989758	1687389	28	6526263	5582966	6054615	667012	11	1,01	
15	810	NPH_3655	2950924	1669063	2309993	906412	39	1444967	1136067	1290517	218425	17	0,56	
14	805	NPH_1638	142219	131181	136700	7805	6	202388	208322	205355	4196	2	1,50	
11	785	NPH_3557	634170	318695	476432	223075	47	11559	10924	11241	449	4	0,02	
10	781	NPH_4094	2914102	1796196	2355149	790478	34	1552135	1622378	1587257	49669	3	0,67	

Peptides used for quant.	C. score	Description NaphS2	Normalized abundance 2MN				Normalized abundance Naph				Ratio Naph/2MN		
			MOH6861A14 MA3_014- 2MN_B1_2	MOH6861A1 5MA3_015- 2MN_B2_2	SD	CV%	MOH6861A1 7MA3_017- 8MA3_018- Naph_A1_2	MOH6861A1 Naph_A2_2	SD	CV%			
14	770	NPH_2219	542743	273272	408008	190545	47	293584	324693	309138	21997	7	0,76
4	769	NPH_6291	605635	428573	517104	125202	24	361637	338426	350031	16413	5	0,68
11	723	NPH_1692	2188259	1619425	1903842	402227	21	8982578	6262856	7622717	1923133	25	4,00
13	682	NPH_7178	503797	294848	399323	147749	37	412358	440679	426519	20026	5	1,07
13	633	NPH_2811	883379	588952	736165	208191	28	703554	587663	645609	81947	13	0,88
9	629	NPH_0950	479419	358891	419155	85226	20	493658	347590	420624	103286	25	1,00
10	595	NPH_1821	233153	134963	184058	69431	38	296918	167147	232033	91762	40	1,26
9	581	NPH_1819	382007	274214	328110	76221	23	313751	235166	274459	55568	20	0,84
9	572	NPH_5978	268361	210434	239398	40960	17	302919	218416	260667	59753	23	1,09
11	564	NPH_3996	191484	136213	163849	39082	24	329451	223987	276719	74574	27	1,69
11	555	NPH_3558	860647	467384	664015	278078	42	92797	102647	97722	6964	7	0,15
10	543	NPH_4429	271488	208583	240035	44480	19	157948	119971	138960	26854	19	0,58
11	537	NPH_1127	614183	414616	514400	141115	27	489887	316423	403155	122658	30	0,78
10	529	NPH_6387	24339	12015	18177	8715	48	12790	13403	13097	433	3	0,72
10	506	NPH_5569	907555	477036	692296	304423	44	889858	880662	885260	6503	1	1,28
9	463	NPH_2560	427172	304176	365674	86971	24	553122	526813	539967	18603	3	1,48
8	454	NPH_2690	618442	503036	560739	81605	15	680475	621176	650825	41931	6	1,16
8	452	NPH_4482	711938	426210	569074	202040	36	557004	502639	529821	38442	7	0,93
9	450	NPH_5480	159763	108975	134369	35912	27	208563	186145	197354	15852	8	1,47
7	444	NPH_6292	1238127	797547	1017837	311537	31	897300	891180	894240	4328	0	0,88
9	442	NPH_5477	250996	154460	202728	68261	34	623782	495869	559825	90448	16	2,76
9	434	NPH_4520	502910	360137	431523	100956	23	489283	431920	460601	40562	9	1,07
8	428	NPH_1639	96838	86584	91711	7251	8	87274	65158	76216	15638	21	0,83
7	419	NPH_3151	493131	289223	391177	144185	37	916328	595100	755714	227143	30	1,93
6	414	NPH_5857	46284	27218	36751	13482	37	99296	75157	87226	17069	20	2,37
8	412	NPH_2691	581977	398390	490183	129815	26	845907	742411	794159	73183	9	1,62
8	409	NPH_5073	952631	485222	718927	330508	46	649127	463695	556411	131120	24	0,77
7	409	NPH_6696	188391	96320	142356	65104	46	155741	155246	155493	350	0	1,09
7	408	NPH_4256	58305	38338	48321	14119	29	41139	35865	38502	3729	10	0,80
7	399	NPH_6970	2057823	1313529	1685676	526296	31	1848002	1448719	1648361	282336	17	0,98
6	396	NPH_1875	221943	128779	175361	65877	38	346938	295802	321370	36159	11	1,83
6	386	NPH_1562	460767	334288	397527	89434	22	310923	370822	340873	42355	12	0,86

Peptides used for quant.	C. score	Description	Normalized abundance 2MN				Normalized abundance Naph				Ratio Naph/2MN		
			MA3_014-2MN_B1_2	MOH6861A14-5MA3_015-2MN_B2_2	SD	CV%	MA3_017-8MA3_018-Naph_A1_2	MOH6861A1-Naph_A2_2	SD	CV%			
5	383	NPH_3272	143793	94659	119226	34743	29	131716	92988	112352	27385	24	0,94
9	364	NPH_4724	132160	94403	113282	26698	24	186832	156868	171850	21188	12	1,52
7	364	NPH_3842	1377	2161	1769	554	31	1829	2908	2368	763	32	1,34
6	355	NPH_3297	183846	158703	171275	17779	10	152524	136334	144429	11448	8	0,84
6	346	NPH_6446	4372021	3008321	3690171	964282	26	2763595	2710118	2736857	37814	1	0,74
6	333	NPH_6822	253094	148784	200939	73758	37	216694	210965	213830	4051	2	1,06
7	317	NPH_1560	393143	223558	303350	119914	39	193300	184723	189012	6065	3	0,61
6	311	NPH_7070	98553	51922	75238	32973	44	82510	72768	77639	6889	9	1,03
5	296	NPH_6824	328159	207721	267940	85163	32	152325	133855	143090	13060	9	0,53
5	295	NPH_2877	279583	137386	208484	100548	48	270231	296092	283161	18286	6	1,36
6	294	NPH_6370	83735	68086	75910	11066	15	136399	168374	152386	22610	15	2,01
5	287	NPH_4572	225996	155863	190929	49592	26	505400	613479	559440	76423	14	2,93
6	277	NPH_1874	125980	85962	105971	28297	27	208426	198610	203518	6941	3	1,92
4	271	NPH_5231	215086	174942	195014	28386	15	298023	264128	281075	23967	9	1,44
5	268	NPH_3917	102816	59007	80911	30977	38	243766	188360	216063	39178	18	2,67
5	264	NPH_5865	95949	97883	96916	1368	1	597232	487613	542422	77513	14	5,60
6	263	NPH_3825	91566	55905	73736	25216	34	83483	51257	67370	22787	34	0,91
5	259	NPH_4798	206836	133682	170259	51728	30	201940	199314	200627	1857	1	1,18
5	257	NPH_1693	554743	393746	474244	113842	24	2283852	1542741	1913297	524045	27	4,03
2	239	NPH_1558	92900	57084	74992	25325	34	105078	169866	137472	45813	33	1,83
5	238	NPH_2958/NPH_6117	1074687	668159	871423	287458	33	910407	743658	827032	117909	14	0,95
5	234	NPH_4257	121305	88359	104832	23296	22	63307	61298	62302	1421	2	0,59
4	230	NPH_3997	150671	104107	127389	32925	26	190115	151998	171057	26953	16	1,34
4	230	NPH_4095	760566	459673	610119	212763	35	632444	574118	603281	41243	7	0,99
4	229	NPH_5961	152549	118199	135374	24289	18	83848	58241	71045	18107	25	0,52
5	226	NPH_2292	23227	13850	18538	6631	36	144350	125975	135162	12993	10	7,29
4	223	NPH_1820	173048	109617	141332	44853	32	243123	144386	193755	69817	36	1,37
5	223	NPH_6221	118287	62131	90209	39709	44	139577	174728	157153	24856	16	1,74
5	216	NPH_4696	108666	63196	85931	32152	37	1406	2213	1809	570	32	0,02
5	209	NPH_2956	279867	192496	236181	61781	26	109575	96751	103163	9068	9	0,44
5	200	NPH_5899	325866	308650	317258	12173	4	321352	271816	296584	35027	12	0,93
4	200	NPH_2810	459935	283732	371833	124595	34	261193	220124	240658	29040	12	0,65

Peptides used for quant.	C. score	Description	Normalized abundance 2MN					Normalized abundance Naph					Ratio Naph/2MN
			MOH6861A14 MA3_014- 2MN_B1_2	MOH6861A1 5MA3_015- 2MN_B2_2	ϕ	SD	CV%	MOH6861A1 7MA3_017- Naph_A1_2	MOH6861A1 8MA3_018- Naph_A2_2	ϕ	SD	CV%	
4	197	NPH_6299	113456	69405	91431	31149	34	105165	98412	101789	4775	5	1,11
3	196	NPH_2998	156784	99864	128324	40249	31	160314	106110	133212	38329	29	1,04
4	190	NPH_1613	46651	30863	38757	11164	29	137730	107455	122592	21408	17	3,16
4	187	NPH_5825	18301	9024	13663	6560	48	114063	131856	122959	12582	10	9,00
4	183	NPH_6563/NPH_0260	120478	59082	89780	43414	48	107158	95984	101571	7901	8	1,13
4	181	NPH_1954	44500	34554	39527	7033	18	33736	34640	34188	639	2	0,86
4	178	NPH_5423	163428	93162	128295	49685	39	208147	186345	197246	15416	8	1,54
3	177	NPH_6762	1378	684	1031	491	48	3378	3232	3305	104	3	3,21
4	169	NPH_5424	119419	66741	93080	37249	40	143037	133998	138517	6392	5	1,49
4	166	NPH_3340	113724	72681	93203	29022	31	104194	113985	109090	6923	6	1,17
3	164	NPH_6672	17607	10303	13955	5165	37	21120	12204	16662	6305	38	1,19
3	163	NPH_1115	87446	45628	66537	29569	44	71946	61094	66520	7674	12	1,00
3	159	NPH_2531	122914	122292	122603	440	0	62556	53584	58070	6344	11	0,47
3	157	NPH_3826	6071	4157	5114	1353	26	33728	31646	32687	1472	5	6,39
4	153	NPH_2532	152406	118029	135217	24308	18	55396	41699	48548	9685	20	0,36
3	150	NPH_1771	43287	39272	41280	2839	7	515	608	562	65	12	0,01
3	149	NPH_5570	368930	203882	286406	116707	41	466736	444781	455759	15524	3	1,59
2	144	NPH_5320	45817	23033	34425	16111	47	170853	154756	162804	11382	7	4,73
3	142	NPH_5230	18651	18894	18773	171	1	39180	36922	38051	1597	4	2,03
3	141	NPH_3006	1233683	681117	957400	390723	41	1166700	943440	1055070	157869	15	1,10
2	139	NPH_3287	17411	12104	14758	3753	25	14599	8890	11745	4037	34	0,80
2	137	NPH_2218	14398	10009	12204	3104	25	10973	10898	10936	53	0	0,90
2	131	NPH_5368	52516	50440	51478	1468	3	25839	20381	23110	3859	17	0,45
2	131	NPH_4847	46360	22800	34580	16659	48	61119	59638	60379	1047	2	1,75
3	129	NPH_7201	59004	39056	49030	14105	29	45071	26656	35864	13021	36	0,73
3	128	NPH_3995	202323	137451	169887	45872	27	283776	236419	260098	33487	13	1,53
3	127	NPH_5576	519995	265582	392789	179897	46	592881	481590	537235	78695	15	1,37
2	124	NPH_3004	352353	179309	265831	122361	46	213358	20205	206781	9300	4	0,78
2	117	NPH_5407	89266	79522	84394	6890	8	25935	21199	23567	3349	14	0,28
2	114	NPH_2628	25457	16253	20855	6509	31	27718	33389	30554	4010	13	1,47
2	114	NPH_3252	231962	186463	209213	32173	15	217849	153021	185435	45841	25	0,89
3	113	NPH_7213	111821	65032	88426	33085	37	99608	66519	83063	23397	28	0,94

Peptides used for quant.	C. score	Description NaphS2	Normalized abundance 2MN					Normalized abundance Naph					Ratio Naph/2MN
			MOH6861A14 MA3_014- 2MN_B1_2	MOH6861A1 5MA3_015- 2MN_B2_2	ϕ	SD	CV%	MOH6861A1 7MA3_017- Naph_A1_2	MOH6861A1 8MA3_018- Naph_A2_2	ϕ	SD	CV%	
2	113	NPH_0973	1364523	847507	1106015	365586	33	1657096	1367074	1512085	205077	14	1,37
3	112	NPH_2876	93265	54550	73907	27375	37	100151	93502	96826	4701	5	1,31
3	111	NPH_1116	58313	33161	45737	17785	39	152251	142816	147533	6672	5	3,23
2	110	NPH_3353	742	829	785	62	8	0	0	0	0	0	0,00
2	110	NPH_1564	164019	103321	133670	42920	32	109771	109301	109536	332	0	0,82
1	108	NPH_2097	16164	22573	19369	4532	23	20035	12781	16408	5129	31	0,85
2	108	NPH_6826	58097	32981	45539	17759	39	27291	25817	26554	1043	4	0,58
2	108	NPH_6194	2756	4074	3415	932	27	3565	5473	4519	1349	30	1,32
2	107	NPH_4202	69486	51973	60729	12384	20	19439	21744	20591	1630	8	0,34
2	106	NPH_5895	18921	14077	16499	3425	21	14203	9427	11815	3377	29	0,72
3	101	NPH_1573	10760	5778	8269	3523	43	17079	15365	16222	1212	7	1,96
2	100	NPH_2174	3903	3691	3797	150	4	4866	4257	4561	430	9	1,20
2	99	NPH_6290	182017	111298	146658	50006	34	176850	156404	166627	14457	9	1,14
2	99	NPH_5858	6905	4183	5544	1924	35	26953	21766	24359	3668	15	4,39
2	94	NPH_6942	6070	3613	4842	1737	36	4126	2359	3242	1250	39	0,67
2	92	NPH_5425	14911	11392	13152	2489	19	15079	9727	12403	3785	31	0,94
2	91	NPH_5579	271923	147885	209904	87708	42	311551	324529	318040	9177	3	1,52
2	90	NPH_7006	91746	50749	71248	28989	41	75356	62574	68965	9038	13	0,97
2	87	NPH_6300	46241	33756	39999	8828	22	28284	30240	29262	1383	5	0,73
2	85	NPH_3841	8826	6587	7707	1583	21	4158	4659	4408	354	8	0,57
2	84	NPH_3228	9388	4633	7010	3362	48	11634	9145	10389	1760	17	1,48
2	83	NPH_2098	32050	38570	35310	4611	13	34909	23011	28960	8413	29	0,82
1	81	NPH_5524	19605	17355	18480	1591	9	6492	4400	5446	1479	27	0,29
1	80	NPH_2615	20144	19645	19894	353	2	17534	13747	15640	2678	17	0,79
2	80	NPH_2826	37382	18887	28134	13078	46	48161	43031	45596	3627	8	1,62
1	80	NPH_6398	5239	4394	4816	597	12	28140	16304	22222	8369	38	4,61
2	79	NPH_3423	9715	10041	9878	230	2	13658	12518	13088	806	6	1,32
1	76	NPH_5512	162044	123870	142957	26993	19	182195	162216	172205	14127	8	1,20
2	75	NPH_5583	18129	10227	14178	5587	39	7474	7567	7520	66	1	0,53
2	70	NPH_3107	3160	2422	2791	522	19	18891	13714	16303	3661	22	5,84
2	68	NPH_3013	14209	10763	12486	2437	20	21809	19623	20716	1546	7	1,66
2	67	NPH_4090	23681	13574	18627	7147	38	24372	23676	24024	492	2	1,29

Peptides used for quant.	C. score	Description	Normalized abundance 2MN					Normalized abundance Naph					Ratio Naph/2MN
			MOH6861A14 MA3_014- 2MN_B1_2	MOH6861A1 5MA3_015- 2MN_B2_2	σ	SD	CV%	MOH6861A1 7MA3_017- Naph_A1_2	MOH6861A1 8MA3_018- Naph_A2_2	σ	SD	CV%	
1	64	NPH_1715	15303	11815	13559	2466	18	10382	5927	8155	3150	39	0,60
1	63	NPH_4203	152623	131192	141908	15154	11	224099	189122	206610	24732	12	1,46
1	60	NPH_6213	9787	6786	8286	2122	26	13422	12404	12913	720	6	1,56
1	59	NPH_2503	4130	6378	5254	1590	30	6160	5155	5657	711	13	1,08
1	55	NPH_0385	6136	3173	4654	2095	45	10511	8447	9479	1460	15	2,04
1	54	NPH_1716	4776	7700	6238	2068	33	4650	7438	6044	1972	33	0,97
1	53	NPH_3383	0	0	0	0	0	22126	17183	19655	3495	18	
1	53	NPH_2290	9600	5619	7609	2815	37	76323	66337	71330	7061	10	9,37
1	52	NPH_6061	7966	4968	6467	2120	33	2920	2797	2859	87	3	0,44
1	49	NPH_3002	507425	313083	410254	137421	33	601141	468379	534760	93877	18	1,30
1	48	NPH_3555	72298	53800	63049	13080	21	26759	26228	26493	375	1	0,42
1	43	NPH_0948	14701	9678	12189	3552	29	20465	17009	18737	2444	13	1,54
1	42	NPH_1092	329	375	352	33	9	189	222	206	24	12	0,58
1	42	NPH_6862	170613	107807	139210	44410	32	173450	122206	147828	36235	25	1,06

Table A16: Proteomic dataset for Tab. 31.

Peptides used for quant.	C. score	Anova (p)	Description	Normalized abundance Naphthalene				Normalized abundance 2-Methylnaphthalene				Ratio DDM Naph/2MN		
				A	B	σ	SD	CV%	A	B	σ		SD	CV%
18	1162,18	6,30E-04	N47_K27480	1467895	2317601	1892748	600833	32	67531	54630	61080	9123	15	31,0
13	818,69	6,00E-04	N47_K27500	1637638	1698086	1667862	42743	3	56808	84497	70652	19579	28	23,6
14	854,81	1,73E-03	N47_K27400	607082	784761	695921	125638	18	14257	16942	15600	1899	12	44,6
4	217	4,85E-04	N47_H23280	47862	62903	55382	10636	19	1660	2300	1980	453	23	28,0
4	216,98	4,90E-04	N47_F14190	44557	36663	40610	5582	14	317	206	262	78	30	155,1
2	89,02	2,88E-02	N47_K27460	53468	56487	54977	2135	4	21	1	11	14	135	5171,5

Peptides used for quant.	C. score	Anova (p)	Description	Normalized abundance Naphthalene				Normalized abundance 2-Methylnaphthalene				Ratio DDM Naph/2MN		
				A	B	σ	SD	CV%	A	B	σ		SD	CV%
10	608	1,11E-03	N47_K27480	195074	224782	209928	21006	10	11338	13772	12555	1721	14	16,7
15	745	5,97E-03	N47_E41400	352575	276477	314526	53809	17	17734	18991	18363	889	5	17,1

Peptides used for quant.	C. score	Anova (p)	Description	Normalized abundance Naphthalene				Normalized abundance 2-Methylnaphthalene				Ratio DDM Naph/2MN		
				A	B	σ	SD	CV%	A	B	σ		SD	CV%
6	305	6,85E-03	N47_A07150	737407	738236	737822	586	0	3249	11047	7148	5514	77	103,2
5	213	2,49E-03	N47_K27600	93372	171078	132225	54947	42	3574	2175	2874	989	34	46,0
2	65	9,35E-03	N47_F14520	20529	35756	28142	10767	38	1350	1293	1321	40	3	21,3

